



HAL
open science

High-Frequency Price Formation Dynamics and Multivariate Intraday Risk Measurement

Hai Dang Ngo

► **To cite this version:**

Hai Dang Ngo. High-Frequency Price Formation Dynamics and Multivariate Intraday Risk Measurement. Economics and Finance. Nantes Université, 2022. English. NNT : 2022NANU3020 . tel-04085092

HAL Id: tel-04085092

<https://theses.hal.science/tel-04085092>

Submitted on 28 Apr 2023

HAL is a multi-disciplinary open access archive for the deposit and dissemination of scientific research documents, whether they are published or not. The documents may come from teaching and research institutions in France or abroad, or from public or private research centers.

L'archive ouverte pluridisciplinaire **HAL**, est destinée au dépôt et à la diffusion de documents scientifiques de niveau recherche, publiés ou non, émanant des établissements d'enseignement et de recherche français ou étrangers, des laboratoires publics ou privés.

THESE DE DOCTORAT DE

NANTES UNIVERSITE

ECOLE DOCTORALE N° 597
Sciences Economiques et Sciences de Gestion
Spécialité : *Sciences Economiques*

Par

Hai Dang NGO

High-Frequency Price Formation Dynamics and Multivariate Intraday Risk Measurement

Thèse présentée et soutenue à Nantes, le 15 Décembre 2022
Unité de recherche : LEMNA, Laboratoire d'Économie et de Management de Nantes-Atlantique

Rapporteurs avant soutenance :

Georgios Sermpinis Professeur, University of Glasgow
Mascia Bedendo Professeur, Università di Bologna

Composition du Jury :

Président :	Alex Frino	Professeur, University of Wollongong
Examineur :	Georgios Sermpinis	Professeur, University of Glasgow
Examineur :	Mascia Bedendo	Professeur, Università di Bologna
Dir. de thèse :	François-Charles Wolff	Professeur, Université de Nantes
Co-dir. de thèse :	Emilios Galariotis	Professeur et Directeur de la recherche, Audencia Business School
Co-encadrant :	Iordanis Kalaitzoglou	Professeur, Audencia Business School

High-Frequency Price Formation Dynamics and Multivariate Intraday Risk Measurement, ©
December 2022

Author:
Hai Dang NGO

Supervisors:
Prof. François Charles WOLFF
Prof. Emiliós GALARIOTIS
Prof. Iordanis KALAITZOGLOU

Institutes:
Université de Nantes, Nantes, France

*To my family, the people I love most - my parents, my sisters and my beloved girlfriend -
for always believing in me and helping me become the person I am today.*

STATEMENT OF AUTHORSHIP

I, Hai Dang Ngo, born October 08, 1990 in Vietnam, declare that this thesis titled *High-Frequency Price Formation Dynamics and Multivariate Intraday Risk Measurement* and the work presented in it are my own. I confirm that this work was done mainly while in candidature for a research degree at the Université de Nantes and Audencia Business School.

Except where reference is made in the text of the thesis, this thesis contains no material published elsewhere or extracted in whole or in part from a thesis accepted for the award of any other degree or diploma. No other person's work has been used without due acknowledgment in the main text of the thesis. This thesis has not been submitted for the award of any degree or diploma in any other tertiary institution.



Hai Dang Ngo

December 15, 2022

ACKNOWLEDGMENTS

My Ph.D. has been a challenging but rewarding experience. I would like to express my gratitude and appreciation to many people who helped me directly and/or indirectly in developing this study and my academic career. It would be impossible for me to complete this work without the invaluable support and encouragement from you. To all of you, I hereby say *Thank You for everything! This would not have been possible without you!*

First and foremost, I would like to express my deepest gratitude to **Prof. Iordanis Kalaitzoglou**, my academic supervisor and mentor for many years. These few words cannot express how much I am grateful to you for your support. You gave me the opportunity to do research with you and introduced me to the field of financial market microstructure. I am extremely lucky to have you as my supervisor and friend. You provide tremendous support for my research and my development in every aspect with your erudite knowledge and heartwarming encouragement. You set an excellent example for me to become not only a responsible and rigorous researcher, but also a helpful and enthusiastic scholar. I am very grateful for your kindness and patience to my capricious research, and I could not have achieved anything in the past five years without your guidance.

In the same spirit, I am additionally indebted to **Prof. Emiliós Galariotis** and **Prof. François Charles Wolff** for advising me, providing me with excellent resources for my research, and keeping me going when things got difficult. The generous financial support of **Prof. Emiliós Galariotis** during the fourth year of my Ph.D. studies is also gratefully appreciated. I also would like to thank all the members of the jury, **Prof. Alex Frino**, **Prof. Georgios Sermpinis**, and **Prof. Mascia Bedendo** for accepting to be part of my Ph.D. journey.

My gratitude extends to all the Ph.D. and postdoctoral researchers in room 361, and all faculty members of the Finance Department at Audencia Business School. I am very grateful to be their colleague and to have the opportunity to share with them joyful moments and excellent professional perspectives after my research hours. A special note is dedicated to **Laurent Pataillot** for his enormous support in helping me translate this thesis into French.

I also take this opportunity to express my appreciation to my two French professors, **Mr. Yves Gendreau** and **Mrs. Françoise Lesimple**. They have helped me tremendously in overcoming difficulties of language barrier and discovering French cultures. In addition, I have been blessed with incredible friends, whom I want to thank for their support during all the years I stayed in France.

Most importantly, I have always been able to rely on my family, my mother, my father, and my sisters for their unconditional love and support. They have never stopped in encouraging me and lifting me up when I was at loose ends. They are the people who have

allowed me to pursue my dreams and become who I am today. My eternal love and gratitude lie with them and it is to them that I dedicate this work in particular.

Finally, I would also like to express my gratitude to my beloved girlfriend who has been a tremendous source of support, inspiration, and motivation during the most difficult phase of my work. She kept me going in my efforts to produce the highest quality research of mine.

RÉSUMÉ

I. INTRODUCTION

Cette thèse porte sur les marchés électroniques modernes et développe des modèles mathématiques sur mesure pour le trading à haute fréquence. Observées à la résolution la plus fine (transaction par transaction), la formation des prix et les transactions intrajournalières présentent des propriétés fondamentalement différentes de celles du trading à plus basse fréquence. En effet, plusieurs “frictions de marché” semblent désormais être la norme plutôt que l’exception, ce qui remet en question l’hypothèse de l’efficience des marchés. Par conséquent, les modèles mathématiques établis de longue date et appliqués à une dynamique de prix à basse fréquence, inadaptés au contexte actuel de trading à haute fréquence, ne parviennent plus à expliquer l’environnement complexe généré par les frictions de microstructure des marchés.

L’un des défis majeurs réside dans les propriétés statistiques des données de trading, notamment l’irrégularité des intervalles inter-événements, l’évolution des prix sur une grille discrète et la nature asynchrone des transactions. Les propriétés traditionnelles, telles que la discrétisation du temps, la continuité des prix, et l’observation de l’information alignée en coupe transversale ne correspondent plus à la réalité. Par conséquent, plusieurs modèles bien établis ne peuvent être appliqués inconditionnellement. En effet, l’approche privilégiée dans la littérature est une sorte d’algorithme de “pseudo-agrégation” à basse fréquence, mais étant donné qu’un certain type de phénomène de négociation à haute fréquence, comme l’arbitrage à faible latence, se produit en fractions de seconde, cet éclaircissement des données entraîne inévitablement une perte d’informations.

Modélisation de la dynamique des prix multivariés en temps continu

L’information asymétrique, la durée de vie des informations, et les effets d’avance-retard sur une dynamique de formation des prix multivariés

Pour remédier à ces lacunes, nous développons dans la première partie de cette thèse une dynamique généralisée de formation des prix, basée sur l’idée que l’information et le temps sont intrinsèquement liés, considérant que l’information a une durée de vie et qu’elle se dégrade avec le temps. Plus précisément, nous proposons une extension du modèle classique “martingale plus bruit” et permettons un traitement plus structurel de la dynamique à haute fréquence qui reflète les sources d’information asymétrique, la durée de vie de l’information (résiduelle) et l’ajustement des prix retardé dans le temps. Pour effectuer des inférences économétriques sur le modèle, nous utilisons un proxy statistique précis pour la décroissance de l’information, dérivé des fonctions décroissantes d’un processus de Hawkes multivarié, et utilisé pour représenter, de manière disjointe, des processus de changement de prix sur une grille discrète. Ceci permet d’estimer l’ajustement (croisé) des prix retardé sur plusieurs actifs à chaque instant, sans nécessairement observer l’arrivée d’un événement. Cette propriété atténue le problème de l’asynchronisme

et de la discrétisation temporelle, et permet d'estimer la corrélation croisée instantanément, à n'importe quelle échelle de temps. Une application empirique sur les actions du DJIA étaye ces postulats théoriques.

Modélisation multivariée du risque de marché en temps continu.

Outre la modélisation de la dynamique du marché, la gestion des risques (risque de marché) est sans aucun doute l'une des activités les plus importantes du praticien des marchés financiers. Les deuxième et troisième parties de la thèse contribuent ainsi à la mesure du risque multivarié à haute fréquence, mesure développée à partir de la dynamique des prix exposée en première partie.

La matrice de variance-covariance basée sur l'intensité.

En particulier, la deuxième partie de la thèse introduit un nouvel estimateur de la structure des moments de second ordre pour le rendement d'actifs, combinant deux approches bien établies sur les mesures de la volatilité à haute fréquence : les approches basées sur la covariation quadratique et les approches basées sur les processus ponctuels. D'une part, avec sa structure paramétrique parcimonieuse basée sur l'intensité conditionnelle, qui est au coeur de l'approche par processus ponctuel, notre modèle préserve les caractéristiques supérieures des estimateurs de volatilité basés sur des processus ponctuels univariés, tout en intégrant les propriétés prépondérantes des données à ultra-haute fréquence. D'autre part, le modèle est défini dans une structure générique d'(auto)covariation temporelle croisée de l'approche par covariation quadratique, ce qui facilite l'estimation de la corrélation croisée entre actifs. Dans une certaine mesure, notre nouvel estimateur de la matrice de variance-covariance basé sur l'intensité n'est pas affecté par les corrélations parasites et l'effet Epps, contrairement aux estimateurs de covariation quadratique, et tient compte simultanément des effets d'avance-retard et des temps endogènes dans les transactions asynchrones. De plus, grâce à sa structure paramétrique, cet estimateur a la capacité de fournir une inférence sur la volatilité locale dans des intervalles intra-journaliers relativement courts, surmontant les limites de la propriété de convergence qui assure la cohérence des mesures de volatilité réalisées sur de telles périodes. Nous testons la robustesse de cet estimateur à l'aide de simulations Monte Carlo étendues.

Value-at-Risk intra-journalier multivariée basée sur l'intensité.

Enfin, la troisième partie de la thèse contribue à un autre aspect de la mesure du risque à haute fréquence, en se concentrant sur la modélisation directe de la queue de la distribution des rendements. Nous proposons une Value-at-Risk (IVaR) intra-journalière multivariée qui généralise les IVaR univariées existantes et prend en compte la structure de corrélation croisée des rendements extrêmes. Notre généralisation multivariée est basée sur la modélisation de l'occurrence de changement de prix bidirectionnels par des intensités conditionnelles stochastiques, ainsi que la prévision des arrivées de transactions futures par simulation Monte Carlo. Notre estimateur surmonte les limites des précédentes approches IVaR basées sur des processus ponctuels et offre une mesure efficace du risque de marché qui tient compte du regroupement de l'arrivée des extrêmes à la fois dans le temps et en coupe transversale. Plus précisément, cet estimateur capture non seulement la corrélation concomitante, mais aussi un autre type de corrélation caractérisé par les données à haute

fréquence, à savoir la corrélation temporelle de type avance-retard. Alors que le premier type de corrélation peut être attribué à la valeur fondamentale des actifs, le second type résulte de la présence de transactions asynchrones, d'informations asymétriques, de trading stratégique et d'apprentissage des prix dans la microstructure du marché. Par conséquent, notre modèle IVaR multivarié, en incorporant fructueusement ces caractéristiques dans ses métriques de risque, donnerait une mesure meilleure et plus informée de l'IVaR pour un seul actif mais également de manière combinée pour un portefeuille intra-journalier.

II. MOTIVATION ET APPROCHES

Cette thèse est motivée à l'origine par le désir de fournir une approche originale aux divers phénomènes qui ont émergé des marchés de trading à haute fréquence et de fournir également des modèles de dynamique des prix et des mesures de risque qui reflètent étroitement les réalités de la microstructure de marché. Nous sommes convaincus que la clé de l'approche de modélisation au niveau microscopique des données de trading à haute fréquence réside dans les temps d'arrivée des événements liés au prix. Lorsque le niveau d'intérêt se situe à la fréquence la plus fine, c'est-à-dire transaction par transaction, la microstructure du marché a un impact significatif sur la manière dont l'information est incorporée dans le prix et, de manière plus importante encore, sur le moment précis où elle l'est. L'intensité de l'arrivée des événements, c'est-à-dire l'inverse des temps d'attente, est le point de rencontre de deux forces fondamentales de la dynamique du marché, l'information et la liquidité, qui constituent le matériau synthétique de la formation des prix O'Hara (1998). L'idée est que le temps joue un rôle dans la mesure de la résolution de l'information, et, plus précisément, dans la mesure de la vitesse à laquelle l'information arrive sur le marché et est progressivement incorporée dans le processus de formation des prix. Par conséquent, un modèle économétrique raisonnable peut être construit de manière à prendre en compte l'arrivée d'événements de prix, à la fois dans les dimensions temporelles et de prix, et à donner la probabilité à chaque instant de l'occurrence d'un mouvement de prix conditionnant l'historique des réalisations. Cette probabilité est appelée intensité conditionnelle.

Nous nous inspirons de la théorie des processus ponctuels, en particulier du processus de Hawkes, pour modéliser directement l'intensité conditionnelle de l'arrivée d'un événement en fonction des informations historiques sur les événements passés. Le processus de Hawkes présente de manière naturelle un système de génération de données basé sur l'intensité conditionnelle, rendant compte de la coexistence et de l'interaction entre les arrivées exogènes et endogènes de nouveaux événements à l'intérieur du système. Les événements exogènes du processus de Hawkes sont déclenchés de la même manière que les événements de prix sont déclenchés par une nouvelle information, tandis que le mécanisme endogène "d'excitation" ressemble à la manière dont le marché apprend et ajuste l'écart de prix dû aux frictions naturelles de la fréquence de transaction par transaction.

Outre la modélisation de l'arrivée d'événements de prix, notre objectif est de disposer de modèles robustes dans toutes les dimensions des actifs, un aspect devenu de plus en plus important dans la mesure du risque. D'une part, l'univers des actifs disponibles pour le trading n'a cessé de s'étendre et, à des fins de diversification, les traders et les investis-

seurs ont désormais de plus en plus d'actifs dans leur portefeuille. Pour détenir ou vendre un actif, il faut prendre en compte non seulement les risques de l'actif lui-même, mais aussi la corrélation avec les risques d'autres actifs. Par conséquent, il n'est pas possible de refléter fidèlement la réalité en supposant que la dynamique des prix de deux actifs apparentés est indépendante, et une modélisation raisonnable de la dynamique doit tenir compte de l'interaction entre eux, en particulier lorsque le trading croisé (également connu dénommé "pricing" croisé ou apprentissage croisé) fait partie intégrante de la microstructure du marché (voir Harford and Kaul, 2005; Hasbrouck, 2001; Pasquariello and Vega, 2013; Tookes, 2008). D'autre part, la relation entre les actifs ne peut pas rester constante, mais change au fil du temps, d'où la nécessité de l'examiner en détail. Le reflet de cette relation est une exigence essentielle, car elle permet non seulement une meilleure mesure du risque, plus informée pour un actif univarié, mais aussi une évaluation correcte des risques de manière combinée pour un portefeuille intra-journalier.

Dans cette thèse, nous tentons de donner des éléments qui contribuent à l'approche mentionnée ci-dessus. Chaque chapitre de cette thèse contribue à cette tâche, la motivation de chacun d'entre eux est présentée ci-dessous.

Dans le chapitre 3, nous sommes motivés par des études antérieures sur l'asymétrie de l'information (Amihud and Mendelson, 1987; Glosten and Milgrom, 1985; Kyle, 1985) et l'apprentissage imparfait (voir en particulier Hasbrouck, 1996 pour une revue des modèles univariés et Buccheri, Corsi and Peluso, 2020 pour le tout premier modèle multivarié) dans un marché à comportement rationnel. Alors que l'asymétrie de l'information génère une certaine hétérogénéité dans la croyance des participants au marché quant à la véritable valeur sous-jacente et déclenche des erreurs de prix, l'apprentissage imparfait conduit à une récupération partielle de l'information résiduelle. En raison de ces deux sources de friction sur le marché, les processus de fixation des prix n'intègrent pas les informations pertinentes immédiatement, mais progressivement sur un intervalle de temps effectif, en contradiction avec les modèles mathématiques classiques de dynamique des prix qui suggèrent un monde parfait et des marchés financiers sans arbitrage. Nous abordons ces restrictions en relaxant l'hypothèse plutôt stricte présente dans toutes les approches précédentes selon laquelle l'information n'est présente qu'au moment de la réalisation. Au contraire, nous introduisons le concept "information résiduelle", en considérant que l'information a une durée de vie et se désintègre au fil du temps. Nous utilisons un proxy statistique précis pour cette information résiduelle décroissante, dérivé de la fonction décroissante d'un processus de Hawkes multivarié utilisé pour représenter de manière disjointe le processus multivarié de changement de prix intra-journalier. Les processus de Hawkes multivariés de changement de prix disjoints permettent de calculer l'estimation de l'ajustement des prix sur chaque actif à chaque instant. Cette propriété atténue la complication qui résulte de l'asynchronisme et de l'irrégularité du temps. La durée de vie de l'information permet également l'existence temporelle de corrélations croisées, appelée effet "avance-retard", qui, en bref, est un phénomène fondamental de la microstructure du marché dans lequel certains actifs ont tendance à suivre les mouvements d'autres actifs avec un certain retard. Ces effets de décalage fournissent une explication alternative pour la tendance vers

zéro de la corrélation croisée entre actifs, illustrée par les effets Epps lorsque la fréquence d'échantillonnage se réduit à la fréquence de transaction. En résumé, ce chapitre apporte une réponse aux questions suivantes: **existe-t-il un mécanisme multivarié de formation des prix à la fréquence des transactions?** Et si tel est le cas, **comment les corrélations croisées entre actifs liés apparaissent-elles naturellement à cette fréquence, en tant que résultat de la nature fondamentalement multivariée du processus de formation des prix ?**

Dans le chapitre 4, nous portons notre attention sur la structure des moments de second ordre du rendement des actifs. En partant du principe que la dynamique multi-actifs de formation des prix décrite au chapitre 3 permet de capturer les dépendances temporelles entre actifs liés, nous sommes motivés par le développement d'un cadre général qui fournit efficacement une inférence intra-journalière sur la covariance intégrée. Nous nous inspirons de la façon dont l'approche basée sur les processus ponctuels, c'est-à-dire l'estimateur de volatilité basé sur la durée des prix (Andersen, Dobrev and Schaumburg, 2009; Engle and Russell, 1998; Gerhard and Hautsch, 2002; Hong et al., 2021; Li, Nolte and Nolte-Lechner, 2015; Tse and Yang, 2012), peut fournir une mesure instantanée de la volatilité univariée grâce à sa structure paramétrique. Ce type d'estimateur de volatilité enregistre de très bonnes performances par rapport à d'autres estimateurs volatilité réalisée bien établis, et est simple à mettre en œuvre. Cependant, son application est limitée à l'estimation de la volatilité univariée car le caractère discret de la modélisation de la durée des prix ne permet qu'un cheminement fixe de l'intensité conditionnelle, incapable de mettre à jour de manière continue les dépendances entre actifs liés et empêchant les modèles de volatilité de la durée des prix de capturer la co-volatilité dans un contexte de trading asynchrone. Au lieu de modéliser la durée des prix, nous proposons de modéliser explicitement l'intensité conditionnelle du mouvement des prix en utilisant le processus multivarié de Hawkes. Nous cherchons également à développer un estimateur qui surmonte les limites des estimateurs basés sur la covariation quadratique, c'est-à-dire la volatilité réalisée, appuyé sur un large échantillon de données pour assurer une estimation cohérente grâce à sa propriété de convergence, et qui fournit une estimation efficace pour un intervalle de temps très court à niveau intra-journalier. Notre généralisation multivariée, l'estimateur de volatilité basé sur l'intensité, fusionne les approches par covariation quadratique et par processus ponctuel. Elle fournit un cadre général qui non seulement préserve les caractéristiques supérieures de l'estimateur de volatilité basé sur la durée du prix en fournissant une inférence intra-journalière sur la variation locale, mais capture également efficacement une caractéristique supplémentaire de la structure de second moment dans l'analyse de portefeuille : la corrélation croisée locale entre actifs. Ce chapitre donne une réponse aux questions suivantes : **un estimateur qui tient compte des effets d'avance-retard fournit-il une estimation plus efficace de la volatilité ? Et est-il possible de capturer une véritable structure de second moment locale à partir de l'observation de processus de prix très "bruyants", transaction par transaction ?**

Le chapitre 5 cherche un autre développement dans la mesure du risque à haute fréquence, basé sur la dynamique de la formation des prix multi-actifs décrite dans le

chapitre 3, et aborde la question de la définition de mesures de risque pratiques pour les traders ou les praticiens qui opèrent leurs activités sur une base intrajournalière. Sur les marchés financiers à haute fréquence, les échanges se caractérisent par leur extrême rapidité et la durée de vie des informations est très courte, puisqu'elle est de quelques secondes, voire de quelques millisecondes (Goldstein, Kumar and Graves, 2014; Hasbrouck and Saar, 2013; Menkveld, 2018; O'Hara, 2015). À de tels horizons, il devient irréalisable de refléter précisément l'ensemble de la distribution des rendements d'actifs. Une solution plus efficace et réalisable consiste à ne considérer que la queue de la distribution, qui caractérise la probabilité des événements extrêmes, plutôt que de prendre en compte inutilement l'ensemble de la distribution de tous les événements de prix. Nous sommes motivés par la littérature sur les mesures de Value-at-Risk intra-journalières (Dionne, Duchesne and Pacurar, 2009; Giot, 2005; Liu and Tse, 2015) qui capturent la queue de la distribution conditionnelle des rendements d'actifs en examinant les temps d'attente avant que des mouvements de prix extrêmes ne se produisent. Jusqu'à présent, la littérature adéquate s'est limitée au cas univarié. Les mesures IVaR univariées étaient à l'origine basées sur la modélisation de la dépendance sérielle de la durée des changements de prix dépassant un seuil. Nous nous écartons de cette modélisation discrète de la durée des prix et modélisons une interdépendance continue dans l'occurrence possible des événements de changement de prix par les intensités conditionnelles stochastiques du processus de Hawkes, ce qui constitue une approche de modélisation par processus ponctuels compatible avec un aspect multivarié. Notre généralisation multivariée est efficace sur des échelles de temps intra-journalières pour des actifs multiples, mais surtout elle prend en compte la structure de corrélation croisée de leurs rendements extrêmes. Elle répond aux questions suivantes : **existe-t-il un moyen efficace d'incorporer les corrélations temporelles de type avance-retard dans la prédiction des rendements extrêmes à haute fréquence ? De plus, la prise en compte de ces caractéristiques dans les mesures de risque permettrait-elle d'obtenir une mesure du risque meilleure ou plus informée ?**

III. VUE D'ENSEMBLE ET ETENDUE DES TRAVAUX

Il s'agit ici d'une thèse cumulative qui s'appuie sur une série de documents de travail. Tous les chapitres sont autonomes, et le plan détaillé de la thèse est le suivant :

Chapitre 2, **Revue de littérature sur la dynamique des prix à haute fréquence et les mesures de risque**, fournit une revue critique de la littérature existante pertinente pour le domaine de recherche de cette thèse. Nous discutons des principaux développements théoriques récents et des études empiriques entourant les thèmes de la dynamique des prix à haute fréquence, de l'estimateur de volatilité et de la « mesure de queue » du risque intra-journalier dans le contexte de la microstructure de marché. Nous mettons également en évidence la littérature qui a contribué aux principales questions relatives à ces trois sujets. Dans la dynamique des prix à haute fréquence, nous discutons de l'irrégularité du temps, de la nature discrète des prix, du trading asynchrone et des effets de décalage. Dans les deux sujets relatifs à la mesure du risque à haute fréquence, nous passons en revue les principales méthodes pour la volatilité réalisée, la volatilité basée sur la durée du prix, et la mesure de queue du risque. Tout au long de notre discussion, nous essayons d'établir

différences et similitudes et essayons également de souligner les points d'intérêt communs dans la littérature et les liens avec notre étude.

Chapitre 3, **Information asymétrique, durée de vie de l'information et effets de retard sur la dynamique de formation des prix à plusieurs variables**, se concentre sur les données de prix de transaction à haute fréquence de plusieurs actifs et cherche un modèle mathématique capable de capturer les complications intégrées aux marchés de trading à haute fréquence et les caractéristiques spéciales des données relevées. Plus précisément, nous étendons le modèle classique "martingale-plus-bruit" pour la dynamique de la formation des prix à haute fréquence afin d'intégrer les erreurs de prix des vraies valeurs sous-jacentes et un mécanisme d'ajustement retardé des prix. Les erreurs de prix sont déclenchées par une information asymétrique, inhérente à la microstructure du marché, et les ajustements de prix retardés sont dus à un apprentissage imparfait de l'information résiduelle. Nous identifions le "pricing" de l'information asymétrique et celui de l'information résiduelle comme des sources séparées du processus de formation des prix. Nous proposons un modèle d'agents multi-types dotés d'informations hétérogènes, et des actifs multiples avec différents degrés d'efficacité du marché et différentes vitesses d'ajustement des prix. La dynamique de formation des prix comporte trois composantes : le prix efficient latent, le prix de quotation ajusté et le prix contaminé observable. En raison des caractéristiques particulières des données transaction-par-transaction, à savoir un espacement temporel irrégulier, des transactions asynchrones et une structure de changement de prix sur grille discrète avec une limite maximale, le modèle ne peut pas être estimé directement par les approches économétriques traditionnelles. Pour tirer des conclusions sur le modèle, nous établissons une liaison entre la dynamique des prix développée et le processus de Hawkes en utilisant une représentation disjointe des changements de prix lors du processus de transaction. La représentation disjointe tire avantage de l'espace d'états discrets dénombrables du changement de prix, alors que les processus de Hawkes multivariés encodent la notation de la causalité entre les états de changement de prix. Les corrélations avance-retard peuvent ensuite être simplement récupérées en intégrant ces interdépendances entre les états discrets de changement de prix. La présence d'effets avance-retard au niveau des actifs peut être mesurée sur tout intervalle arbitraire. En séparant les sources motrices en liquidité d'une part et en contenu informationnel des transactions d'autre part, nous révélons l'impact de chaque composant sur la force des corrélations d'avance-retard entre actifs. Le modèle est testé sur une section transversale des actions du DJIA avec des estimations non-paramétriques et paramétriques pour soutenir nos postulats théoriques.

Chapitre 4, **Estimation de la matrice de covariance des rendements d'actifs multivariés avec une représentation par martingale de l'intensité de Hawkes**. Outre la formation du processus de prix à la fréquence la plus fine, la compréhension de la dynamique de la matrice de variance-covariance est également nécessaire pour les traders et les praticiens du trading à haute fréquence, car elle détermine l'exposition des actifs à une variété de facteurs de risque, ce qui ouvre des possibilités pour construire des mesures de risque efficaces et des portefeuilles optimaux. Le deuxième chapitre de cette thèse développe un

estimateur basé sur l'intensité de la matrice de variance-covariance intégrée avec des données tick-by-tick bruyantes et asynchrones. Nous établissons le lien entre la théorie de la covariation quadratique des rendements des actifs et celle de la structure des moments de second ordre des processus ponctuels. Plus précisément, l'estimateur est conçu pour avoir une structure générique d'autocovariance (croisée) temporelle, puis ces autocovariances (croisées) peuvent être formulées en termes de moments conditionnels de premier ordre et de second ordre des processus de comptage associés à des états de changement de prix disjoints. Nous prouvons que dans le cas particulier d'une fonction de décroissance fixe exponentielle, il existe une forme analytique de ces moments dérivant d'une structure de martingale de l'intensité conditionnelle de Hawkes. Ainsi, nous pouvons obtenir une spécification entièrement paramétrique de l'estimateur de covariance intégrée basé sur l'intensité, exprimée en termes de paramètres estimés du processus de Hawkes multivarié de changements de prix disjoints. La correspondance entre la covariation quadratique des rendements des actifs et les processus ponctuels de changements de prix disjoints est placée sous une hypothèse de semi-martingale contaminée par le bruit pour le prix de transaction observable. En supposant raisonnablement que les bruits de microstructure ne sont mis à jour qu'au moment de la transaction et indépendamment des prix efficients, nous proposons un moyen efficace, également basé sur les intensités des processus ponctuels disjoints, d'estimer directement le biais encouru par les bruits, ce qui complète la robustesse de notre estimateur de variance-covariance intégré basé sur l'intensité

La performance de l'estimateur est évaluée à l'aide d'une étude de simulation. Nous découvrons l'impact sur l'estimateur des caractéristiques de microstructure telles que l'activité de trading, la non-synchronicité des transactions et le bruit de microstructure. Plus important encore, nous démontrons la performance relative en échantillon fini de notre estimateur basé sur l'intensité par rapport aux autres estimateurs de référence de la littérature.

Chapitre 5, **Processus ponctuels disjoints de Hawkes sur l'extension multivariée de Value-at-Risk intra-journalière**. Un autre volet de la mesure du risque à haute fréquence que nous trouvons utile pour appliquer notre dynamique de formation des prix multi-actifs est la modélisation directe de la queue de la distribution des rendements d'actifs. Parmi les mesures "de queue" du risque, la plus simple mais largement applicable et universelle étant la Value-at-Risk intra-journalière (IVaR). Nous constatons que la littérature existante manque encore d'un cadre multivarié de la mesure IvaR, aussi nous proposons un modèle qui peut combler l'absence d'un modèle de Value-at-Risk (IVaR) intra-journalier pour de multiples actifs. Notre généralisation multivariée est basée sur la modélisation de la probabilité des événements de changement de prix, et sur la prévision des trajectoires futures des rendements par simulation de type Monte Carlo. Pour étudier la queue de la distribution des rendements, nous nous concentrons sur la réalisation d'événements de mouvements de prix bidirectionnels, qui sont déclenchés si le changement de prix cumulatif à la hausse (à la baisse) est égal ou supérieur à un seuil. Nous modélisons la probabilité d'occurrence de ces événements par un modèle multivarié de Hawkes avec un noyau exponentiellement décroissant. Contrairement aux modèles à durée discrète, les in-

tensités conditionnelles de Hawkes multivariées mettent à jour leur set d'informations de manière continue, ce qui permet de prendre en compte les effets temporels propres et les effets croisés induits par tout nouvel événement arrivant dans la dynamique des prix.

Pour faciliter les prévisions d'événements futurs, nous développons également un algorithme de détection d'arrivée basé sur un compensateur conditionnel autorégressif, qui estime les intensités conditionnelles cumulatives attendues lors d'un nouvel événement de changement de prix. Nous évaluons la mesure multivariée dans la prévision de l'IVaR à l'aide de trois backtests bien connus sur les réalisations de violations : le test de couverture inconditionnelle de Kupiec (1995), le test de séquence de "hits" corrélés d'Engle and Manganelli (2004), et le test de violation aléatoire de Candelon et al. (2010). Nous appliquons l'estimateur IVaR à une sélection de deux paires d'actions à forte et à faible activité de trading cotées dans l'indice Dow Jones Industrial Average et nous étudions l'impact du choix du seuil de changement de prix et de l'intervalle de prévision sur la performance de l'estimateur.

Chapitre 6 conclut cette thèse. Tout d'abord, nous résumons la contribution principale comprenant : une extension du modèle standard univarié d'ajustement retardé des prix dans un cadre multi-actifs, qui fournit une dynamique de formation des prix tenant compte de manière plus complète des caractéristiques spéciales de la microstructure de marché à la fréquence transaction-par-transaction ; un estimateur efficace de la matrice de variance-covariance réalisée qui résiste aux effets d'avance-retard, au bruit de microstructure et à l'asynchronisme des transactions ; et enfin une généralisation multivariée de la Value-at-Risk intra-journalière. Nous soulignons ensuite certaines implications importantes de ces développements pour les chercheurs universitaires et les praticiens des marchés de trading à haute fréquence. Enfin, nous soulignons les aspects intéressants que nous n'avons pas entièrement couverts dans cette thèse et nous fournissons une discussion approfondie des sujets et domaines potentiels, en ce qui concerne la modélisation multivariée de la dynamique des prix, les estimateurs de volatilité réalisée et la Value-at-Risk intra-journalière, qui pourraient être intéressants pour de futures activités de recherche.

ABSTRACT

The thesis focuses on modern electronic markets and develops tailor-made mathematical models of high-frequency trading. When focusing on the finest frequency trading, such as transaction-by-transaction, intraday price formation and trading exhibit fundamentally different properties compared to lower trading frequencies. Several “market frictions” appear to be the norm, rather than the exception, and this poses a great challenge to the efficient market hypothesis. Consequently, long-established mathematical models, that are applied to lower-frequency price dynamics, are no longer adequate in the context of high-frequency trading and fail to explain the complex environment generated by the frictions of market microstructure.

A primary challenge of doing so is the statistical properties of the recorded trading data, including irregular spacing time, discrete grid-like price, and asynchronous trading. The traditional properties, the discreteness of time, the continuity of price, and the aligned observation of cross-sectional information do not hold, and, thus, several well-established models cannot be applied unconditionally. The preferred approach in the literature is some kind of “pseudo-aggregation” algorithm at lower frequency, but given that some kinds of high-frequency trading phenomena, like low-latency arbitrage, occur in fractions of a second, this data thinning inevitably results in information loss.

Modelling Multivariate Price Dynamics in Continuous Time

Asymmetric Information, Information Life Span, and Lead-Lag Effects on a Multivariate Price Formation Dynamics

To address this shortcoming, in the first part of this thesis, we develop a generalized price formation dynamic based on a view that information and time are inherently linked, considering that information has a lifespan and decays over time. More precisely, we extend the classic “martingale-plus-noise model” and allow for a more structured treatment of high-frequency dynamics that capture the sources of asymmetric information, information life span, and temporally lagged price adjustment. To draw econometric inferences from the model, we use a precise statistical proxy for the decay of information derived from the decaying functions of a multivariate Hawkes process, which is used to represent, in a disjointed manner, grid-like price change processes. This is the main contribution of this work and enables estimations of lagged price (cross-)adjustment on multiple assets to be computed at every point in time, without necessarily observing the arrival of an event. This property alleviates the issue of asynchronicity and time discretization and enables the estimation of cross-correlation instantaneously and at any time scale. An empirical application on DJIA stocks supports these theoretical postulations.

Modelling Multivariate Market Risk in Continuous Time

Alongside modelling market dynamics, managing risks (market risk) is undoubtedly one of the most important activities of the practitioner on the financial market. The second

and third parts of the thesis thus contribute to high-frequency risk measurement, developed on the ground of high-frequency trading price dynamics in the first part.

Intensity-Based Variance-Covariance Matrix

In particular, the second part of the thesis introduces a novel estimator of second-order moment structure of asset returns, combining two well-established approaches on high-frequency volatility measures, that is, quadratic covariation and point process-based approaches. On the one hand, with its parsimonious parametric structure based on conditional intensity, which is the core of point process approach, our model preserves superior features of univariate point process-based volatility estimators in addressing salient properties of ultra-high-frequency data. On the other hand, the model is defined within a generic temporal cross-(auto)covariation structure of the quadratic covariation approach, decomposing the cross-(auto)correlation between assets into contemporaneous and correlation, facilitating the estimation of the second-order moment structure in the context of high-frequency trading with irregular and non-synchronous transaction times. To some extent, our novel intensity-based variance-covariance matrix estimator is not affected by spurious correlations and Epps effects, in contrast to quadratic covariation estimators, and accounts for simultaneous lead-lag effects and endogenous times in asynchronous trading. In addition, with a parametric structure, the estimator has the ability to provide inference on local volatility over relatively short intraday intervals, overcoming the limitations of convergence property ensuring consistently realized volatility measures in such periods. We test the robustness of the estimator with extensive Monte Carlo simulations.

Intensity-Based Multivariate Intraday Value-at-Risk

Finally, the third part of the thesis contributes to another strand of high-frequency risk measurement, focusing on direct modelling of the tail distribution of asset returns. We propose a multivariate intraday Value-at-Risk (IVaR) that generalizes previous univariate IVaR and takes into account the cross-correlation structure of asset extreme returns. Our multivariate generalization is based on modelling the occurrence of bidirectional price change events by stochastic conditional intensities and forecasting arrivals of future transactions by Monte Carlo simulation. The estimator overcomes the limitations of previous IVaR based on point process approaches and offers an efficient market risk measure that accommodates the clustering of the arrival of extremes both in time and cross-sectionally. More specifically, the new intraday market risk measure captures not only the risk from contemporaneous correlation, but also from another type of correlation characterized by high-frequency data, that is, the temporal lead-lag correlation. While the former can be attributable to fundamental asset values, the latter arises as a consequence of the presence of asynchronous trading, asymmetric information, strategic trading, and price learning in the market microstructure. Therefore, our multivariate IVaR model, by successfully incorporating these features into its risk metrics, would give a better/more informed measure of IVaR in one asset and in a combined way for an intraday portfolio.

CONTENTS

Declaration of Authorship	iii
Acknowledgments	v
Résumé	vii
Abstract	xvii
List of Figures	xxii
List of Tables	xxiii
Abbreviations	xxv
1 INTRODUCTION	1
1.1 Research Context	1
1.1.1 From low-frequency to high-frequency trading	1
1.1.2 The failure of classical models at the microscopic level of market structure	2
1.1.3 The challenging features of high-frequency trading data	3
1.2 Motivation and Approaches	4
1.3 Overview and Scope of work	8
2 LITERATURE REVIEW ON HIGH FREQUENCY PRICE DYNAMICS AND RISK MEASURES	11
2.1 Transaction price dynamics and market microstructure	11
2.1.1 Models for the timing of trades	12
2.1.2 Models for the discreteness of prices	17
2.1.3 Models for the non-synchronicity and the lead-lag effects	20
2.2 High Frequency Data and Market Risk measure	23
2.2.1 Realized volatility	24
2.2.2 Instantaneous volatility	28
2.2.3 Intraday Value-at-Risk measures	30
3 ASYMMETRIC INFORMATION, INFORMATION LIFE SPAN, AND LEAD-LAG EFFECTS ON A MULTIVARIATE PRICE FORMATION DYNAMICS	33
3.1 Introduction	34
3.2 Theoretical framework	37
3.2.1 The multi-asset asymmetric lagged adjustment model	37
3.2.2 Lead-lag effects	43

3.2.3	Generalization of previous multi-asset lagged adjustment model	46
3.3	An equivalent Hawkes point process representation and estimation	47
3.3.1	Hawkes processes representation of disjoint observed price change dynamics	48
3.3.2	Parameterization and estimation of Hawkes processes	53
3.4	Empirical findings: the interdependence of price changes	54
3.4.1	Data description	54
3.4.2	Disjoint price change transaction point processes	55
3.4.3	Statistical interdependence between price change levels	58
3.5	Model Calibration	63
3.5.1	Non-parametric estimation	63
3.5.2	Parametric estimation	73
3.6	Conclusion	80
4	MULTIVARIATE COVARIANCE VARIANCE MATRIX ESTIMATION WITH MAR- TINGALE REPRESENTATION OF HAWKES INTENSITY	83
4.1	Introduction	84
4.2	Quadratic Covariation and Integrated Covariance	86
4.3	Quadratic covariation and Intensity Based Covariance Estimator	89
4.3.1	Conditional Estimator of Quadratic Covariation	89
4.3.2	Intensity Based Estimator	92
4.4	Martingale Representation and Conditional Covariance of Point Processes . .	96
4.4.1	Multivariate Hawkes Point Processes	96
4.4.2	Martingale Representation of Hawkes Intensities	97
4.4.3	Conditional Covariance of Point Processes	98
4.4.4	Towards a fully parametric closed-form conditional covariance of point processes	100
4.5	Simulation Study	102
4.5.1	Simulation Design	102
4.5.2	Estimator and Tuning Parameters	104
4.5.3	Simulation results	105
4.6	Conclusion	110
5	DISJOINT HAWKES POINT PROCESSES ON MULTIVARIATE EXTENSION OF IN- TRADAY VALUE-AT-RISK	113
5.1	Introduction	114
5.2	Review existing Intraday Value-at-Risk models	117
5.2.1	The Giot model	118
5.2.2	The Dionne-Duchesne-Pacurar model	119
5.2.3	The Liu-Tse model	120
5.2.4	Limitations of existing univariate IVaR models for a multivariate ex- tension	121
5.3	Multivariate intensity-based Intraday Value-at-Risk model	121

5.3.1	Disjointing Hawkes point processes of price dynamics	122
5.3.2	The compensator of counting function.	123
5.3.3	The autoregressive conditional compensator - ACC model.	124
5.3.4	Evaluation of IVaR by Monte Carlo simulation	125
5.4	Back-testing IVaR	126
5.4.1	Unconditional coverage test	126
5.4.2	Dynamic quantile test	127
5.4.3	Duration-based GMM	127
5.5	Empirical application	128
5.5.1	Data description	128
5.5.2	Empirical results	129
5.6	Conclusion	144
6	CONCLUSIONS	147
6.1	Summary and Main Findings	147
6.2	Implications	150
6.3	Limitations and Future Researches	151
6.4	Final Remarks	153
	APPENDICES	155
A	APPENDIX	155
A.1	Hawkes process models	155
A.1.1	Point Process	155
A.1.2	Hawkes Point Processes	156
A.2	The disjoint representation and marked Hawkes point processes	157
A.3	Parameter estimation and goodness-of-fit test	160
A.4	Additional Tables and Figures	161
	BIBLIOGRAPHY	161

LIST OF FIGURES

Figure 3.1	An illustration about the shape of lagged adjustment kernels Ψ . . .	40
Figure 3.2	Transaction point processes marked by price changes of six selected DJIA stocks	56
Figure 3.3	Average excitement kernel norms $\int_0^\infty \Phi(t)dt$ amongst observed discrete price change states of pairwise stocks.	64
Figure 3.3	Average excitement kernel norm $\int_0^\infty \Phi(t)dt$ amongst observed discrete price change states of pairwise stocks (<i>cont.</i>)	65
Figure 3.3	Average excitement kernel norm $\int_0^\infty \Phi(t)dt$ amongst observed discrete price change states of pairwise stocks (<i>cont.</i>)	66
Figure 3.4	Average cross-adjustment of all the pairs formed by six selected stocks (non-parametric estimation).	68
Figure 3.5	Average self-adjustment of all six selected stocks in different pairwise relations (non-parametric estimation).	69
Figure 3.6	Self-adjustment of all six selected stocks in different pair-wise relations over all trading days in the sample (non-parametric estimation).	72
Figure 3.7	Estimated η normalized per second of each asset in different pairwise relation over all trading day.	74
Figure 3.8	Average cross-adjustment of all the pairs formed by six selected stocks (parametric estimation)	76
Figure 3.9	Average self-adjustment of all six selected stocks in different pairwise relations (parametric estimation).	77
Figure 3.10	The lead-lag correlation within one second for different pairwise assets over all trading days (parametric estimation).	79
Figure 5.1	Price change duration processes over a trading week	131
Figure 5.2	5-min IVaR out-of-sample forecasts with 2, 3, and 4 ticks thresholds	133
Figure 5.3	15-min IVaR out-of-sample forecasts with 2, 3, and 4 ticks thresholds	134
Figure 5.4	30-min IVaR out-of-sample forecasts with 2, 3, and 4 ticks thresholds	135
Figure 5.5	60-min IVaR out-of-sample forecasts with 2, 3, and 4 ticks thresholds	136

LIST OF TABLES

Table 3.1	Descriptive statistics for six selected stocks listed on DJIA index . . .	55
Table 3.2	Empirical results of pair-wise interdependence for six selected DJIA stocks.	59
Table 3.3	Empirical results of pair-wise interdependence for six selected DJIA stocks (<i>continued</i>).	60
Table 3.4	Empirical results of pair-wise interdependence for six selected DJIA stocks (<i>continued</i>).	61
Table 3.5	The average daily estimate of the lead-lag correlation within one second for different pairwise assets (non-parametric estimation). . .	71
Table 3.6	Statistical testing for the random walk of exogenous information. . .	75
Table 3.7	Average daily parametric estimation of lead-lag correlations within one second for different pairwise assets (parametric estimation). . .	78
Table 3.8	The means and standard deviations of the estimated decay parameters β^d for the asset d	80
Table 4.1	Parameters values for simulating the efficient price vectors.	103
Table 4.2	Simulation results for integrated volatility estimators.	106
Table 4.3	Simulation results for integrated volatility estimators.	107
Table 4.4	Simulation results for integrated covariance/correlation estimators. .	109
Table 5.1	Descriptive statistics for four selected stocks listed on the DJIA index.	128
Table 5.2	Descriptive statistics for OUB and OLB point processes	130
Table 5.3	Probability of observing IVaR failures for two selected pairs of stocks	132
Table 5.4	5-min IVaR backtesting results for two selected pairs of stocks	138
Table 5.5	15-min IVaR backtesting results for two selected pairs of stocks . . .	138
Table 5.6	30-min IVaR backtesting results for two selected pairs of stocks . . .	139
Table 5.7	60-min IVaR backtesting results for two selected pairs of stocks . . .	139
Table 5.8	5-min IVaR backtesting results for two selected pairs of stocks . . .	140
Table 5.9	15-min IVaR backtesting results for two selected pairs of stocks . . .	141
Table 5.10	30-min IVaR backtesting results for two selected pairs of stocks . . .	143
Table 5.11	60-min IVaR backtesting results for two selected pairs of stocks . . .	144
Table A.1	Empirical results of pair-wise interdependence for selected DJIA stocks (<i>continued</i>)	161
Table A.2	Empirical results of pair-wise interdependence for selected DJIA stocks (<i>continued</i>)	162
Table A.3	Empirical results of pair-wise interdependence for selected DJIA stocks (<i>continued</i>)	163
Table A.4	Empirical results of pair-wise interdependence for selected DJIA stocks (<i>continued</i>)	164

Table A.5 Empirical results of pair-wise interdependence for selected DJIA
stocks (*continued*) 165

ABBREVIATIONS

AACD	Two-state Asymmetric Autoregressive Conditional Duration Model
ACC	Autoregressive Conditional Compensator Model
ACD	Autoregressive Conditional Duration Model
ACI	Autoregressive Conditional Intensity Model
ACM	Autoregressive Conditional Multinomial Model
BSM	Black-Scholes-Merton Model
CAPM	Capital Asset Pricing Model
EMH	Efficient Market Hypothesis
GMM	Generalized Method of Moments
Hawkes-POT	Hawkes-Peak Over Threshold Model
INAR	Integer-valued Autoregressive Time Series
IIVaR	Intensity-based Intraday Value-at-Risk
IRC	Intensity-based Realized Covariance
IVaR	Intraday Value-at-Risk
MALA	Multi-asset Asymmetric Information Lagged Adjustment Prices Model
MLA	Multi-asset Lagged Adjustment Prices Model
NYSE	The New York Stock Exchange
OLB	Over-Lower Bound Price Change Point Process
OUB	Over-Upper Bound Price Change Point Process
PDV	Price Duration-based Volatility
SCI	Stochastic Conditional Intensity Model
RC	Realized Covariance
RK	Realized Kernel
VAR	Vector of Autoregressive Processes
VaR	Value-at-Risk

INTRODUCTION

1.1 RESEARCH CONTEXT

1.1.1 *From low-frequency to high-frequency trading*

In the early days of the 1970s, Fisher Black envisaged the future of a stock exchange:

A stock exchange can be embodied in a network of computers, and the costs of trading can be sharply reduced, without introducing any additional instability in stock prices, and without being unfair either to small investors or to large investors. (Black 1971b, p. 87)

Back in his days, trading floors with trading desks were crowded by people, rushing to execute hand-carried orders to intermediate for a vast majority of transactions in the financial market. Today, the world of trade that Fisher had in mind is very close. The old-fashioned trading floors of most major stock exchanges have been largely replaced by automated electronic trading machines. The modern facility is no longer a place, but an alternative computer system over which transactions are entered, routed, executed, and cleared electronically with little or no human intervention.

A new type of trader, the high-frequency algorithmic trader, has emerged and became the main participant in the market, accounting for much more than half of the total trading volume ¹. These traders harness their technical advantages, encode their strategy into computer algorithms, and beat the market by being extremely fast. Their trades are typically characterized with odd lots, that is, trades for less than 100 shares of stock (O'Hara, Yao and Ye, 2014), and with very short-lived positions, that is, the trade lifespan can be measured in microseconds or even on the order of nanoseconds (Hasbrouck, 2019; Menkveld, 2016, 2018). While much has been made of high-frequency traders, the behaviour of traditional, non high-frequency traders is also radically different, as is the market in which their trading occurs (O'Hara, 2015). The technological advancements behind high-frequency trading pervade the marketplace, with algorithmic trading as the mechanism for virtually all trading. Services previously provided by brokers, dealers, and specialists are now largely executed by a sub-human-attention speed of computer algorithms. Not only high-frequency traders, but also non high-frequency traders, or even everybody else in the

¹ Aitken, Cumming and Zhan (2015) document that high-frequency traders are responsible for between 50% and 70% of all trades in financial markets or even up to 75% on some occasions. O'Hara (2015) and O'Hara, Yao and Ye (2014) indicate that 50% or more of the total volume of financial transactions can be attributed to this group of traders

market, are now relying on increasingly sophisticated trading algorithms to optimize their transactions.

Therefore, financial markets have been transformed from traditional “human, low-frequency” to modern “electronic, high-frequency” markets. This transformation leads to fundamental changes, from the way traders trade to the way markets are structured. With markets and trading being radically different, the classical models used in the past are no longer adequate, and the traditionally employed methodologies are also no longer applicable. Therefore, the modelling of price dynamics and risk measures must also evolve to reflect the new realities of the high-frequency world.

1.1.2 *The failure of classical models at the microscopic level of market structure*

Before the realm of high-frequency trading, classical mathematical finance models, such as the Efficient Market Hypothesis (EMH), the Capital Asset Pricing model (CAPM), and the Black-Scholes-Merton framework (BSM), play a central role in describing asset price formation dynamics in financial markets. These long-established models were built on perfect-world settings where information related to the true asset values is immediately disseminated and is equally interpreted among market participants. Financial markets are all-powerful computational engines capable of aggregating and processing all the beliefs and demands of all market participants, and immediately reflecting in price processes the full set of information currently available. The fundamental mechanism of traditional financial markets, indeed, supports this notion in the context that market observations are simply closing prices of lower frequencies, such as daily, weekly, monthly, or annually (Fama, 1998).

However, the modern high-frequency world operates differently. In this world, market participants always have some kinds of heterogeneity with respect to their endowment of information. Price formation dynamics is the game of a multitude of interconnected agents, each trading is heterogeneously characterized by imperfect and partial information of the agents, confined by specific institutional and regulatory constraints (see, e.g. Admati and Pfleiderer, 1988; Easley and O’hara, 1992; Kyle, 1985). The movements of the game are observed and recorded with the highest frequency ever, where each event represents the action of the agents at the transaction. At this frequency, various “market frictions” arise, including asymmetric information, strategic trading, and price learning, as natural phenomena (Glosten and Milgrom, 1985; Holden and Subrahmanyam, 1992; Kyle, 1985; Vives, 1995), in contradiction to the perfect world implied by the classical models. In other words, in the context of high-frequency trading, the traditional price formation dynamics is simply inadequate and fails to explain the complex environment generated by the frictions of this modern market microstructure.

The modern market is different and so are recorded high-frequency trading data. It is inherently characterized by several special features such as irregular spacing time, discrete grid-like price, and asynchronous trading and the traditional properties of low-frequency data, such as the discreteness of time, the continuity of price, and the aligned observation

of cross-sectional information do not hold, and, thus, several well-established models cannot be applied unconditionally. The preferred approach in the literature is some kind of “pseudo-aggregation” algorithm at a lower frequency, but given that some kind of high-frequency trading phenomena, like low-latency arbitrage, occurs in fractions of a second, this data thinning inevitably results in information loss.

Therefore, the classical models are lagging behind the development of the financial market and are no longer applicable to high-frequency trading. One of the fundamental questions is, if the classical models are not valid, then how are the prices formulated in terms of information revelation over time? The answer to this question is to develop a new price formation dynamic that is tailor-made to accommodate the special features of the market microstructure and efficiently capture the information-revelation process embedded in the transaction-by-transaction frequency data.

1.1.3 *The challenging features of high-frequency trading data*

In a rational expectations market, the trading behaviours of market participants are heterogeneously characterized by their endowment of information and reflect on their corresponding executed trading process. The information revelation is then successively embedded in the special features of recorded high-frequency transaction data: irregularly spacing transaction time, discrete observable price, and non-asynchronous trading. Thus, the tailor-made model of price formation dynamics in high-frequency trading necessarily accounts for these features.

First, high-frequency trading data are inherently characterized by irregular trading intervals. The time elapsed between observations is not of fixed duration, and the discreteness of timing, which is essential in traditional econometrics, no longer holds unconditionally. However, the timestamps of the trading events are not random and mutually independent. Instead, the trading events are chronologically ordered by a matching engine, and are time-stamped by a single clock (Aquilina, Budish and O’Neill, 2021). More importantly, the timing of trades can potentially be informative about the price process. The trading duration is well recognized as a consistent proxy of liquidity, as it carries significant information about the state of the market (see, e.g. Dufour and Engle, 2000; Easley and O’hara, 1992; Glosten and Milgrom, 1985; Gouriéroux, Jasiak and Le Fol, 1999; O’Hara, 2015). Dufour and Engle (2000) documents strong evidence of the effect of trade duration on price adjustment based on historical trades, while Engle (2000) and Engle and Russell (1994) finds significant co-movement between trading intensity (the inverse of trade duration) and price volatility. Therefore, the role of trading times cannot be ignored in the price formation process and treated as an independent series as in the classical framework on lower frequency data.

However, explicitly modelling the time process is not an easy task, as it requires modelling not only the behaviour of traders and, in particular, how much of the information known by insiders has been made public (Glosten and Milgrom, 1985), but also any friction and imperfection that may be present in the trading mechanism (Easley and O’hara,

1992). Most traditional econometric models constructed on a calendar-time framework are not capable of doing this. Traditional approaches convert “event time” to calendar time, aggregating all this meaningful information and its respective impact on price discovery to a single time point, thus neglecting the economic significance of each event.

Second, when modelling comes to analyze multivariate data sets, the time discretization of recorded transaction-by-transaction data turns out to be even more complicated. Trading activities of different instruments are observed at different time points, raising a barrier in observing the same information cross-sectionally at the same time. This is the root of the Epps effect, that is, the bias toward zero of cross-correlation observed when shrinking the sampling frequency to zero (see, e.g. Epps, 1979; Hayashi and Yoshida, 2005).

Finally, the observable transaction price is not continuous, as the classical assumptions of traditional price dynamic models, and the price movements must fall onto the grid due to the rule of a minimum unit of price measurement. The discrete minimum tick size is a necessary feature of a modern automated market to prevent an explosion of message under the current market design and to artificially constrain the liquidity cost of the market (see, in particular, Chao, Yao and Ye, 2017, 2018; Li, Wang and Ye, 2021; Yao and Ye, 2018, among others). Furthermore, because the institution implements some rules restricting the maximum amount that the price can move from one event to another, observable price movements often take only a handful of values (Darolles, Gouriéroux and Fol, 2000; Engle and Manganelli, 2004). Thus, at the transaction-by-transaction frequency, the price discreteness with limited maximal becomes another dominant feature of the data.

As price changes are quoted as multipliers of a smallest divisor, the use of traditional continuous distributions to characterize the price process is far from being appropriate. At the transaction-by-transaction level, the price changes also have a nontrivial probability mass only at zero and close-to-zero levels. The conventional formulation relying on continuous probability distributions with non-bounded support cannot accommodate these features of high-frequency transaction prices.

1.2 MOTIVATION AND APPROACHES

This thesis was originally motivated by the desire to provide an original approach to various phenomena that have emerged from high-frequency trading markets and to provide models of price dynamics and risk measures that closely mirror the realities of the market microstructure. Considering a multivariate, cross-sectional price formation that incorporates well-embedded features of high-frequency trading data, the thesis also aims to address shortcomings of previously mentioned traditional modelling.

We review previous literature and we recognize that irregular times and asynchronous trading are major challenges that introduce bias or results in loss of information in intraday estimates. We address exactly these issues, considering that at a microscopic level, the time of trading (business times or event times) appears to be inextricably bounded to the evolution of prices and other microstructure phenomena. In other words, the arrival times of price events play a key role for modelling the price formation at the microscopic

level of high-frequency trading data. When the level of interest is at the finest frequency of transaction-by-transaction, the microstructure of the market has a significant impact on how and, more importantly, on when information is incorporated into prices. The intensity of event arrival, the inverse of waiting times, is where two fundamental forces of market dynamics, information and liquidity, meet and constitute the synthetic material for the formation of prices (O'Hara, 1998). The idea is that time plays a role in measuring information resolution, and more precisely, in measuring the speed at which the information hits the market and is gradually incorporated into the price process. Consequently, a reasonable econometric model can be constructed in the way of accounting for the arrival of price events, both in time and price dimensions, and give the probability at every instant of time, the so-called conditional intensity, of when a price movement conditioning occurs on the historical realizations.

We are inspired by point processes theory, in particular, the Hawkes point process, in the way of directly modelling the conditional intensity of event-arrival conditioning on historical information of past event occurrences. The Hawkes process features in a natural way a data-generating system based on conditional intensity, accounting for the co-existence and the interplay between the exogenous and endogenous arrivals of new events inside the system. The exogenous events of the Hawkes process are triggered in a similar way that price events are triggered by a new release of information, whereas the endogenous mechanism "excitation" resembles the manner in which the market learns and adjusts the deviation of price due to the natural frictions of the transaction-by-transaction frequency.

In addition to modelling the arrival of price events, our target is to have models that are robust across asset dimensions, which has become increasingly important in risk measurement. On the one hand, the universe of available trading assets has been continuously expanding, and, for diversification purposes, traders and investors have more and more assets in their portfolio. Holding or selling one asset is required to take into account not only the risks of the asset itself but also the correlation with the risks of other assets. As a result, it is not a true reflection of reality to assume that the price dynamics of two related assets are independent and reasonable dynamic modelling needs to take into account the interaction between them, especially when cross-asset trading (also known as cross-asset pricing and cross-asset learning) is an inherent part of the market microstructure (see Harford and Kaul, 2005; Hasbrouck, 2001; Pasquariello and Vega, 2013; Tookes, 2008). On the other hand, the relationship among trading assets cannot remain constant, but will change over time, which gives rise to the need to look at it in detail. Capturing this relationship is an essential requirement, as it not only allows a better and more informed risk measure of a univariate asset, but also provides a proper assessment of risks in a combined way for an intraday portfolio.

In this thesis, we attempt to give elements that contribute to the above-mentioned approach. Each chapter of this thesis has a place in this venture. In the following, we present the motivation behind each of them.

In [Chapter 3](#), we are motivated by previous studies on asymmetric information (Amihud and Mendelson, 1987; Glosten and Milgrom, 1985; Kyle, 1985) and imperfect learning (see,

in particular, Hasbrouck, 1996 for a review of univariate models and Buccheri, Corsi and Peluso, 2020 for the very first multivariate model) in a rationally behaving market. While the former generates some kinds of heterogeneity in the belief of market participants with respect to the true underlying value and triggers pricing errors, the latter leads to partial recovery in the residual information. Due to these two sources of market friction, the price processes do not immediately incorporate price-relevant information but instead gradually over an effective time interval, in contradiction to a perfect world and arbitrage-free financial market implied by classical mathematical price dynamics models. We address these frictions by relaxing the rather strict assumption present in all previous approaches that information is present only at realization times. In contrast, we introduce the concept of “residual information”, considering that the information has a lifespan and decays over time. We use a precise statistical proxy for this decaying residual information derived from the decaying function of a multivariate Hawkes process, which is used to represent, in a disjoint manner, the intraday multivariate price-change process. The multivariate Hawkes processes of disjoint price change allow for the estimation of price adjustment on each asset to be computed at every point in time. This property alleviates the complication that arises as a consequence of the asynchronicity and the irregularity of time. The lifespan of information also allows for the temporal existence of cross-correlations, which is termed “lead-lag effect”, that, in short, is a fundamental phenomenon of a market microstructure in which some assets tend to follow the movements of other assets with a time delay. The lead-lag effects provide an alternative explanation for the bias towards zero of cross-correlation between related assets documented by Epps effects when the sampling frequency shrinks to the transaction frequency. In summary, this chapter provides an answer to the following questions. **Does a multivariate price formation mechanism exist at transaction-by-transaction frequency?. If so, then how do the cross-correlations among related assets naturally arise at this frequency, as a result of the multivariate fundamental of the price formation process.**

In Chapter 4, we turn our attention to the second-order moment structure of asset returns. On the ground that the multi-asset price formation dynamics in Chapter 3 has favourable results in capturing temporal dependencies between related assets, we are motivated to develop a general framework that efficiently provides an intraday inference on integrated covariance. We are inspired by the way the point process-based approach, i.e. price duration-based volatility estimator (Andersen, Dobrev and Schaumburg, 2009; Engle and Russell, 1998; Gerhard and Hautsch, 2002; Hong et al., 2021; Li, Nolte and Nolte-Lechner, 2015; Tse and Yang, 2012), with its parametric structure, can provide an instantaneous measure of univariate volatility. This type of volatility estimator is documented with a very nice performance against a well-established realized volatility estimator, and is simple to implement. However, its application is confined to only univariate volatility estimation because the discreteness of price duration modelling allows only fixed path conditional intensity, which is unable to update the dependencies between related assets continuously and deters the price duration volatility models from capturing co-volatility in a setting with asynchronous trading. Instead of modelling the price duration, we suggest

modelling explicitly the conditional intensity of the price movement using the multivariate Hawkes process. We also aimed at developing an estimator that overcomes the limitations of quadratic covariation-based estimators, i.e. realized volatility, which must rely on a large sample of data to ensure consistency estimation by its convergence property, and provides an efficient estimation for a very short time interval at the intraday level. Our multivariate generalization, the intensity-based volatility estimator, amalgamates both quadratic covariation and point-process approaches. It provides a general framework which not only preserves a superior feature of the price duration-based volatility estimator in providing intraday inference on local variation, but also efficiently captures an additional feature of the second-moment structure in portfolio analysis: local cross-correlation between assets. The chapter gives an answer to questions **Does an estimator accounting lead-lag effects provides a more efficient estimation of volatility?** and **Is it possible to capture a local true second-moment structure from very noisy observable transaction-by-transaction price processes?**.

Chapter 5 searches for another development in high-frequency risk measurement based on the dynamics of multi-asset price formation dynamics in Chapter 3, and addresses the question of how to define practical risk measures for traders or practitioners who operate their activities on an intraday basis. In high-frequency financial markets, trading is characterized by being extremely fast and information has very short lifespans, living in time frames of seconds to seconds or even a few milliseconds (Goldstein, Kumar and Graves, 2014; Hasbrouck and Saar, 2013; Menkveld, 2018; O'Hara, 2015). Within these horizons, accurately capturing the entire distribution of asset returns becomes impracticable and unfeasible. A more efficient and feasible solution is to consider only the tail of the distribution, which characterizes the probability of extreme events, rather than unnecessarily account for the whole distribution of all price events. We are motivated by the literature on intraday Value-at-Risk measures (Dionne, Duchesne and Pacurar, 2009; Giot, 2005; Liu and Tse, 2015) that capture the tail of the conditional distribution of asset returns by looking at the waiting times for extreme price movements to occur. So far, the literature on this topic has been confined to the univariate case. The univariate IVaR measures were originally based on the modelling of serial dependence in duration for price change exceeding a threshold. We deviate from this discrete price-duration modelling and model continuous interdependence in the likelihood of price change events occurring by stochastic conditional intensities of the Hawkes process, which is a "multivariate-friendly" point-process modelling approach. Our multivariate generalization is effective on intraday time scales and for multiple assets, and more importantly, it takes into account the cross-correlation structure of their extreme returns. It answers the following questions: **Is there any efficient way to incorporate temporal lead-lag correlations into the prediction of high-frequency extreme returns?** and **Whether accounting for these features into risk metrics would give a better/more informed risk measure?**

In the next section, we will give a more detailed scope of work for each chapter.

1.3 OVERVIEW AND SCOPE OF WORK

This is a cumulative thesis that is based on a series of working papers. All chapters are self-contained, and the detailed outline of the thesis is as follows:

Chapter 2, Literature Review on High Frequency Price Dynamics and Risk Measures, provides a critical review of the major existing literature relevant to the field of research in this thesis. We discuss the main recent theoretical developments and empirical studies surrounding the topics of high-frequency price dynamics, the volatility estimator, and intraday tail risk measure in the context of the market microstructure. We also highlight the literature contributed on major issues relating to the above three topics. In the high-frequency price dynamics, we discuss irregular trading time, discrete price, asynchronous trading, and lead-lag effects. In the two topics on high-frequency risk measurement, we review the main methods for realized volatility, price duration-based volatility, and the tail-risk measure. Alongside our discussion, we attempt to draw differences and similarities, and emphasize points of common interest amongst the literature and connections to our studies.

Chapter 3, Asymmetric Information, Information Life Span, and Lead-lag Effects on a Multivariate Price Formation Dynamics, focuses on the high-frequency transaction price data of multiple assets and seeks a mathematical model that is capable of capturing embedded complications of high-frequency trading markets and special features of the recorded data. To be specific, we extend the classic “martingale-plus-noise” model for high-frequency price formation dynamics to accommodate pricing errors of true underlying values and a lagged price adjustment mechanism. The pricing errors are triggered by asymmetric information, an inherent part of the market microstructure, and the lagged price adjustments are due to imperfect learning of residual information. We identify the pricing of asymmetric information and residual information as separable sources driving the price formation process.

We propose a model of multi-type agents with heterogeneous information endowments, and multi-assets with different degrees of market efficiency and different speeds of price adjustment. Standing on the viewpoints of market makers who set the prices on the market, we introduce the price-formation dynamics composed of three components: latent efficient price, adjusted quote price, and observable contaminated price. Due to special features of the transaction-by-transaction dataset, i.e. irregular spacing time, asynchronous trading, and the discrete grid-like structure of a price change with maximal limit, the model cannot be directly estimated by traditional econometric approaches. To draw inferences from the model, we build a bridge between the developed price dynamics and Hawkes point process using a disjoint price change representation of the transaction process. The disjoint representation takes advantage of the countable discrete state space of the price change, and the multivariate Hawkes processes encode the notation of causality between the price change states. Then, the lead-lag correlations can be simply recovered by taking integration of this interdependence among discrete price change states. The presence of lead-lag effects at the asset level can be measured over any arbitrary interval. By separating the

driving sources into liquidity and the information content of trade, we reveal the impacts of each component on the strength of lead-lag correlations between assets.

The model is tested on a cross-section of DJIA stocks with both non-parametric and parametric estimation to support theoretical postulations.

Chapter 4, Multivariate Variance Covariance Matrix Estimation with Martingale Representation of Hawkes Intensity, contributes to the estimation of second-order moment structure of high-frequency trading asset returns. In addition to the formation of the price process at the finest frequency, understanding the dynamics of the variance-covariance matrix is also necessary for high-frequency traders and practitioners, since it determines asset exposures to a variety of risk factors, opening up possibilities to construct efficient risk measures and optimal portfolios. The second chapter of this thesis develops an intensity-based estimator of integrated variance-covariance matrix with noisy and asynchronous tick-by-tick data. We establish the link between the theory on quadratic covariation of asset returns and that on the second-order moment structure of the point process. In detail, the estimator is designed to have a generic structure of temporal (cross-)autocovariance. Then, this (cross-)autocovariance can be formulated in terms of the conditional first- and second-order moments of counting processes associated with disjoint price change states. We prove mathematically that in a particular case of exponential fixed decay function, there exists a closed form of these moments deriving from a martingale structure of Hawkes conditional intensity. Thus, we can obtain a fully parametric specification of the intensity-based integrated covariance estimator, expressed in terms of the estimated parameters from the multivariate Hawkes process of disjoint price change states.

The mapping between the quadratic covariation of asset returns and the point processes of disjoint price changes is placed under a noise-contaminated semi-martingale hypothesis for the observable transaction price. And by a reasonable assumption that the microstructure noises are only updated at transaction times and independent of the efficient prices, we propose an efficient way, also based on the intensities of the disjoint point processes, to estimate directly the bias incurred by the noises, which complements the robustness of our intensity-based integrated variance-covariance estimator.

The performance of the estimator is evaluated using a simulation study. We uncover how the impacts of microstructure features such as trading activity, non-synchronicity trading, and microstructure noise to the estimator. More importantly, we demonstrate the relative finite sample performance of our intensity-based estimator compared to other benchmark estimators in the literature.

Chapter 5, Disjoint Hawkes Point Processes on Multivariate Extension of Intraday Value-at-Risk, contributes to another strand of high-frequency risk measurement. To be more specific, we apply our multi-asset price formation dynamics in a direct modelling of tail distribution of asset returns. Amongst tail-risk measures, with the greatest simplicity but wide applicability and universality is intraday Value-at-Risk (IVaR). We recognize that the existing literature still lacks a multivariate framework of the IVaR measure. Thus, we propose a model that can fill the gap of an intraday Value-at-Risk (IVaR) model for multiple assets. Our multivariate generalization is based on modelling the likelihood of

price change events occurring, and forecasting the future paths of returns by a Monte Carlo simulation. To study the tail of return distributions, we focus on the realizations of bidirectional price movement events, which are triggered if the cumulative price change on the upward (downward) equals or exceeds a threshold. We model the likelihood of occurring these events by multivariate Hawkes with exponential decay kernel. Contrasting with discrete duration-type models, the multivariate Hawkes conditional intensities update their information set continuously, thus accounting for both temporal self- and cross-asset effects induced by any new event arriving in the price dynamics.

To facilitate future events forecasts, we also develop an arrival detection algorithm based on an autoregressive conditional compensator, which estimates expected cumulative conditional intensities to arrive at a new price change event. Then, the Monte Carlo simulation is adopted to simulate the return distribution, from which the IVaR is calculated for any arbitrary intraday time interval.

We evaluate the multivariate measure in IVaR forecasting using three well-known backtests on violation realizations: unconditional coverage test by Kupiec (1995), correlated hit sequence test by Engle and Manganelli (2004), and random violation test by Candelon et al. (2010). We apply the multivariate IVaR estimator to two selected pairs of stocks with high- and low-trading activities listed on the Dow Jones Industrial Average index and investigate the impact of choosing the price change threshold and the forecast interval on the performance of the estimator.

Chapter 6 concludes this thesis. First, we summarize the main contribution, including an extension of standard univariate lagged price adjustment model to a multi-asset framework that provides more comprehensive price formation dynamics to accommodate special features of the market microstructure at transaction-by-transaction frequency; an efficient estimator realized variance-covariance matrix that robust to lead-lag effects, microstructure noise, and asynchronous trading; and a multivariate generalization of intraday Value-at-Risk. Then, we highlight some important implications of these developments for both academic researchers and practitioners on high-frequency trading markets. Finally, we point out interesting aspects that we did not fully cover in this thesis and provide a thorough discussion of potential topics and areas, with respect to multivariate price dynamics modelling, a realized volatility estimator, and intraday Value-at-Risk, that may be interesting for future research activities.

LITERATURE REVIEW ON HIGH FREQUENCY PRICE DYNAMICS AND RISK MEASURES

2.1 TRANSACTION PRICE DYNAMICS AND MARKET MICROSTRUCTURE

In the early 1900s, a French doctoral student Louis Bachelier defended his thesis “Théorie de la Spéculation” (Theory of Speculation) which is today recognized as the birth certificate of modern mathematical finance. In his thesis, he set the very first footprint on the mathematics of Brownian motion and applied its trajectory to stock price dynamics and option price modelling. He wrote the main idea of his work in the following sentence: “The mathematical expectation of the speculator is zero”. Later, in 1973, Nobel prize winners - Fischer Black, Myron Scholes, and Robert Merton introduced a major breakthrough in mathematical finance with their new methodology for the pricing of financial instruments, the so-called Black-Scholes-Merton model. In the same spirit with Bachelier’s work, the asset prices are supposed to be Brownian diffusion, which is as the notion of risk. This diffusion dynamic consistently coheres with a hypothesis: current asset prices incorporate all relevant information, and if any subsequent price change happened, it is the result of the arrival of new information, which arrives randomly and cannot be predicted. This hypothesis is often known as the Efficient Market Hypothesis (EMH). In both Bachelier’s and Black-Scholes-Merton frameworks, EMH play a central role and the market is a perfect world. In this full information setting, new information, which leads the investor to revise their estimate of future cash flows, would be immediately disseminated and interpreted by all market participants, and then, the prices would immediately adjust to a new equilibrium value.

Over the past decades, the introduction of available massive ultra-high frequency datasets into market microstructure research has opened up questions about the validity of the EMH. In contrast to the world of EMH, in the modern financial market there are always informed agents who are endowed with superior knowledge of price-relevant information over other uninformed agents (Glosten and Milgrom, 1985; Kyle, 1985). The informed trader only transacts when there is superior information available and would like to capitalize on that information before it becomes public. Their actions are watched by other market participants through their excessive supply or demand for liquidity (Bloomfield, O’Hara and Saar, 2005; O’Hara, 1998). Meanwhile, uninformed agents, by observing the market, try to extract private information signals and use them as advantages. The revelation of information and the corresponding price adjustment are not likely to be immediate

but gradual through transitions that are governed by the trading strategies of the agents (O'Hara, 1998, 2003). Thus, the EMH does not seem to hold unconditionally when the market is considered at the microscopic level. However, if the EMH is not valid, then one of the fundamental questions is how the prices adjust to new information and what role the above trading setups play in the price adjustment.

In a rational expectations market, the agents have some kind of heterogeneity with respect to their level of information, and their trading behaviours heterogeneously characterize their corresponding executed transaction processes. The recorded transaction processes then successively reveal privately informed information on the price processes. The practical implications are empirically testable hypotheses, and thereupon, dynamic models on the price formation process by studying recorded ultra-high frequency data. As a complete description of the market, which contains all transactions and transaction-associated characteristics like transaction time, transaction price, posted bid/ask prices, and volumes are recorded, the ultra-high frequency trading data allow for a detailed analysis of the trading activity and its price discovery characteristics, which enables a study of market dynamics at the lowest possible scale. However, these new datasets come with new challenges characterized by their special features, irregular temporal spacing, price discreteness, and non-synchronicity with complex lead-lag effects. Therefore, the implementation of econometric analysis and modelling must take these into account.

The primary roots of our modelling price dynamics are classified into three main fields of work according to the challenges posed by ultra-high frequency data: the time of trades, the discreteness of price, and the asynchronicity with complex lead-lag effects. These three lines of inquiry evolved sufficiently in the literature, so that it is possible to summarize them separately. The following discussion proceeds to do this, but also attempts to draw differences and connections and emphasize points of common interest.

2.1.1 *Models for the timing of trades*

Economic questions on trading activity in the market microstructure, i.e. how price processes adjust given the characteristics of order flows, should be studied at the transaction-by-transaction frequency. At this level, the constructed economic models are driven not only by the question at hand, but also by assumptions on the role of the trading times.

2.1.1.1 *The sampling of time and the information loss*

Most of the classical financial econometric analyses are implemented in regular, fixed-time frameworks. The frequencies of these time intervals were previously yearly, monthly, weekly, or daily, but with the availability of ultra-high frequency data sets, the intervals of hours, minutes, seconds, or even milliseconds are being used for the econometric modelling. A sceptical approach is to convert the data by imposing an artificially regular spacing time series on natural irregular spacing realizations. Thus, the econometric analysis typically proceeds without considering the original form of the data, or in other words, ignoring the role of the timing of events. The simplest way of this approach is to use the most re-

cent price at the end of a time interval as the observation for that interval. Huang and Stoll (1994) use this way for the prevailing mid-quote prices in their prediction of stock short-run price change on the basis of micro-structure factors. Andersen et al. (2001) use the last trade price to construct a model-free estimate of daily exchange rate volatility and correlation. To reduce the sensitivity to measurement errors in prices, perhaps a more sophisticated way is to introduce a sampling scheme which is appropriate to the context of an economic question. For example, for the purpose of estimating ex-post integrated volatility, Andersen et al. (2001) and Andersen et al. (2003) uses a weighted average to interpolate the first and last prices of small intervals, Hayashi and Yoshida (2005) analyzes overlapping tick-by-tick returns, Jacod et al. (2009) and Podolskij and Vetter (2009) propose a pre-averaging scheme in their modulated realized covariance. Another way of time sampling is to use the finest frequency to set a time clock so that there is at most one observation per time interval. The problem of this way is the possibility of missing values when the inter-trade duration is larger than the presetting time period. The calendar price is either the next price or the stale price. Hasbrouck (2001) takes this approach to record the time of a trade to the nearest second in his proposed random walk efficient price augmented by trade-related effects. Later, Aït-Sahalia, Fan and Xiu (2010), Barndorff-Nielsen et al. (2011), Hautsch, Kyj and Oomen (2010) and Zhang (2011) adopt the so-called refresh-time sampling schemes in their multivariate realized kernel estimator. Generally, although these three ways of artificially discretizing time intervals are very handy and straightforward in practice, they are not without cost. Indeed, the discretization blurs the timing of events, causes bias associated with temporally aggregating with variance, and induces spurious lead-lag correlations or destroys true short-term lead-lag effects (see, e.g. Huth and Abergel, 2014; Russell and Engle, 2010).

Another simple approach in application is, perhaps, to assume that the arrival times of past transactions have no impact on the distribution of the marks. This approach is taken by Hasbrouck (1991) in his bivariate vector regression (VAR) model applied to mid-quote price and transaction volume data to investigate the price impact of a trade on future transaction prices. Within his framework, the impact of a trade on the prices comes from the unexpected component of that trade, i.e. trade innovation, which accounts for the persistent price impact rather than the total trade, which also includes a predictable, transient portion conveying no new information. Because the model operates in transaction time, these price impacts are also measured in transaction time, and the price impact is measured in units of transactions. Consequently, the measure involves an undesirable loss of information, since the relations between the price and the timing of trades are lost.

2.1.1.2 *The role of trading times*

Theoretical frameworks of Admati and Pfleiderer (1988), Diamond and Verrecchia (1987), Easley and O'hara (1992) and Garman (1976) claim a role for the trade arrival time process in market microstructure modelling. They suggest that the timing of trades carries information. The importance of time is also confirmed by the studies of Engle (2000) and Engle and Russell (1994) on the co-movement of trading intensity and volatility. This leads

Dufour and Engle (2000) to consider expanding VAR structure in Hasbrouck (1991) to allow the time between trades to impact market price behaviour. In their empirical analysis, they define a liquid market as a market in which trades have a lower impact on prices and, consequently, it takes a while for new trade-related information to be fully incorporated into prices. They find strong evidences of the effect of trade duration on the price adjustment process. More precisely, the time between trades is informative, and a higher trading intensity is associated with a higher price impact of trades, a faster price adjustment to new trade-related information, and a stronger positive autocorrelation of trades. Thus, the incorporation of times into the price dynamics allows one to measure the value and the speed of price change after trades. The corresponding time elapsed from a trade that induces a price revision of a given amount is a natural framework for studying the liquidity process and assessing the level of liquidity risk.

In their research, Dufour and Engle (2000) accounts for the influence of trade duration on the price adjustment process, but still maintains the assumption of exogenous times for both price and trade-relevant information. This assumption may be too restrictive, and one can certainly visualize situations where price movements would influence the arrival rates of trades. For example, a sudden drop in the asking price could call forth a series of market buy orders and thus increase the transaction rate. Similarly, a wider spread should reduce the transaction rate, given that all else being equal. In fact, many contributions to the market microstructure literature (see, e.g. Easley and O'hara, 1992; Engle, 2000; Engle and Russell, 1994) provide some preliminary empirical evidence on the correlation between prices and inter-trade times.

2.1.1.3 *Discrete modelling of trading duration*

Building on the previous researches, Engle and Russell (1998) and Russell and Engle (2005) propose the Autoregressive Conditional Duration - Autoregressive Conditional Multinomial (ACD-ACM), which is the first one jointly modelling the distribution of transaction duration and transaction prices. They treat transaction price data as the joint distribution of weakly exogenous inter-trade duration and price changes, which can be decomposed into the product of the conditional distribution of price changes and the marginal distribution of inter-trade duration. In other words, if the contemporaneous relationship between the arrival times and price changes is not of interest, the model is simply a marked point process where the arrival times may depend on the past arrival times and the past marks of price changes, regardless of the values of the contemporaneous price change. Their modelling of duration, ACD, has a great advantage of flexibility, which stems from various choices for parameterizations of the duration's conditional mean and its identical independent density. The flexibility drives a diversification to accommodate different characteristics of analyzed data in the line shape for the event arrival intensity, e.g. exponential distribution (monotonic) (Engle and Russell, 1998), Weibull distribution (hump-shaped) (Engle and Russell, 1998), (U-shaped) Gamma distribution (Lunde, 1999), Blurr distribution (a type of non-monotonic shape) (Grammig and Maurer, 2000), Generalized F distribution (a type of non-monotonic shape) (Hautsch, 2001), or a mixture of distributions (a mixture of shape)

(Luca and Gallo, 2004) and also in the auto-regressive conditional mean form, e.g. standard linear ACD (Engle and Russell, 1998), threshold nonlinear ACD (Zhang, Russell and Tsay, 2001), Fractionally Integrated ACD (Jasiak, 1999), logarithmic ACD (Bauwens and Giot, 2000), augmented ACD (Fernandes and Grammig, 2006), stochastic conditional duration (Bauwens, 2006)¹.

Nevertheless, many interesting economic questions concerning the financial market microstructure can only be addressed using multivariate models. Although ACD-type models seem particularly well suited to analyze the joint distribution of transaction data for a single asset, it is difficult to extend to the case of multiple assets due to the discrete nature of duration modelling in the ACD (Russell, 1999). In the ACD, the information set is assumed to remain intrinsically unchanged between arrival times. The conditional intensity function, up to an identical duration density, can be time-varying, but it has a fixed path depending only on past observations. Thus, the intensity is unable to update before its arrival terminates although new information from other coexisting point processes did arrive, and thus there is an implicit loss of information. Taking the case of bivariate point processes of transaction and quote revisions as an illustration, if multiple quote revisions occur without intervening transactions and in the absence of an information event, then there is no adjustment, according to the ACD model, in the new transaction arrival rate. On the contrary, a scenario consistent with asymmetric information models would be that the change in price quotes chokes off the trading flow and leads the market back to a “normal” trading level (Dufour and Engle, 2000). From an inventory model perspective, in addition, a change of quote would immediately attract opposite side traders (O’Hara, 1998). The problem is that it is difficult to model the distribution of a duration when new information can arrive within a duration. A multivariate framework requires another approach of modelling.

2.1.1.4 *Continuous modelling of conditional intensity*

A more natural approach is to specify a model directly through the conditional intensity for each type of market event. The conditional intensity function is a central concept in point process theory (see, e.g. Daley and Vere-Jones (2006) and Karr (2017)) and is defined as the conditional instantaneous rate of event occurrence given the information set. Since the intensity function is defined in continuous time and thus allows for a continuous updating of the information set, it is a more natural concept to overcome the difficulty that the individual events of a multivariate point process occur asynchronously. More specifically, the common information set upon which each intensity is conditioned is updated continuously as new information arrives, thus allowing other types of event to have an immediate impact on the intensity as they occur in continuous time. In a pioneering work, Bowsher (2007) recognized the flexibility and the advantages of using the class of multivariate point processes that can be specified by a conditional intensity vector. He introduced bivariate Hawkes processes in order to model the joint dynamics of trades and quote changes of a stock.

¹ For an in-depth survey of ACD type model we refer to Pacurar (2008) among others.

The Hawkes process is a class of multivariate point processes that were introduced in the 1970s by Hawkes (1971) and Hawkes and Oakes (1974), notably to model the occurrence of seismic events. The Hawkes processes feature, in a natural way, a data-generating process with causal structure, built on the self-excitation and cross-excitation of arrived events, and thus account simultaneously for the co-existence and interplay between the exogenous impact on the system and the endogenous processes². It has also been widely used to model the role of endogenous activity in the financial market microstructure, where only a minor fraction of market movements can be explained by relevant news releases (exogenous factors), with important consequences for market stability and risk management (see e.g. Bacry, Mastromatteo and Muzy, 2015; Bowsher, 2007; Chavez-Demoulin and McGill, 2012; Filimonov and Sornette, 2012; Rambaldi, Filimonov and Lillo, 2018). This popularity can be explained, above all, by their great simplicity and flexibility, as anticipated by Bowsher (2007). The model is amenable to statistical inference, and closed-form formulae can be obtained in some particular situations. Moreover, since their parameters are very straightforward in meaning, they lead to a clear interpretation of many aspects of the complex dynamics of market microstructure events. In the case of modelling a discrete-time point process, the Hawkes modeling approach is mathematically equivalent to the ACD-based approach in the quantification of endogeneity (Filimonov, Wheatley and Sornette, 2015), but is intuitively more appealing.

Intensity-based modelling in the financial econometric literature has also used the autoregressive conditional intensity model (ACI) (Russell, 1999) and its extension. Russell (1999) use ACI model for modelling interdependence in the bivariate processes of market order and limit order arrivals. In another approach to the limit order book, Hall and Hautsch (2007) introduce additional explanatory covariates into the bivariate ACI to model the arrival of buy and sell trades, taking into account the changes in the limit order book caused by a new limit order, a change in an existing limit order, or a cancellation of a limit order. Bauwens (2006) propose an stochastic extension of the ACI model which adds a latent Gaussian autoregressive component to the log-intensity in their stochastic conditional intensity (SCI). More recently, Li, Nolte and Nolte (2021) proposed a Markov switching structure to the ACI in their Markov-Switching ACI model. They applied the model to detect distinct regimes in intraday volume and price duration dynamics, which support their perspective on the regime-switching behaviour of intraday volatility. The core component of all of these ACI models is specified in "event time", which results in a difficult understanding of the properties of the continuous conditional intensity process, or equivalently, the distribution of the multivariate point process. Therefore, the model still lacks extension and thus, remains limited to some applications compared to its opponents, e.g., ACD and Hawkes processes.

² See Kirchner (2016b) and Schatz, Wheatley and Sornette (2021) for the extension of Hawkes process for both endogenous and exogenous dynamics

2.1.2 *Models for the discreteness of prices*

Discreteness of prices in modern financial markets poses an additional complication in the analysis of ultra-high frequency data. For the U.S. markets, the graduation to decimalization is now complete³, but we still find price changes clustering on only a handful of values. This discreteness can have an important influence on the analysis of price dynamics, and thus there exists a vast literature on it. According to the objective interest, we classify the literature into two lines. The first line mainly focused on the notion of a “true” or efficient price in analysis of discrete prices. The efficient price is defined as the expected value of the asset given all currently available public information, and it is distinguished from the observed price, which is the efficient price contaminated by rounding error and market microstructure noise. The focus of these studies, therefore, was on the relationship between the efficient price and the discrete observed prices. The second line, vice versa, is not interested in the structural components of discrete prices. Instead, they directly model the price dynamics with a reduced-form model with quantally discrete-valued price change variables.

2.1.2.1 *Classical structural price dynamics models*

The classic models of discreteness for inferences on efficient price were driven by assumptions about the specifications of trading costs and rounding errors. Depending on the specification used, the models have different implications on the behaviour of a transaction price: allowing it to evolve as a rounded random walk, a rounded signal-plus-noise, or a value randomly selected from two rounded random walks (the bid and the ask quotes). Initially, discrete transaction prices were modelled as random walk processes, rounded to the nearest grid point (see, e.g. Ball, 1988; Gottlieb and Kalay, 1985). The traders first negotiate a continuous price, which is then discretized. The continuous efficient price is inherently unobserved and only discrete contaminated prices are observed. Hence, much emphasis was placed on how inference about the efficient price is influenced by measurement errors induced by discreteness. Then, Harris (1990) combine the models of Gottlieb and Kalay (1985) and Roll (1984) to describe the key features of the observed price, the discreteness, and the bid-ask spread (the cost of market making), which is a rounded signal-plus-noise dynamic. The model yields quantitative implications for the biases in the standard variance and in the serial correlation estimators: the discreteness increases the price variances and adds negative serial covariance to price change series, but these biases are dependent on the variance of the true underlying value and on the cost of market-making. Harris (1990)’s model is still very simplistic because of its restrictive assumption of constant volatilities for the efficient price and the bid-ask spread. As new information arrives, the volatility of the efficient price will change and consequently change the risk of holding the asset, which is somewhat a correlative of bid-ask spread in the sense of the cost of market-making expos-

³ In order to conform to international trading standards and to make it easier for traders to interpret prices and place trades, the U.S. Securities and Exchange Commission (SEC) mandated all exchanges convert to a decimalization system no later than April 9, 2001. The minimum tick size was reduced from 1/16th of a US dollar to one cent for stocks selling at prices greater than or equal to US1\$.

ure. The bid-ask spread will also vary accordingly, violating the assumption of the model. Hasbrouck (1999a,b), in his research, confirms this correlated stochastic variation of these two components.

Hasbrouck (1999a,b) extends Harris (1990)'s model by relaxing this assumption with time-varying volatilities for the efficient price and the bid-ask spread and suggests a framework handling discrete, clustered bid and ask quotes as opposed to only the transaction prices. The dynamics of his model are of more complex structure and are not suitable for the type of analysis presented by Harris (1990). Instead, Hasbrouck (1999b) focuses on characterizing the dynamics of the exposure costs to the quote and, second, estimating the model for the volatility of the efficient price given only observations of the perturbed discrete bid and ask prices. The model also allows for asymmetry in the costs of exposure, which is in line with the practice that the specialist, in some states of the world, may set quotes more conservatively on one side of the market than the other. However, the asymmetric costs of exposure incurred by only the rounding effects in Hasbrouck (1999a,b) are still simple and not sufficient to explain an asymmetric information environment, where market makers learn about the private information of informed traders from order flows and subsequently adjust the cost of trading to avoid potential risk to informed traders (O'Hara, 1998, 2003). Zhang, Russell and Tsay (2008) have appealed to this perspective of asymmetric information microstructure theory and suggest incorporating the characteristics of the order flows into the perception of market makers about the exposure costs. By making distinctions between unexpected volumes initiated by the buyer and the seller, they find that the ask and bid components of the spread change asymmetrically about the efficient price as a function of the order flow.

The models mentioned with their structural price dynamics seem to involve many interesting microstructure features. But they are not free of problems. Because the efficient price and the market-making costs are intrinsically latent variables and only the discrete bid and ask quotes are observable, the estimation of (Hasbrouck, 1999a,b)'s and (Zhang, Russell and Tsay, 2008)'s models by traditional methods like likelihood and moment is difficult. Alternatively, Hasbrouck (1999b) proposes casting the model in a non-Gaussian, non-linear state-space representation and estimated via maximum likelihood, and Hasbrouck (1999a) proposes another technique, a Markov chain Monte Carlo method and a Gibbs sampler, treating the price at any given update as an unknown parameter.

2.1.2.2 *Reduced-form price dynamics models*

If the structural parameters are not of primary interest, then an alternative is to model transaction prices directly with a reduced-form model for quantally discrete-valued random variables. Econometric models of this approach often employ ordered probit models. Hausman, Lo and MacKinlay (1992) propose modelling the transaction by transaction price changes where previous structural models linking unobserved continuous efficient price change to observed discrete price change are replaced by a reduced-form probit mapping function defined via a set of breakpoints. The effects of the observable explanatory variables (e.g. irregular timing of trade, volume, future returns, bid-ask spread, and sign of

trade) flow to a dependent variable of the latent efficient price change via a linear specification, which then maps into the observed discrete price change. Conditional on particular values of the explanatory variables, the predictions of the model are given as probabilities of pre-specified discrete price changes. Hausman, Lo and MacKinlay (1992) apply the model to analyze the movement of the stock price at NYSE. By incorporating explanatory variables regarding the content of information in a sequence of trades, they examine the impact of asymmetric information to price dynamics in his model. In particular, they study how transaction prices respond to a sequence of buyer-initiated trades versus a sequence of seller-initiated trades, and find evidence that persistent selling predicts falling prices and persistent buying predicts rising prices. They also suggest that the relation between conditional variance of the underlying value may depend on the contemporaneous duration with evidence that a long waiting time leads to higher variance per transaction. In the same approach, Bollerslev and Melvin (1994) replace linear regression with a GARCH specification, the output of which (conditional volatility forecasts) is fed into a probit model for discrete bid-ask spread at FX markets.

Although the probit-type models and the first line of classic discreteness both allow the price dynamic to accommodate special features of the market microstructure, i.e. discreteness, market-making costs, rounding errors, and order flow characteristics, there are several structural differences. Contrary to the latter, the probit-type models require latent continuous efficient price dependent only on observable data. This helps to incorporate conditional information much easier but also rules out attractive and basic features of the classic discreteness models, namely the dependence of the latent price on its prior values. Also, considered as a reduced-form structure, a probit model of observed price change may fit well with observed data, but there is no obvious candidate for the underlying efficient price change structure. Thus, many interesting micro-structure features may not be easily resolved with the probit models. However, probit models are more general in certain aspects. Most notably, the mapping from the latent continuous price change to the observed discrete price change is described by a probit link with a set of breakpoints that need only be ordered. This allows for a degree of flexibility in the implicit rounding function that is not available in the structure models. Broadly speaking, probit models are reduced-form specifications with robustness and flexibility in modeling data but are difficult in some respects to interpret structurally.

More recently, Russell and Engle (2005) propose an ACM-ACD, generalizing previous works on probit models for transaction data to take into account the joint distribution of discrete price change and irregular trading time. The connection between them arises from the view that the discrete price grid is predefined as permeable barriers in the outcome space of the continuous latent price. If transactions are assumed to occur when the latent price crosses one of these barriers, the observable crossing times can be used to infer the structural parameters of the latent price processes. Thus, transaction price data are modelled as the joint distribution of weakly exogenous inter-trade duration and price changes, which then can be decomposed into the product of the conditional distribution of price changes and the marginal distribution of inter-trade duration. The price changes

are treated as a multinomial random variable and modelled by an autoregressive conditional multinomial model (ACM) for the price transition probabilities while the marginal distribution of the inter-trade duration is captured by the ACD model (Engle and Russell, 1998).

In the same spirit as Russell and Engle (2005), Rydberg and Shephard (1999a,b, 2000, 2003) suggest a trivariate component model, decomposing the transaction price data into three distinct processes: non-zero price change, direction of price change, and magnitude of price change. Bien, Nolte and Pohlmeier (2006) and Liesenfeld, Nolte and Pohlmeier (2008) propose a very close integer count hurdle model to extend the domain of discrete price change state in the ACM model. All these component models are in the same spirit as Russell and Engle (2005) that use an autoregressive structure for discrete price change. Although the decomposition breaks the estimate down into a sequence of simpler problems, it does come with a cost. To estimate the model sequentially, the first component cannot depend on lagged values of the components coming afterward. For example, in the Rydberg and Shephard (2003) model, the non-zero price cannot be a function of past direction or magnitude of price changes, or the direction can not depend on the past magnitude. The importance of this restriction surely depends on the economic questions at hand.

Unlike the approach of Russell and Engle (2005), in our approach, we do not focus on and decompose each transaction into separate components, price change and trading time. Instead, we “zoom out” from transaction-by-transaction time series and split them into multivariate transaction time series realized by discrete price change, e.g. the number of ticks. We follow the spirit of the ordered probit models of Bollerslev and Melvin (1994) and Hausman, Lo and MacKinlay (1992) to create a mapping between latent efficient price change and observable discrete price change, but ours has a remarkable improvement. First, we provide a sophisticated structure of the price dynamics, which accommodates major features of the market microstructure such as asymmetric information and lead-lag effects, and its straightforward and precise connection to the dynamics of observed discrete price change. The dynamics of observed discrete change is also significantly improved by replacing naive regression by a specification of exogenous-endogenous activities using the Hawkes process. Second, our model is robust for both univariate and multivariate frameworks, while existing models are only applicable to the univariate asset. Therefore, our model is more generalized in terms of structure and dimension, and more importantly, enables more direct and structural interpretation with hypotheses of market microstructure theory.

2.1.3 *Models for the non-synchronicity and the lead-lag effects*

A core question that essentially emerges from multivariate price dynamics modelling is whether correlation among assets naturally arises at the tick-by-tick level as a result of the multivariate fundamental of the price discovery process, and equivalently, there exists an indispensable multivariate transaction price generation mechanism. The comprehensive empirical studies of tick-by-tick stock returns often documented an issue of correlation

in non-synchronous trading: It has a bias towards zeros, the so-called Epps effects (Epps, 1979). In this context, there exists a difference in the trading activity, one asset can trade more infrequently than others, and the observed trades are often, if not always, at different timestamps. As a consequence, empirical contemporaneous tick-by-tick correlation statistics are obtained at null. However, the zeros in the contemporaneous statistics do not testify to the non-existence of a multivariate price formation mechanism. If one considers a perfectly frictionless world of Bachelier and Black, Scholes, Merton, where asymmetric information does not exist and observed prices processes immediately impound all relevant information, then with that being the case the price movements between two assets are contemporaneously correlated but not cross-autocorrelated. However, in the natural frictional alternative of market microstructure theory, the prices do not instantaneously adjust when new information arrives (Amihud and Mendelson, 1987; Glosten and Milgrom, 1985; Hasbrouck and Ho, 1987; Kyle, 1985). Instead, the price formation process is delayed due to various market frictions, such as lagging information dissemination and price smoothing by informed traders to maximize their information advantages. Thus, the high-frequency asset price dynamics are often documented to be characterized by a phenomenon, the so-called lead-lag effects, that the price dynamic of one asset tends to follow the one of other assets with a time delay. (Bucheri, Corsi and Peluso, 2020; Chan, 1992; Chiao, Hung and Lee, 2004; Huth and Abergel, 2014; Jong and Nijman, 1997).

2.1.3.1 *Lead-lag effects in low frequency trading*

The manner in which information is incorporated into stock prices and consequently causes the lead-lag effects has long been of primary concern in financial economics. On the lower frequency, it was studied under the term “cross-autocorrelation”, the analogue of lead-lag effects in regularly spaced trading times. Lo and MacKinlay (1990) document an important difference in the cross-autocorrelation patterns between large- and small-firm returns. The cross-autocorrelation where the large firm is the leader and the small firm the lagger is higher than the cross-autocorrelation where the small firm is the leader and the large firm the lagger. This difference points to some friction that delays information from being incorporated into all stock prices simultaneously. Brennan, Jegadeesh and Swaminathan (1993), Chordia, Roll and Subrahmanyam (2000) and Mech (1993) propose that the lead-lag patterns arise due to the difference in adjustment speeds amongst stocks to economy-wide shocks. The shocks should first be incorporated into the prices of the more actively traded larger stocks, resulting in the observed cross-autocorrelation patterns in stock returns.

More recently, Bernhardt and Mahani (2007), Boulatov, Hendershott and Livdan (2012) and Chordia, Sarkar and Subrahmanyam (2011) point out the role of privately observed systematic information (informed trading) in triggering the lead-lag pattern. In their theoretical framework, Chan (1993) show how imperfect learning of signals by market makers about private information in stock returns leads to positive lead-lag effects in a model without informed trading factor. Bernhardt and Mahani (2007) and Boulatov, Hendershott and Livdan (2012) assume that the market makers can only update their pricing function

condition on the order flow information of the asset they trade only. In other words, there exist imperfections in the learning of market makers. Both researches employ an informed trading factor in their model. The former considers short-lived information, whereas in the latter the information is long-lived. With short-lived information, the informed order flow is independent across time, and past returns are unrelated to past informed order flow. In contrast, long-lived information makes informed order flows positively autocorrelated. We consider that long-lived information in (Boulatov, Hendershott and Livdan, 2012) is a more realistic scenario, especially in the intraday or transaction-by-transaction level of our studies.

2.1.3.2 *Lead-lag effects in high frequency trading*

Investigation of lead-lag effects has been a long story in the economics literature at various time scales, mostly at daily or longer than daily, but relatively minor for high-frequency data. The lead-lag patterns in intraday data can expect to be sharply distinct from those of low-frequency data, and even within intraday time horizons, the patterns at the transaction-by-transaction level can be very different from those of the other level, such as minute-to-minute (Hayashi and Koike, 2017, 2018). Indeed, the modern financial market contains different types of participants, each of which has different perspectives about the market: different risk appetites, different sources of capital and information, and different investment/trading horizons. These differences are then incorporated into the formation of prices on a different time scale (Muller et al., 1993). The practical implication here is the existence of a distinct structure of lead-lag effects at the transaction-by-transaction level.

At the transaction-by-transaction level, theoretical and empirical justifications for the lead-lag effects on stocks have been quite scarce compared to those at a lower frequency, partly due to the difficulties in modelling irregular trading times, and observed discrete and noise-contaminated prices of ultra-high frequency data that we mentioned in previous Sections § 2.1.1 and § 2.1.2. To deal with these difficulties, the most common way in modelling lead-lag effects is either imposing an artificial regularly spacing time or introducing a sampling scheme rather than considering modelling endogenous time. For example, Dao, McGroarty and Urquhart (2018), Hoffmann, Rosenbaum and Yoshida (2013) and Huth and Abergel (2014) generalize the overlapping tick-by-tick prices method of Hayashi and Yoshida (2005) to calculate “lead-cross-autocorrelation” and “lag-cross-autocorrelation” patterns of lead-lag effects. Hayashi and Koike (2017, 2018) impose the finest observable resolution of the data as time unit of the price realizations and use a wavelet-based method for a multi-scale analysis of lead-lag effects. Very recently, Buccheri, Corsi and Peluso (2020) introduce a multi-asset version of the price adjustment model of Hasbrouck and Ho (1987) to capture lagged dissemination of information across stocks. The model is then cast into a linear Gaussian state-space representation and can be conveniently estimated through a standard Kalman-EM algorithm. However, instead of taking into account the roles of trading times, their model aggregates all high-frequency prices at a one-second frequency and treats asynchronous observation as a typical missing value problem. Moreover, the

stringent factor of informed trading, which also invokes lead-lag effects, is not yet taken into account in their model.

Recognizing this missing gap in the multivariate framework of price dynamics, we are motivated to derive a novel model that accommodates endogenous trading times, imperfect dissemination of information and informed trading, and, more importantly, lead-lag effects. Our model consists of the features of lagged price adjustment and informed trading into random walk processes. The dynamics is then mapped into multivariate discrete state Hawkes point process for convenient parameter estimation and inference. The study of Bacry et al. (2013) is similar to ours in the way of using Hawkes point processes to model price movements. However, our model is distinguished by a more generalized framework supported by a theoretical foundation of price dynamics and thus is a different but more convenient approach to study lead-lag effects. The non-trivial lead-lag effects derived from the model is the evidence of the indispensable multivariate transaction price generation mechanism, which serves as the preliminary purpose of our studies.

2.2 HIGH FREQUENCY DATA AND MARKET RISK MEASURE

Alongside modeling market dynamics, managing risks (market risk) is undoubtedly one of the most important activities of the practitioner on the financial market. In truth, the performance of a financial position is bound tightly with its associated trade-off market risk. Market risk can be defined as the risk of a change in the value of a financial position due to changes in the value of the underlying components on which that position depends (Mcneil, Frey and Embrechts, 2015). A great performance of a position is rewarded only if the outcome of underlying values adheres to market risk appetites which are measured clearly, accurately, and practically.

Although the idea and practice of evaluating market risk and trade-off return is not new to the financial econometric literature, what is novel in the last two decades are newly developed risk measurement methods relying on harnessing high frequency data. As the full record of every movement in financial markets, high frequency data offer market practitioners the ability to study and incorporate into their methodology real-time market information of the financial market that are impossible to identify with low-frequency data. In particular, new types of data pave the way for digging up insights about the dynamic properties of volatility, i.e. the main source of market risk and driving force of extreme prices movements, i.e. news announcement and their impacts on the financial markets, from which our knowledge of market risks has gained tremendously. There is a new range of risk measures developed from high frequency data and they have been emerging as a new body of financial study, namely high frequency risk measurement.

One of the most successful approaches in the area of high frequency risk measurement is modelling of the dynamics of the second-order moments of asset returns, which is also known as realized volatility ⁴. Realized volatility is simple to compute (it is equal to the

⁴ Here and throughout, we use the generic term "volatility" in reference both to variance (or standard deviation) or covariance (standard deviation and correlation). When it is important, the precise meaning will be clear from the context.

sum of squared high frequency returns) and is a consistent estimator of integrated volatility under general conditions (see Andersen et al., 2001; Andersen et al., 2003; Andersen, Bollerslev and Meddahi, 2005; Barndorff-Nielsen et al., 2011; Barndorff-Nielsen and Shephard, 2002a, 2004; Barndorff-Nielsen, Shephard and Winkel, 2006). These models are now established as one of the most influential and challenging approaches in financial econometrics, due to its capability of capturing not only traditional stylized effects in asset returns but also crucial aspects for ultra-high frequency data.

Another strand of high frequency risk measurement focuses on direct modelling of a tail distribution of asset returns, among which the greatest simplicity but wide applicability and universality is intraday Value-at-Risk (IVaR). This type of risk measure is very useful, as it provides extreme loss on the tail given a coverage probability of risk, without requiring knowledge of the main body of the distribution. IVaR is often calculated on very short intervals, e.g. 15 minutes, 30 minutes... (see Banulescu et al., 2015; Chavez-Demoulin and McGill, 2012; Dionne, Duchesne and Pacurar, 2009; Giot, 2005; Tse and Yang, 2012) and thus overcomes the difficulty of traditional daily VaR in providing the practitioner with forecasts of market risks in (near) real-time basis.

2.2.1 *Realized volatility*

The most critical feature of asset return is arguably its second-moment structure, and understanding this feature lies at the heart of options pricing, portfolio selection, and risk management applications. Therefore, it is not surprising that an enormous number of volatility models based on daily returns have been developed over the years, including ARCH (Engle, 1982), GARCH (Bollerslev, 1986), EGARCH (Nelson, 1991), and stochastic volatility specifications (Taylor, 2008); and their performance has been intensively analyzed in financial econometrics⁵. The fact that all these models consider latent conditional volatility, and thus the validity of these models in practice strictly depends upon presumed distributional properties or specific (parametric) dynamics form of the volatility. Indeed, Bollerslev (1987), Carnero (2004) and Malmsten and Teräsvirta (2004), among others, point out in their studies that most of these latent volatility models fail to describe several stylized properties that are observed in financial time series satisfactorily. Additionally, using a latent variable as a proxy of volatility complicates its forecasting and makes it difficult to evaluate the performance of volatility models.

The search for an adequate framework for the estimation and prediction of the conditional volatility of financial assets returns has led to the analysis of high frequency data. In fact, the volatility modelling literature has taken a significant step forward. By introducing quadratic variation theory into measuring ex-post variation of asset prices, Andersen et al. (2001) and Andersen et al. (2003) and Barndorff-Nielsen and Shephard (2002a,b), propose a new approach called “realized” volatility that exploits the information in high-frequency returns. Basically, the approach is to estimate volatility by summing all intraday high fre-

⁵ For an substantial literature review on latent volatility literature, we refer to Asai, McAleer and Yu (2006) and Bauwens, Laurent and Rombouts (2006), among others

quency squared returns sampled at very short intervals. The idea is that if the sample path of volatility is continuous, then increasing the sampling frequency yields arbitrarily precise estimates of volatility at any given time (Merton, 1980). The new proxy of volatility is no longer latent, but an observable and “realized” process; thus, it can be modelled directly rather than being treated as a latent variable. The statistical properties of the realized volatility are extensively studied in Barndorff-Nielsen and Shephard (2002b), Meddahi (2002), Andersen et al. (2003), Mykland and Zhang (2009). It has led to a considerable improvement in our understanding of how the data-generating process of financial prices may be characterized and how prices can be correlated between different assets (Aït-Sahalia and Jacod, 2012).

However, using a non-parametric setting, the approach is not without difficulties. Unlike those low frequency data that are homogeneously spaced, tick-by-tick transactions occur irregularly and asynchronously. In addition, the observed transaction price of high-frequency data comes with market microstructure noise (Jacod, Li and Zheng, 2017). Thus, the realized quantities that can be estimated from high frequency data are not confined to volatility. There is an upward bias on realized volatility due to the market microstructure noise and a downward bias on realized co-volatilities in the multivariate framework due to the asynchronicity. These two biases can partially or even fully offset the incremental benefits of using intraday information, and therefore may render the use of high-frequency data practically unattractive. The bias from asynchronicity will be mentioned in a later section on multivariate realized volatility. Now we focus only on the univariate case with only the bias of microstructure noise.

2.2.1.1 *Univariate realized volatility estimators*

Several existing studies have already proposed different approaches to mitigate these issues. For example, in the univariate asset framework, Aït-Sahalia, Mykland and Zhang (2005) propose sampling as frequently as possible at the cost of modelling the microstructure noise. This paper assumes constant volatility so that it can perform the maximum likelihood estimation. Xiu (2010) extend Aït-Sahalia, Mykland and Zhang (2005)’s to a quasi-maximum likelihood estimator, which is consistent, efficient and robust with respect to stochastic volatility. Also in the context of stochastic volatility, Zhang, Mykland and Aït-Sahalia (2005) present a nonparametric two-scale realized volatility estimator, which is the first consistent estimator in the presence of noise. This estimator takes the average of many RV estimators partially to eliminate the effects of the noise, and the remaining noise effects are debiased by an estimator on the noise variance. Subsequently, Zhang (2006) extend his previous two-scale to multi-scale realized volatility, improving the convergence rate in Zhang, Mykland and Aït-Sahalia (2005) to the optimal rate a model can achieve as shown by Gloter and Jacod (2001). Barndorff-Nielsen et al. (2008) have designed various realized kernels that can be used to deal with endogenous noise and endogenously spaced data, and their convergence rates are the same as those of the multi-scale realized volatility. Jacod et al. (2009) and Podolskij and Vetter (2009) introduced the pre-averaging method, which involves first averaging the observed prices over a moderate number of

time points to reduce the measurement error. Another side of the research searches for optimal sampling frequencies and the commonly accepted sampling interval for high frequency data is to sample at 5-minute intervals (Andersen and Bollerslev, 1997; Bandi and Russell, 2008; Bandi and Russell, 2006; Hansen and Lunde, 2006a; Li et al., 2013; Liu, Patton and Sheppard, 2015).

We recall that it may not be appropriate to apply these pioneer models directly to transaction-by-transaction data. Oftentimes, in order to satisfy the conditions assumed, data cleaning procedures that involve substantial subsampling are necessary, such as reducing the frequency of data from tick-by-tick to minute-by-minute or at best second-by-second. Moreover, the transaction times are not only irregularly spaced, but also endogenous, depending on the price process. Developments have been made to relax the assumptions. Among other works, Li et al. (2013) and Li, Zhang and Zheng (2013) studied endogenous observation times; Li, Xie and Zheng (2016) considered a situation where dependent microstructure noise can be modelled as a function of trading information while allowing for endogenous observation times and jumps; Jacod, Li and Zheng (2019) propose an estimator on tick-by-tick data, which achieves the optimal rate of convergence, under a setting of irregular and endogenous observation times; decaying autocorrelation noise and jumps.

2.2.1.2 *Multivariate realized volatility estimators*

When it comes to an application of multiple assets, the estimation of integrated covariance matrix (co-volatility) is even more challenging due to the so-called non-synchronous trading effect. As pointed out by Buccheri et al. (2019), Dao, McGroarty and Urquhart (2018), Epps (1979), Huth and Abergel (2014) and Large (2007a), information arrives at different frequencies for different assets and information related to one asset can affect the price formation process of another asset, thus inducing additional microstructure effects among correlated assets, so-called stale prices, and temporal lead-lag effects. The standard approach of realized measures (Barndorff-Nielsen and Shephard, 2004) relied on an artificially regularly spaced time scheme and cannot take into account the difference in the timestamps of the last ticks, thus ignoring these effects and creating an attenuation bias⁶. In this context, pioneering contributions have been made by Hayashi and Yoshida (2005) and Martens (2004), proposing refresh time sampling and a pseudo-aggregation algorithm of asynchronous observations, respectively, to correct the realized covariance estimator. However, their estimators do not consider the microstructure noise that plagues the use of high frequency data more generally.

Several recent papers have proposed techniques in varying complexity estimators for simultaneously dealing with asynchronicity and market microstructure noise. Voev and Lunde, 2006 propose an bias-corrected Hayashi–Yoshida estimator in a more realistic world of noisy prices, but their estimator does not achieve consistency. Zhang (2011) has demonstrated theoretically the existence of a bias associated with the standard RC estimator due

⁶ This attenuation bias was first noted empirically for sample correlation matrices by Epps (1979), and is commonly referred to as the Epps effect

to the asynchronicity of the data and advocates a consistent multivariate version of his two-scale realized covariance estimator, which is capable of simultaneously eliminating biases in asynchronous and noisy data. Christensen, Kinnebrock and Podolskij (2010) rely on a multivariate extension of the univariate pre-averaging approach and the Hayashi-Yoshida estimator and advocates the (adjusted) modulated realized covariance estimator, which also have noise robustness and can resolve the asynchronous data problem. However, these estimators all assume high-level market microstructure noise, for example, exogenous and i.i.d to achieve their asymptotic properties.

Aware of these missing parts in the noise, Barndorff-Nielsen et al. (2011) introduce their multivariate realized kernel. Their estimator is the first estimator that simultaneously guarantees positive semi-definiteness, accommodates asynchronicity, and is also robust for general assumptions on microstructure noise. First, they utilize refresh-time sampling to limit the effect of non-asynchronicity of a multivariate data set. Then, they employ lead-lag autocovariance terms to mop up the remaining effects of the noise and asynchronicity. The autocovariance structure combined with an appropriate weight function allows for a consistent positive semi-definite estimator. However, the desirable feature of positive semi-definiteness comes at the cost of substantial data loss in high dimensions. It is shown in Barndorff-Nielsen et al. (2011) that the multivariate realized kernel works well in moderate dimensions when all the assets are very frequently traded. Moreover, full multivariate kernels are challenged with heterogeneous liquidity, since the refresh-time sampling scheme will be limited by the least frequently traded asset. Still, the estimator does not achieve an optimal rate of convergence and suffers from a bias in non-linear transformations of the estimated covariance matrix, for example, realized correlations and regression coefficients. Thus, the use of it is constrained in potential applications.

More recently, there have been several extensions on generalizing multivariate semi-martingale price dynamics with more complex endogenous noise and asynchronous trading⁷. Bibinger (2012) extends the multi-scale volatility estimators to the covariance estimation. Christensen, Podolskij and Vetter (2013) and Koike (2015) combine the pre-averaging estimator of Christensen, Kinnebrock and Podolskij (2010) with the Hayashi and Yoshida (2005) method for synchronization. Park, Hong and Linton (2016) extend the work of Mancino and Sanfelici (2011) and Mancino and Sanfelici (2008) and develop a Fourier method-based estimator of realized covariance. Varneskov (2016b) develops a general multivariate additive noise model for synchronized asset prices and extends Varneskov (2016a)'s univariate flat-top realized kernels to estimate its quadratic covariation. Li et al. (2022) extend the least squares-based estimators of Curci and Corsi (2012) and Nolte and Voev (2012) to a multivariate quadratic covariation estimator, which is consistent in the presence of asynchronicity and endogenous noise.

To sum up, the aforementioned methods all require certain choice to deal with irregular spacing times and non-synchronicity of trading. In the univariate case, it is a data-cleaning

⁷ There exists also an extension of realized measures allowing for (co-)jumps in the price processes. However, we do not concern (co-)jumps in our studies. For the literature on this extension, we refer to Ait-Sahalia and Jacod (2012), Ait-Sahalia and Xiu (2016), Ait-Sahalia and Yu (2009), Brownlees, Nualart and Sun (2020), Jacod, Li and Zheng (2019), Koike (2015) and Varneskov (2016a), among others

procedure that involves substantial subsampling, such as reducing the frequency of data from tick-by-tick to minute-by-minute or, at best, second-by-second. For multiple assets, there are two main approaches of dealing with asynchronous observations: firstly, apply a synchronization scheme and estimate all elements of the covariance matrix jointly; and secondly, align the observations by a pseudo-aggregation algorithm and estimate the covariance matrix element-wise. As such, all paradigms may come with the cost of losing information. The information lost can be a consequence of either removing valuable data or ignoring the endogenous impact of trading time. The latter in the multivariate case, resulting from pseudo-aligning the observations, are even more severe as it additionally introduces spurious lead-lag correlations or unnecessarily destroys true short-term lead-lag effects (Buccheri et al., 2019; Curme et al., 2015; Huth and Abergel, 2014). Last but not least, these estimators, to obtain effective results, require an essential step of prudently selecting sampling intervals, bandwidths, or other tuning parameters. The selection necessitates ensuring a solid sample size to invoke the consistency of the estimators, which often limits the use of realized measures to the finest frequency of only daily integrated (co-)variation. For short intraday intervals, such as an hour or 15 minutes, it is doubtful if the sample size is large enough to justify the applicability of the asymptotics of the realized estimators (Tse and Yang, 2012). Therefore, their implementation can raise subtle issues, especially, for high frequency or intraday traders who often practise in a real-time basis.

In [Chapter 4](#), we introduce a multivariate realized estimator that is robust for those issues. Our proposed volatility estimator has the important advantage of employing all the information available in all price series, and thereby making use of all the trades of any asset. Furthermore, in sharp contrast to alternative estimators, our estimator is not affected by spurious correlations and Epps effects, while taken into account simultaneously the lead-lag effects amongst correlated assets and the endogenous times of trading. Finally, since the estimator is a point process-based volatility estimator, it has a parametric structure and ability to provide intraday inference on local volatility, as opposed to an integrated (co-)variation estimator from the realized measures.

2.2.2 *Instantaneous volatility*

A potential candidate that has the capability to overcome the above-mentioned problems of realized volatility is the price duration-based volatility estimator. This type of estimator was first initiated in the high frequency trading context by Engle and Russell (1998). They quantify the instantaneous volatility of the price process by modelling the arrival rate of price duration, i.e. the waiting time for the price process to generate a certain given price change. The instantaneous volatility is determined by the product of the conditional price intensity function, which characterizes the probability that a price event will occur in the next instant conditional on the history of price events, and the price change threshold. However, their main results concentrate only on the serial dependency found in the process

of price intensities, and the estimated instantaneous volatility is used as a by-product to test their relationship to hypotheses emerging from market microstructure literature.

After the suggestion of Engle and Russell (1998), price duration-based volatility has received so far very little attention in the literature, compared to the realized volatility estimator. The limited number of studies that focus on developing a volatility estimator based on this approach can be mentioned. For example, Gerhard and Hautsch (2002) consider a direct specification of the volatility estimator directly on price duration. Andersen, Dobrev and Schaumburg (2009) introduce a volatility measure in a dual approach of measuring the duration per unit of price change. Tse and Yang (2012) proposes using augmented ACD model (Fernandes and Grammig, 2006) for price duration to measure the integrated volatility over an interval. Li, Nolte and Nolte-Lechner, 2015 incorporate other market microstructure variables in the parametric structure of ACD model and study of the effect of inclusion of those variables on the quality of volatility estimates. Li, Nolte and (Lechner) (2018) derive asymptotic results for the general class of renewal process estimators, including also the price duration-based volatility estimator. Very recently, Hong et al. (2021) improve upon Tse and Yang (2012)'s parametric price duration estimator by replacing the Exponential distribution with a Burr distribution that can better capture a long-memory dependence in price duration. In addition, they provide practical ways based on bid/ask spread to appropriately choose the threshold parameter, which determines the size of the price change that defines the event times.

As pointed out by Tse and Yang (2012), this estimator enjoys a full parametric assumption for the dynamic price duration process, which can better off the estimator in the manifold. First, data beyond the volatility estimation window can be used to improve the estimated parameter, which in turn leads to a more precise volatility estimation. Second, according to Li, Nolte and Nolte-Lechner (2015), the parametric structure of ACD models facilitates the inclusion of other market microstructure covariates, which not only can further improve the quality of volatility estimation, but also provides a framework for analyzing the relationship between volatility and other market microstructure covariates at a high frequency level. Moreover, with a parametric assumption, not only an integrated variance estimator, but also a local volatility estimator (intraday volatility or real-time volatility) can be obtained, as opposed to realized volatility mentioned in the previous section. By simulation, Tse and Yang (2012) show that the price duration-based volatility estimator is more efficient than the realized volatility estimators, and Hong et al. (2021) find that it has a better forecast performance than the realized volatility type estimators. However, this estimator did not receive equal attention as the realized volatility type estimators, partly due to its confinement to only a univariate case.

The difficulties of extending above price duration volatility estimators to multivariate framework are two-fold: on the discreteness of price duration and on the non-decreasing monotone of integrated volatility. First, the discreteness of price duration, as we pointed out in Section § 2.1.1, allows only fixed-path conditional intensity, which is unable to update new information arrivals within waiting times and deters the price duration models from capturing co-volatility in a setting with asynchronous tradings. Second, the price

duration volatility model has to rely on the non-decreasing monotonic property of integrated volatility to construct a renewal point process in integrated variation time. However, within a multivariate framework with another concern of co-variation (co-volatility), the non-decreasing monotone is no longer valid. Therefore, the covariation estimation needs a tailor-made econometrics model to ameliorate the impact of asynchronous trading between assets, particularly the Epps and lead-lag effects mentioned in Section § 2.1.3.

Motivated by the above studies of a point process approach-based volatility estimator, we derive in Chapter 4 a multivariate estimation of integrated (co)-variation based on the conditional intensities. In order to account for the interdependence between assets, instead of ACD-type models, we suggest using multivariate Hawkes processes to model the continuous conditional intensity function of price change transaction, i.e. transaction marked by the number of ticks it moves the price. With its parsimonious representation of self-cross exciting effects in the conditional intensity, our model still preserves superior features of the price duration-based estimator, while it can take into account the interdependence between assets by addressing salient properties of ultra-high frequency data sets.

2.2.3 *Intraday Value-at-Risk measures*

Computerized trading, aided by the rise of ultra-high frequency data, has been dominant in the modern financial markets. This type of trading is characterized by a very short investment horizon, at time frames of minutes to minutes or even a few microseconds (Hasbrouck, 2019; Menkveld, 2018; O'Hara, 2015). Within these horizons, accurately capturing the entire distribution of price dynamics becomes impracticable and unfeasible. For example, to invoke consistency through its asymptotic properties, the estimate of the second-moment structure relying on popular realized volatility requires a large amount of infilled data which are often difficult to obtain in such small windows (Tse and Yang, 2012). Meanwhile, a more efficient and feasible way is to consider only the tail, which represents the probability of extreme events, rather than the whole distribution of price movements. In the time scales where much of the volatility is evoked by the noise, the measures of extreme events seem to be more qualified market risk information than the back and forth bounces or the excessive number of zero movements of price due to market microstructure. Therefore, a part of the literature on high frequency risk measures has shifted its research to tail risk measures, and the one of simplicity but wide applicability and universality is intraday Value-at-Risk (IVaR). According to (Coroneo and Veredas, 2012; Dionne, Duchesne and Pacurar, 2009; Giot, 2005; Tse and Yang, 2012), IVaR is a useful tool to define risk profiles, monitor risk, and measure performance; for market makers, screen traders, high frequency traders, or anyone else who strategically opens and closes positions during the day. IVaR provides a more complete picture than a daily VaR measure, accounting for intraday information. However, the literature on IVaR measures, to the best of our knowledge, involves only a univariate framework.

The econometric modelling of intradaily market risk using tick-by-tick data was first studied in Giot (2005), where the authors recognize the importance of assessing intradaily

trading risks in a modern financial market. By assuming that the fat-tailed properties of return distributions on daily data are still valid on intraday data, he resamples the data to regularly spaced returns and studies the performance of the one-step ahead VaR predicted by normal GARCH, Student GARCH, RiskMetrics. In addition, to take into account the information conveyed by the irregularly spaced trading times on IVaR, he uses a price duration volatility estimator with a log-ACD model (Bauwens and Giot, 2000). Based on his empirical findings, the IVaR based on price duration volatility surprisingly underperforms its counterpart using the standard time series models, e.g. the Student-GARCH model. He also comments that the underperformance might be the consequence of the normal distribution assumption on the return, and of the time transformations to the regularly time-spaced world for evaluation purposes with other approaches. Later, Dionne, Duchesne and Pacurar (2009) investigate the use of irregularly spaced tick-by-tick data and propose an IVaR which is based on an ultra high frequency GARCH-type model (Engle, 2000) combining with a Monte Carlo simulation. They demonstrate rather satisfactory results for their IVaR, which incorporates tick-by-tick information, in their evaluation using backtesting methods. Coroneo and Veredas (2012) propose an estimate of IVaR based on a distribution-free quantile regression approach for equidistant sampled high frequency return. Their approach allows for the construction of conditional return moments measures simply depending on explanatory variables and without necessary knowledge about the functional forms of these moments or of the return distribution. More recently, Liu and Tse (2015) apply a two-state asymmetric auto-regressive conditional duration model (AACD) (Tay et al., 2011) to model bidirectional price duration events, which are classified into upward and downward directional price movements. The estimated AACD is then cast into a Monte Carlo simulation to forecast ex-ante return distribution, from which IVaR is calculated. The results of the backtest show that IVaR calculated using a sophisticated bidirectional price duration scheme outperforms previous methods using simply absolute threshold price duration in Dionne, Duchesne and Pacurar (2009) and Giot (2005).

The common point of the above-mentioned univariate IVaR methods is to look at slices of the conditional distribution of the transaction point process, i.e. the transactions that move the price at least a certain price change level, without any reliance on global distribution. Specifically, the strategy pursued in these methods is to concentrate on the waiting times to occur extreme price transaction events, which is demonstrated to be significantly serial dependent. The IVaR forecasts are then determined by the conditional expected duration between the extreme price events, which can be consecutively estimated by the ACD models. However, as our critical review in Section § 2.1.1 shows, the discreteness of ACD models hinders the extension of IVaR to a multivariate framework, which requires a consideration of cross-effects between assets in an asynchronous transaction context. The problem is that the ACD-type model is unable to adjust the arrival rate of a new price event when novel information arrives within a duration. It has to wait until the arrival of the point process terminates, which causes a loss of cross-dependence information between assets. A more appropriate approach that overcomes the difficulties of ACD models in a multivariate framework is directly modelling the continuous conditional intensity func-

tion; thus, it allows for a continuous updating of the information set in the extreme price event processes.

A predominant model type for this purpose, in temporal settings, is based on multivariate Hawkes processes (Bacry, Mastromatteo and Muzy, 2015; Bowsher, 2007; Hawkes, 1971; Hawkes and Oakes, 1974). Hawkes processes have also been used to model extreme price movements at a rather low frequency (Bieñ-Barkowska, 2020; Chavez-Demoulin, Davison and McNeil, 2005; Chavez-Demoulin, Embrechts and Sardy, 2014; Embrechts, Liniger and Lin, 2011; Grothe, Korniiichuk and Manner, 2014; Hautsch and Herrera, 2019). In a high frequency trading context, the pioneer work of Chavez-Demoulin and McGill (2012) extends Chavez-Demoulin, Davison and McNeil (2005)'s Hawkes-Peak Over Threshold (Hawkes-POT), which models the clustering behaviour of extreme events over a threshold, to intraday risk measures. The idea is to couple the Hawkes process and classical extreme value theory in a model, where the former captures the intensity of threshold exceedance events and the latter for the clustering of excess size in the occurrences. The Hawkes-POT has the same spirit as the previously mentioned approach, that is to focus on temporal dependence of extreme price events in the tail, the part directly contributing to the risk, while ignoring the less important structure of moderate price events. Although the model, using the Hawkes process, has a lot of flexibility in modelling the occurrences of extreme price events, the Hawkes-POT still exists only in a univariate framework due to the complexity of its structure and its exceedance threshold selection (Chavez-Demoulin, Embrechts and Sardy, 2014).

Considering the recent developments in modelling IVaR, we realize that there is still a gap for an IVaR model that has the ability of taking into account the temporal cross-dependence structure, for multiple assets, of extreme price events in the view that they are clustering in the tail of distributions. Most often, it is not a true reflection of reality to assume that the price movements of two related assets are independent, especially when one considers the probability of their extreme moves, which are often the result of common information (Cousin and Bernardino, 2013; Grothe, Korniiichuk and Manner, 2014). For the univariate case, the marginal probability structure might be sufficient, but when it comes to the multi-asset framework, they might interact with each other in extreme events, which consequently cause contagion or simply lead-lag effects, as we mentioned in Section § 2.1.3. In Chapter 5, we develop a multivariate IVaR model that incorporates these elements into its risk metrics in a high frequency trading context, which would give a better/more informed measure of IVaR in one asset and in a combined way in an intraday portfolio.

ASYMMETRIC INFORMATION, INFORMATION LIFE SPAN, AND LEAD-LAG EFFECTS ON A MULTIVARIATE PRICE FORMATION DYNAMICS

Abstract

The information content of trades has a life. We define the life span of trade information as an effective time scale on which the information lives and contributes to price formation processes. In terms of long-lived information, the price adjustment turns out to be sluggish in the sense that it takes time to incorporate the information fully. According to this logic of information discovery, we introduce a multi-asset price formation model in transaction frequency, which generalizes previous microstructure models of lagged price adjustment. The model can be considered as a combination of microstructure models on lagged price adjustment and on asymmetric information. Econometric inference from the model proves the indispensability of a multi-asset price formation mechanism at the finest microscopic frequency. The model also shows its advantage in recovering the lead-lag structure of the true underlying values not only at the cross-transaction level, but also for any arbitrary interval. Our application to a set of selected DJIA stocks provides empirical evidence of the existence of a multi-asset transaction-by-transaction price formation mechanism and sheds light on its market microstructure determinants.

Keyword: Asymmetric information, information life span, Lagged price adjustment, Lead-lag effects, Hawkes process, asynchronous trading.

3.1 INTRODUCTION

If financial prices are semi-martingales, all relevant information about underlying values should be immediately disseminated, equally interpreted, and instantaneously incorporated into price processes. In a modern real financial market, there always exist heterogeneous market participants (Glosten and Milgrom, 1985; Kyle, 1985), endowed with different knowledge regarding the underlying values and capitalizing on their own information advantages. At the high-frequency trading level, various complications arise, including asymmetric information, strategic trading, and price learning, as natural phenomena (Glosten and Milgrom, 1985; Holden and Subrahmanyam, 1992; Kyle, 1985; Vives, 1995). The complex environment generated by such features is in contradiction with the arbitrage-free efficient market implied by the semi-martingales behaviour. So, if the semi-martingale prices are not valid, then the fundamental questions are how information is diffused at tick level and how do prices react to information diffusion. It is to discover a price formation mechanism that elicits dispersed information from heterogeneously informed agents on the true value of what underlies it. By this mechanism, the price processes converge to the true values not immediately, but gradually with a speed, namely the speed of price adjustment.

To do so, we consider a new property of information: information has a lifespan, that is, the time it takes for information to be assimilated into the price dynamics. Such a lifespan converges to zero under the null that the observed price processes impound all available information and behave as semi-martingales. But under the natural “frictional” alternative rooted in market microstructure theories, the lifespan of information deviates from zero and causes sluggishness in the recovery of the true underlying value.

What leads to the existence of the information lifespan? In a rational behaviour market, informed agents have some kinds of heterogeneity with respect to the underlying value and trade on their own information with the intermediation of zero-expected profit market makers in the presence of noise or a liquidity trader (Glosten and Milgrom, 1985; Kyle, 1985; O’Hara, 1998). Each of the informed traders has some belief about the unknown underlying values, and their collective beliefs reveal the true efficient prices. They trade wisely, exploit their advantages in information, and their trading strategies hinder other traders and market makers from accessing their information. Informed traders submit market orders to market makers who set prices efficiently, conditional on the aggregate order flow. More precisely, the market makers may not buy and sell randomly, but set quoted prices upon observing the order book and examining their previous transactions. In the sense that they observe a noisy signal of the aggregate information, the market makers can make errors in their pricing of order flows, but they can also retrieve improved information from their historical trades to set better quoted prices. However, their lagged adjustments are not perfect either, and only partially missing information can be recovered and incorporated in future quoted prices. The described imperfection of price adjustment makes the impacts of trades last for an interval of time, that is, the lifespan of trade (information). In

other words, there exists a duration after which the information content of trade becomes obsolete and no longer has an impact on the future price movement.

Motivated by this logic of information discovery, we introduce a multi-asset price formation mechanism at transaction-by-transaction frequency, which generalizes previous microstructure models of lagged price adjustment (see Hasbrouck, 1996 for a review on univariate lagged price adjustment models and Buccheri, Corsi and Peluso, 2020 for a very first model on multivariate assets). The lagged price adjustment models, also known as partial price adjustment models, were originally introduced in the market microstructure to account for temporal own- and cross-correlations, which are also termed lead-lag effects amongst high frequency returns. Our multivariate generalization, namely multivariate asymmetric lagged adjustment model (MALA), departs from the work of Buccheri, Corsi and Peluso (2020) which can be considered as the multivariate lagged adjustment (MLA) of aggregated prices, and decomposes the puzzle of lagged adjustment into two distinct and subsequent imperfections of the market: inherent asymmetric information at the transaction frequency and partial adjustment to the information content of trade. The MALA, to a large extent, strengthens the theoretical results in the MLA and provides new insights into the imperfections of price adjustment which provide a comprehensive description of price formation in more general settings.

Without modelling informed trading, the classical lagged price adjustment models show how the imperfect price adjustment arises as a consequence of delaying dissemination of information, i.e. some assets trade ahead and carry information about other assets. The prices react in a constant and same manner to all kinds of information without accounting for the distinction between the impacts from the information of order flow and the information of trade. The MALA relaxes these assumptions and takes into account the distinct impact of asymmetric information. By including informed trading, the MALA allows for an additional and more detailed explanation relating the lead-lag correlation to asymmetric information and trading. Bernhardt and Mahani (2007), Boulatov, Hendershott and Livdan (2012) and Chordia, Sarkar and Subrahmanyam (2011) point out the role of privately observed systematic information, i.e. informed trading, in causing positive cross-autocorrelation, the analogue of lead-lag effects on lower frequency trading with regularly spaced time. Also, considering that the information content of trade is long-lived and has a lifespan, we extend the constancy assumption and apply a fast-decaying impact of trade over time. If the information content of trade is short-lived, then the trade sequence is independent across time, and the returns are uncorrelated in asynchronous trading according to Epps effects. If information is long-lived, as in our model, then trades across assets become temporally correlated and give rise to lead-lag effects.

Furthermore, the MALA also contributes to the current literature on lead-lag effects, which has received some attention (see Bernhardt and Mahani, 2007; Buccheri, Corsi and Peluso, 2020; Chan, 1992, 1993; Chiao, Hung and Lee, 2004; Hayashi and Koike, 2017, 2018, 2019; Hoffmann, Rosenbaum and Yoshida, 2013; Huth and Abergel, 2014; Jong and Nijman, 1997), but still lacks a well-established econometric framework that describes the existence of lead-lag effects from the finest microscopic perspective of market microstructure. Eco-

nometric inference on the MALA allows us to measure lead-lag correlations formally in the latent underlying values not only at any arbitrary fixed sampling interval but also at cross-transaction frequency, which provides evidence for the inevitability of multi-asset price formation processes at transaction-by-transaction level. Furthermore, by separating two sources demonstrating the strength of lead-lag effects, i.e. trade-carrying information and liquidity, the MALA provides a comprehensive picture on these two driving sources of lead-lag correlations. The current literature on lead-lag correlation has mainly considered only one of the two, the information content of trade or the liquidity, and ignored the combined effects between them.

Econometric inference of the MALA can be conveniently obtained by casting the model into a Hawkes system of disjoint price change point processes. The transition dynamics is a vector of autoregressive processes (VAR) for the observed price changes, which account for the microstructure noises as additive white-noise error terms. Because the distinguishing feature of transaction-by-transaction prices is discreteness, i.e. such finely sampled price changes take on only five or six distinct states, the joint dynamics of trading time and dependent price movements can be decomposed and modelled as multivariate disjoint price change processes corresponding to all possible observed discrete states. The counting processes of these disjoint price change states can be viewed as nonzero integer-valued autoregressive time series (INAR), and thus their conditional distribution can be fed into the exo(geneous)-endo(geneous) mechanism of multivariate Hawkes processes (Kirchner, 2016b; Wheatley, Wehrli and Sornette, 2019). The Hawkes model was first developed by Hawkes (1971) and Hawkes and Oakes (1974), highlighting the basic idea of autoregression in a continuous setting in a compact and meaningful way, and thus has attracted a considerable amount of interest in financial econometrics (see Bacry, Mastromatteo and Muzy, 2015; Hawkes, 2017 for recent reviews). This approach allows us to estimate the parameters using all the information available on the transaction processes and avoid the limitations of the state-space approach proposed by Buccheri, Corsi and Peluso (2020) to estimate the MLA. For instance, while the latter has to aggregate the price at an optimal frequency for feasible estimation by the Kalman-EM algorithm, the former can handle all observations at the transaction level, at which only one transaction corresponding to the traded asset is observed at each timestamp, and the latter is not able to manage. Also, estimating at the transaction level, the former provides the true correlation incurred by each transaction, and the lead-lag correlation between assets can be simply recovered for any arbitrary interval instead of only at a fixed interval in the latter.

Similarly to the MLA, the MALA has a one-to-one correspondence between the matrix of lead-lag coefficients in the VAR of observed prices and the matrix of adjustment speeds in the price formation of true underlying values. The statistical significance of lead-lag correlations at the transaction level can thus prove the indispensability of multi-asset price formation mechanism at the finest frequency. Together with liquidity level, i.e. trading activity, we also propose a measure of lead-lag effects amongst assets. The MALA is then tested on a cross section of DJIA high-frequency transaction data. The significant cross-asset adjustment kernels recovered from the estimated Hawkes excitement coefficients

provide empirical evidence for the existence of a multi-asset price formation at transaction-by-transaction frequency. We also examine in detail the relationship between liquidity level and lead-lag effects amongst selected assets. The results obtained generally confirm the common empirical finding that high liquid assets often play the role of leaders in the market. However, there is also the case that some assets are less active in trading but highly informative, i.e. their trade carries large amount of information on prices, and can lead the dynamics of more liquid assets. Finally, the robustness of the model is tested with respect to the random walk of exogenous components.

The chapter continues as follows. Section § 3.2 provides a theoretical framework for our MALA model. The section also provides a formal formulation of the lead-lag effects resulting from the price dynamics of the MALA. In Section § 3.3, we put forward a disjoint price change representation to transition VAR of observed price changes, which we will cast into multivariate Hawkes point process for estimation. Section § 3.4 studies descriptive analysis of the data and empirical interdependence between states of price change. In Section § 3.5, we discuss the results from both methods of estimation: non-parametric and parametric. Conclusions and directions for future research are contained in Section § 3.6.

3.2 THEORETICAL FRAMEWORK

3.2.1 *The multi-asset asymmetric lagged adjustment model*

We consider a multivariate price formation framework that features multiple assets with different price adjustment speeds and multiple agents who own different degrees of information. The model captures the effects described in the Introduction § 3.1: informed traders possess superior information about the true underlying values and submit market orders contingent on their advantages of information. Hypothesized publicly-informed market makers set quoted prices, conditional on their observation of the aggregate order flows and their revision of historical transaction prices. Finally, the observed prices taken on the market are prices contaminated by market microstructure noise. Therefore, the model has three components: efficient price processes, adjusted price quotes, and observed contaminated prices. For coherence with the market microstructure literature, the former is specified in continuous time, whereas the two latter prices are specified in discrete time.

We assume that the efficient log-price \mathbf{Y}_t is a D -dimensional vector that evolves as a Brownian semi-martingale defined on some filtered probability space $(\Omega^Y, \mathcal{F}, (\mathcal{F}_t), \mathcal{P})$, where in particular, $(\mathcal{F}_t) \subseteq \mathcal{F}$ is an increasing family of σ -fields satisfying \mathcal{P} -completeness and right continuity:

$$\mathbf{Y}_t = \int_0^t \mathbf{A}_s ds + \int_0^t \mathbf{\Theta}_s d\mathbf{W}_s, \quad \mathbf{\Sigma}_t = \mathbf{\Theta}_t \mathbf{\Theta}_t^\top \quad (3.1)$$

where $t \in [0, T]$, \mathbf{A}_t is a D -dimensional vector of predictable locally bounded drifts, $\mathbf{\Theta}_t$ is a $D \times D$ -dimensional volatility matrix, and \mathbf{W}_t is a D -dimensional vector of independent Brownian motions. The interval $[0, T]$ can be thought of as representing the trading day.

Let $0 \leq t_1^d, \dots, t_{N^d(T)}^d \leq T$ denote the strictly increasing observation times of the transaction process for asset d , with $d \in [1, D]$, and $N^d(t)$ denote the right continuous counting function that counts the cumulative number of transactions in the point process d up to time t . We also denote $0 \leq t_1, \dots, t_{N(T)} \leq T$ as the pooled point process of all D marginal point processes, which means $N(t) = \sum_{d=1}^D N^d(t)$ and the duration between traded in the pooled transaction process is $\tau_i = t_{i+1} - t_i$, $i \in [1, N(T)]$. In ultra-high-frequency data, the effect of drift is very minor and negligible. Thus, we assume that the drift term in Eqn. 3.1 is zero for simplicity. Denoting $\Delta \mathbf{Y}_{t_{i+1}} = \mathbf{Y}_{t_{i+1}} - \mathbf{Y}_{t_i}$ the log-returns of the efficient price, we can write:

$$\Delta \mathbf{Y}_{t_{i+1}} = \int_{t_i}^{t_{i+1}} \Theta_s d\mathbf{W}_s \quad (3.2)$$

These efficient log-returns reflect all information about the underlying values that occurred within the interval $[t_i, t_{i+1})$. They are the returns that, abstracting from microstructure effects, would only be observable in an imaginary perfect world. In that world, price-relevant information is distributed and interpreted by all market participants, and when new information arrives, prices are instantly adjusted to reflect all available information. However, in a modern real financial market, there always exist heterogeneous informed traders who have better knowledge of relevant price information and try to capitalize on the information they have (Glosten and Milgrom, 1985; Kyle, 1985; O'Hara, 1998). Each informed trader has a small piece of information about the efficient price \mathbf{Y} , and the collective information of all informed traders reveals \mathbf{Y} . They submit market orders contingent on the information they have about \mathbf{Y} . Moreover, in order to maximize their advantages, the informed traders also strategically exploit the information by minimizing the informational impact of his trades. Their trading strategy hinders the market maker's ability to access complete information about \mathbf{Y} .

Informed traders have an information advantage over market makers because of their private signals, but market makers observe noisy signals of the aggregate position of informed traders. Market makers cautiously analyze the noisy signals and also examine their previous transactions, uncovering hidden information, and setting their price quotes. In response to the noisy signals of the incoming order flows, they adjust the price quotes by a vector of coefficients γ to the true movements of the underlying values $\gamma \Delta \mathbf{Y}$ where γ can be thought of as parameters that reflect the probability of informed traders, the mispricing of market makers, or to a large extent, the efficiency of the market. If the signals do not contain noise, γ will be the identity vector and the quoted prices will be completely adjusted to the signals.

Although market makers make errors in their pricing of noisy order flows, they can retrieve improved information on previous transaction prices. But these lagged adjustments of market makers are not perfect either and recover partially missing information. This feature of imperfect lagged adjustment was studied in partial lagged adjustment models with constant coefficients by Amihud and Mendelson (1987), Buccheri, Corsi and Peluso (2020), Damodaran (1993) and Hasbrouck and Ho (1987). We adapt these models to take into account inherent features at the transaction-by-transaction level, such as informed trading and decaying information over time, by assuming the imperfection of lagged ad-

justment processes can be characterized by a function of elapsed time from the occurrence of transactions.

Denoting P_{t_i} , $i = 1, \dots, N(T)$ as a D -dimensional vector of quoted prices. To set price quotes at time t_i , in addition to adjusting to the noisy signals by $\gamma \Delta Y_{t_i}$, market makers also revise the deviation of the previous quote to the efficient prices with the speed of adjustment given by functions $\Psi_{t_{i-1}}(\tau_i)$, where $\tau_i = t_i - t_{i-1}$ is the time elapsed between two consecutive price quotes and the subscript t_{i-1} denotes the transaction incurring adjustment. The improved information is then reflected in the new quote at time t_i by an amount $\Psi_{t_{i-1}}(\tau_i)(Y_{t_{i-1}} - P_{t_{i-1}})$.

At t_0 , the beginning of the trading day, we assume that the observed prices reflect all related information. It is a reasonable assumption because, at the opening, there is an important feature of stock markets that resembles a call auction market. All market and limit orders are submitted to market makers (in the role of specialists), and market makers will accumulate them and determine opening prices. We consider the opening prices that are adjusted to all the demand and supply of the market:

$$P_{t_0} = Y_{t_0} \quad (3.3)$$

where P_{t_0} denotes the D -dimensional adjustment prices at time t_0 .

At t_1 , the first trade on the trading day, traders start submitting their market orders using the information they have. Observing only noisy signals of order flows in the first trade, market makers set trading prices cautiously by assigning the probability that the trade is motivated by informed traders, reflected by a D -dimensional vector of parameters γ . Note that γ contains non-negative and time-varying coefficients that enable different uncertainty levels of the market over a trading day. The quoted prices P_{t_1} are given by:

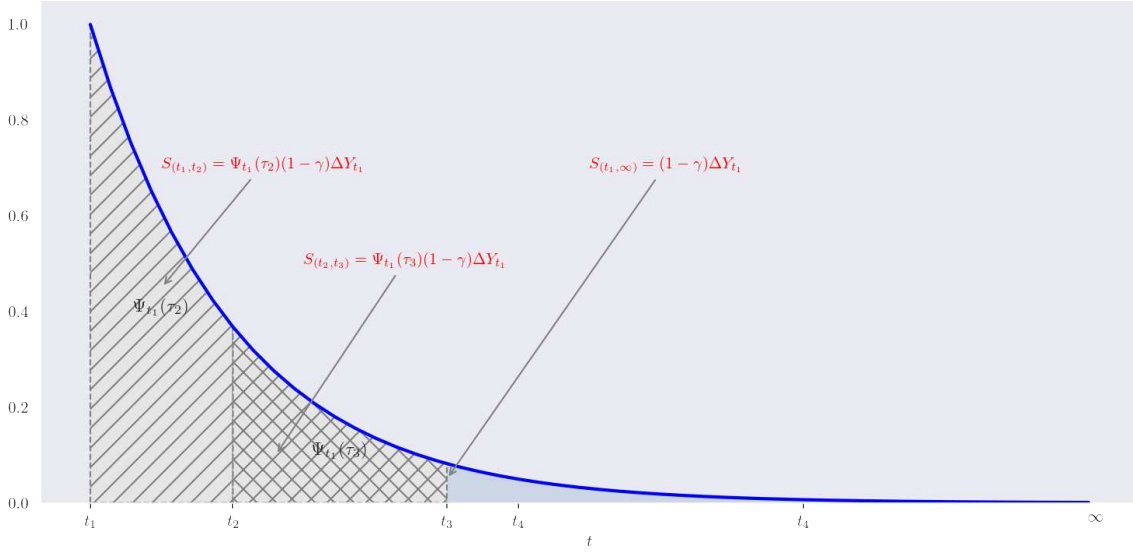
$$Y_{t_1} = Y_{t_0} + \int_{t_0}^{t_1} \Theta_s dW_s \quad (3.4)$$

$$P_{t_1} = P_{t_0} + \gamma \Delta Y_{t_1} \quad (3.5)$$

Because the efficient prices and the adjustment prices are not observable, we consider the D -dimensional vector of observed log-price processes X_{t_i} that is contaminated by market microstructure noise, i.e. transaction costs. It is worth mentioning here that due to asynchronous trading, only one component of X_{t_i} corresponding to the traded asset is observed at each time t_i , while the movements of the remaining assets are not observable. The vector of prices, X_{t_1} , contaminated by microstructure noise u_{t_1} are observed as:

$$X_{t_1} = P_{t_1} + u_{t_1} \quad (3.6)$$

At t_2 , market makers continue to observe the aggregated order flows of the second trade, jointly examining the deviation of the previous transaction from the efficient prices, and

Figure 3.1: An illustration about the shape of lagged adjustment kernels Ψ 

Notes: The blue line illustrates adjustments on quoted prices t_2, t_3, \dots incurred by a transaction occurring at t_1 . The shaded areas under the blue line, denoted by $S_{(\cdot, \cdot)}$, are innovations recovered from the missing information $(1 - \gamma)\Delta Y_{t_1}$

accordingly adjusting their second price quotes with improved information. The informed trading and imperfect learning are accommodated explicitly by the following specification:

$$P_{t_2} = P_{t_1} + \gamma\Delta Y_{t_2} + \Psi_{t_1}(\tau_2)(Y_{t_1} - P_{t_1}) \quad (3.7)$$

$$X_{t_2} = Y_{t_2} + u_{t_2} \quad (3.8)$$

where the corresponding change in the adjustment price that reflects relevant information obtained by the market makers is:

$$\Delta P_{t_2} = \gamma\Delta Y_{t_2} + \Psi_{t_1}(\tau_2)(1 - \gamma)\Delta Y_{t_1} \quad (3.9)$$

Note that $\Psi_{t_1}(\tau_2)$ in Eqn. 3.9 measures the adjustment that market makers make to improve their mispricing at t_1 , that is, missing information on efficient price changes in previous quotes $(1 - \gamma)\Delta Y_{t_1}$.

Moving on, let us discuss the trade at t_3 . Similarly, market makers continue to adjust the price correspondingly to order flows and previous transactions, including the most recent t_2 but also the transaction t_1 :

$$\begin{aligned} \Delta P_{t_3} &= \gamma\Delta Y_{t_3} + \Psi_{t_2}(\tau_3)(Y_{t_2} - P_{t_2}) \\ &= \gamma\Delta Y_{t_3} + \sum_{i=1}^2 \Psi_{t_2}(\tau_3)(\Delta Y_{t_i} - \Delta P_{t_i}) \\ &= \gamma\Delta Y_{t_3} + \Psi_{t_2}(\tau_3)(1 - \gamma)\Delta Y_{t_2} + \Psi_{t_2}(\tau_3)\Psi_{t_1}(\tau_2)(1 - \gamma)\Delta Y_{t_1} + \Psi_{t_2}(\tau_3)(1 - \gamma)\Delta Y_{t_1} \\ &= \gamma\Delta Y_{t_3} + \Psi_{t_2}(\tau_3)(1 - \gamma)\Delta Y_{t_2} + \Psi_{t_1}(\tau_3)(1 - \gamma)\Delta Y_{t_1} \end{aligned} \quad (3.10)$$

The third equality is obtained by substituting Eqn. 3.9, whereas the last equality is derived by the following property that we impose on the adjustment function:

$$\Psi_{t_1}(\tau_3) = [1 - \Psi_{t_1}(\tau_2)]\Psi_{t_2}(\tau_3) \quad (3.11)$$

Recall that the first term on the LHS of the above equation quantifies the remaining amount of missing information on the changes in the efficient price at the transaction t_1 . The second term measures the adjustment to the missing information, but as it occurs at its origin t_2 . The product of them, the term on the RHS, measures the innovation recovered during the interval $\tau_3 = t_3 - t_2$ from the mispricing at t_1 .

Extending Eqn. 3.11 to multiple periods, the adjustment kernels are defined such that:

$$\Psi_{t_i}(\tau_{i+j}) = \prod_{p=1}^{j-1} [1 - \Psi_{t_{i+p-1}}(\tau_{i+p})]\Psi_{t_{i+j-1}}(\tau_{i+j}) \quad (3.12)$$

An example of an adjustment kernel satisfying the above property is the integration of an exponential function, that is, $\Psi_{t_i}^{dr}(\tau_j) = \int_{t_{j-1}}^{t_j} e^{-\beta^{dr}(t-t_i)} dt$ with β^{dr} being the coefficient controlling the slope of the function or the adjustment speed based on the transaction of the asset r to the quoted price of the asset d , $d, r \in [1, D]$ (see Fig. 3.1).

The choice of adjustment kernels, $\{\Psi_{t_i}^{dr}(\tau)\}_{d,r \in [1,D]}$, is critical for the speed of updating missing information from previous transactions about the true efficient prices \mathbf{Y}_{t_i} on the current price quotes \mathbf{P}_{t_i} . If $\Psi_t(\tau) = \mathbb{I}_D$, then $\Delta \mathbf{P}_{t_i} = \gamma \Delta \mathbf{Y}_{t_i}$, the only missing part of the current trade is from the asymmetric information component and will be fully recovered in the next transaction. Instead, if the diagonal element $0 < \{\Psi_{t_i}^{dd}(\tau)\}_{d \in [1,D]} < 1$, the adjustment process is gradual, and consequently there exists missing information on \mathbf{P}_{t_i} not only from informed trading on the current trade, but also from delayed adjustment on previous trades. It is important to note here that $\Psi_t(\tau)$ may be non-diagonal. According to Buccheri, Corsi and Peluso (2020), the non-diagonal $\{\Psi_t^{dr}(\tau)\}_{d,r \in [1,D], d \neq r}$ implies that the adjustment process of one asset is affected by the adjustment process of other assets, which results in lead-lag effects that we will discuss in the next section § 3.2.2.

In addition to the property in Eqn. 3.12, we make the following assumptions about the adjustment price kernel $\Psi_t(\tau) = \{\Psi_t^{dr}(\tau)\}_{d,r \in [1,D]}$:

- (H1) $\Psi_t(\tau)$ is component-wise causal, i.e. for $\tau < 0$, $\Psi^{dr}(\tau) = 0, \forall d, r \in [1, D]$.
- (H2) $\Psi_t(\tau)$ is component-wise positive, i.e. $\Psi_t^{dr}(\tau) \geq 0, \forall d, r \in [1, D]$.
- (H3) $\Psi_t(\tau)$ is additive, i.e. for $\tau_i, \tau_{i+1} \geq 0$, $\Psi_t(\tau_i) + \Psi_t(\tau_{i+1}) = \Psi_t(\tau_{i-1, i+1})$ where $\tau_i = t_i - t_{i-1}$, $\tau_{i+1} = t_{i+1} - t_i$, and $\tau_{i, i+1} = t_{i+1} - t_{i-1}$.
- (H4) $\lim_{\tau \rightarrow \infty} \sum_{r=1}^D \Psi_t^{dr}(\tau) ds = 1, \forall d \in [1, D]$.
- (H5) $\Psi_t^{dr}(\tau)$ are accelerated decaying functions on $\tau \forall d, r \in [1, D]$, i.e. for $j > i \geq 1$, the differential $(\Psi_t^{dr})'(\tau_i) \gg (\Psi_t^{dr})'(\tau_j)$ where $\tau_i = t_i - t_{i-1}$, and $\tau_j = t_j - t_{j-1}$
- (H6) $\Psi_t^{dr}(\tau_i) \gg \Psi_t^{dr}(\tau_i) \Psi_t^{pq}(\tau_j) \forall d, r, p, q \in [1, D]$ for $j > i \geq 1$

The Assumptions **(H1)**, **(H2)**, **(H3)** and **(H4)** are natural conditions of the price adjustment kernels. **(H1)** indicates that the market makers cannot infer information on the trade that has not yet arrived. **(H2)**, the more transactions are observed, the more extra signals of the true underlying values are recovered by market makers to improve the adjustment prices. **(H3)** is simply the additive properties of information extracted from past transaction prices and of price adjustment between two distinct periods. **(H4)** ensures the maximal retrieved information is always lower than the true information of the underlying values. The two remaining assumptions **(H5)**, **(H6)** determine the shape of the adjustment price functions over time. Specifically, **(H5)** is about the amount of information that can be retrieved from the past prices. The farther away a transaction is, the less impact of that trade's information content on the current price quotes. Finally, **(H6)** is about "obsolescence" of the information. If a signal on the true underlying value is already retrieved, that signal is exhausted, and continuing to dig into that signal does not provide more improved information to the price processes.

The model is then extended to subsequent transactions. We note that there are a total of $N(T)$ transactions during the period $[0, T]$ that represents a trading day. We have the following results:

Proposition 1. *Assume that the price adjustment kernel, $\Psi_t(\tau) = \{\Psi_t^{dr}(\tau)\}_{d,r \in [1,D]}$, satisfies the Assumptions **(H1-H6)**. At transaction t_{i+1} , the three components of prices are given by:*

$$\mathbf{Y}_{t_{i+1}} = \mathbf{Y}_{t_i} + \int_{t_i}^{t_{i+1}} \Theta_s d\mathbf{W}_s \quad (3.13)$$

$$\mathbf{P}_{t_{i+1}} = \mathbf{P}_{t_i} + \gamma \Delta \mathbf{Y}_{t_{i+1}} + \Psi_{t_i}(\tau_{i+1})(\mathbf{Y}_{t_i} - \mathbf{P}_{t_i}) \quad (3.14)$$

$$\mathbf{X}_{t_{i+1}} = \mathbf{P}_{t_{i+1}} + \mathbf{u}_{t_{i+1}} \quad (3.15)$$

Eqn. 3.15 is observable transaction prices, which are contaminated by additive micro-structure noise, taken by traders. Instead, Eqn. 3.14 can be represented as a VAR that describes the dynamics of the latent quoted price set by market makers. The quoted prices can be decomposed into three components: (1) \mathbf{P}_{t_i} , the information incorporated in the past price, (2) $\gamma \Delta \mathbf{Y}_{t_{i+1}}$ the current price innovation that is adjusted in response to the noisy signals of aggregate order flows, and (3) $\Psi_{t_i}(\tau_{i+1})(\mathbf{Y}_{t_i} - \mathbf{P}_{t_i})$ the price revision after retrieving improved information on the historical transaction prices. The last term accounts for the additional signals not only from the stock itself but also from other related stocks. The change in the price quotes can be represented as follows:

$$\Delta \mathbf{P}_{t_{i+1}} = \gamma \Delta \mathbf{Y}_{t_{i+1}} + \sum_{j=1}^i (1 - \gamma) \Psi_{t_j}(\tau_{i+1}) \Delta \mathbf{Y}_{t_j} \quad (3.16)$$

The adjustment of market makers on the price quotes $\Delta \mathbf{P}_{t_{i+1}}$ starts from (1) their history-based revisions $\sum_{j=1}^i (1 - \gamma) \Psi_{t_j}(\tau_{i+1}) \Delta \mathbf{Y}_{t_j}$, which are updated with the speed functions $\Psi_{t_j}(\tau_{i+1})$, and combine with (2) their interpretation of the noisy signals about the efficient price changes $\gamma \Delta \mathbf{Y}_{t_{i+1}}$, of which the uncertainty of the market makers is reflected in the parameters γ . Thus, the model assumes that not only can informed traders determine

prices, but also market makers can set prices based on their own information. The market makers do not observe information directly, but instead can observe aggregate order flows of informed traders, revise their belief on historical transactions, and determine prices conditional on those elements.

Finally, one might question the non-convergence of our model that the quoted prices always deviate from their true underlying values. Let us assume that there exists a period without asymmetric information, where the market makers have an entire picture of the true underlying values. In practice, this period can be at the end of the trading day when a closing call auction takes place. Similarly to an open-call auction, all orders are aggregated and matched up with one another at the prices determined by the market makers. These last transaction price changes can be regarded as those that reflect all relevant information available and have no uncertainty, i.e. $\gamma = \mathbf{0}^\top$. Furthermore, since informed traders would prefer to act with their superior information before the markets are closed, avoiding the information that can be published during the overnight period, the markets have a tendency of being significantly more opaque towards the end of a continuous trading session. Regarding the last transactions of the continuous trading session, the missing information on the underlying values is trivial, and a shorter duration is required for complete adjustment on these trades. The closing call auction often lasts for a duration that is substantially longer than the lifespan of trade. Therefore, it is realistic to consider that the last quoted prices of the close-call auction converge to their efficient ones at the end, i.e. $\mathbf{P}_{t_{N(T)}} = \mathbf{Y}_{t_{N(T)}}$.

3.2.2 Lead-lag effects

In the previous section, we constructed a model of price dynamics for multiple assets in an environment that allows for asymmetric information and imperfect price adjustment. For a stock d in a portfolio of D stocks, its price change dynamics is given by the following corollary:

Corollary 1. *Given a portfolio of D stocks following the price dynamics of Proposition 1. The price dynamics of the stock d , $d \in [1, D]$ at an observed transaction t_{i+1}^d is as follows:*

$$\Delta Y_{i+1}^d = \int_{t_i}^{t_{i+1}^d} \sigma_s^d dW_s^d \quad (3.17)$$

$$\begin{aligned} \Delta P_{i+1}^d &= \gamma^d \Delta Y_{i+1}^d + \sum_{r=1}^D \sum_{j=1}^{N^r(t_i^d)} (1 - \gamma^r) \Psi_j^{dr}(\tau_{i+1}^d) \Delta Y_j^r + \\ &\quad + \sum_{r=1}^D \sum_{j=N^r(t_i^d)+1}^{N^r(t_{i+1}^d)} (1 - \gamma^r) \Psi_j^{dr}(t_{i+1}^d - t_j^r) \Delta Y_j^r \mathbb{1}_{r \neq d} \end{aligned} \quad (3.18)$$

$$\Delta X_{i+1}^d = \Delta P_{i+1}^d + \Delta u_{i+1}^d \quad (3.19)$$

Note that we simplify the notation by denoting subscripts i, j as transaction indexes and superscripts d, r as the corresponding stock of that transaction, e.g., $\Delta Y_{i+1}^d, \Delta P_{i+1}^d, \Delta X_{i+1}^d$ are the efficient, adjusted, and observed price changes of stock d over the interval $[t_i^d, t_{i+1}^d]$. The

indicator function $\mathbb{1}_{r \neq d}$ in the third term of Eqn. 3.18 indicates adjustments on historical price changes of other stocks r that occur between two consecutive transactions, $[t_i^d, t_{i+1}^d)$, of the stock d , while the second term is adjustments of other past price changes that occur before the transaction t_i^d .

In general, the corollary implies that when market makers revise their pricing errors caused by asymmetric information, they retrieve improved information not only in the previous transaction price changes of the stock itself, but also in those of other related stocks. Consequently, current adjustments of the quoted prices are correlated with the past price changes of the other stocks, which can be justified through the adjustment function $\Psi_t(\tau) = \{\Psi_t^{dr}(\tau)\}_{d,r \in [1,D]}$. The past price changes of some stocks might have greater impacts on the revision of the other stocks than the other stocks have on themselves, i.e. $\Psi_t^{dr}(\tau) > \Psi_t^{rd}(\tau)$, $\forall d, r \in [1, D]$, and $d \neq r$. This feature is contemplated in the microstructure literature under the term of “lead-lag” effects (Buccheri, Corsi and Peluso, 2020; Dao, McGroarty and Urquhart, 2018; Hayashi and Koike, 2017, 2018; Huth and Abergel, 2014). However, there still lacks a framework that formally investigates the mechanism in which asymmetric information and imperfect lagged adjustment drive serial dependence in the manner of lead-lag effects, even though the data-generating process was assumed to be temporally independent. Here, we fill this gap in the context of our multivariate price dynamics model. In the other way around, the non-trivial (co-)variation recovered from lead-lag effects is the evidence of the indispensable multivariate transaction price generation mechanism of our model.

First, let us give some intuition behind the adjustment processes with a simple case of bivariate stocks. In the first trade, market makers receive a favourable signal about the first stock, and because the market markers do not have the true underlying information, they cautiously adjust the prices of stocks only partially upward in response to the favourable information. In the subsequent trades, in order to set the prices for the first stock, they revise previous transactions that are not only of the first stock but also of the second one. If the second stock’s price also increases in the last transactions, they will be more confident and adjust the price of the first stock further upward, and, vice versa, they will revise downward. Following this logic, we consider the autocovariances and the cross-autocovariances of two assets d, r . Indeed, the literature on realized (co-)variation of stocks is well documented that the realized (co-)variation can be retrieved by evaluating the realized (cross-) autocovariation of price changes (see, particularly, Barndorff-Nielsen et al., 2011; Varneskov, 2016b)

Without loss of generality, we assume that the market microstructure noises u_t follow an independent normal distribution and are exogenous to the efficient price processes. Furthermore, we consider that the transaction costs are significantly smaller than the change in the true underlying values, and thus the noise variances can be negligible compared to the variation in the efficient price processes. These assumptions might be unrealistic in some circumstances of significant asymmetric information where market makers can set non-trivial transaction costs. However, our main concentration is to discover the impacts

of lead-lag effects on (co-)variation relationship, and imposing these assumptions smooths out irrelevant and troublesome impacts of noise components.

By the Corollary 1, the (cross-) autocovariation is weighted by the time-decaying adjustment kernel. To measure the impact of the lead-lag effects on the (cross-) autocovariation via an information change, we evaluate the difference of conditional (cross-) autocovariation as the results of the change in its conditional information set. Specifically, at two distinct transactions, e.g. t_i^d and t_{i+h}^d with h denoting a distance in the transaction indexes, the efficient price changes are defined on two filtrations $\mathcal{F}_{t_i^d}$ and $\mathcal{F}_{t_{i+h}^d}$ ¹. For simplicity, we take $h = -1$, that is, there is a new signal on the efficient price of the asset d at t_i^d , and it is contained in $\mathcal{F}_{t_i^d}$ but not in $\mathcal{F}_{t_{i-1}^d}$. We also consider two scenarios. On the one hand, at t_i^d market makers observe only information about the transaction t_i^d on the asset d and adjust their price quotes. On the other hand, they also observe other information on the asset r , a transaction t_j^r that arrives between $[t_{i-1}^d, t_i^d]$, and is included in $\mathcal{F}_{t_i^d}$. Innovation in conditional (cross-) autocovariation, caused by the difference between two information sets $\mathcal{F}_{t_i^d}$ and $\mathcal{F}_{t_{i-1}^d}$, can be derived from the Corollary 1 for the two scenarios as follows:

First scenario: $t_j^r < t_{i-1}^d$

$$\mathbb{E}[(\Delta X_i^d)^2 | \mathcal{F}_{t_i^d}] - \mathbb{E}[(\Delta X_i^d)^2 | \mathcal{F}_{t_{i-1}^d}] = (\gamma^d)^2 (\sigma_i^d)^2 \quad (3.20)$$

$$\mathbb{E}[\Delta X_i^d \Delta X_{i-1}^d | \mathcal{F}_{t_i^d}] - \mathbb{E}[\Delta X_i^d \Delta X_{i-1}^d | \mathcal{F}_{t_{i-1}^d}] = 0 \quad (3.21)$$

$$\mathbb{E}[\Delta X_i^d \Delta X_j^r | \mathcal{F}_{t_i^d}] - \mathbb{E}[\Delta X_i^d \Delta X_j^r | \mathcal{F}_{t_{i-1}^d}] = 0 \quad (3.22)$$

Second scenario: $t_{i-1}^d < t_j^r < t_i^d$

$$\begin{aligned} \mathbb{E}[(\Delta X_i^d)^2 | \mathcal{F}_{t_i^d}] - \mathbb{E}[(\Delta X_i^d)^2 | \mathcal{F}_{t_{i-1}^d}] &= (\gamma^d)^2 (\sigma_i^d)^2 + (1 - \gamma^r)^2 [\Psi_j^{dr}(\tau_{i-j}^{dr})]^2 (\sigma_j^r)^2 + \\ &\quad + 2\gamma^d (1 - \gamma^r) \Psi_j^{dr}(\tau_{i-j}^{dr}) \sigma_{i-j}^{dr} \end{aligned} \quad (3.23)$$

$$\mathbb{E}[\Delta X_i^d \Delta X_{i-1}^d | \mathcal{F}_{t_i^d}] - \mathbb{E}[\Delta X_i^d \Delta X_{i-1}^d | \mathcal{F}_{t_{i-1}^d}] = \gamma^d (1 - \gamma^r) \Psi_j^{dr}(\tau_{(i-1)-j}^{dr}) \sigma_{(i-1)-j}^{dr} \quad (3.24)$$

$$\begin{aligned} \mathbb{E}[\Delta X_i^d \Delta X_j^r | \mathcal{F}_{t_i^d}] - \mathbb{E}[\Delta X_i^d \Delta X_j^r | \mathcal{F}_{t_{i-1}^d}] &= \gamma^d \gamma^r \sigma_{i-j}^{dr} + \gamma^r (1 - \gamma^d) \Psi_{i-1}^{dd}(\tau_i^{dd}) \sigma_{(i-1)-j}^{dr} + \\ &\quad + \gamma^r (1 - \gamma^r) \Psi_j^{dr}(\tau_{i-j}^{dr}) (\sigma_j^r)^2 \end{aligned} \quad (3.25)$$

where $\sigma_{(\cdot)}^d, \sigma_{(\cdot)}^r, \sigma_{(\cdot)}^{dr}$ are the variance and covariance components of the efficient price processes $\Theta_{(\cdot)}$ in Eqn. 3.1. We also denote $\tau_{i-j}^{dr} = \tau_i^d \cap \tau_j^r$ as the intersection² of two waiting times for transactions i, j of stocks d, r , i.e. $\tau_i^d = t_i^d - t_{i-1}^d, \tau_j^r = t_j^r - t_{j-1}^r$ and σ_{i-j}^{dr} as the corresponding covariation of efficient prices over that intersected duration.

Our primary goal is to measure the difference in the innovation of (cross-) autocovariation between two scenarios, from which we can determine whether lead-lag effects exist. It is obvious that there is a significant difference between the two scenarios. When only information on the asset d is observed (the first scenario), the innovation in the variation

¹ We note here that there is also σ -algebra generated by noises at different trading times. However, since we consider only the impact of the lead-lag effects arising from the information on efficient price changes, we simply assume that we have complete filtration of this component

² We note that the notation of intersected duration τ_{i-j}^{dr} is distinguished with the one of accumulated duration $\tau_{i,i+1} = \tau_i + \tau_{i+1}$ in the previous section

of the observed price change in Eqn. 3.20 is due to only a new noisy signal in the transaction t_i^d . However, when a piece of (leading) information is observed in asset r between two consecutive transactions of asset d (the second scenario), the market maker adjusts the price of asset d not only based on its own noisy signal and trading history, but also based on additional information about asset r . The innovations in the (cross-) autocovariation are significantly different from the first scenario. The revisions of (cross-) autocovariation in Eqn. 3.23, Eqn. 3.24, and Eqn. 3.25 take into account the price variations in the asset d itself, $(\sigma_i^d)^2$, and the price variations in the related asset r , $(\sigma_j^r)^2$, and also contemporaneous price cross-correlations between the two assets, $\sigma_{i-j}^{dr}, \sigma_{(i-1)-j}^{dr}$. Thus, the information about the efficient price change of one asset leads to two other sources driving the (cross-) autocovariation: one simply arises as the results of contemporaneous (cross-) correlation between assets and the other temporal (cross-) correlation incurred by lagged (cross-) adjustment. An implication is that market makers can infer additional information using the price changes of related stocks, even though the true value of the investigated stock is not observable.

3.2.3 Generalization of previous multi-asset lagged adjustment model

Compared to the previous literature, on the one hand, our results confirm the finding in the most recent research of Buccheri, Corsi and Peluso (2020). First, some assets leading others emerge not from the difference in the level of trading activity but from the lagged adjustment coefficients. These adjustments are measured as time-varying functions of the time elapsed from the observation of the leading information. Second, there exists another source of lead-lag effects that are not related to contemporaneous cross-asset correlation. This source of lead-lag effects arises as a consequence of non-zero diagonal coefficients in the lagged adjustment kernel rather than the cross-asset pricing. To illustrate this finding, we set $\sigma_{(\cdot)}^{dr} = 0$, which means that the efficient prices are independent. Based on Eqn. 3.23 and Eqn. 3.25, it is obvious that the innovation in the price variation and cross-autocovariation of the asset d is driven by the variation in the efficient price of the asset r , weighted by the lagged adjustment coefficients.

On the other hand, the definition of the lead-lag adjustment in our model generalizes the one of Buccheri, Corsi and Peluso (2020). In their work, the MLA, Buccheri, Corsi and Peluso (2020) implicitly assume the constancy of the adjustment coefficients. This assumption is quite simple and restrictive, and as the authors remarked, it confines the MLA model to account for changes in market volatility and liquidity conditions. Indeed, by using aggregated transaction prices at one second frequency, the MLA neglects the timing of trades that might convey information about market volatility and liquidity. The MLA can also destroy true short-term lead-lag effects by aggregating the price change that occurs over a time interval of less than one second. In addition, the MLA applies the same adjustment kernel to all adjustments without distinguishing information on a noisy signal of order flows or information on historical trades. Thus, the MLA does not accommodate the special feature of asymmetric information, which is inherent at the transaction-by-transaction level. The

lagged adjustment in MLA arises as the consequence of delaying in information dissemination between assets, i.e. some assets trade ahead and carry information about others. Meanwhile, the price dynamics in our model, the MALA, additionally accounts for the response of market makers to asymmetric information. The lead-lag effects emanate from two distinct and subsequent imperfections of the market: heterogeneous beliefs on the true underlying values and temporally lagged adjustment on historical trades. Thus, our model can be seen as the generalization of Buccheri, Corsi and Peluso (2020)'s model. To illustrate this point, let us consider the case in which market makers have the same adjustment to both noisy order flows and historical trades. The price dynamics in Proposition 1 turns out to be exactly the same as the ones in Buccheri, Corsi and Peluso (2020):

Corollary 2. *Assume that γ has $D \times D$ -dimension and $\gamma = \Psi_t(\tau)$ is the matrix of adjustment coefficients. At transaction t_{i+1} , the three components of prices are given by:*

$$\mathbf{Y}_{t_{i+1}} = \mathbf{Y}_{t_i} + \int_{t_i}^{t_{i+1}} \Theta_s d\mathbf{W}_s \quad (3.26)$$

$$\mathbf{P}_{t_{i+1}} = \mathbf{P}_{t_i} + \Psi_{t_i}(\tau)(\mathbf{Y}_{t_{i+1}} - \mathbf{P}_{t_i}) \quad (3.27)$$

$$\mathbf{X}_{t_{i+1}} = \mathbf{P}_{t_{i+1}} + \mathbf{u}_{t_{i+1}} \quad (3.28)$$

If the matrix $\Psi_{t_i}(\tau)$ is of constant adjustment coefficients, $\Psi_{t_i}(\tau) = \Psi$, the price dynamics turns out to be the ones in the multi-asset lagged adjustment model.

By taking into account the timing factor, the lagged adjustments, and then lead-lag effects, are not immediate but last over time. Their functional forms are shaped by the Assumptions (H1)-(H6) and Eqn. 3.12 in the previous section. Generally, the adjustment coefficients vary with the time elapsed from the point when the information occurs. A key implication of taking into account the timing factor is that the longer the waiting time between transactions, the larger and more precise adjustment should be made.

3.3 AN EQUIVALENT HAWKES POINT PROCESS REPRESENTATION AND ESTIMATION

While Section § 3.2.1 represented a structural model that is capable of accommodating the intrinsic features of the market microstructure at the transaction level, its two components, the quoted and the efficient prices in Eqn. 3.14 and Eqn. 3.15 are not observable but latent processes. Also, due to asynchronous trading at the transaction level, only one component of $\Delta \mathbf{X}_{t_i}$ corresponding to the traded asset is observed at each t_i , whereas the observations of other assets are missing. Thus, the parameters in Proposition 1 are not amenable to direct measurement. It is therefore useful to cast the model into an alternative representation, that is, from the viewpoint of price change, an observational equivalence.

The triple price dynamics in Proposition 1 can be summarized by the following autoregressive dynamics of the observed prices:

Proposition 2. Let (\mathbf{X}_t) be the multivariate observable price time series of D assets from Proposition 1. Then (\mathbf{X}_t) can be represented as a vector of autoregressive processes as follows:

$$\Delta \mathbf{X}_{t_{i+1}} = \boldsymbol{\eta}_{t_{i+1}} + \sum_{j=1}^i \boldsymbol{\psi}_j(\tau_{i+1}) \Delta \mathbf{X}_{t_j} - \mathbf{u}_{t_{i+1}} - \sum_{j=1}^i \boldsymbol{\psi}_j(\tau_{i+1}) \mathbf{u}_{t_j} \quad (3.29)$$

where $\boldsymbol{\eta}_{t_{i+1}} = \gamma \Delta \mathbf{Y}_{t_{i+1}}$ and $\boldsymbol{\psi}_j(\tau_{i+1}) = \gamma^{-1}(1 - \gamma) \boldsymbol{\Psi}_j(\tau_{i+1})$.

By our Assumptions of exogenous and independent normal white noises and random walk efficient prices, the above equation is a vector of autoregressive processes on observed prices, expressing the fact that the knowledge on the past observed price changes is useful for forecasting the current observed price changes. The D -variate vectors $\boldsymbol{\eta}$ and \mathbf{u} contain noisy signals and market microstructure noises, which, in principle, can be considered as all exogenous factors.

The second term of lagged observed prices weighted by time-decaying adjustment kernel $\boldsymbol{\psi}$ encodes long-memory endogenous activities that capture the conditional dynamics depending on past price changes. The $D \times D$ -matrix $\boldsymbol{\psi}_j(\cdot)$ contains self-adjustments and cross-adjustments of the next price changes based on historical price changes of the asset itself or of other assets. For example, for $d \neq r$ $\boldsymbol{\psi}_j^{dr}(\tau_{i+1}) \Delta X_j^r$ is the cross-adjustments between assets that quantifies how much the next price change of the asset d at transaction t_{i+1} in response to a past price change of the asset r at time t_j during the interval $\tau_i = t_{i+1} - t_i$. Similarly, $\boldsymbol{\psi}_j^{dd}(\tau_{i+1}) \Delta X_j^d$ is a self-adjustments effect of type- d events.

Therefore, Eqn. 3.29 can be seen as endo(geneous) - exo(geneous) activities, and given the observations of discrete price changes, our statistical problem is to identify the exo and endo parts in the dynamics of price adjustment. This exo-endo mechanism is actually very similar to the one underlying ‘‘Hawkes processes’’, that have attracted a considerable amount of interest recently (for recent reviews, see Bacry, Mastromatteo and Muzy, 2015; Hawkes, 2017). For a rigorous theoretical foundation of Hawkes processes, we will discuss in the Appendix. The Hawkes model highlights the basic idea of the autoregressive process: given an event, the conditional intensity, the conditional expected number of events in a unit of time, can be formulated as a linear combination of jumps on past events. By its definition, the conditional intensity is implemented in continuous setting, and robust to the irregularly spaced as well as asynchronous trading time. Thus, it is possible to investigate the conditional distribution of observed price change dynamics through an analogous and tractable framework of Hawkes processes that address all the above-mentioned issues of the dataset at the transaction level.

3.3.1 Hawkes processes representation of disjoint observed price change dynamics

Although Eqn. 3.29 is the representation of the unconditional distribution, what is more primary to our consideration is the conditional distribution of observed price changes, which unveils the mechanism of price formation processes, conditioning upon a particular sequence of order flows and historical price changes. To facilitate the formulation of a

conditional distribution on the observed prices, we assume that the observed prices are generated by filtration (\mathcal{H}_t) , the σ -algebra generated by $(\mathbf{X}_s)_{s \leq t}$. For illustration, if we assume that the response of a market maker to asymmetric information, γ , is \mathcal{F}_t -adapted, i.e. being driven by the information set of efficient prices, the link between the filtration of price dynamic components, by the independence of between microstructure noises and efficient price, is given as: $\mathcal{H} = \mathcal{F} \times \mathcal{G}$, $\mathcal{H}_t = \bigcap_{s>t} \mathcal{F}_s \times \mathcal{G}_s$ where \mathcal{G}_s is the σ -algebra generated by microstructure noises. We follow Christensen, Kinnebrock and Podolskij (2010) and Varneskov (2016b) for this setup. Because the noises are only updated at exactly the times of transaction, the conditional distribution of observed price change conditioned on its historical realizations and new price innovations can be deduced as follows:

$$\mathbb{E} \left[\Delta \mathbf{X}_{t_{i+1}} \middle| \mathcal{H}_{t_{i+1}^-} \right] = \boldsymbol{\eta}_{t_{i+1}} + \sum_{j=1}^i \boldsymbol{\psi}_j(\tau_{i+1}) \Delta \mathbf{X}_{t_j} \quad (3.30)$$

Denoting $\Delta \mathbf{N}(\tau_i) = \mathbf{N}(t_i) - \mathbf{N}(t_{i-1})$ as a D -variate vector of counting functions that count the number of transactions for each asset d over the interval $[t_{i-1}, t_i)$, $\tau_i = t_i - t_{i-1}$ and for some instants $dt \ll t$, $t^- = \lim_{dt \rightarrow 0} t - dt$, $d\mathbf{N}_t = \lim_{dt \rightarrow 0} \mathbf{N}(t) - \mathbf{N}(t^-)$. Due to the Assumptions of singular and ordered transaction point processes (see the Appendix), $d\mathbf{N}_t$ can take only a vector of zeros, or an identity vector of which all elements are zeros except for one entry at the index of the traded asset taking value 1. For each transaction that occurs at time t , it is marked by a price change value, m_t , which can be any number of discrete minimum tick sizes³, positive and negative. However, in empirical analysis (see Section § 3.4.2), we find that, for high liquid assets, more than 99% of the price changes fall on one of just seven different values, that is, $\forall d \in [1, D], \Delta X^d = 0, \pm 1 \text{ tick}, \pm 2 \text{ ticks}; \Delta X^d \leq -3 \text{ ticks}; \text{ and } \Delta X^d \geq 3 \text{ ticks}$. Therefore, we follow Hausman, Lo and MacKinlay (1992), Liesenfeld, Nolte and Pohlmeier (2008) and Russell and Engle (2005) and assume that m_t takes values from a finite state space of price change \mathcal{M} and denote M as the number of possible outcomes of \mathcal{M} . Eqn. 3.30 can be represented with counting functions and price change values such as:

$$\mathbb{E} \left[\Delta \mathbf{N}(\tau_{i+1}) m_{t_{i+1}} \middle| \mathcal{H}_{t_{i+1}^-} \right] = \boldsymbol{\eta}_{t_{i+1}} + \sum_{j=1}^i \boldsymbol{\psi}_j(\tau_{i+1}) m_{t_j} d\mathbf{N}_{t_j} \quad (3.31)$$

For each outcome $m_{t_{i+1}}$ in \mathcal{M} at transaction t_{i+1} :

$$\mathbb{E} \left[\Delta \mathbf{N}(\tau_{i+1}) \middle| \mathcal{H}_{t_{i+1}^-} \right] = \frac{\boldsymbol{\eta}_{t_{i+1}}}{m_{t_{i+1}}} + \sum_{j=1}^i \frac{\boldsymbol{\psi}_j(\tau_{i+1})}{m_{t_{i+1}}} m_{t_j} d\mathbf{N}_{t_j} \quad (3.32)$$

For some intuitions behind the development of an alternative representation by Hawkes processes, since the observed transaction price changes usually take only a handful of discrete values, the transaction process of the asset d can be partitioned into M mar-

³ The discrete minimum tick size is a necessary feature of the modern automated market to prevent an explosion of messages under the current market design and to constrain the liquidity cost of the market artificially. For the complexity of the discreteness, we refer to Chao, Yao and Ye (2017, 2018), Li, Wang and Ye (2021) and Yao and Ye (2018) among others

ginal transaction process associated with each price change values of its state space \mathcal{M} . In other words, for each element $N^d(t)$ in the D -variate vector, $N(t)$, we can generate a new M -variate vector of counting processes $\{N^{d,m}(t)\}_{m \in \mathcal{M}^d}$ by disjointing the (ground) transaction process $N^d(t)$ according to its state of price changes. The disjoint price change processes and the ground transaction process are mapped through the following manner: $N^d(t) = \sum_{m \in \mathcal{M}} N^{d,m}(t)$. The properties of disjoint processes is discussed in the Appendix. The motivation for the disjointing representation is to simplify the complication of joint modelling non-synchronous trading times and dependent price movements of multiple assets⁴. Intuitively, the problem of marked transaction processes of multiple assets can be represented as multivariate disjoint price change processes and can be simply treated as multivariate Hawkes processes. Given an outcome $m_{t_{i+1}}$ at transaction t_{i+1} , the analytical expression of Eqn. 3.31 for each asset d is:

$$\mathbb{E} \left[\Delta N^{d,m}(\tau_{i+1}) \middle| \mathcal{H}_{t_{i+1}^-} \right] = \frac{\eta_{t_{i+1}}^d}{m_{t_{i+1}}} + \sum_{r=1}^D \sum_{j=1}^i \frac{\psi_j^{dr}(\tau_{i+1})}{m_{t_{i+1}}} m_{t_j} dN_{t_j}^{r,m} \quad (3.33)$$

For simplicity, we replace the notation of each combination (d, m) and (r, m) , where $d, r \in [1, D]$ and $m \in \mathcal{M}$ with M states, by k, l , where $k, l \in [1, K]$ and $K = D \times M$. Also, for each value of the price change $m \in \mathcal{M}$ at t_{i+1} and its previous realized values, $m_{t_j}, j \leq i$, we can denote $\eta_{t_{i+1}}^k = \frac{\eta_{t_{i+1}}^d}{m_{t_{i+1}}}$ and $\psi_j^{kl}(\tau_{i+1}) = \frac{\psi_j^{dr}(\tau_{i+1})}{m_{t_{i+1}}} m_{t_j}$. For all $k \in [1, K]$, we can express Eqn. 3.33 as:

$$\mathbb{E} \left[\Delta N^k(\tau_{i+1}) \middle| \mathcal{H}_{t_{i+1}^-} \right] = \eta_{t_{i+1}}^k + \sum_{l=1}^K \sum_{j=1}^i \psi_j^{kl}(\tau_{i+1}) dN_{t_j}^l \quad (3.34)$$

Due to the Assumptions of the efficient price and the adjustment function, $\eta_{t_{i+1}}^k$ and $\phi_j^{kl}(\tau_{i+1})$ can be formed by locally integrable functions over the interval $[t_i, t_{i+1})$. Thus, for $t \in [t_i, t_{i+1})$, denoting $\mu^k = \frac{\partial \eta_{t_{i+1}}^k}{\partial t}$ and $\phi_j^{kl}(t) = \frac{\partial \psi_j^{kl}(\tau_{i+1})}{\partial t}$. It is worth noting that μ^k can be a function of time t , that is non-homogeneous. However, we assume the constancy of μ^k , and $\eta_{t_{i+1}}^k$ is restricted to functions of only first-order differential with t . The rationale for this choice is discussed in the next section. By definition of the conditional intensity:

$$\lambda^k(t | \mathcal{H}_t) = \frac{\partial \mathbb{E} \left[\Delta N^k(\tau_{i+1}) \middle| \mathcal{H}_{t_{i+1}^-} \right]}{\partial t} \quad (3.35)$$

Taking the differentiation of both sides of Eqn. 3.34, we obtain the following proposition:

Proposition 3. *Given the multivariate price dynamics for D assets in Proposition 1 and the Assumption that the observable price changes of each asset, ΔX^d , take only finite discrete values,*

⁴ The dependence of price change is not only amongst assets, but also between the price change and the time of trading. For references on the relationship between the trading time and the trading price change, we refer to Dufour and Engle (2000) and Russell and Engle (2005)

$m \in \mathcal{M}$ with M states, the conditional probability of a transaction arrived with price change value m can be represented as the formulation of Hawkes point processes:

$$\lambda^k(t|\mathcal{H}_t) = \mu^k + \sum_{l=1}^K \sum_{j=1}^i \phi_j^{kl}(t) dN_{t_j}^l \quad (3.36)$$

where k, l are the indexes that denote each combination of (d, m) and $1 \leq k, l \leq K, K = D \times M$. The non-negative μ^k , in Hawkes model, is called baseline intensity and $\phi_j^{kl}(\cdot)$ is called excitement coefficient, which corresponds to the exogenous impacts of noisy order flows and the endogenous impacts of lagged price changes, respectively.

Furthermore, denoting K^d as a set of the indexes of the disjoint price change processes for the asset d , the coefficients of the autoregressive representation of ΔX^d , in Eqn. 3.30, are given as:

$$\eta_{t_{i+1}}^d = \sum_{k \in K^d} \int_{t_i}^{t_{i+1}} \mu^k m^k dt \quad (3.37)$$

$$\psi_j^{dr}(\tau_{i+1}) = \sum_{k \in K^d} \sum_{l \in K^r} \int_{t_i}^{t_{i+1}} \frac{\phi_j^{kl}(t)}{m^l} m^k dt \quad (3.38)$$

where m^k, m^l are the price change values associated with the excitement coefficient $\phi_j^{kl}(t)$.

The proposition reflects an alternative view on observed price change sequences as a special exo-endo problem characterized by Hawkes conditional intensities. Basically, for each component of the K -variate observed price change processes, we observe the arrival of exogenous events that stems from (in)homogeneous Poisson processes with “immigration” rates $\mu^1, \dots, \mu^k, \dots, \mu^K$, which can be the representation of new information about aggregate order flows. This exogenous event in the component l originated at transaction t_j triggers other K inhomogeneous Poisson processes in the components $k = 1, \dots, K$ with intensities $\phi_j^{kl}(t)$, which can generate subsequent “offspring” price changes events. And each of these realized “offspring” events again provokes other K inhomogeneous Poisson processes and produces the “offspring” of its own in the same way; and so on, inducing the clustering of events as a cascade of inhomogeneous Poisson processes. These so-called endogenous events are triggered by occurred events rather than by new information, which is in a similar manner to the lagged adjustment process based on historical transactions. We note that the terms “immigrant”, “offspring”, and “branching ratio” came from the theory of branching processes, as the Hawkes process can be considered as a branching-type process.

Following the Hawkes model, we can choose the offspring intensity, i.e. self-excitement and cross-excitement coefficients, such that $\phi_j^{kl}(t) dN_{t_j}^l = \phi^{kl}(t - t_j^l) dN_{t_j}^l$, in which the impact of a previous price change t_j^l on the future conditional intensity is weighted by a function of time distance $t - t_j^l$, completely in accord with previous Assumptions on the adjustment kernel. In its general form, the equation Eqn. 3.36 is represented by the following equation:

$$\lambda(t) = \mu + (\Phi \star dN)(t) \quad (3.39)$$

where $\Phi(t) = \{\phi^{kl}(t)\}$ is a $K \times K$ matrix, $\mu = \{\mu^k\}$ is a K -variate vector, $\mathbf{N}(t) = \{N^k(t)\}$ is a K -variate vector of identity or zeros, and \star denotes the “matrix convolution” notation:

$$(\Phi \star d\mathbf{N})(t) = \int_0^t \Phi(t-s) d\mathbf{N}(s) \quad (3.40)$$

The matrix Φ describes the influences between disjoint price change states. More specifically, the coefficients ϕ^{kk} account for self-excitation effects, encoding the influences of disjoint states of the asset d on other disjoint states of the asset d itself, and the coefficients ϕ^{kl} with $k \neq l$ account for cross-excitation effects, encoding the influences of disjoint states of the asset d on disjoint states of the other counterpart assets r . Thus, it is natural to decompose the $K \times K$ matrix Φ into D sub-matrices $M \times M$. For illustration, we consider D with only two assets d, r :

$$\Phi(t) = \begin{pmatrix} \Phi^{dd}(t) & \Phi^{dr}(t) \\ \Phi^{rd}(t) & \Phi^{rr}(t) \end{pmatrix} \quad (3.41)$$

where:

- $\Phi^{dd}(t), \Phi^{rr}(t)$: accounts for the self-adjustment on the next price changes based on the price changes of the asset itself.
- $\Phi^{dr}(t), \Phi^{rd}(t)$: accounts for the cross-adjustment on the next price changes based on the price changes of other assets.

In Proposition 3, the vector of autoregressive price change processes in discrete time can be interpreted as its counterpart Hawkes processes in continuous time. The interpretation stems from disjointing transaction sequences into sub-transaction sequences associated with a discrete value of price change. And the counting process of each disjoint price change sequence can be viewed as \mathbb{N}_0 valued integer time series (INAR). The close relation between Hawkes point processes and INAR time series has been investigated in Kirchner (2016b), and Kirchner (2016a), who propose an approximation of the Hawkes process using the INAR model. Their studies can be considered as a theoretical foundation of the existence and uniqueness of the equivalence presented in Proposition 3.

Despite its simplicity, the alternative representation by Hawkes processes can capture the characterization of the autoregressive observed price dynamics in Proposition 2 with the presence of asynchronous trading and missing observations. However, the derivation of adjustment coefficients specifying other components of price dynamics in Proposition 1 is unfortunately more complex without additional assumptions on asymmetric information and will not be further developed here. We leave this task for future research. The perspective here is to forego precise estimation of structural parameters in hope of achieving an alternative characterization of price dynamics from which we disentangle the lead-lag effects embedded in the price formation process.

3.3.2 Parameterization and estimation of Hawkes processes

From the Proposition 3, the baseline intensities of multivariate disjoint point processes implicitly defines the arrivals (immigration) of new efficient price innovation. Due to the independence of efficient price innovations, the baseline intensities should be renewed at each immigrant point, and the immigration process of new innovations can be described by a renewal intensity rate. In that sense, the waiting times between the innovations are independently and identically but arbitrarily distributed. Such a specification can provide a superior quality of capturing changes in information flows. However, we do not have a realization on the arrival of information flows, and so the flexibility of the renewal immigration process comes with a cost that makes direct estimation, i.e. by the maximum likelihood method, for multivariate disjoint price change point processes practically impossible Wheatley, Filimonov and Sornette (2016). In the framework of this thesis, we follow standard Hawkes processes and assume the constancy of the baseline intensity vector μ within the period analyzed. This suggests that new innovations about efficient price arrive exogenously at each disjoint price change point process of the system in Poisson processes. As long as the Hawkes representation is re-estimated on a daily basis, the assumption of constancy of μ is not restrictive.

Next, another problem that implicitly determines the conditional distribution of the observed price dynamics concerns the choice of the excitement function ϕ . In most cases, ϕ of Hawkes processes is a somewhat arbitrary parametric kernel, and the main decision between exponential or power-law functions. It is easy to show that these two functional families of ϕ yield an adjustment price kernel Ψ that satisfies all the requirements in Assumptions (H1-6). Amongst two kernels, the exponential excitement function yields a Markovian structure for the conditional intensity Hawkes (2017) and so it is mathematically more attractive. Also, the likelihood function of exponential decay is easier to handle by recursive representation Ogata (1988). Thus, in our studies, we chose the exponential decay function for the excitement kernels, which makes the conditional intensity functions have the form:

$$\lambda^{kl}(t) = \mu^{kl} + \sum_{l=1}^K \int_0^t \alpha^{kl} \beta^{kl} e^{-\beta^{kl}(t-s)} dN^l(s) \quad (3.42)$$

where $\alpha = \{\alpha^{kl}\}_{k,l \in [1,K]}$ is a valued-matrix of impact coefficients, $\beta = \{\beta^{kl}\}_{k,l \in [1,K]}$ are decay coefficients. From the theory of branching processes, $q^{kl} = \frac{\alpha^{kl}}{\beta^{kl}}, 0 \leq q^{kl} \leq 1$ are called branching coefficients, which are the expected number of offspring at each point, and $Q = \{q^{kl}\}_{k,l \in [1,K]}$ is the branching matrix. We can infer from Proposition 3 that the amount of lagged information retrieved by the revision is measured by the branching coefficients and the speed of adjustment on historical transactions is determined by the decay function. The impact of the previous transaction (the excitement) decreases exponentially over time according to the decay parameters. For the purpose of measuring the lead-lag effects between stocks, it is natural to impose one decay parameter for all disjoint price change processes belonging to one asset:

$$\beta^d := \beta^{k1} = \beta^{k2} = \dots = \beta^{kl} \quad (3.43)$$

for all k that indexes the combinations (d, m) of the asset d with $m \in \mathcal{M}^d$.

Last but not least, we note that exponential or power-law kernels cannot catch the switching in the regime or the non-monotonicity of the excitement. So, in the first step, we calculate the non-parametric point-wise estimation that can identify the complicated shapes of excitement in the data. These point-wise estimates also give us some hints to specify the shape of the excitement kernel, respectively, decay functions as well as the impact coefficients in our final parametric model. In particular, we use the Expectation-Maximization algorithm in `tick` library which was developed in Bacry, Dayri and Muzy (2012), Bacry et al. (2018), Bacry, Jaisson and Muzy (2016) and Bacry and Muzy (2016). For further details on the likelihood function of the estimation, we refer the reader to the Appendix.

3.4 EMPIRICAL FINDINGS: THE INTERDEPENDENCE OF PRICE CHANGES

3.4.1 *Data description*

Our data set in this empirical application includes high-frequency transaction data of six stocks listed on the Dow Jones Industrial Average (DJIA) index: Apple (ticker symbol AAPL) and International Business Machines (ticker symbol MSFT); American Express (ticker symbol AXP) and Visa (ticker symbol V); Chevron (ticker symbol CVX) and Exxon Mobil (ticker symbol XOM). The first two of the selected stocks, namely Group I including AAPL and IBM, belong to the technology sector, whereas the second two stocks, namely Group II including AXP and V, belong to the financial services sector and the remaining two, namely Group III including CVX and XOM, belong to the oil and energy sector. The data of all stocks are extracted from the Trade and Quote (TAQ) database that recorded trading information in the three-month period from 01/02/2019 to 30/04/2019, a total of 62 business days. The timestamp precision of each data point is a millisecond. Following the data-cleaning algorithm employed by (Barndorff-Nielsen et al., 2011) to remove potential errors, we (i) consider transactions in the main trading session from 9:30 to 16:00, which is considered to ensure maximum liquidity, and (ii) exclude data within the first and last fifteen minutes of the trading session to eliminate the effects of opening, closing call auctions, and overnight session. When several simultaneous transactions were observed, we (iii) used the volume-weighted average price. Next, we (iv) delete non-trade transactions with zero volume, and with negative or zero transaction prices. We also (v) remove observations that have transaction prices above the ask price plus bid-ask spread or below bid price minus bid-ask spread. Table 3.1 shows several descriptive statistics related to the trading activity of the six stocks together.

In particular, amongst six stocks, AAPL has the highest number of trades per day with the average waiting time between two consecutive trades at 0.3 seconds, which can be considered as the stock having the most liquidity. Whereas AXP and IBM are considered as the stocks having less liquidity stocks in terms of the number of trades and the average duration between two consecutive trades of these stocks are of 1.73 and 1.43 seconds, respectively. For all six selected stocks, the distributions of transaction price changes are

Table 3.1: Descriptive statistics for six selected stocks listed on DJIA index

Indicators	Group I		Group II		Group III	
	AAPL	IBM	AXP	V	CVX	XOM
Average Number of Trade	77500	15917	12842	27933	26593	27533
Max Number of Trade	148859	44814	19612	51105	156357	49974
Min Number of Trade	51490	10851	8881	19931	15146	20316
Nonzero Trade	36042	7997	5681	12499	12466	8679
Nonzero Percentage	45.93	50.09	44.29	44.85	47.45	31.47
Positive Extreme Trade	60	70	37	39	68	1
Positive Extreme Percentage	0.07	0.45	0.27	0.13	0.20	0.00
Negative Extreme Trade	64	73	36	39	71	1
Negative Extreme Percentage	0.06	0.43	0.28	0.13	0.20	0.00
Price Average	185.63	139.19	109.65	152.05	121.62	79.58
Trade Duration Average	0.30	1.43	1.73	0.80	0.97	0.81

Notes: For each asset, we show the average statistics per day for some indicators such as number of trades; number of non-zero trades that move stock price; number of positive and negative extreme trades that move stock price more than 3 ticks; price average; and the average trade duration between consecutive observations.

approximately symmetric. The frequencies of two opposite movements but with the same number of ticks are roughly similar. On average, the non-zero trades that move stock prices occurred with 40% to 50% frequency, excepting for XOM with the frequency of only 31.47%. The extreme trades that move prices greater than 3 ticks occurred with very minor frequencies of less than 0.5%. Especially, XOM has, on average, only 2 transactions per day that move the price more than 3 ticks. Illustrations and histograms of transaction point processes by price changes are presented in Figure 3.2. Virtually, all the mass in each histogram is concentrated in five or seven cells - there are few extreme price movements of more than 3 ticks, which highlights the importance of discreteness in transaction prices.

3.4.2 Disjoint price change transaction point processes

Given the price discreteness of transaction-by-transaction data and the sparseness of extreme price change moves, we assume that transaction point processes are marked with a finite number M^d of discrete price change states. We partition these marked transaction point processes as M^d -variate vector of multivariate disjoint price change transaction point processes. In choosing M^d , we have to balance price resolution against the practical constraint that a too large M^d will yield no observation in the extreme states. Using the descriptive statistics in the previous section as a guide, we set $M^d = 6$, d denoting the index of the stocks { AAPL, AXP, CVX, IBM, V }, that implies six-states price change spaces $\mathcal{M}^d = \{\Delta X^d | \Delta X^d \geq 3 \text{ ticks}, \Delta X^d = \pm 2 \text{ ticks}, \Delta X^d = \pm 1 \text{ tick}, \text{ and } \Delta X^d \leq -3 \text{ ticks}\}$. A special case of XOM has a very small frequency of movements greater than 3 ticks, we choose $M^d = 4$ and reduce its discrete price change space to four states $\mathcal{M}^d = \{\Delta X^d | \Delta X^d \geq 2 \text{ ticks}, \text{ and } \Delta X^d = \pm 1 \text{ tick}\}$. The two extreme states include up-

Figure 3.2: Transaction point processes marked by price changes of six selected DJIA stocks



Notes: The panels on the left represents transactions marked by different price change states occurred during 14:00:00 - 14:30:00 14/02/2019. The panels on the right displays the histogram of transactions by price changes on 14/02/2019.

ward price movements of 3 (2 for XOM) or more ticks and downward price movements of 3 (2 for XOM) or more ticks. The vector of disjoint price change process for asset d , as an instance with $M^d = 6$, is given by:

$$dN^d(t) = (dN^1(t), \dots, dN^m(t), \dots)^\top = \begin{cases} [1, 0, 0, 0, 0, 0]^\top & \text{if } \Delta X^d(t) \leq -3 \text{ ticks.} \\ [0, 1, 0, 0, 0, 0]^\top & \text{if } \Delta X^d(t) = -2 \text{ ticks.} \\ \vdots & \vdots \\ [0, 0, 0, 0, 0, 1]^\top & \text{if } \Delta X^d(t) \geq 3 \text{ ticks.} \end{cases} \quad (3.44)$$

where $m \in [1, M^d]$.

In order to analyze the price dynamics for multiple assets, we proceed by concatenating the vectors of multivariate disjoint point processes to a new K -dimensional vector with $K = \sum_d M^d$, which is given by:

$$dN(t) = (dN^1(t), dN^2(t), \dots, dN^k(t), \dots)^\top, \quad k \in [1, K] \quad (3.45)$$

where k is indexing each combination of the price change state index and the asset index, (m, d) . The K -variate disjoint states correspond to all observable discrete events in the transaction point processes of the D assets. The interdependence between D assets is represented by the cross- and self-influencing dynamics between the K disjoint discrete states. Therefore, the disjointing transaction point processes provide a compact, yet meaningful summary of a transaction price dynamic without specifying complicated price and time-joint distribution. Instead, the disjoint framework allows us to account for real-time excitement effects from one state that influences the likelihood of inducing another state in the system. For the sake of parsimony and simplicity, we consider only a finite discrete state space of observed price change.

Although the observed price change can be any number of ticks, positive or negative, our assumption of finite number of states, M^d , poses no problems since we let some states in \mathcal{M}^d represent a multiple number of states in the observed price change, e.g the states ≤ -3 ticks, and ≥ 3 ticks. The finite M^d also keeps the number of unknown parameters finite. But this parsimony comes with a cost of losing price resolution as the model cannot distinguish the price movements of 3 ticks or of greater than 3 ticks, and similarly for price movements of -3 ticks or fewer than 3 ticks. In principle, we can increase the resolution of the price by simply adding more states, i.e. increasing M^d . However, in practice the data will impose a limit on the fineness of price resolution simply because there will be no observations in the extreme states when M^d is too large, e.g the case of stock XOM with $M^d = 6$ in our study. As a result, the subset of coefficients of those states cannot be identified and cannot be estimated.

Finally, although the definition of the state space of price changes \mathcal{M}^d does not require a symmetry between the positive and negative sides, the symmetrical histogram of price changes in Figure 3.2 suggests a symmetric definition of the state space.

3.4.3 Statistical interdependence between price change levels

Before moving to a detailed analysis of non-parametric and parametric modelling, we present here some empirical findings on the interdependence between disjoint point processes of price change states, see Tables 3.2, 3.3, and 3.4. These findings give a preliminary numerical summary of the relations between disjoint point processes in the modelling in the next section. In Tables 3.2, 3.3, and 3.4, we document the average results over all trading days separately for 6 pairs of assets with the three former AAPL-IBM, AXP-V, and CVX-XOM belonging to the same groups and the three latter IBM-XOM, AAPL-AXP, and CVX-V belonging to different groups. For other asset pair relations, we refer the readers to the Appendix.

First, we calculate empirical *unconditional* probabilities of transactions associated with each state, i.e. $\mathbb{P}\text{r}(dN^k(t_i) = 1)$, which is documented in the last row **Total** in each panel. Next, we calculate empirical *conditional* probabilities of the occurrence of an event state k (in row) given that the preceding occurrence is an event of state l (in column), i.e. $\mathbb{P}\text{r}(dN^k(t_i) = 1 | dN^l(t_{i-1}) = 1)$. In each panel, the results of the conditional probability are documented by values without parentheses on the first line of each cell. In addition, to illustrate the change in the occurrence probability of one event state k with and without the influence of the last occurred events state l , we also represent the ratios of the *conditional* probabilities to *unconditional* probabilities for the occurrence of event state k :

$$\text{Leverage ratio} = \frac{\mathbb{P}\text{r}(dN^k(t_i) = 1 | dN^l(t_{i-1}) = 1)}{\mathbb{P}\text{r}(dN^k(t_i) = 1)} \quad (3.46)$$

which are values in parentheses on the second line of each cell. These ratios are called leverage ratios because they indicate the change in the probability of occurrence for one state induced by the arrival of other states. For example, denoting k for (AAPL, ≥ 3 ticks) and l for (AAPL, ≤ 3 ticks), the probability of unconditional occurrence for state k in the next event is only 0.74%. However, given that the last event is state l , the conditional probability of the occurrence for state k rises to 15.7%, giving the leverage ratio of 34.3. The leverage ratio greater than 1 can be considered as one state, which actually is triggered by another state, that can be seen as self- or cross-excitation effects. The significant excitements are highlighted by bold values, which are greater than 2 for states belonging to the same asset and greater than 1.2 for states belonging to different assets. On the other hand, a ratio smaller than 1 can be an indicator of inhibition effects, i.e. the occurrence of one state prevents other states from occurring. However, such an inhibition effect requires a different specification of conditional intensities, which is beyond the scope of this thesis, and thus we do not account for it in the analysis.

We note that each panel in the tables can be divided into four separated quadrants, which is equivalent to the decomposition of the Hawkes kernel matrix in Eqn. 3.41. The top-left (Q1) and bottom-right (Q4) quadrants include the cells of excitement that are generated by the self-adjustment conditional in a previous state of the asset itself. Whereas, the top-right (Q2) and bottom-left (Q3) ones are of the excitements from the cross-adjustment

Table 3.2: Empirical results of pair-wise interdependence for six selected DJIA stocks.

		AAPL						IBM					
		≤ -3	-2	-1	1	2	≥ 3	≤ -3	-2	-1	1	2	≥ 3
AAPL	≤ -3	0.57 (0.90)	0.29 (0.44)	0.23 (0.30)	0.71 (0.97)	2.58 (4.47)	15.08 (35.93)	1.34 (1.99)	0.79 (1.25)	0.56 (0.88)	0.40 (0.60)	0.56 (0.87)	0.87 (1.47)
	-2	2.53 (0.52)	2.09 (0.40)	2.19 (0.41)	6.72 (1.32)	20.77 (4.43)	17.57 (3.83)	6.25 (1.28)	5.11 (1.00)	4.20 (0.80)	3.27 (0.62)	3.93 (0.75)	5.26 (1.04)
	-1	16.65 (0.48)	18.00 (0.52)	25.00 (0.72)	49.20 (1.42)	41.11 (1.18)	32.58 (0.94)	29.84 (0.86)	32.10 (0.92)	32.83 (0.94)	27.90 (0.80)	27.11 (0.78)	26.23 (0.75)
	1	30.75 (0.89)	40.26 (1.16)	49.00 (1.42)	24.27 (0.71)	17.87 (0.52)	17.08 (0.49)	27.56 (0.80)	27.50 (0.80)	28.17 (0.82)	33.70 (0.98)	33.24 (0.96)	31.77 (0.92)
	2	19.73 (4.25)	21.56 (4.53)	6.88 (1.33)	1.94 (0.36)	2.04 (0.40)	2.26 (0.45)	5.04 (0.96)	4.24 (0.81)	3.57 (0.68)	4.64 (0.88)	5.48 (1.07)	6.69 (1.35)
	≥ 3	15.70 (34.30)	3.06 (4.99)	0.71 (0.94)	0.20 (0.27)	0.25 (0.35)	0.46 (0.58)	1.25 (1.76)	0.66 (0.86)	0.50 (0.64)	0.69 (0.94)	0.93 (1.42)	1.39 (1.85)
IBM	≤ -3	1.31 (2.54)	0.81 (1.40)	0.58 (1.02)	0.43 (0.75)	0.55 (0.99)	0.81 (1.46)	0.49 (0.96)	0.24 (0.46)	0.19 (0.32)	0.62 (1.06)	1.91 (3.89)	6.62 (16.25)
	-2	2.40 (1.39)	2.02 (1.16)	1.77 (1.03)	1.31 (0.76)	1.33 (0.77)	1.39 (0.81)	1.31 (0.77)	1.20 (0.71)	1.12 (0.65)	2.99 (1.76)	6.89 (4.25)	5.17 (3.18)
	-1	5.05 (0.70)	6.11 (0.86)	6.93 (0.98)	5.34 (0.76)	4.10 (0.58)	3.55 (0.49)	7.17 (1.06)	8.30 (1.22)	10.22 (1.50)	15.24 (2.20)	10.97 (1.57)	8.33 (1.21)
	1	3.50 (0.49)	4.02 (0.57)	5.06 (0.71)	7.39 (1.04)	6.49 (0.92)	5.77 (0.80)	7.29 (1.05)	11.06 (1.59)	15.30 (2.20)	9.45 (1.38)	7.79 (1.15)	6.22 (0.93)
	2	1.22 (0.73)	1.23 (0.73)	1.23 (0.73)	1.84 (1.09)	2.04 (1.21)	2.25 (1.32)	5.64 (3.54)	6.80 (4.27)	2.75 (1.67)	0.92 (0.54)	0.95 (0.56)	1.13 (0.68)
	≥ 3	0.59 (0.89)	0.56 (0.92)	0.43 (0.72)	0.64 (1.08)	0.88 (1.57)	1.21 (2.07)	6.81 (15.16)	2.01 (3.79)	0.58 (0.98)	0.18 (0.30)	0.23 (0.36)	0.31 (0.63)
Total		0.74	5.17	34.75	34.51	5.24	0.78	0.57	1.73	7.10	7.11	1.69	0.59
		AXP						V					
		≤ -3	-2	-1	1	2	≥ 3	≤ -3	-2	-1	1	2	≥ 3
AXP	≤ -3	0.31 (0.43)	0.28 (0.35)	0.19 (0.25)	0.64 (0.87)	2.27 (3.84)	9.50 (20.91)	1.94 (3.04)	1.25 (2.01)	0.67 (0.97)	0.51 (0.71)	0.86 (1.29)	1.21 (2.06)
	-2	1.58 (0.69)	1.34 (0.56)	1.14 (0.47)	3.31 (1.42)	9.13 (4.25)	6.94 (3.40)	3.75 (1.79)	3.00 (1.36)	2.37 (1.02)	1.75 (0.75)	1.93 (0.87)	2.18 (0.98)
	-1	8.86 (0.72)	10.38 (0.83)	13.11 (1.06)	22.45 (1.78)	15.65 (1.24)	11.30 (0.90)	10.30 (0.82)	11.31 (0.90)	12.46 (0.99)	9.37 (0.74)	7.49 (0.59)	6.25 (0.50)
	1	11.56 (0.92)	16.43 (1.29)	22.53 (1.77)	12.96 (1.03)	10.82 (0.87)	8.99 (0.72)	6.16 (0.49)	7.59 (0.59)	9.10 (0.71)	12.95 (1.02)	11.94 (0.94)	10.66 (0.85)
	2	7.66 (3.70)	8.85 (4.17)	3.12 (1.35)	0.97 (0.41)	1.28 (0.56)	1.63 (0.73)	2.05 (0.91)	1.79 (0.79)	1.67 (0.73)	2.48 (1.09)	3.18 (1.42)	3.54 (1.60)
	≥ 3	8.66 (18.51)	2.34 (3.93)	0.55 (0.76)	0.18 (0.25)	0.26 (0.43)	0.34 (0.50)	1.39 (1.96)	0.72 (1.18)	0.51 (0.75)	0.71 (1.04)	1.20 (1.88)	1.63 (2.74)
V	≤ -3	2.88 (4.14)	1.50 (1.75)	0.91 (0.97)	0.53 (0.56)	0.87 (0.97)	1.56 (1.61)	0.51 (0.55)	0.44 (0.61)	0.27 (0.30)	0.87 (0.96)	3.32 (4.54)	14.31 (23.94)
	-2	6.60 (1.50)	5.95 (1.35)	4.31 (0.95)	2.90 (0.65)	4.00 (0.92)	5.52 (1.35)	2.75 (0.70)	2.44 (0.56)	2.13 (0.47)	5.75 (1.32)	15.45 (3.84)	14.13 (3.57)
	-1	25.48 (0.88)	27.54 (0.95)	28.58 (0.99)	22.41 (0.77)	20.74 (0.72)	19.53 (0.67)	13.79 (0.48)	17.20 (0.60)	22.53 (0.79)	40.92 (1.42)	33.52 (1.16)	26.93 (0.93)
	1	20.21 (0.69)	20.95 (0.72)	22.01 (0.75)	28.48 (0.98)	28.04 (0.96)	25.62 (0.88)	25.91 (0.89)	34.22 (1.17)	42.00 (1.44)	22.41 (0.77)	18.41 (0.64)	15.60 (0.54)
	2	4.57 (1.11)	3.59 (0.85)	2.96 (0.67)	4.28 (0.96)	5.48 (1.25)	7.04 (1.69)	16.38 (4.11)	16.49 (4.11)	5.53 (1.29)	2.00 (0.45)	2.32 (0.53)	3.03 (0.73)
	≥ 3	1.63 (2.05)	0.84 (0.98)	0.58 (0.62)	0.88 (0.97)	1.46 (1.63)	2.04 (2.15)	15.05 (27.98)	3.53 (5.08)	0.76 (0.83)	0.27 (0.31)	0.39 (0.48)	0.53 (0.67)
Total		0.71	2.33	12.61	12.73	2.30	0.70	0.92	4.41	28.88	29.16	4.36	0.90

Notes: Conditional probabilities of occurrences of event type k (in rows) given the last occurrence of event type l (in columns): $\Pr(dN^k(t_i) = 1 | dN^l(t_{i-1}) = 1)$. The result is reported in percentage. The last row **Total** presents the unconditional probabilities of each type of events.

Table 3.3: Empirical results of pair-wise interdependence for six selected DJIA stocks (*continued*).

		CVX					XOM				
		≤ -3	-2	-1	1	2	≥ 3	≤ -2	-1	1	≥ 2
CVX	≤ -3	0.44 (0.47)	0.23 (0.21)	0.20 (0.17)	0.97 (0.86)	3.27 (3.10)	13.45 (12.84)	3.01 (2.96)	1.56 (1.44)	0.75 (0.67)	1.08 (0.89)
	-2	2.05 (0.44)	2.03 (0.43)	1.88 (0.39)	6.21 (1.28)	15.39 (3.19)	12.30 (2.63)	6.73 (1.42)	5.85 (1.22)	3.35 (0.69)	3.63 (0.76)
	-1	10.54 (0.48)	12.75 (0.58)	17.90 (0.81)	33.01 (1.47)	24.35 (1.10)	18.95 (0.86)	20.61 (0.93)	23.74 (1.07)	16.54 (0.74)	14.07 (0.63)
	1	18.43 (0.83)	24.97 (1.11)	33.26 (1.48)	18.08 (0.82)	14.09 (0.64)	10.84 (0.49)	12.00 (0.53)	15.51 (0.69)	24.57 (1.10)	20.91 (0.94)
	2	12.61 (2.68)	15.52 (3.28)	6.19 (1.29)	1.70 (0.36)	1.87 (0.39)	2.07 (0.45)	2.68 (0.55)	3.11 (0.65)	5.97 (1.27)	7.00 (1.52)
	≥ 3	13.94 (14.52)	3.57 (3.37)	0.91 (0.77)	0.20 (0.17)	0.21 (0.19)	0.38 (0.38)	1.08 (0.93)	0.74 (0.65)	1.62 (1.50)	2.47 (2.32)
	Total	1.15	4.85	22.27	22.37	4.79	1.15	0.43	21.22	21.42	0.34
XOM	≤ -2	1.05 (2.31)	0.56 (1.26)	0.44 (1.06)	0.23 (0.56)	0.30 (0.67)	0.35 (0.79)	0.17 (0.30)	0.09 (0.20)	0.77 (1.85)	9.52 (26.06)
	-1	26.28 (1.21)	25.20 (1.17)	23.66 (1.11)	15.88 (0.75)	15.08 (0.70)	14.71 (0.68)	6.59 (0.33)	8.60 (0.41)	38.00 (1.84)	33.57 (1.64)
	1	14.29 (0.66)	14.92 (0.69)	15.39 (0.72)	23.40 (1.08)	24.95 (1.15)	25.99 (1.18)	36.04 (1.73)	40.24 (1.94)	8.35 (0.40)	7.60 (0.36)
	≥ 2	0.37 (1.03)	0.25 (0.73)	0.18 (0.51)	0.32 (0.95)	0.48 (1.46)	0.97 (3.03)	11.09 (41.51)	0.56 (1.69)	0.06 (0.17)	0.15 (0.31)
	Total	1.15	4.85	22.27	22.37	4.79	1.15	0.43	21.22	21.42	0.34
IBM	≤ -3	0.90 (0.71)	0.52 (0.39)	0.41 (0.27)	1.28 (0.89)	3.91 (3.06)	13.50 (12.35)	2.33 (1.59)	1.65 (1.10)	1.15 (0.80)	1.28 (0.85)
	-2	2.32 (0.53)	2.22 (0.51)	2.31 (0.52)	5.88 (1.35)	13.09 (3.11)	10.42 (2.51)	4.41 (1.01)	4.60 (1.04)	3.42 (0.78)	2.97 (0.68)
	-1	11.85 (0.67)	14.06 (0.79)	18.30 (1.03)	26.80 (1.50)	20.17 (1.13)	15.43 (0.86)	13.45 (0.75)	16.69 (0.93)	13.90 (0.77)	10.29 (0.57)
	1	13.91 (0.77)	19.95 (1.11)	27.15 (1.51)	17.96 (1.01)	14.31 (0.80)	11.09 (0.62)	10.19 (0.56)	13.00 (0.72)	17.88 (0.99)	16.31 (0.90)
	2	11.21 (2.78)	13.40 (3.28)	5.61 (1.32)	2.11 (0.48)	2.21 (0.51)	2.43 (0.57)	2.81 (0.68)	3.16 (0.74)	4.61 (1.07)	4.50 (1.08)
	≥ 3	13.71 (11.53)	4.37 (3.34)	1.24 (0.83)	0.40 (0.26)	0.50 (0.33)	0.74 (0.49)	1.57 (1.15)	1.15 (0.77)	1.73 (1.17)	2.61 (1.66)
	Total	1.15	4.85	22.27	22.37	4.79	1.15	0.43	21.22	21.42	0.34
XOM	≤ -2	0.84 (1.57)	0.59 (1.19)	0.41 (0.78)	0.28 (0.57)	0.39 (0.74)	0.51 (0.91)	0.34 (0.54)	0.15 (0.28)	0.94 (1.86)	10.72 (23.23)
	-1	25.64 (1.00)	25.54 (1.00)	24.88 (0.97)	20.44 (0.80)	19.80 (0.77)	20.18 (0.79)	9.78 (0.38)	12.64 (0.50)	43.86 (1.72)	39.73 (1.57)
	1	19.18 (0.74)	19.03 (0.74)	19.45 (0.75)	24.54 (0.95)	25.25 (0.98)	24.92 (0.96)	42.83 (1.67)	46.28 (1.80)	12.40 (0.48)	11.38 (0.44)
	≥ 2	0.44 (0.88)	0.32 (0.80)	0.23 (0.55)	0.33 (0.83)	0.37 (0.94)	0.78 (1.81)	12.31 (37.45)	0.68 (1.63)	0.11 (0.25)	0.21 (0.45)
	Total	1.45	4.39	17.96	18.04	4.28	1.49	0.53	25.60	25.82	0.43

Notes: Conditional probabilities leverage represents the ratio of the conditional occurrence probability of event type k given the last occurrence of event type l and the unconditional probability of each type of events.

Table 3.4: Empirical results of pair-wise interdependence for six selected DJIA stocks (*continued*).

		AAPL						AXP					
		≤ -3	-2	-1	1	2	≥ 3	≤ -3	-2	-1	1	2	≥ 3
AAPL	≤ -3	0.55 (0.74)	0.30 (0.46)	0.24 (0.32)	0.74 (0.98)	2.64 (4.33)	15.55 (34.64)	1.70 (2.30)	0.80 (1.26)	0.57 (0.86)	0.39 (0.52)	0.69 (0.96)	1.00 (1.51)
	-2	2.72 (0.53)	2.16 (0.39)	2.32 (0.42)	7.02 (1.30)	21.42 (4.32)	18.64 (3.88)	7.32 (1.45)	5.35 (1.01)	4.26 (0.77)	3.30 (0.60)	4.41 (0.81)	5.61 (1.06)
	-1	17.71 (0.48)	18.96 (0.52)	26.42 (0.72)	51.46 (1.40)	43.11 (1.17)	33.64 (0.92)	31.59 (0.86)	33.36 (0.91)	33.90 (0.92)	28.83 (0.78)	27.60 (0.75)	26.74 (0.73)
	1	31.64 (0.86)	42.03 (1.15)	51.13 (1.40)	25.86 (0.71)	18.88 (0.52)	18.35 (0.50)	26.69 (0.73)	28.49 (0.78)	29.43 (0.81)	34.86 (0.96)	34.26 (0.94)	32.42 (0.89)
	2	20.53 (4.16)	22.42 (4.46)	7.16 (1.31)	2.08 (0.37)	2.12 (0.39)	2.48 (0.48)	5.76 (1.06)	4.58 (0.85)	3.72 (0.66)	4.86 (0.87)	5.67 (1.04)	7.14 (1.34)
	≥ 3	16.52 (35.50)	3.20 (4.99)	0.74 (0.93)	0.22 (0.28)	0.29 (0.41)	0.56 (0.75)	1.00 (1.20)	0.84 (1.16)	0.49 (0.62)	0.69 (0.88)	1.02 (1.49)	1.50 (2.35)
AXP	≤ -3	0.89 (3.51)	0.48 (1.52)	0.31 (0.98)	0.25 (0.75)	0.32 (1.03)	0.54 (1.72)	0.31 (1.93)	0.18 (0.53)	0.11 (0.32)	0.36 (1.03)	1.36 (5.26)	5.56 (26.73)
	-2	1.19 (1.15)	1.19 (1.16)	1.06 (1.01)	0.82 (0.77)	0.82 (0.78)	0.92 (0.94)	1.03 (1.03)	0.86 (0.87)	0.73 (0.66)	2.03 (1.97)	5.78 (6.04)	4.45 (4.67)
	-1	4.26 (0.74)	4.98 (0.86)	5.56 (0.96)	4.24 (0.74)	3.34 (0.58)	2.47 (0.44)	6.63 (1.24)	7.45 (1.38)	9.14 (1.68)	15.27 (2.74)	10.35 (1.87)	7.69 (1.39)
	1	2.61 (0.44)	3.19 (0.55)	4.06 (0.70)	5.88 (1.01)	5.31 (0.92)	4.73 (0.80)	7.91 (1.42)	11.19 (1.97)	15.51 (2.74)	8.70 (1.58)	7.89 (1.44)	6.45 (1.20)
	2	0.79 (0.85)	0.79 (0.75)	0.75 (0.73)	1.12 (1.09)	1.28 (1.28)	1.40 (1.38)	4.97 (5.24)	5.62 (5.93)	1.81 (1.73)	0.62 (0.57)	0.81 (0.75)	1.26 (1.31)
	≥ 3	0.59 (2.05)	0.29 (0.92)	0.24 (0.76)	0.33 (1.05)	0.48 (1.67)	0.72 (2.76)	5.09 (23.52)	1.26 (4.62)	0.32 (0.97)	0.10 (0.33)	0.15 (0.48)	0.20 (0.64)
Total		0.77	5.44	36.69	36.44	5.52	0.81	0.33	1.06	5.75	5.83	1.04	0.32

		CVX						V					
		≤ -3	-2	-1	1	2	≥ 3	≤ -3	-2	-1	1	2	≥ 3
CVX	≤ -3	0.42 (0.49)	0.27 (0.32)	0.21 (0.22)	0.88 (0.90)	2.97 (3.35)	12.29 (14.22)	2.68 (2.95)	1.41 (1.55)	0.90 (0.99)	0.70 (0.76)	1.02 (1.07)	1.58 (1.65)
	-2	2.12 (0.54)	2.01 (0.51)	1.83 (0.46)	5.51 (1.36)	13.85 (3.38)	10.63 (2.70)	5.47 (1.40)	4.74 (1.19)	3.94 (0.99)	3.05 (0.75)	3.35 (0.83)	3.58 (0.87)
	-1	10.80 (0.59)	12.53 (0.68)	17.03 (0.93)	29.63 (1.58)	21.77 (1.17)	17.47 (0.94)	13.65 (0.74)	15.95 (0.86)	17.34 (0.94)	14.72 (0.78)	12.09 (0.65)	11.17 (0.58)
	1	16.73 (0.90)	22.55 (1.20)	30.08 (1.60)	16.49 (0.89)	13.34 (0.72)	10.79 (0.59)	10.54 (0.55)	12.24 (0.65)	14.21 (0.75)	18.07 (0.97)	16.63 (0.89)	13.80 (0.74)
	2	11.35 (2.88)	13.79 (3.46)	5.43 (1.34)	1.60 (0.41)	1.90 (0.48)	2.28 (0.61)	3.92 (0.99)	3.37 (0.84)	3.02 (0.76)	4.04 (1.02)	4.94 (1.27)	5.46 (1.38)
	≥ 3	12.10 (14.56)	3.21 (3.60)	0.83 (0.83)	0.20 (0.21)	0.23 (0.27)	0.29 (0.28)	1.49 (1.55)	1.07 (1.14)	0.69 (0.75)	0.97 (1.05)	1.54 (1.66)	2.51 (2.96)
V	≤ -3	1.74 (2.52)	1.07 (1.49)	0.65 (0.87)	0.47 (0.65)	0.69 (1.01)	1.18 (1.97)	0.38 (0.51)	0.30 (0.42)	0.22 (0.30)	0.70 (1.06)	2.72 (5.28)	11.76 (27.05)
	-2	5.45 (1.57)	4.25 (1.24)	3.14 (0.90)	2.31 (0.67)	2.89 (0.87)	3.51 (1.06)	2.19 (0.72)	1.90 (0.57)	1.73 (0.50)	4.70 (1.46)	12.84 (4.39)	11.82 (3.99)
	-1	19.39 (0.87)	20.61 (0.92)	21.04 (0.95)	17.49 (0.79)	16.71 (0.75)	14.95 (0.67)	11.62 (0.54)	14.26 (0.66)	18.37 (0.86)	33.26 (1.56)	27.81 (1.30)	22.77 (1.07)
	1	15.24 (0.68)	16.08 (0.72)	16.99 (0.76)	21.59 (0.96)	20.63 (0.92)	19.91 (0.88)	22.34 (1.01)	28.37 (1.31)	34.50 (1.60)	17.99 (0.83)	14.91 (0.69)	12.82 (0.59)
	2	3.61 (1.10)	2.91 (0.88)	2.33 (0.70)	3.17 (0.92)	4.04 (1.19)	4.91 (1.46)	13.24 (4.45)	13.52 (4.57)	4.49 (1.40)	1.58 (0.47)	1.87 (0.57)	2.35 (0.72)
	≥ 3	1.04 (1.62)	0.72 (1.14)	0.44 (0.63)	0.66 (0.90)	0.97 (1.36)	1.80 (2.89)	12.49 (33.02)	2.89 (5.66)	0.59 (0.87)	0.21 (0.32)	0.30 (0.44)	0.38 (0.53)
Total		0.97	4.08	18.74	18.80	4.03	0.98	0.71	3.38	22.03	22.26	3.33	0.69

Notes: Conditional probabilities leverage represents the ratio of the conditional occurrence probability of event type k given the last occurrence of event type l and the unconditional probability of each type of events.

based on historical trade of other assets. Also inside each quadrant, we can further divide into four sub-quadrants: the top-left (SQ1) and bottom-right (SQ4) indicate the excitements between same-sign states, i.e. from a negative (positive) state to a negative (positive) state, while the top-right (SQ2) and bottom-left (SQ3) are for the excitements between opposite sign states, i.e. from a positive (negative) state to a negative (positive) state. Looking at these (sub-) quadrants, we can shed light on the main characteristics of the multivariate disjoint point processes as follows:

1. The interdependence is roughly similar across panels of different pairs of stocks and is centre-symmetric in each quadrant.
2. In self-adjustment quadrants, Q1 and Q4, the significant excitements with remarkably high leverage ratios are in the sub-quadrants SQ2 and SQ3, which are composed of opposite-sign states. This observation indicates that the predominant behaviour of the price process is price reversion rather than price continuation.
3. Meanwhile, for cross-asset adjustment, Q2 and Q3, the significant excitements are in the sub-quadrants, SQ1 and SQ4, composed of same sign states, which indicate the tendency moving in the same direction of two price processes is higher than moving in the opposite direction. This can be attributed to positive cross-autocorrelation or lead-lag effects between assets.
4. Amongst the cells, the strongest excitements are between extreme states, e.g $(AAPL, \leq -3) \Leftrightarrow (AAPL, \geq 3)$; $(IBM, \leq -3) \Leftrightarrow (IBM, \geq 3)$; $(AAPL, \leq -3) \Leftrightarrow (IBM, \leq -3)$; $(AAPL, \geq 3) \Leftrightarrow (IBM, \geq 3)$ etc.
5. There are some stocks that consistently lead other stocks, for example, $AAPL \rightarrow IBM$, $AAPL \rightarrow AXP$. The pairwise leverage ratio in the quadrants representing the impact of AAPL on other assets is higher than in the quadrant representing the opposite direction.
6. There is evidence of lead-lag correlations between assets belonging to different groups, illustrated by strong leverage ratios in the Q2 and Q3 quadrants. These lead-lag between-groups effects, i.e $APPL \Leftrightarrow IBM$, $AXP \Leftrightarrow V$, $CVX \Leftrightarrow XOM$, are in general stronger than the within-groups effects, i.e $APPL \Leftrightarrow AXP$, $IBM \Leftrightarrow XOM$, $CXV \Leftrightarrow V$.

In general, we can say that there exist temporal dependencies between states of disjoint price change point processes. Some states stimulate the occurrence of states in the same asset or in other assets, which can be seen as self-adjustment or cross-adjustment in the model of Proposition 1. We will address these dependencies with the Hawkes processes modelling approach in the next section.

3.5 MODEL CALIBRATION

3.5.1 Non-parametric estimation

The goal of this section is to specify a non-parametric Hawkes model for transaction price data without postulating a specific form for an adjustment (decay) kernel. As we mentioned, the parametric specification tends to be oversimplified or even incapable of capturing the adjustment kernel in some scenarios, e.g. the adjustment to information involves regime-switching or information simply decaying periodically and in an oscillatory way. In such a case, a data-driven and non-parametric approach is more appropriate to investigate the ground truth of the kernel shape. In our study, non-parametric estimation give point-wise excitements between disjoint observed discrete price states. On that ground, we make inferences about the point-wise adjustment of price dynamics. The results also verify the assumptions and selections of the excitement function that we previously chose for the parametric estimation in a later section.

In the first step, we estimate the baseline intensities μ^k and the non-parametric kernel matrix ϕ^{kl} of the conditional intensities in the Proposition 3 for K -dimensional Hawkes point processes, which result from disjointing transaction data of pairwise stocks. Since the Hawkes conditional intensities are an instantaneous representation of the autoregressive observed price processes in the Proposition 2, we can retrieve the incremental of the noisy signals from order flows, i.e. $\eta^d dt$, and the point-wise incremental of the adjustment kernel, i.e. $\psi^{dr} dt$, of the autoregressive price dynamics from the obtained estimation in the first step. All estimations are employed on a daily basis, and we consider transaction time series to be independent across trading days. Consequently, the estimation procedure described previously is applied independently every day, and then the daily results are averaged to get the final estimates.

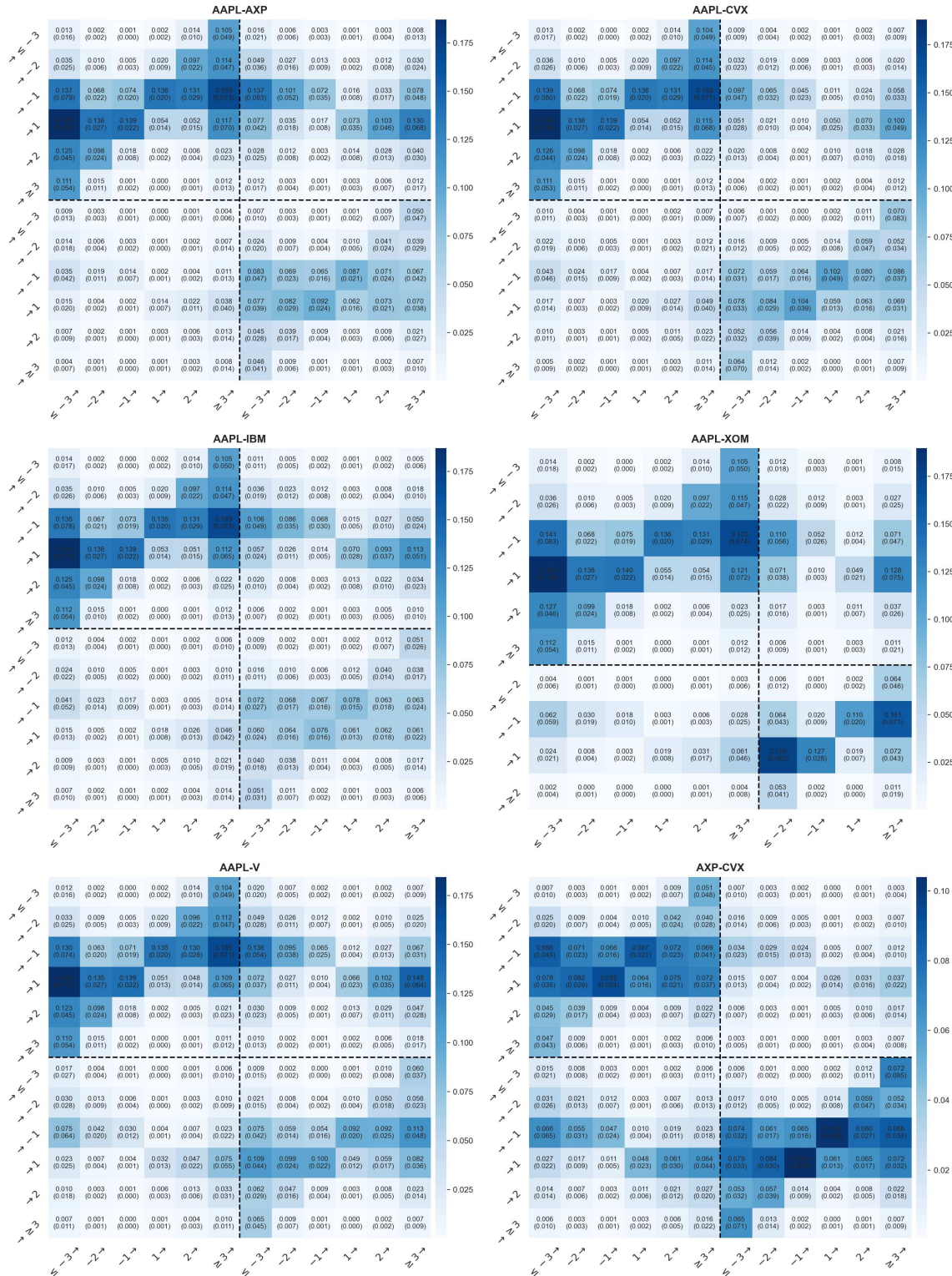
3.5.1.1 The excitement kernel norms of disjoint price change states

Figure 3.3 shows the average estimate of the matrix-valued excitement kernel norms:

$$\mathbf{G} = \{G^{kl}\}_{k,l \in [1,K]}, G^{kl} = \|\phi^{kl}\|_1 = \int_0^\infty \phi^{kl}(t) dt$$

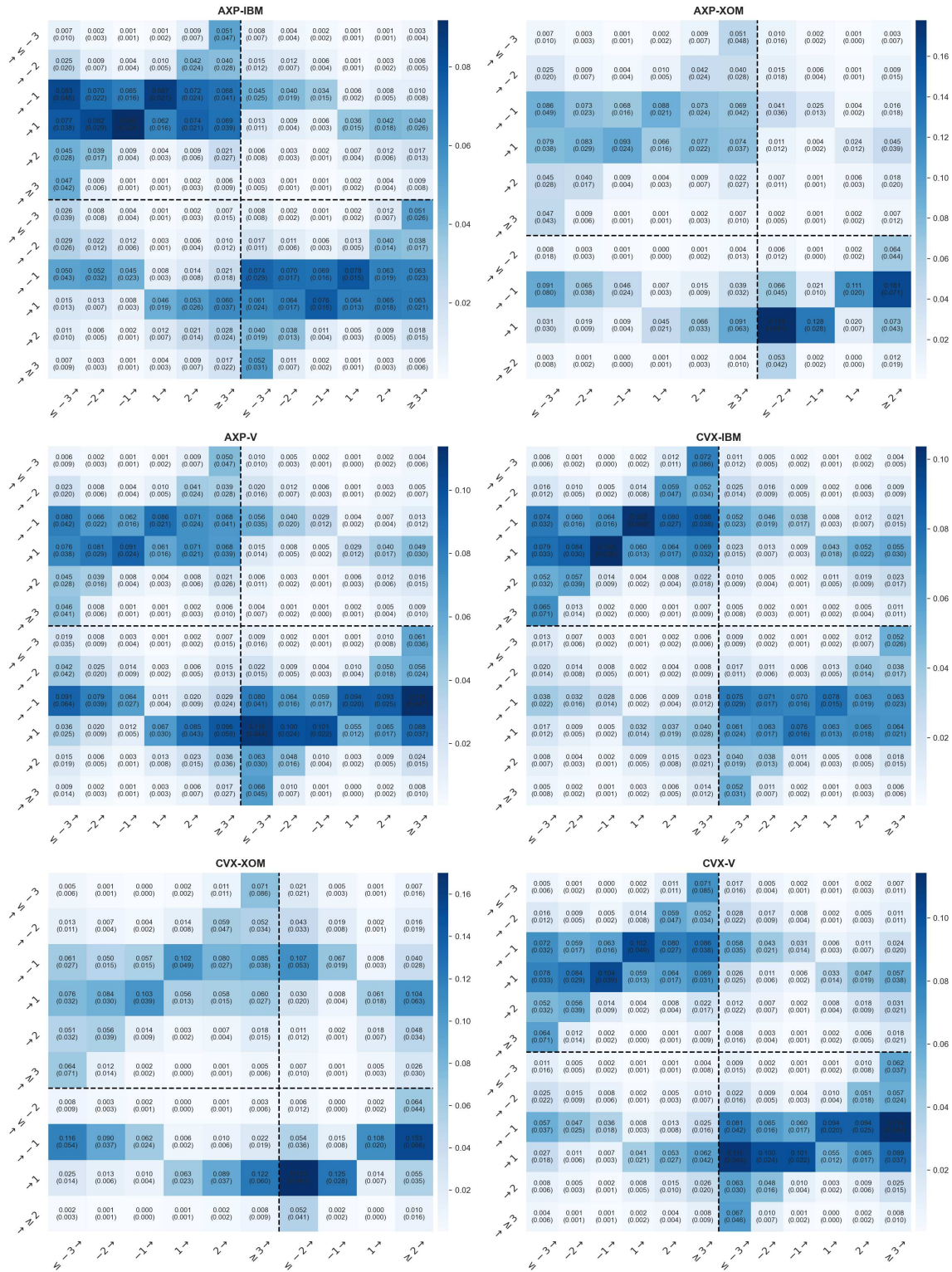
We recall that the kernel $\phi^{kl}(t)$ is only the “bare” point-wise impact of a transaction of state l on the likelihood of a transaction occurrence with state k . In order to account for the impact associated with all the cascades triggered by some event, ones have to estimate the kernel norms G^{kl} . The kernel norms G^{kl} illustrate the mean number of transaction event states k triggered by a single transaction of state l , and measure the total of self-excitation and cross-excitation between states. Furthermore, in the framework of our price adjustment dynamics, the kernel norms also represent the total information on the true underlying level that is retrieved from the trade occurring at one state. For the sake of simplicity, we represent the norm values using a colour map with more intense blue cells corresponding to higher kernel norms. In each cell, the value in the first line is the average

Figure 3.3: Average excitement kernel norms $\int_0^\infty \Phi(t)dt$ amongst observed discrete price change states of pairwise stocks.



Note: The top-left (Q1) and bottom-right (Q4) quadrants include the cells of excitement that are generated by the self-adjustment conditional on the previous state of the asset per se. The top-right (Q2) and bottom-left (Q3) ones are of the excitements from the cross-adjustment based on the historical trade of other assets. In each cell, the first line is the average of the excitement norm over all trading days while the second one is the covariance of the norm.

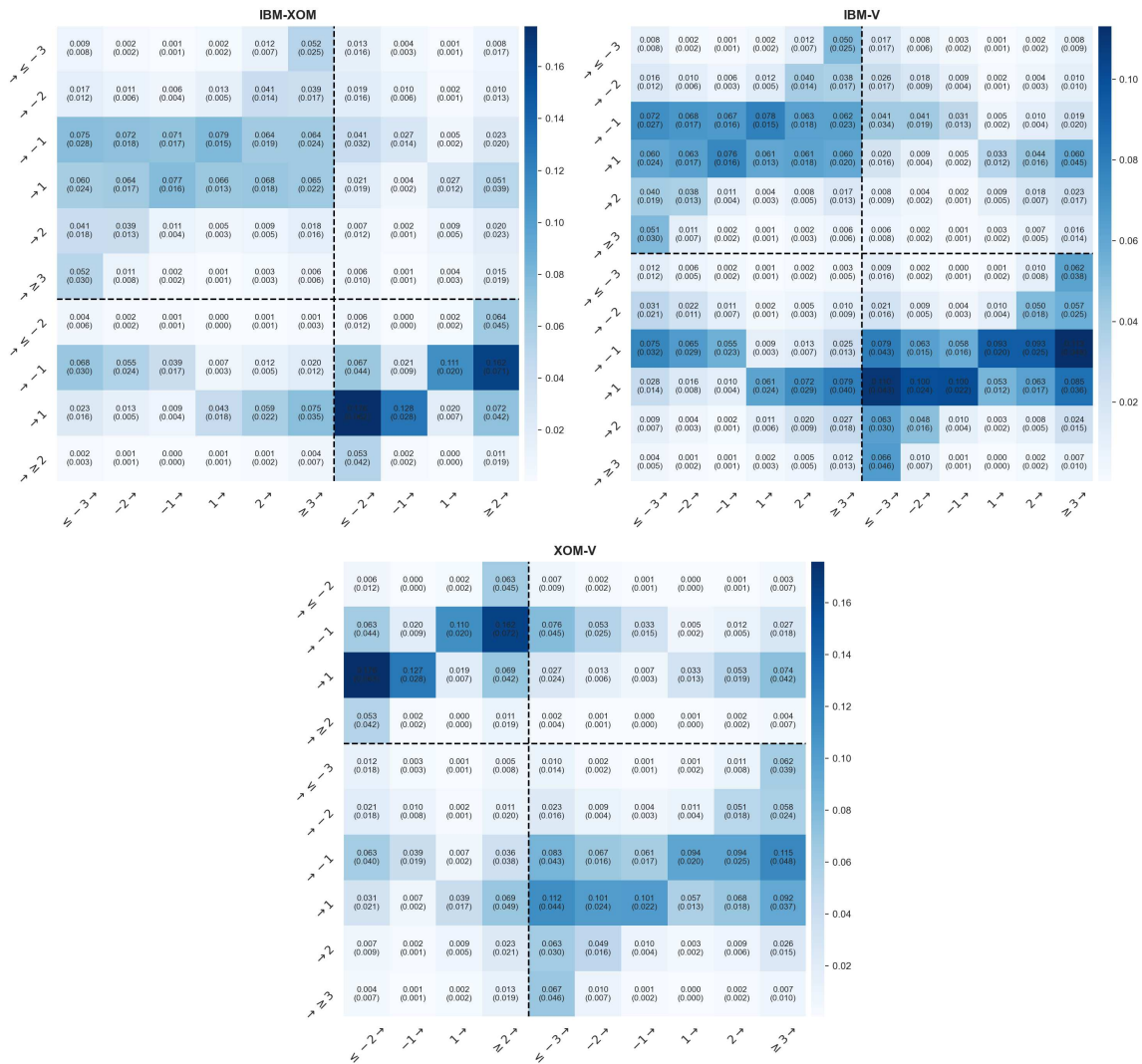
Figure 3.3: Average excitement kernel norm $\int_0^\infty \Phi(t)dt$ amongst observed discrete price change states of pairwise stocks (*cont.*)



estimate of kernel norms over all trading days, while the value in the second line is the covariance.

As expected, the overall descriptive analysis in the previous section about the interdependence amongst disjoint price change states is fairly well recovered by the shape of

Figure 3.3: Average excitement kernel norm $\int_0^\infty \Phi(t)dt$ amongst observed discrete price change states of pairwise stocks (*cont.*)



the average kernel norm matrix. In particular, the four quadrants of any pairwise assets are symmetrical across the centre. For instance, the kernel $\phi^{(AAPL, \leq -3) \rightarrow (AAPL, \geq 3)}$ seems to have the same norm as the kernel $\phi^{(AAPL, \geq 3) \rightarrow (AAPL, \leq -3)}$. The blue colour of cells in the quadrants Q1 and Q4 are stronger than in the other two quadrants Q2 and Q3. Larger excitement norms between within-asset states indicate a stronger tendency of moving price within one asset than of switching between cross-asset states. As such, the price adjustment is mainly through revising information from the historical trades of the asset itself. Furthermore, heavy blue cells in the leftmost and rightmost columns in each quadrant display strong excitations originating from extreme states, i.e. ≥ 3 and ≤ -3 . This feature confirms that the extreme states carry large amounts of information and thus prompt large adjustments in the price formation.

One can also notice that a striking feature appearing in all pairwise panels is the anti-diagonal shape of the Q1 and Q4 quadrants and the diagonal shape of Q2 and Q3. The former indicates that, on the one hand, one movement in the price mainly triggers another

within-asset movement of similar or smaller magnitude, but with an opposite sign. This within-asset exciting structure implies a strongly mean-reverting behaviour, which is the main characteristics of the price dynamics in the market micro-structure and which is also a potential source that prompts the absence of the price correlation between assets in the long-range. On the other hand, the latter accounts for the influence of one asset's state on transaction intensity of states belonging to other assets. It is found to be less significant to the former and clearly has an opposite pattern: a price move from one asset triggers a price move of other assets in the same direction, i.e. an upward to an upward, a downward to a downward. This co-movement of the assets can be attributed to the positive lead-lag correlation. Also, we can notice smaller kernel norms in the cells that mark the impact of opposite direction states between assets, e.g. $G^{(XOM, \leq -2) \rightarrow (AAPL, 1)}$, $G^{(XOM, \geq 2) \rightarrow (AAPL, -1)}$. This negative lead-lag correlation can arise as a consequence of combined effects of negative auto-correlation and positive contemporaneous correlation.

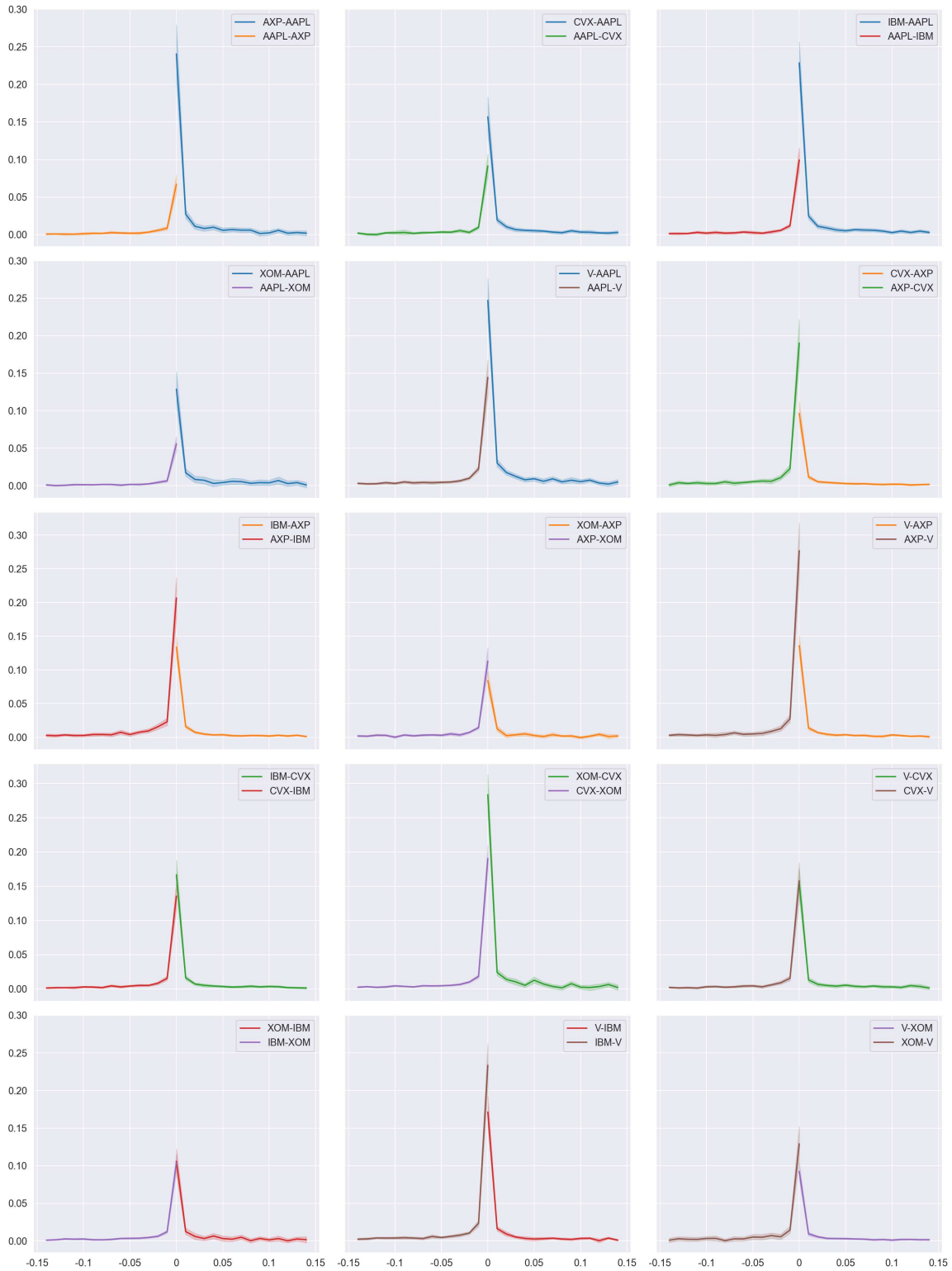
3.5.1.2 *The cross-transaction lead-lag effects*

A more detailed examination of lead-lag effects can be obtained by looking at the point-wise price adjustment incurred by each transaction, i.e. ψ^{dr} with d, r denoting the indexes at asset level. In Figures 3.4 and 3.5, we plot the step-wise increments accumulated by the adjustment kernel, $\int_{t_i}^{t_{i+1}} \psi^{dr}(u) du$, within each step of duration $t_{i+1} - t_i = 10\text{ms}$. Figure 3.4 illustrates the cross-adjustment increments from the trade of the cross-asset, and Figure 3.5 illustrates the self-adjustment increments incurred by the trade of the asset itself. The shaded line denotes the 95% confidence interval. A nonzero estimate of the adjustment kernel at positive (negative) step points implies the lead-lag relation at the transaction level generated by the first (second) relationship displayed in the legend. As suggested in the analysis of the excitement kernel norms, we find strong evidence of positive cross-adjustment effects and negative self-adjustment effects in all selected pairs. Both cross- and self-adjustments start from the highest magnitude of approximately 0.1 - 0.3 at the first 10 ms and decay to zero over the support of about 150 ms. The strongest adjustments are in the time range of 10 to 50 ms, which is significantly less than the average waiting time of a trade (see Table 3.1). The magnitude and effective timescale of the adjustments at the transaction level are relatively close to the relevant literature on lead-lag effects using transaction data (see, e.g. Dao, McGroarty and Urquhart, 2018; Hayashi and Koike, 2019; Huth and Abergel, 2014). More importantly, the results on the effective timescale confirm the inevitability of modelling transaction-by-transaction price dynamics and the advantages of our model over the opposition of an aggregated price (see, in particular, Buccheri, Corsi and Peluso (2020)). While aggregating prices destroy all correlations that are exhausted at a rate higher than the sampling frequency, our model can account for true short-term lead-lag correlations at the finest frequency of transaction level. Thus, the lead-lag correlation between assets can be simply recovered by integrating for any arbitrary interval.

We remind the reader that the adjustment kernel increments plotted in Figures 3.4 and 3.5 measure the point-wise price impact of a trade to other trades, and thus can be inter-

puted as the information content of trade. On the one hand, it is clear from Figure 3.4 that the cross-asset information content is in an inverse relation with the liquidity level.

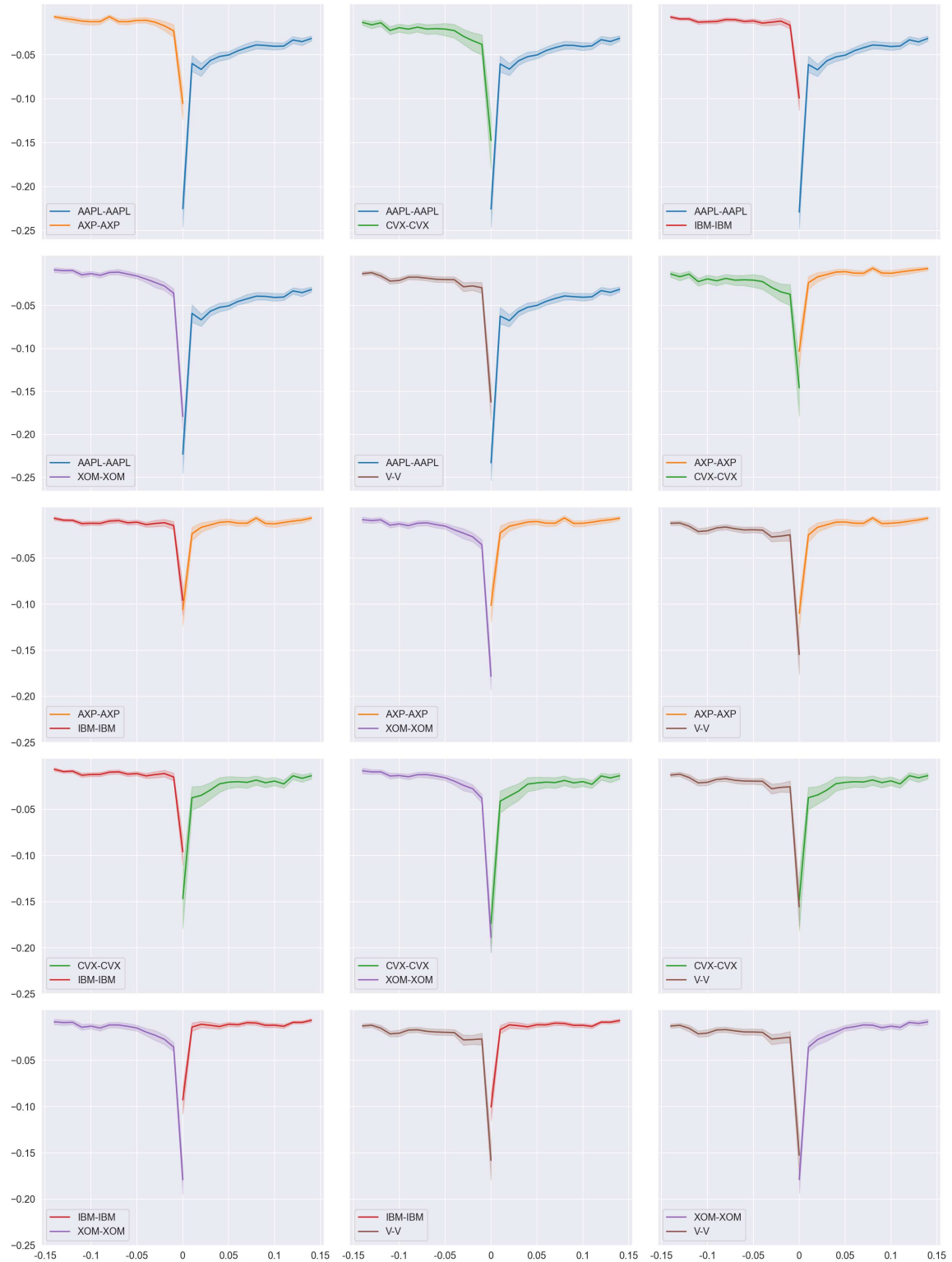
Figure 3.4: Average cross-adjustment of all the pairs formed by six selected stocks (non-parametric estimation).



Notes: Averages are computed overall the business days in the sample. The line shade denotes 95% confidence intervals. Correlations at positive time points imply that the second asset displayed in the legend leads the first asset and the other way around for negative time points.

For instance, APPL is considered as the highest liquidity asset in term of the number of trades from Table 3.1, but its trades convey little information to the price adjustment of

Figure 3.5: Average self-adjustment of all six selected stocks in different pair-wise relations (non-parametric estimation).



Notes: Averages are computed overall the business days in the sample. The line shade denotes 95% confidence intervals.

other assets compared to the impacts from other assets to AAPL's price. Meanwhile, AXP is the lowest liquidity asset and its trade contributes substantially to the price formation of other assets. The small amount of cross-asset information contained in trades of liquidity assets can be attributed to the extremely short duration between consecutive trades (Wuensche, Theissen and Grammig, 2011). When fast trading prevails, there remains little informational change additionally incorporated into trade. Accordingly, the information role of trade is diminished. Also, to a lesser extent, it can be explained by the splitting of meta-orders (Gomes and Waelbroeck, 2014)), which also lowers information content per trade about the correlation with other assets.

On the other hand, Figure 3.5 illustrates that the trade of liquidity assets is in a positive correlation with the strength of self-adjustment. However, the negative strength of auto-correlation indicates that the self-adjustment arises merely as a consequence of the bouncing back and forth of the transaction price between bid and ask prices rather than a true movement in the efficient price. And because of high trading intensity, this buying and selling bouncing even dominates in magnitude the actual efficient price movements and automatically generates strong negative auto-correlation in the trade sequences. Furthermore, we also notice that the negative auto-correlation in the self-adjustment of one asset remains approximately unchanged in different pairwise relations. This consistency of autocorrelation can serve as a robustness check to verify that the self-adjustment effects recovered by our models are not altered in relation to assets of different liquid levels. In other words, the self-adjustment is independent of the cross-adjustment. Compared to the cross-adjustment, the self-adjustments in Figure 3.5 are surprisingly not as strong as previously indicated by the analysis of kernel norms, but even weaker. This might be due to the symmetric excitation of within-asset price change states, where the price reversal is dominance. It, thus, leads to offsets between the within-asset excitements and diminishes the auto-correlation.

3.5.1.3 *The cross-asset lead-lag effects*

Previously, we examined the adjustment effects across transactions, i.e. the impact from a trade to the occurrence of other trades, which can be interpreted as the information content of a trade. The comparison between liquidity levels and the strength of the adjustment kernels shows that high-liquid assets have a low information content per trade. However, this result cannot determine the lead-lag relationship at the asset level. One asset can be highly informative per trade but low trading activity, and consequently, incurs a small aggregated impact on prices of other assets. In the other way around, high liquidity asset with high number of trade but low information content can stimulate a large price impact in total. Thus, to uncover the lead-lag correlation at asset level, it is necessary to account for the liquidity together with the cross-transaction information content. We consider the average elapsed time between two consecutive trades as a proxy of liquidity and incorporate it into the measure of cross-asset lead-lag effects by taking the ratio:

$$\text{Lead-lag correlation} = \frac{\int_0^{\infty} \psi^{dr}(u) du}{\text{Average trade duration}} \quad (3.47)$$

In the above equation, the liquidity of asset is described by the average inter-transaction time between consecutive trades, which is also the inverse ratio of the number of trades within a fixed time, i.e. one second in our context. Thus, the term “lead-lag correlation” quantifies the average adjustment induced by one asset to the formation of the price of another asset in one second. Figure 3.6 displays the daily dynamics of the one-second lead-lag correlation for all pairwise assets, and Table 3.5 illustrates the average estimation over all trading days. We also report in the table the statistics of two sample t-tests, which test whether there exists a “leader” between two assets. It is clear from Figure 3.6 that all lead-lag correlations are all nonzero with high significance. We also find strong evidence of leadership from the results in Table 3.5. For instance, AAPL, the most heavily traded asset, appears to be the most informative asset since it leads almost all the other assets. In contrast, IBM and AXP are led by all other assets. The summary of results in Table 3.5 yields the following lead-lag order among all selected assets:

$$\text{AAPL} \rightleftharpoons \text{XOM} \rightarrow \text{V} \rightleftharpoons \text{AXP} \rightleftharpoons \text{CVX} \rightarrow \text{IBM} \quad (3.48)$$

Table 3.5: The average daily estimate of the lead-lag correlation within one second for different pairwise assets (non-parametric estimation).

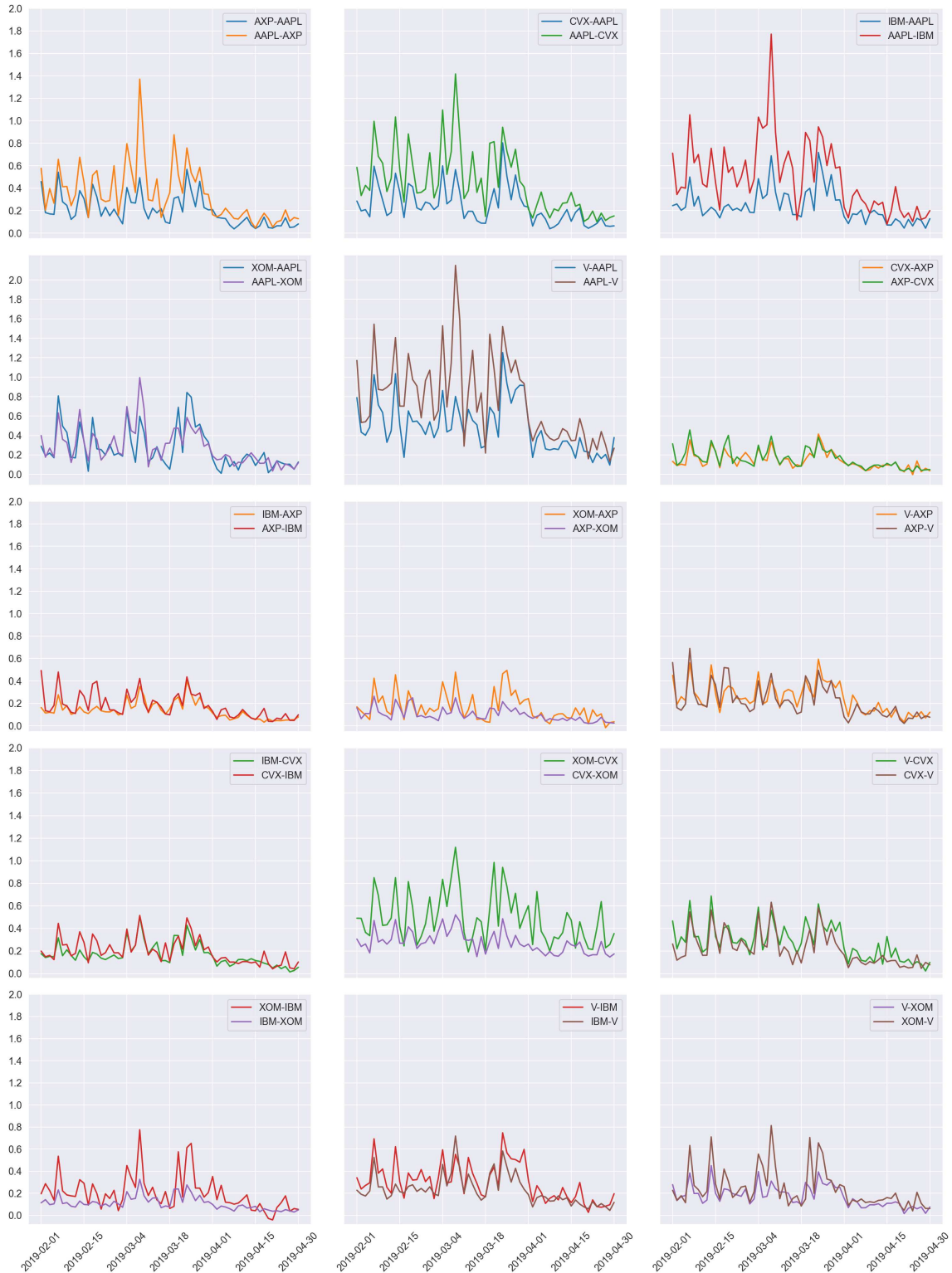
		Group I		Group II		Group III	
		AAPL	IBM	AXP	V	CVX	XOM
Group I	AAPL		0.237	0.201	0.491	0.240	0.264 ^(ns)
	IBM	0.499****		0.179**	0.303**	0.198*	0.204****
Group II	AXP	0.349****	0.138		0.246 ^(ns)	0.143 ^(ns)	0.165***
	V	0.769****	0.233	0.221 ^(ns)		0.223	0.243**
Group III	CVX	0.459****	0.167	0.161 ^(ns)	0.284*		0.492****
	XOM	0.284 ^(ns)	0.112	0.100	0.175	0.278	

Notes: The column indexes denotes the leading assets and the row indexes are the lagged assets. The value with superscript are the lead-lag correlation with significant leadership. The significant levels are obtained based on the p-value of the two-sample t-test: ****: $p \leq 0.0001$, ***: $p \leq 0.001$, **: $p \leq 0.01$, *: $p \leq 0.05$, and ^(ns): $p > 0.05$. The value without superscript denotes the correlation provoked by the follower.

We note that, from Table 3.1, AAPL is the highest liquid asset in terms of the number of trades and the duration of trade, but CVX and IBM are not the least traded asset on average. In fact, CVX, IBM, XOM, and V are relatively similar in the level of liquidity, whereas AXP is the least liquid asset. It is surprising that XOM has much less liquidity than AAPL but has a very similar lead correlation. There is no clear distinction about the leader between these two assets. XOM seems to be highly informative and leads all remaining assets, although the differences in liquidity are small. Similarly, the lead role of AXP in relationships with CVX and IBM is not related to their liquidity levels, because CVX and IBM are considered to have higher liquidity. Thus, the common empirical finding that highly liquid assets are leaders is not always true in our analysis, and we draw a similar

conclusion to the work of Buccheri, Corsi and Peluso (2020): The presence of lead-lag correlation is not only due to its differences in the level of liquidity, which is expressed in terms of trading activity, but also to the information content of trade that contributes to the cross-asset price formations. We recall from Proposition 1 that the quote prices are

Figure 3.6: Self-adjustment of all six selected stocks in different pair-wise relations over all trading days in the sample (non-parametric estimation).



adjusted based on information retrieved from historical trades of not only the asset itself but also other assets. The past price change of some stocks d could be more informative and thus contribute a larger impact on the revision of other stocks r than other stocks r have on themselves, which emerge from $\Psi^{dr} > \Psi^{rd}$. Such differences, in turn, generate a higher correlation on the “lead” side than on the “lag” side.

Clearly, there exists statistical evidence of lead-lag correlation between not only within-group assets but also cross-group assets. On the one hand, in terms of lead correlation, i.e. the correlation generated by one asset leading another asset, the cross-group effects are generally weaker than within-group effects. From Table 3.5, AXP, CVX, IBM, and XOM (in columns) exhibit the highest lead correlations in relation to within-sector assets. In other cases, we observe smaller correlations. For instance, $AXP-V > AXP-AAPL > AXP-IBM > AXP-CVX > AXP-XOM$. On the other hand, in terms of lag correlation, i.e. the correlation in which one asset is led by another asset, the largest correlations are mostly from the relationship with the most liquid asset, AAPL. The exceptional case is of group III assets, energy sector, in which the largest lag correlations of CVX and XOM are still in relation to within-group assets, XOM and CVX, respectively.

3.5.1.4 *The exogenous information*

In the next step, it is useful to investigate the remaining estimated component of the observed price dynamics, η . We recall that while Ψ demonstrates adjustment processes of endogenous lagged information, $\eta dt = \gamma dY_t$ determines the immigration of exogenous information interpreted by the market maker. If η is well captured by the Hawkes system, the process of η should follow a random walk. Figure 3.7 plots the estimate of normalized η per second for each asset in different pairwise relations over all trading days. We can notice that the estimation of η are roughly similar in relations with different assets. Table 3.6 provides some statistics of the estimated η and Jarque-Bera test, testing whether the realization of the estimated η has the skewness and kurtosis that match a normal distribution.⁵ The obtained test statistics confirm that it is not sufficient to reject the null of normal distribution. This indicates that it is highly likely that the estimated η does not violate the random walk assumption and thus verifies the robustness of our model.

3.5.2 *Parametric estimation*

From the previous section, we have identified some ground truth on the price dynamics using non-parametric estimation of multivariate disjoint Hawkes processes. However, the point-wise estimation of the adjustment kernel on the time grid by the non-parametric method is not adequate under some circumstances, i.e. estimating the parametric covariance matrix of multivariate price series (see Chapter 3), or forecasting extreme values (see Chapter 5). And it is necessary to formulate the kernel over time with a fully paramet-

⁵ Because this test in a small sample is overly sensitive to extreme observation and consequently often rejects the null hypothesis when it is true, we eliminate very few outliers, i.e. about 1-4 observations compared to original sample of 61, before performing the test.

ric model. It is obvious from the plot of non-parametric point-wise estimates in Figures 3.4 and 3.5 that the adjustment (excitement) kernel is likely to be fast-decaying and non-increasing. The most potential candidates in the relevant literature are exponential decay and power decay. In this section, we choose exponential decay for adjustment (excitement)

Figure 3.7: Estimated η normalized per second of each asset in different pairwise relation over all trading day.



Table 3.6: Statistical testing for the random walk of exogenous information.

	AAPL \rightleftharpoons AXP		AAPL \rightleftharpoons CVX		AAPL \rightleftharpoons IBM		AAPL \rightleftharpoons XOM		AAPL \rightleftharpoons V	
Sample size	61	60	61	60	61	59	61	59	61	60
Mean \times 100	0.022	0.000	0.022	0.000	0.022	0.001	0.024	-0.003	0.022	-0.001
Std \times 100	0.019	0.006	0.019	0.011	0.019	0.009	0.019	0.005	0.019	0.012
Skewness	-0.124	-0.050	-0.109	0.140	-0.183	0.444	-0.125	0.521	-0.109	0.594
Kurtosis	-0.907	1.659	-0.827	0.201	-0.867	0.568	-0.687	-0.004	-0.955	-0.183
JB-stat	2.354	5.101	1.985	0.205	2.354	2.277	1.501	2.565	2.531	3.532
<i>p</i> -value	0.308	0.078*	0.371	0.902	0.308	0.320	0.472	0.277	0.282	0.171

	AXP \rightleftharpoons CVX		AXP \rightleftharpoons IBM		AXP \rightleftharpoons XOM		AXP \rightleftharpoons V		CVX \rightleftharpoons IBM	
Sample size	60	59	59	59	60	57	61	60	59	59
Mean \times 100	0.000	0.001	0.000	0.002	0.001	-0.002	0.000	0.000	-0.0006	0.001
Std \times 100	0.006	0.010	0.005	0.007	0.006	0.004	0.007	0.010	0.010	0.007
Skewness	-0.103	-0.456	0.020	0.108	-0.056	0.250	0.286	0.412	-0.499	0.603
Kurtosis	1.523	1.258	1.239	0.996	1.263	-0.031	1.644	-0.108	1.224	0.824
JB-stat	4.333	4.669	2.645	1.734	2.850	0.604	5.886	1.708	4.894	4.449
<i>p</i> -value	0.115	0.097*	0.266	0.420	0.241	0.739	0.053*	0.426	0.087*	0.108

	CVX \rightleftharpoons XOM		CVX \rightleftharpoons V		IBM \rightleftharpoons XOM		IBM \rightleftharpoons V		XOM \rightleftharpoons V	
Sample size	59	59	60	60	59	58	59	60	58	60
Mean \times 100	0.003	-0.003	0.001	0.000	0.003	-0.003	0.002	0.000	-0.003	0.001
Std \times 100	0.011	0.005	0.011	0.010	0.007	0.004	0.007	0.009	0.004	0.010
Skewness	-0.060	0.641	0.242	0.395	0.505	0.240	0.183	0.201	0.470	0.295
Kurtosis	0.562	0.037	1.169	-0.208	1.066	-0.398	0.893	-0.360	-0.113	-0.250
JB-stat	0.458	3.846	2.933	1.691	4.276	1.053	1.586	0.845	2.124	1.094
<i>p</i> -value	0.795	0.146	0.231	0.429	0.118	0.591	0.453	0.655	0.346	0.579

Notes: We report the means and standard deviations of the estimated η^d of the asset d in its pairwise relationship with other assets, as well as the t-values and p-values for the Jarque-Bera test. The first (second) column of each pair illustrates the results for the first (second) asset in the pair. The Jarque-Bera test measures if the estimated η^d follows random walk. The rejection levels are based on the *p*-value. ***, **, and * refer to rejections at 1%, 5%, and 10%, respectively.

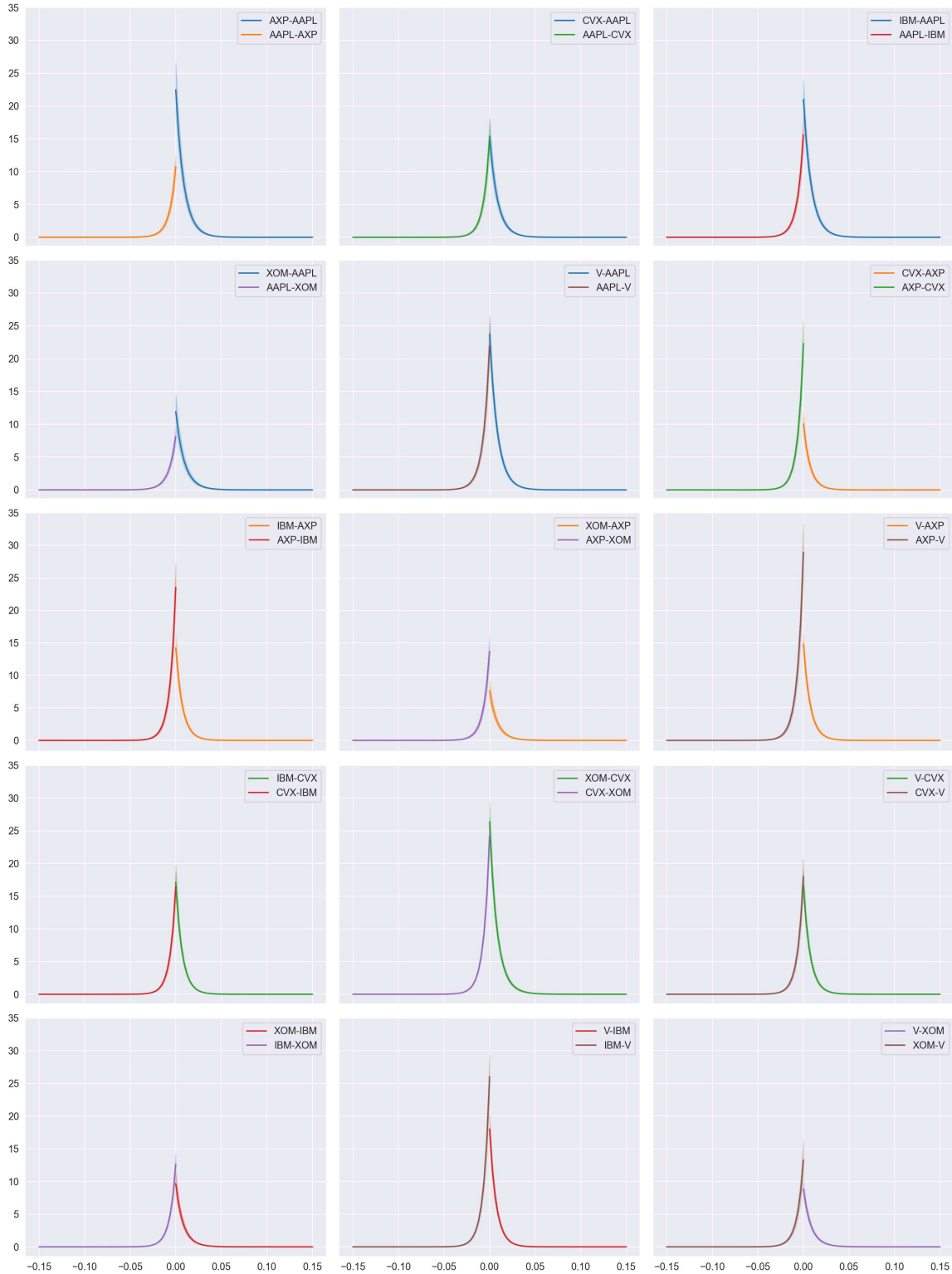
kernels in our parametric estimation to take advantage of its simplistic likelihood function (see Section § 3.3.2).

We remind the reader some of the parametric Hawkes terminologies from the previous section: the strength of an excitement from type- l state to type- k state is measured by a branching coefficient $q^{kl} = \alpha^{kl} / \beta^k$ and this excitement decreases exponentially over time according to a decay function $\phi^{kl}(t) = \alpha^{kl} \beta^k e^{-\beta^k t}$, where α^{kl} is the impact coefficient and β^k is the decay coefficient. We note that if we estimate a full set of coefficients, the MLE does not guarantee convergence as results of the non-convex likelihood function and excessive number of coefficients. Therefore, we first use grid search to determine the decay coefficients, β , by the least-squares method. Then, the remaining parameters, i.e. baseline intensities μ and impact coefficients α , are calculated by MLE. Because of the independence amongst disjoint price change point processes, we can optimize the likelihood function corresponding to each of them separately. Then, the parametric price adjustment at asset level, $\psi^{dr}(t)$ can be recovered from the estimated excitement kernels by Proposition 3. The average of these estimation over all trading days yields the final results.

The purpose of the study on parametric estimation is two-fold. On the one hand, it serves as a robustness check to verify that the parametric estimation is in line with the ground truth of non-parametric one, and thus confirms its validity. On the other hand, by

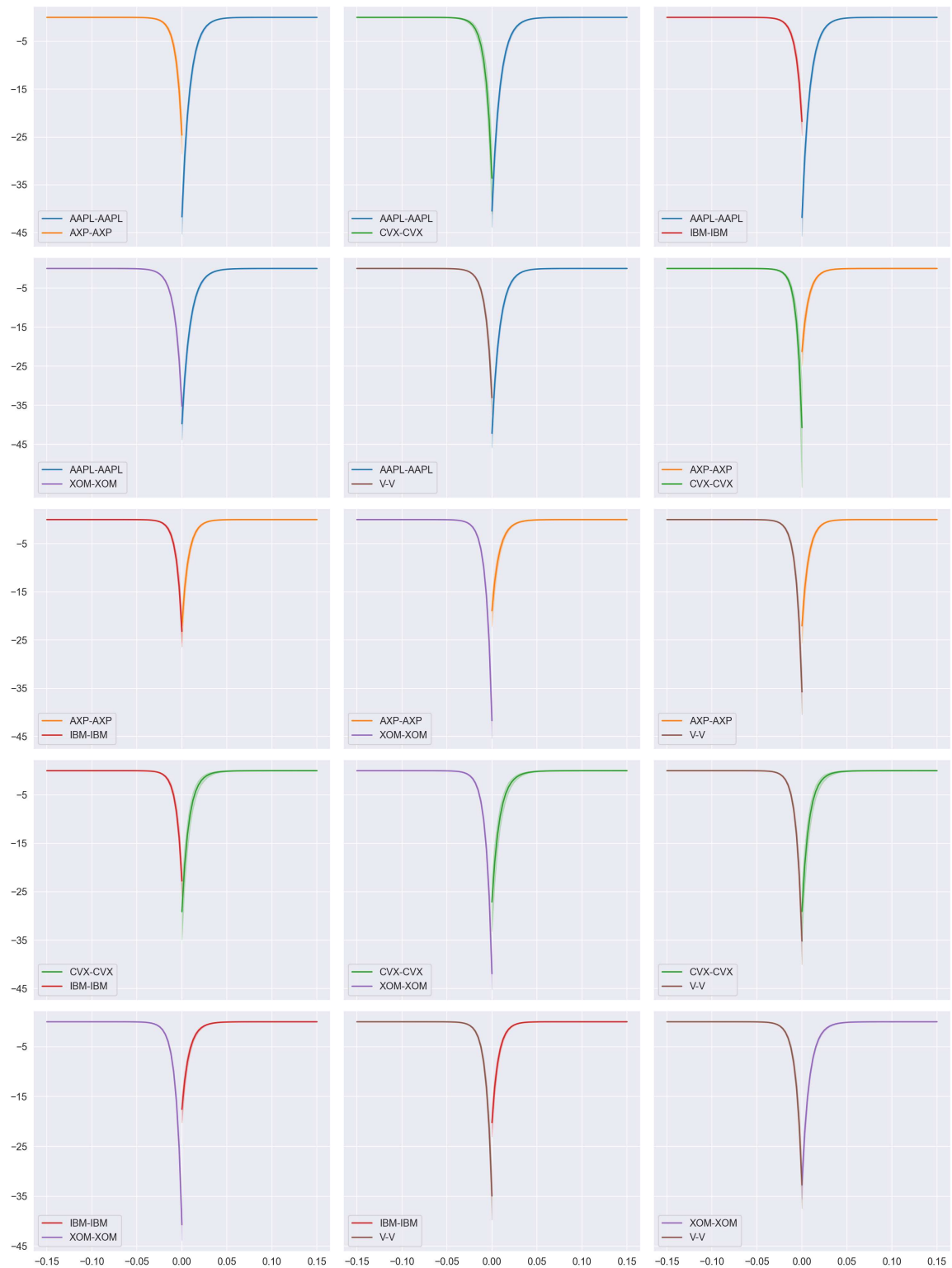
examining the estimated kernel shape, i.e. the decay coefficients β , we can clarify some fundamental properties of the trade information: the life span of the information or the time

Figure 3.8: Average cross-adjustment of all the pairs formed by six selected stocks (parametric estimation)



Notes: Averages are computed over all business days in the sample. The line shade denotes 95% confidence intervals. Correlations at positive time points imply that the second asset displayed in the legend leads the first asset and the other way around for negative time points

Figure 3.9: Average self-adjustment of all six selected stocks in different pair-wise relations (parametric estimation).



Notes: Averages are computed over all business days in the sample. The line shade denotes 95% confidence intervals.

for a trade to be completely incorporated into the price and obsolete; and also, whether this life span of information can be explained by the liquidity of assets.

Figures 3.8 and 3.9 illustrate the estimate of the price adjustment $\psi^{dr}(t)$ on the asset d incurred by a transaction of the asset r . The former shows the cross-adjustment effects, which is the case of $d \neq r$, whereas the latter displays the self-adjustment effects with $d = r$. We note that the two current figures in this section, 3.8 and 3.9, capture the development of price adjustment over time, whereas the previous Figures 3.4 and 3.5 illustrate point-wise estimates of the effect only, i.e. integrated price adjustment over each step of 10 ms. Non-zero adjustment effects at positive (negative) points of the time axis imply lead-lag relations at the transaction level in the first (second) pair displayed in the legend. The line shade denotes the 95% confidence interval. As done in the previous non-parametric estimation, it is interesting to study the cross-transaction lead-lag correlation through the parametric estimated adjustment kernel. The purpose of the study on parametric estimation is two-fold. On the one hand, it serves as a robustness check to verify that the parametric estimation is in line with the ground truth of non-parametric one and thus confirms its validity. On the other hand, examining the kernel shapes, which are determined by decay coefficients, clarifies the fundamental properties of trade information: how the impact or the information content of a trade is decayed and then how long that information is to be completely incorporated into the price and obsolete; and more importantly, whether this lifespan of information is explained by the liquidity of assets.

Table 3.7: Average daily parametric estimation of lead-lag correlations within one second for different pairwise assets (parametric estimation).

		Group I		Group II		Group III	
		AAPL	IBM	AXP	V	CVX	XOM
Group I	AAPL		0.136	0.118	0.271	0.139	0.147
	IBM	0.362****		0.088 ^(ns)	0.171**	0.105 ^(ns)	0.106***
Group II	AXP	0.257****	0.077 ^(ns)		0.146**	0.076	0.086**
	V	0.524****	0.123	0.111		0.117	0.117 ^(ns)
Group III	CVX	0.341****	0.091 ^(ns)	0.083 ^(ns)	0.161**		0.287****
	XOM	0.219**	0.061	0.054	0.099 ^(ns)	0.165	

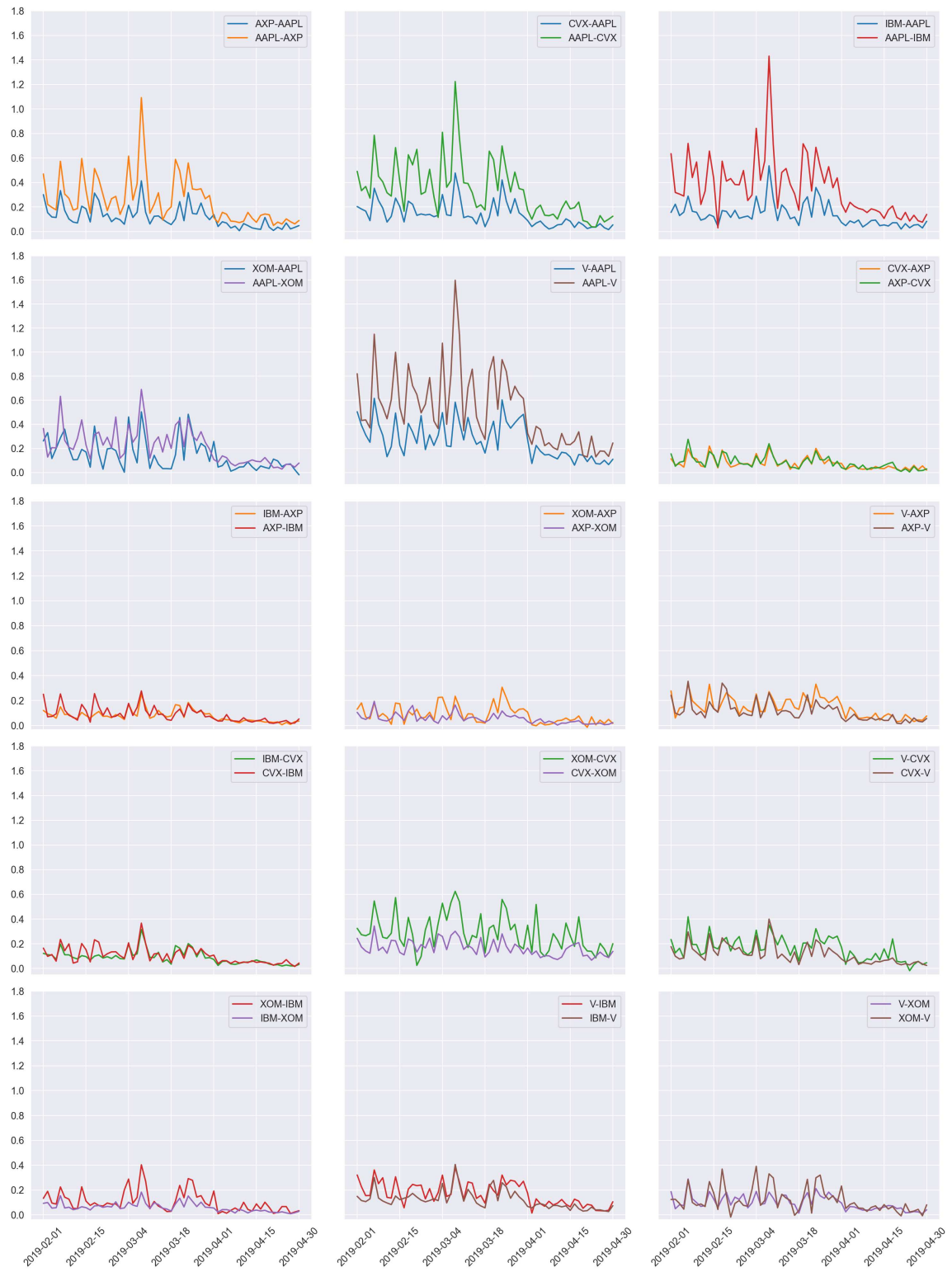
Notes: The column indexes denotes the leading assets and the row indexes are the lagged assets. The value with superscript are the lead-lag correlation with significant leadership. The significant levels are obtained based on the p-value of the two-sample t-test: ****: $p \leq 0.0001$, ***: $p \leq 0.001$, **: $p \leq 0.01$, *: $p \leq 0.05$, and ^(ns): $p > 0.05$. The value without superscript denotes the correlation provoked by the follower.

From Figures 3.8 and 3.9, we notice that taking the integration of adjustment kernels over the interval of 10 ms yields relatively similar results obtained by the non-parametric estimation. In other words, imposing the parametric formulation of exponential decay to adjustment (excitement) kernels does not change significantly the estimation of lead-lag effects, and our conclusion remains unchanged between the two estimation methods. Indeed, by looking at Table 3.7 and Figure 3.10, a very similar result on the order of lead-lag relationship is obtained:

$$\text{AAPL} \rightarrow \text{XOM} \Leftrightarrow \text{V} \rightarrow \text{AXP} \Leftrightarrow \text{CVX} \Leftrightarrow \text{IBM} \quad (3.49)$$

Similar to non-parametric estimation, the order of lead-lag relationship confirms that the liquidity level is not only the factor demonstrating the presence of lead-lag correlations but also the information content of trade. However, in this parametric estimation, the liquidity plays another role in determining the extent over which the correlation exists

Figure 3.10: The lead-lag correlation within one second for different pairwise assets over all trading days (parametric estimation).



beyond contemporaneity. We remind the reader that the lead-lag correlation arises as the consequence of the imperfect lagged adjustment: the price errors are adjusted by revising signals of historical trades, but the adjustments take time to incorporate fully the information content of trade. Otherwise stated, the trade information and its impact on prices have a lifespan. And it is the difference in the liquidity or transparency level between assets that the information has a different speed of dissemination and thus a different lifespan.

Table 3.8 reports the the average estimated decay coefficients of all assets over all trading days and pairwise relationships. We notice that AAPL and XOM, which is proven to be highly informative securities by leading other assets, have the lowest decaying coefficients. In addition, the speed of decay increases with the liquidity of the asset. In other words, the trade information of low-liquid assets takes more time to be assimilated and incorporated into the price of high-liquid assets. This result can plausibly be explained in that the transmission of information between assets is influenced by the level of liquidity and the high liquid assets with a high level of transparency enables a faster transmission of information. Indeed, highly transparent assets reduce the risk of adverse selection and the market makers are more confident in initiating an adjustment when receiving a signal from historical trades of these assets.

Table 3.8: The means and standard deviations of the estimated decay parameters β^d for the asset d .

	Group I		Group II		Group III	
	AAPL	AXP	CVX	IBM	XOM	V
Mean	117.8	152.1	148.3	151.2	124.4	146.6
Std	10.8	28.6	25.3	20.6	25.0	17.6

Therefore, it is the life span of trade that the information are disseminated gradually and give rise to the temporal existence of cross-correlation, which is termed as the lead-lag correlation. In non-synchronous trading, the contemporaneous correlation is often considered to vanish, which is documented as Epps effects. And the existence of lead-lag effects beyond the contemporaneous time confirms the inevitability of our framework for multivariate price dynamics at transaction-by-transaction level.

3.6 CONCLUSION

In this chapter, we extend standard univariate models of lagged price adjustment to a multi-asset framework, in which asymmetric information and lagged adjustment are formally taken into account. Lagged adjustment emerges in our framework as a revision of trades to adjust pricing errors caused by asymmetric information. By assuming that lagged adjustment is not perfect and it takes time to incorporate fully the information from trades, we introduce into the model a new feature of the trades: the recovered information from trades has a lifespan and it decays over time. The lead-lag effects naturally arise as a consequence of price revision, which is conditional on not only trades of the asset itself but also trades of other assets. The strength of adjustment induced by the trades of other assets is determined by non-zero non-diagonal coefficients in the lagged adjustment matrix Ψ .

The dynamics of an auto-regressive observed transaction price can be represented as multivariate disjoint price change point processes. By foregoing the precise specification of the joint distribution between the price and the time of trades, the disjoint representation allows us to focus on the evolution of transactions associated with a finite number of the most frequent price change states. The disjoint price change dynamics then can be cast into the multivariate Hawkes processes. As a byproduct of the interdependence between disjoint discrete price change states, we obtain the estimate of the observed price dynamics that are robust to non-asynchronous trading and microstructure noise.

The model is tested on a cross-section of DJIA stocks. It is first estimated non-parametrically and the point-wise estimation sheds light on the shape of the parametric adjustment kernel. The exponential decay function that satisfies all the required assumptions about the adjustment kernel shape was chosen for parametric estimation. At the price change level, the estimation of the model is in line with descriptive analysis, and the calibrated model seems reasonable from an economic perspective. e.g. the dominant price movement is to switch amongst within-asset states, and the adjustment of prices is mainly driven by the information of the historical trades on the asset itself rather than on the cross assets. The within-asset excitements implies a strongly mean-reverting behaviour, whereas the cross-asset excitements indicate the co-movement of asset returns in the extreme states.

At asset level, the analysis provides empirical evidence for the existence of a multi-asset price formation mechanism. In particular, we find significant cross-transaction effects between assets, that is the impact incurred by a trade to other trades or the information content of the trade about prices. And it is the lifespan of this trade information giving rise to the existence of temporal (lead-lag) cross-correlation, which vanishes in contemporaneous time of asynchronous trading. Such lead-lag correlation is then normalized by the factor of average duration to measure the lead-lag relationship between assets. The results obtained confirm the common empirical finding that highly liquid assets often play the leader roles. However, there exist some significant exceptions of some low liquid assets, which contain highly informative trades and carry more information about prices, leading other stocks with higher levels of liquidity. The results also find that lead-lag correlations are exhibited not only between assets within a sector but also between assets from different sectors, though with a smaller strength of correlation.

Finally, with the available parametric specification, it might be tempting to use our model for building a new measure of covariance matrix that accounts for the temporal lead-lag correlation. However, at transaction-by-transaction level the observed prices are presumably seriously biased by market micro-structure noise and this has to be handled with care. Also, with significant evidence of extreme return co-movement, there will be promising empirical applications on developing a tail risk measure using our framework.

4

MULTIVARIATE COVARIANCE VARIANCE MATRIX ESTIMATION WITH MARTINGALE REPRESENTATION OF HAWKES INTENSITY

Abstract

In this chapter, we propose a novel estimator of second-order moment structure of asset returns, combining two well-established approaches towards high-frequency volatility measures, that is, quadratic covariation and point process-based approaches. On the one hand, with its parsimonious parametric structure based on conditional intensity, which is the core of point process approach, our model preserves superior features of univariate point process-based volatility estimators in addressing salient properties of ultra-high-frequency data. On the other hand, the model is defined within a generic temporal cross-(auto)covariation structure of the quadratic covariation approach, facilitating the estimation of cross-correlation between assets. To some extent, our novel intensity-based variance-covariance matrix estimator is not affected by spurious correlations and Epps effects, in contrast to quadratic covariation estimators, and accounts for simultaneously lead-lag effects and endogenous times in asynchronous trading. In addition, with a parametric structure, the estimator has the ability to provide inference on local volatility over relatively short intraday intervals, overcoming the limitations of convergence property ensuring consistent realized volatility measures on such periods. We test the robustness of the estimator with extensive Monte Carlo simulations.

Keyword: Variance-covariance matrix, quadratic covariation, Hawkes process, intensity-based volatility, lead-lag effects, asynchronous trading.

4.1 INTRODUCTION

Over the past two decades, the literature on modelling the second-order moment structure of asset returns has taken a step forward by harnessing high frequency data. A new approach, “realized” volatility, introduced by Andersen et al. (2001), Andersen et al. (2003) and Barndorff-Nielsen and Shephard (2002b, 2004), has transformed the measure of (co-) variation of asset prices by exploiting information on fine-grained returns. Conditional volatility is no longer a latent variable, but observable, and thus has led to a considerable improvement in our understanding of the data generating process.

The realized volatility is simply estimated by summing all intraday high frequency returns sampled at very short intervals. The basic idea is that if the sample path of volatility is continuous, then increasing the sampling yields arbitrarily precise estimates of volatility at any given point in time. In other words, the realized volatility relies exclusively on the large sample size of high frequency returns to ensure the efficiency and consistency of the estimators. However, due to the necessity of solid sample size, the use of realized measures is often confined to the finest frequency of only daily integrated (co-)variation. For short intraday intervals, such as an hour or 15 minutes, it is doubtful if the sample size of the return is large enough to justify the applicability of the asymptotic of the realized estimators Tse and Yang (2012). Hence, in spite of its simplistic nature, the implementation of realized volatility can raise subtle issues, especially, for high frequency or intraday traders who often practise in a real-time basis with a very short investment horizon. Hasbrouck and Saar (2013) document that high-frequency traders can operate with a latency of only a few milliseconds, while blinking an eye takes a few hundred milliseconds. Even more extreme, Goldstein, Kumar and Graves (2014) report that it is possible to trade in a microsecond environment.

This chapter is devoted to address this issue in the high frequency econometric literature by developing a locally integrated covariation estimator. Our estimator, namely intensity-based realized covariance (IRC), is built on the disjoint price change point processes for multi-assets in the previous chapter. The IRC can be considered as a multivariate generalization of the previous univariate realized volatility model based on the point process approach, i.e. price duration-based volatility (PDV) (see Hong et al., 2021 for the most recent study on PDV estimators). The latter were originally introduced by Engle and Russell (1998) to account for serial dependency in the price duration process over a threshold, of which the univariate instantaneous volatility was estimated as a by-product. Our multivariate generalization, the IRC, amalgamates both quadratic covariation and point process approaches. It provides a general framework which not only preserves PDV’s superior feature of providing intraday inference on local variation but also efficiently captures an additional feature of second-moment structure in portfolio analysis: local cross-correlation between assets.

Univariate volatility models based on the point process approach, PDV, were proposed, among others, by Andersen, Dobrev and Schaumburg (2009), Engle and Russell (1998), Gerhard and Hautsch (2002), Hong et al. (2021), Li, Nolte and (Lechner) (2018), Li, Nolte

and Nolte-Lechner (2015) and Tse and Yang (2012). The theoretical concept underlying these models is that by modelling price duration, i.e. the waiting time to generate a certain change in the price process, the instantaneous volatility can be represented as the product of the conditional price intensity, i.e. the inverse of price duration, and the price change threshold. These estimators have been neglected in the literature, despite being very simple to implement and Andersen, Dobrev and Schaumburg (2009), Hong et al. (2021) and Tse and Yang (2012) documenting their very nice performance against realized volatility estimators. As pointed out by Tse and Yang (2012), this estimator enjoys a full parametric assumption for the dynamic price duration process, which can improve the estimator in the manifold. First, data beyond the volatility estimation window can be used to improve the estimated parameter, which in turn leads to a more precise volatility estimation. Second, according to Li, Nolte and Nolte-Lechner (2015), the parametric structure of the ACD models facilitates the inclusion of other market microstructure covariates, which not only can further improve the quality of volatility estimation, but also provides a framework for analyzing the relationship between volatility and other market microstructure covariates at the high frequency level. Moreover, with a parametric assumption, not only an integrated variance estimator, but also a local volatility estimator (intraday volatility or real-time volatility) can be obtained, as opposed to realized volatility. However, this estimator did not receive equal attention as the realized volatility-type estimators, partly due to its confinement of only univariate variation estimation.

Nevertheless, many interesting economic questions can only be addressed using multivariate models. Although the PDV estimators seem particularly well suited for estimating univariate variation, it is difficult to extend them to a multivariate framework. The reason lies in the nature of price duration volatility: on the discreteness of price duration and on the non-decreasing monotone of integrated volatility. First, the discreteness of price duration allows only fixed path conditional intensity, which is unable to update new information arrivals within waiting times, and deters the price duration models from capturing co-volatility in a setting with asynchronous tradings (Russell, 1999). Second, the price duration volatility model must rely on the non-decreasing monotonic property of the integrated volatility to construct a renewal point process in the integrated variation time (Li, Nolte and (Lechner), 2018). Within a multivariate framework with another concern of covariation (co-volatility), the non-decreasing monotone is no longer valid. Furthermore, the estimation of covariation is even more challenging due to the so-called non-synchronous trading effect. As pointed out by Buccheri, Corsi and Peluso (2020), Dao, McGroarty and Urquhart (2018), Epps (1979), Huth and Abergel (2014) and Large (2007b), price-relevant information arrives at different frequencies for multiple assets, and information related to one asset can affect the price formation process of another asset, thus inducing additional microstructure effects among them, the so-called stale prices and temporal lead-lag effects. The point process approach-based covariation estimation, thus, needs to be tailor-made to overcome the limitations of univariate estimators and to mitigate the impacts of asynchronous trading in the multivariate case.

Motivated by the robustness of disjoint price change point processes in modelling multivariate price dynamics (see [Chapter 3](#)), we continue to apply this approach to estimate integrated (co-)variation for multiple assets in our IRC. Instead of modelling a discrete duration of only the transaction price truncated over a threshold, the IRC utilizes multivariate Hawkes processes to model, in continuous settings, conditional intensities of all possible observed discrete states of price change, taking advantage of discreteness of the high frequency transaction-by-transaction price and a finite number of price change states. We also establish the link between the theory on quadratic covariation of asset returns and that on the second-order moment structure of the point process. In detail, the conditional quadratic covariation of semi-martingale prices is reformulated as a sum of conditional (cross-)autocovariance between disjoint price change point processes. Then, under a martingale representation of conditional intensity, a parametric structure of the conditional (cross-)autocovariance can be obtained and expressed in terms of the estimated parameters from the multivariate Hawkes process.

The mapping between the quadratic covariation of asset returns and the point processes of disjoint price changes is placed under a noise-contaminated semi-martingale hypothesis for the observable transaction price. The microstructure noise, justified economically in our framework, may simply arise as a consequence of bid-ask bound effects and trading on the spread. And by a reasonable assumption that the microstructure noises are only updated at transaction times and independent of the efficient prices, we propose an efficient way, also based on the intensities of the disjoint point processes, to estimate directly the bias incurred by the noises, which complements the robustness of our IRC estimator.

The structure of this chapter is as follows. Section [§ 4.2](#) briefly discusses the theory of quadratic covariation and links to integrated covariance. In Sections [§ 4.3](#) and [§ 4.4](#), we put forward the theoretical framework for the IRC estimator. [§ 4.5](#) present the simulations and analysis of the results. Finally, [§ 4.6](#) concludes.

4.2 QUADRATIC COVARIATION AND INTEGRATED COVARIANCE

We start with conditions on the price processes and introduce the theory of quadratic covariation, which is akin to integrated covariance. We assume a D -dimensional vector of latent semi-martingale true underlying values or efficient prices which is driven by Brownian shocks. Postulating the semi-martingale assumption on the efficient prices is natural and consistent with classical continuous-time modeling in finance (see, e.g. [Duffie, 2010](#)). These Brownian semi-martingale efficient prices evolve on a rich enough filtered probability space $(\Omega^Y, \mathcal{F}, (\mathcal{F}_t)_{t \geq 0}, \mathcal{P})$, where, in particular, $(\mathcal{F}_t) \subseteq \mathcal{F}$ is an increasing family of σ -fields satisfying \mathcal{P} -completeness and right continuity ([Protter, 2013](#)), and given by:

$$\mathbf{Y}_t = \int_0^t \mathbf{A}_s ds + \int_0^t \mathbf{\Theta}_s d\mathbf{W}_s, \quad \mathbf{\Sigma}_t = \mathbf{\Theta}_t \mathbf{\Theta}_t^\top \quad (4.1)$$

where $t \in [0, T]$, \mathbf{A}_t is a D -dimensional vector of predictable locally bounded drifts, Θ_t is a $D \times D$ -dimensional volatility matrix, and \mathbf{W}_t is a D -dimensional vector of independent Brownian motions. The interval $[0, T]$ can be thought of as representing the trading day.

We wish to capture the erratic behaviour implied by Brownian dynamics, which is represented by the integrated covariance matrix $\mathbf{IC} = \int_0^T \Sigma_t dt$. We note that the assumption of Brownian semi-martingale efficient prices above admits the presence of leverage effects, i.e. non-zero correlations between the efficient price \mathbf{Y}_t and the volatility Θ_t , but excludes the discontinuous movements, or jumps.¹

For the sake of our forthcoming presentation about the link between quadratic covariation and integrated covariance, we (temporarily) assume in this section that the noise is completely modelled, and only the efficient prices remain. It is well established that if the efficient prices behave as Brownian semi-martingale processes, then the integrated covariance converges to the quadratic covariation, i.e. the summation of increasing finer sampled cross-products of the efficient returns (see, e.g. Protter, 2013):

$$\langle \mathbf{Y} \rangle_t := \text{p-lim}_{h \rightarrow 0} \sum_{j=1}^{T/h} [\mathbf{Y}_{jh} - \mathbf{Y}_{(j-1)h}] [\mathbf{Y}_{jh} - \mathbf{Y}_{(j-1)h}]^\top \quad (4.2)$$

As the properties of Brownian semi-martingale, there exists a unique decomposition of efficient prices into the sum of two vectors of adapted right-continuous processes, one of which has a finite variation path, and the other is a local martingale:

$$\mathbf{Y}_t = \mathbf{A}_t + \mathcal{M}_t \quad (4.3)$$

where $\mathbf{A}_t \in \mathcal{FV}^c$, $\mathbf{A}_0 = 0$ and \mathcal{M}_t is a multivariate stochastic volatility process that satisfies the following:

$$\mathcal{M}_t = \int_0^t \Theta_s d\mathbf{W}_s$$

with the corresponding instantaneous covariance at time t is as:

$$\Sigma_t = \Theta_t \Theta_t^\top \text{ with } \int_0^t \Sigma_s^{dr} ds < \infty, \forall t < \infty \text{ and } d, r \in \{1, \dots, D\}$$

Also, by the properties of the local martingale and the continuous finite-variation process, the quadratic covariation process of \mathbf{Y} equals the quadratic covariation of the martingale components, that is, also the integrated covariance:

$$\langle \mathbf{Y} \rangle_t = \int_0^t \Sigma_s ds \quad (4.4)$$

This result holds regardless of the presence of jumps in the local martingale component (see, e.g. Barndorff-Nielsen and Shephard, 2004). From Eqn. 4.2 and Eqn. 4.3, we obtain the integrated covariance formulation of efficient price processes as their quadratic covariation:

¹ In the presence of jumps, the problem of separating the continuous part from the jump part could be preemptively tackled by pre-testing the data for jumps using jump identification tests that are able to locate the position of jumps inside the day (e.g. Lee and Mykland, 2007). Our methodology can then be applied to the resulting jump-filtered series.

$$\mathbf{IC} = \int_0^T \boldsymbol{\Sigma}_s ds = \text{p-lim}_{h \rightarrow 0} \sum_{i=1}^{n=T/h} [\mathbf{Y}_{jh} - \mathbf{Y}_{(j-1)h}] [\mathbf{Y}_{jh} - \mathbf{Y}_{(j-1)h}]^\top \quad (4.5)$$

The quadratic covariation is pivotal in financial economics (see, e.g. the reviews by Andersen, Bollerslev and Diebold, 2010; Barndorff-Nielsen and Shephard, 2007) and we thus take Eqn. 4.5 as defining the target that we are interested in estimating. Andersen et al. (2001), Andersen et al. (2003) and Barndorff-Nielsen and Shephard (2002b, 2004), amongst others, suggest constructing an artificially regular spaced high frequency returns time series by choosing a sufficiently small fixed time interval h , $J = T/h$, and the ex-post integrated covariance can be estimated by a “realized” covariance (RC) matrix:

$$\mathbf{RC}^{(J)} = \sum_{j=0}^{J-1} [\mathbf{Y}_{(j+1)h} - \mathbf{Y}_{jh}] [\mathbf{Y}_{(j+1)h} - \mathbf{Y}_{jh}]^\top \quad (4.6)$$

However, the transaction prices we observe, in reality, are not the efficient prices, \mathbf{Y}_t , but the ones, \mathbf{X}_t , which are contaminated by market microstructure noises, \mathbf{U}_t :

$$\mathbf{X}_t = \mathbf{Y}_t + \mathbf{U}_t \quad (4.7)$$

Furthermore, due to asynchronous trading, only a component of \mathbf{X}_t corresponding to the traded asset is observed at each time t , while the movements of the remaining assets are not observable. The transaction timestamps are not regularly spaced and are not synchronous between assets. Thus, the realized quantities that can be estimated from high frequency data are not confined to quadratic covariation. There is an upward bias on the realized variation due to the market microstructure noise and a downward bias on the realized covariation due to the asynchronicity in a multivariate framework. These two biases can partially or even fully offset the incremental benefits of using intraday information, and hence may render the use of high-frequency data practically unattractive. Due to them, it may not be appropriate to apply directly pioneer realized covariance models to transaction-by-transaction data, but necessarily involve data cleaning procedures. The tick-by-tick returns can be substantially resampled to an optimal but much lower frequency of minute-by-minute or second-by-second at best (see Andersen and Bollerslev, 1997; Bandi and Russell, 2008; Bandi and Russell, 2006; Corsi, Peluso and Audrino, 2014; Hansen and Lunde, 2006a; Li et al., 2013; Liu, Patton and Sheppard, 2015); or they can be applied to an artificial time scheme to pseudo-align observations (Barndorff-Nielsen et al., 2008, 2011; Jacod et al., 2009; Podolskij and Vetter, 2009; Varneskov, 2016a,b). These paradigms can improve the robustness and efficiency of the RC estimators, but they also come at the cost of important information losses. The losses are due not only to removing substantial observations but also to neglecting and modifying the intrinsic value of a trade-characterized variable: the transaction time. Indeed, it is widely documented that the transaction time is not only irregular, but also endogenous and mutually dependent on the transaction price (Dufour and Engle, 2000; Jacod, Li and Zheng, 2019; Li et al., 2013; Li, Zhang and Zheng, 2013). Moreover, pseudo-aligning observations additionally introduce spurious lead-lag correlations or unnecessarily destroy true short-term lead-lag effects. (Buccheri, Corsi and Peluso, 2020; Curme et al., 2015; Huth and Abergel, 2014).

In the next section, we will propose a new volatility estimator, namely intensity-based realized covariance (IRC), that has the important advantage of employing all the information available in all the transaction price series, thereby making use of all the trades of any asset and also accounting for the endogenous impact of trading times. Specifically, according to the multi-asset price formation mechanism developed in the previous chapter [Chapter 3](#), we recognize that the information of each observed price series can contain the information of the other series. By capturing the interdependence amongst assets in the conditional intensity function, the IRC methodology pulls all the available multivariate information in computing each single pair of covariance.

4.3 QUADRATIC COVARIATION AND INTENSITY BASED COVARIANCE ESTIMATOR

4.3.1 *Conditional Estimator of Quadratic Covariation*

To spell out the foregoing model, let \mathbf{X} be the D -dimensional vector of the transaction price. Each component X^d is observed at $0 \leq t_1^d, \dots, t_{N^d(T)}^d \leq T$ that corresponds to the transaction process of the asset d , with $d \in [1, D]$, and $N^d(t)$ denotes the right continuous counting function that counts the cumulative number of transactions in the point process d up to time t . We also denote $0 \leq t_1, \dots, t_{N(T)} \leq T$ as the pooled point process of all D -variate marginal point processes, which means $N(t) = \sum_{d=1}^D N^d(t)$ and the duration between traded in the pooled transaction process is $\tau_i = t_{i+1} - t_i$, $i \in [1, N(T)]$.

As we indicated in previous sections, the efficient prices are not directly observable. Instead, the actual observed prices are contaminated with market microstructure noises. To facilitate the estimation of the integrated covariance from noisy observed prices, we describe how the market microstructure noises take place and relate to the efficient prices given in [Eqn. 4.4](#) by making assumptions as follows:

- (H1)** The microstructure noises are only updated at exactly the times where there exists the arrival of trades.
- (H2)** The microstructure noises are stationary, mutually independent, with mean zero, and are also uncorrelated with the efficient price.

Assumption **(H1)** does not require that U_t exists for every t , in other words, our interest in the microstructure noise is only at observation times t_i . In Assumption **(H2)**, we assume a diagonal covariance matrix of microstructure noise, which means that the microstructure noises are not correlated across the assets. These settings on microstructure noise have been studied in many pioneer models of realized volatility (see Christensen, Kinnebrock and Podolskij, 2010; Voev and Lunde, 2006; Zhang, 2006, 2011; Zhang, Mykland and Ait-Sahalia, 2005). Although Assumption **(H2)** may be empirically questionable due to its simplistic nature, it greatly simplifies the methodological implementation of our integrated covariance estimator. Also, it is feasible to generalize the noise covariance matrix to the non-diagonal but with an additional computational effort. However, due to the

intrinsic non-synchronicity of market microstructure noise, i.e. Assumption **(H1)**, its empirical covariance matrix tends to be approximately diagonal. In the later section § 4.5, we will show with the simulation results that even if non-diagonal noise covariance elements exist, the deterioration of the precision of the estimator is limited and does not affect its ranking with respect to the competing estimators.

By the assumptions about the microstructure noise, the essence of the setups for the IRC estimator is that the observed prices X_{t_i} are white noise-contaminated fluctuations around the efficient price Y_{t_i} and that contamination occurs only at exactly the time of transactions. Thus, the mapping between the (co-)variation of the two prices can be obtained through the conditional expectation given the information set generated right before the moment that the noises are updated and lead to the departure from the efficient prices. To facilitate the conditional expected estimation, we assume that the observed prices are generated by filtration (\mathcal{H}_t) , the σ -algebra generated by $(X_s)_{s \leq t}$. The link between the filtration of two price components, by the independence of between the microstructure noises and the efficient prices, is given as: $\mathcal{H} = \mathcal{F} \times \mathcal{G}$, $\mathcal{H}_t = \bigcap_{s > t} \mathcal{F}_s \times \mathcal{G}_s$ where \mathcal{G}_s is the σ -algebra generated by exogenous microstructure noises (see Christensen, Kinnebrock and Podolskij, 2010). We do not observe the two information sets \mathcal{F}_T , \mathcal{G}_T separately, but the aggregated one \mathcal{H}_t , which reveals only information about the observed prices. The integrated covariance matrix of the efficient price cannot be estimated directly, but through the information of observed price processes. Denoting the instantaneous increments of the efficient price as $dY(t) = \lim_{\delta \rightarrow \infty} Y_{t+h} - Y_t$, we can write the conditional expectation of integrated covariance in Eqn. 4.5 as:

$$\hat{\mathbf{I}}\mathbf{C}_T = \mathbb{E}_T\left[\int_0^T \boldsymbol{\Sigma}(u)du\right] = \int_0^T \mathbb{E}_u[d\mathbf{Y}(u)d\mathbf{Y}(u)^\top] \quad (4.8)$$

where $\mathbb{E}_T[\cdot]$, $\mathbb{E}_u[\cdot]$ denotes the expectation conditioning on the observed price path at the endpoint T and at the time point u , respectively. The change from $\mathbb{E}_T[\cdot]$ to $\mathbb{E}_u[\cdot]$ in the third equality simply due to $\mathcal{H}_u \subset \mathcal{H}_T$ with $u \in [0, T]$ and $d\mathbf{Y}(u)$ is \mathcal{F}_u -measurable, so it is \mathcal{H}_u -measurable.

Estimation of the asset return covariance matrix for this efficient price plus noise model involves two challenges. First, the contamination by microstructure noises can induce an explosive behaviour in the estimated variation when the sampling frequency increases (see Eqn. 4.9). Second, the non-synchronicity makes observation times rarely simultaneous and incurs additional microstructure effects amongst correlated assets, the so-called stale prices, and temporal lead-lag effects (see Chapter 3). The proposed estimator must be specified to mitigate the upward bias of the noise variation, also to capture cross-contemporaneous and cross-temporal dependence with the observed price such that additional microstructure features are taken into account, for example, bid-ask bounce effects (Roll, 1984), asymmetric information (Glosten and Milgrom, 1985), strategic learning (Diebold and Strasser, 2013), and lead-lag information transmission (Buccheri, Corsi and Peluso, 2020).

Inspired by the (cross-)autocovariation approach in the realized kernel (RK) estimators, that is, the realized covariance is defined within the realized autocovariation structure (see,

e.g. Barndorff-Nielsen et al., 2008, 2011; Varneskov, 2016a,b), we propose our estimator having the structure as follows:

Proposition 4. *Let Assumptions (H1) and (H2) be satisfied, and let $h < T$, we can rewrite Eqn. 4.8 as:*

$$IRC_T = \int_0^T \int_u^{u+h} \mathbb{E}_v[d\mathbf{X}(u)d\mathbf{X}(v)^\top] - \int_0^T \text{diag}(\mathbb{E}_u[d\mathbf{U}(u)d\mathbf{U}(u)^\top]) \quad (4.9)$$

where $\text{diag}(\cdot)$ represents the matrix with only non-zero diagonal elements (d, d)-th.

Proof. For each $v \in [u, u+h], \forall u \in [0, T]$, we have:

$$\begin{aligned} \mathbb{E}_T[d\mathbf{X}(u)d\mathbf{X}(v)^\top] &= \mathbb{E}_v[d\mathbf{Y}(u)d\mathbf{Y}(v)^\top] + \mathbb{E}_v[d\mathbf{Y}(u)d\mathbf{U}(v)^\top] + \\ &\quad \mathbb{E}_v[d\mathbf{U}(u)d\mathbf{Y}(v)^\top] + \mathbb{E}_v[d\mathbf{U}(u)d\mathbf{U}(v)^\top] \end{aligned} \quad (4.10)$$

By Assumption (H2) and the properties of the Brownian semi-martingale: $d\mathbf{Y}(u) \perp d\mathbf{U}(v) \forall u, v$; $d\mathbf{Y}(u) \perp d\mathbf{Y}(v) \forall u \neq v$; and $d\mathbf{U}^d(u) \perp d\mathbf{U}^r(v) \forall u \neq v, d \neq r \forall d, r \in [1, D]$ (the symbol \perp is used to denote stochastic independence). Therefore, we obtain the following equation:

$$\int_u^{u+h} \mathbb{E}_v[d\mathbf{X}(u)d\mathbf{X}(v)^\top] = \mathbb{E}_u[d\mathbf{Y}(u)d\mathbf{Y}(u)^\top] + \text{diag}(\mathbb{E}_u[d\mathbf{U}(u)d\mathbf{U}(u)^\top]) \quad (4.11)$$

This gives us the complete proof of the Proposition. \square

Here, we redefine the conditional contemporaneous (cross-) covariation at each instant time u , i.e. $\mathbb{E}_u[d\mathbf{X}(u)d\mathbf{X}(u)^\top]$, to be the integration of all conditional temporal (cross-) covariation from the return at that instant time, $\mathbb{E}_v[d\mathbf{X}(u)d\mathbf{X}(v)^\top]$ over the bandwidth interval, i.e. $v \in [u, u+h]$. At different times within the bandwidth interval, the temporal term is increasingly limited in covariation when the time difference $v - u$ increases. The temporal covariation of time differences greater than h , i.e. outside the bandwidth interval, is assigned to be zero. In other words, the value of h demonstrates the extent to which the covariation exists beyond contemporaneity. This temporal covariation is akin to cross-transaction effects, that is, some (price move) information carried by a trade is also carried by other trades due to lead-lag adjustment (see Chapter 3). And how long the trade lives in the price formation processes, i.e. the lifespan of trade, gives rise to the temporal existence of covariation, alongside contemporaneous covariation, which vanishes in asynchronous trading settings according to Epps effects.

Although the first term of the IRC has a generic structure of (cross-) autocovariance, as in RK estimators, there are some important differences. We consider a continuous estimator that replaces the “orders” of autocovariance by the “time differences” of autocovariance. The time differences determine the impact of a transaction on another transaction and thus the strength of covariation between them. Meanwhile, the RK, in a discrete setting, weighs the strength of covariation by a function of the difference in numerical orders between observed returns (see, in particular, Barndorff-Nielsen et al. (2008)). However, the order differences are not similar to the elapsed times between transactions. Indeed, the order of return events is demonstrated by an observation pseudo-aligning scheme, that ignores

the endogenous role of trading times and that can additionally introduce spurious cross-transactions effects or unnecessarily exhaust these effects.

The second term, i.e. the de-noise term, in Eqn. 4.9 aims at estimating the second-order moment of the noise. Because the noise covariance matrix is assumed to be diagonal, this term is our concern only in estimating integrated variance. Therefore, we can separate Eqn. 4.9 for the case of integrated variance and covariance as follows:

$$\hat{I}\hat{C}_T^{d,d} = \int_0^T \int_u^{u+h} \mathbb{E}_v[dX^d(u)dX^d(v)] - \int_0^T \mathbb{E}_u[dU^d(u)^2] \quad (4.12)$$

$$\hat{I}\hat{C}_T^{d,r} = \int_0^T \int_u^{u+h} \mathbb{E}_v[dX^d(u)dX^r(v)] \quad (4.13)$$

Utilizing the specifications of microstructure noise in Assumptions **(H1)** and **(H2)**, we can rewrite the de-noise term for the case of integrated variance as:

$$\begin{aligned} \mathbb{E}_T\left[\int_0^T dU^d(u)^2\right] &= \mathbb{E}_T\left[\sum_{t_i^d \leq T} (dU^d(t_i^d))^2\right] = \sum_{t_i^d \leq T} \mathbb{E}_{t_i^d}[(dU^d(t_i^d))^2] \\ &= - \sum_{t_i^d \leq T} \mathbb{E}_{t_i^d} \left[\lim_{\delta \rightarrow 0} [X^d(t_i^d + \delta) - X^d(t_i^d)][X^d(t_i^d) - X^d(t_i^d - \delta)] \right] \\ &= - \sum_{t_i^d \leq T} \mathbb{E}_{t_i^d} [dX^d((t_i^d)^+)dX^d(t_i^d)] \end{aligned} \quad (4.14)$$

where $(t_i^d)^+ = \lim_{h \rightarrow 0} t_i^d + h$ denotes the instant time immediately after t_i^d . The first and second equality are due to the assumption that microstructure noises are updated only at transaction times and equal to zero elsewhere, i.e. the transaction cost does not exist unless there occurs a transaction. The remaining equality is due to the independence between the microstructure noises and the efficient prices.

The intuition of the de-noise method in Eqn. 4.14: The estimation of the de-noise term is essentially based on differentiating. Taking differences seems redundant if the time series U_i^d is observable. However, in our framework, the U^d is masked by the efficient price Y^d , and we can observe only X_i^d if the transaction occurs at t_i^d . A local deviation of the observed price from the efficient price, e.g. at transaction t_i^d , can be considered as a temporary and transitory jump. And after a transaction, the hidden price immediately reverts to its true value before another jump in the next transaction. Taking differences in an instant δ removes the effect of the efficient price. The intuition of such a removal is that the increment of the efficient price is much smaller than the jump of the noise under instantaneous time change.

4.3.2 Intensity Based Estimator

In the previous section, the conditional integrated covariance of the efficient price is formulated within the conditional temporal covariation structure of the observed price (see

² We simplify the notation by denoting the subscript i as the transaction index of the variables and the superscript d as the corresponding asset of that transaction, e.g. dU_i^d . We use this notation interchangeably with previous ones, e.g. $dU^d(t_i^d)$.

Eqn. 4.9 and Eqn. 4.14). Such conditional covariation arises as a consequence of strong and often complex temporal dependence existing in the high-frequency transaction price. Motivated by the robustness of the multivariate disjoint price change point processes in modelling the transaction-by-transaction interdependence of multi-asset price dynamics in Chapter 3, we continue to apply this approach to the observed transaction prices.

The intuition of the disjointing price change is that the movements of the observed transaction price are restricted to take a handful of integer values that are multiples of a smallest non-zero price change, i.e. tick³. The modelling of finite multinomial probabilities associated with such disjoint price change states is feasible by the conditional intensity approach of the Hawkes process without complex specifications on the multivariate distribution between asset returns and on the joint distribution between trading times and price changes. The interdependence between multiple assets and between trading times and price changes can be simply retrieved through temporal cross- and self-excitation in the conditional intensity dynamics of disjoint price changes.

Following the notation in Chapter 3, we consider an K -dimensional vector of disjoint point processes $\{N^k(t)\}_{k=1}^K$ with $K = \sum_{d=1}^D M^d$ where M^d is the number of price change states in the state space \mathcal{M}^d associated with the asset d . The strictly increasing observation times of the k -th point process $t_1^k, t_2^k, \dots, t_i^k, \dots$, indicate the timestamps corresponding to the state x^k . We also set $N^k(t)$ as a right-continuous counting function which counts the cumulative number of transactions in the point process k up to time t . This counting function $N^k(t)$ is characterized by its conditional intensity vector $\lambda^k(t)$, which measures the instantaneous quantity of event arrival in the point process k -th conditional on its information set:

$$\lambda^k(t) = \lim_{dt \rightarrow 0} \frac{\mathbb{Pr}\{N^k(t) - N^k(t - dt) > 0 | \mathcal{H}_t\}}{dt} \quad (4.15)$$

The information set \mathcal{H}_t realizes the path of observed price processes that also includes arrival times and transactions counts for all disjoint states. Following Bacry, Jaisson and Muzy (2016), Engle and Russell (1998), Hawkes (1971), Hawkes and Oakes (1974) and Russell and Engle (2005) among others, we impose some assumptions on the (ground) transaction point processes:

(H3) Each ground transaction point process $\{N^d(t)\}_{d=1}^D$ is assumed to evolve with “after effects” and “conditionally orderly”, which leads to the following properties:

$$\mathbb{Pr}\{N^d(t) - N^d(t - dt) = 1 | \mathcal{H}_t\} = \lambda^d(t)dt + o(dt) \quad (4.16)$$

$$\mathbb{Pr}\{N^d(t) - N^d(t - dt) > 1 | \mathcal{H}_t\} = o(dt) \quad (4.17)$$

On the one hand, a ground transaction point process is considered to evolve with after-effects if for any $t > 0$, the likelihood of occurring a transaction at t depends on the

³ The discrete minimum tick size is necessary feature of modern automated market to prevent an explosion of messaging under the current market design and to constrain the liquidity cost of the market artificially. For the complexity of price discreteness, we refer to Chao, Yao and Ye, 2017, 2018; Li, Wang and Ye, 2021; Yao and Ye, 2018 among others

sequence of transaction occurred only before but not after t , i.e. the interval $[0, t)$. This means that each past transaction only has impacts on the future transaction occurrence, after its presence. On the other hand, a ground transaction point process satisfying conditionally orderly is that, for a sufficiently short time interval, there exist at most one transaction. In other words, conditioned on the information set up to t , \mathcal{H}_t , the probability of occurring two or more transactions is infinitesimally relative to the probability of occurring one transaction. These two conditions in Assumption **(H3)** are fully consistent with empirical properties of high frequency transaction data. In reality, the transactions, indeed, are executed sequentially by matching bid and ask orders queuing in a limit order book according to priority rules (see, e.g. Aquilina, Budish and O’Neill, 2021). Note that Assumption **(H3)** avoids only the simultaneity in a single transaction process, but does not prevent the possibility of simultaneous transaction occurrences between multiple assets.

However, our empirical findings on multiple asset transaction-by-transaction data show that there is an insignificant number of simultaneous transactions between assets, especially for transactions that move price in our study. Therefore, it is appropriate to impose the following assumption when converting the transaction point processes into the multivariate disjoint price change point processes.

(H4) Each disjoint price change point process evolves conditionally orderly with after-effects. And the probability of simultaneously transaction occurrences between disjoint point processes are negligible, leading to the following properties:

$$\Pr\{[N^k(t) - N^k(t - dt)] = 1 | \mathcal{H}_t\} = \lambda^k(t)dt + o(dt) \quad (4.18)$$

$$\Pr\{[N^k(t) - N^k(t - dt)] > 1 | \mathcal{H}_t\} = o(dt) \quad (4.19)$$

$$\Pr\{[N^k(t) - N^l(t - dt)][N^l(t) - N^l(t - dt)] \geq 1 | \mathcal{H}_t\} = o(dt) \quad (4.20)$$

where $k, l \in [0, K]$, $k \neq l$ indexing the component of K -dimensional vector of disjoint price change point processes.

As a consequence of Assumption **(H4)**, the counting increment of each disjoint point process over an instant time takes only two values 0 or 1, and the realization of counting function can be viewed as non-decreasing valued integer time series. The (Eqn. 4.15) can be rewritten as:

$$\lambda^k(t) = \frac{\Pr\{dN^k(t) = 1 | \mathcal{H}_t\}}{dt} = \frac{\mathbb{E}_t[dN^k(t)]}{dt} \quad (4.21)$$

where $dN^k(t) = \lim_{dt \rightarrow 0} N^k(t) - N^k(t - dt)$.

Thanks to representing the transaction price as disjoint price change point processes, we can construct the observed price as follows:

$$X^d(t) = X^d(0) + \sum_{k|m^k \in \mathcal{M}^d} \int_0^t m^k dN^k(u) \quad (4.22)$$

where m^k denotes a disjoint state of price change from the transaction price process of the asset d .

And the conditional first- and second-order moments of price increment over infinitesimal time are:

$$\mathbb{E}_u[dX^d(u)] = \sum_{\{k : m^k \in \mathcal{M}^d\}} \mathbb{E}_u[dN^k(u)]m^k = \sum_{\{k : m^k \in \mathcal{M}^d\}} \lambda^k(u)m^k du \quad (4.23)$$

$$\mathbb{E}_v[dX^d(u)dX^r(v)] = \sum_{\{k : m^k \in \mathcal{M}^d\}} \sum_{\{l : m^l \in \mathcal{M}^r\}} \mathbb{E}_v[dN^k(u)dN^l(v)]m^k m^l \quad (4.24)$$

where $u \leq v$ and $k, l \in [0, K]$. We note that for $d = r$ and $u = v$, which is the case of conditional contemporaneous variation, we can rewrite [Eqn. 4.24](#) as:

$$\mathbb{E}_u[(dX^d(u))^2] = \sum_{\{k : m^k \in \mathcal{M}^d\}} \mathbb{E}_u[dN^k(u)](m^k)^2 = \sum_{\{k : m^k \in \mathcal{M}^d\}} \lambda^k(u)(m^k)^2 \quad (4.25)$$

which has a similar formulation to the PDV estimator (Andersen, Dobrev and Schaumburg, 2009; Engle and Russell, 1998; Gerhard and Hautsch, 2002; Hong et al., 2021; Li, Nolte and (Lechner), 2018; Li, Nolte and Nolte-Lechner, 2015; Tse and Yang, 2012). By imposing a parametric specification on the conditional intensity $\lambda^k(u)$, both the IRC and PDV enjoy the full parametric formulations. As aforementioned advantages in the introduction, the parametric form assumption, speaking from a practical point of view, guarantees a feasible estimation even for a short intraday interval, which contains a small number of observations, and yields an estimate of local intraday volatility. These estimators can even be better off using data beyond the estimation window or including other market microstructure covariates to improve the quality of estimates. Compared to realized volatility estimators, non-parametric approach makes them relying exclusively on the sample size to ensure the efficiency and consistency, and thereby, the estimation is often confined to daily or higher frequency.

The IRC also has a number of important differences from the PDV. On the one hand, the IRC accounts for variations from all observed states of price change, whereas the PDV considers only one absolute state, a fixed price change threshold, to represent all movements in the price process. That price change threshold plays a specific role of truncating small variations, which is assumed coming from micro-structure noises, i.e. bid-ask bounce effects. The selection of such threshold is an empirically appropriate data-driven preference rather than a theoretically optimized value (see, e.g. Hong et al., 2021). Therefore, the applicability of the PDV estimators is still questionable despite their easy implementation and very nice performance against RV estimators. Our estimator, in a different way, treats the bias of microstructure noise as separable quantities. Such quantities arise as the consequence of temporary local deviations from the efficient prices at the time of transaction, and thus can be directly estimated and subtracted from conditional temporal variations of the signal-plus-noise process (see [Eqn. 4.14](#)). On the other hand, the IRC consists of both contemporaneous and temporal (co-)variations, while the PDV focuses on only the contemporaneous part. To some extent (see [Chapter 3](#)), the temporal part accounts for the lead-lag effects and compensates for the loss of the contemporaneous part incurred by asynchronous trading, asymmetric information, and imperfect price formation. Therefore, the IRC

is not only the multivariate generalization of the PDV estimator but also accommodates a more general framework of price formation dynamics.

4.4 MARTINGALE REPRESENTATION AND CONDITIONAL COVARIANCE OF POINT PROCESSES

Taking Eqn. 4.12, Eqn. 4.13 and Eqn. 4.24 together, we have formulated the conditional integrated covariance in terms of the conditional first- and second-order moments of disjoint price change transaction point processes. It remains to construct a closed-form of the point process second-order moments. In order to do so, we will place ourselves in the context of multivariate Hawkes point processes and discuss the martingale representation of conditional intensity function, from which such closed-form of the point process covariance can be derived.

4.4.1 Multivariate Hawkes Point Processes

The k -th component in the K -dimensional vector of conditional intensities, $\lambda^k(t)$, measures the instantaneous quantity of the event arrival of the k -th point process conditional on its information set, and can be formulated as a linear combination of all past events that occurred before t , not only in the k -th process, but also in the others:

$$\lambda^k(t) = \mu^k + \sum_{l=1}^k \int_{-\infty}^t \phi^{kl}(t-s) dN^l(s) \quad (4.26)$$

where $\{\mu^k\}_{k \in [1,K]}$ is a vector of exogenous intensities and $\{\phi^{kl}(t)\}_{k,l \in [1,K]}$ is a matrix-valued decay kernel assumed to be positive and causal. By matrix representation and using convolution notation, we can express the K -dimensional conditional intensity vector, $\boldsymbol{\lambda}(t) = \{\lambda^k(t)\}_{k \in [1,K]}$ as:

$$\boldsymbol{\lambda}(t) = \boldsymbol{\mu} + \int_{-\infty}^t \boldsymbol{\phi}(t-s) d\mathbf{N}(s) = \boldsymbol{\mu} + (\boldsymbol{\phi} \star d\mathbf{N})(t) \quad (4.27)$$

where $\boldsymbol{\mu} = \{\mu^k\}_{k \in [1,K]}$, $\boldsymbol{\phi}(t) = \{\phi^{kl}(t)\}_{k,l \in [1,K]}$ are vector and matrix of sizes K and $K \times K$ respectively. The operator \star stands for convolution.

Proposition 5. *If point processes \mathbf{N}_t satisfy Assumptions (H3) and (H4), the vector of conditional intensities $\boldsymbol{\lambda}(t)$ has an unconditional mean vector $\boldsymbol{\Pi}$ as:*

$$\mathbb{E}(\boldsymbol{\lambda}(t)) = \boldsymbol{\Pi} = (\mathbb{I} - \hat{\boldsymbol{\phi}}_0)^{-1} \boldsymbol{\mu} \quad (4.28)$$

where $\hat{\boldsymbol{\phi}}_z = \{\hat{\phi}_z^{kl}\}_{k,l \in [1,K]} = \{\mathcal{L}\{\hat{\phi}^{kl}\}(z)\}_{k,l \in [1,K]} = \{\int_0^\infty e^{-zt} \phi^{kl} dt\}_{k,l \in [1,K]}$ denotes the Laplace transform of the decay kernel matrix $\boldsymbol{\phi}$ with the frequency parameter z .

Proof. From the formulation of the conditional intensity, i.e. Eqn. 4.21, we have:

$$\mathbf{\Pi} = \mathbb{E}(\boldsymbol{\lambda}(t)) = \mathbb{E}(d\mathbf{N}(t))/dt \quad (4.29)$$

Combining with Equation (4.27), we get:

$$\mathbf{\Pi} = \boldsymbol{\mu} + \int_{-\infty}^t \boldsymbol{\phi}(t-s)ds\mathbf{\Pi} = \boldsymbol{\mu} + \int_0^{\infty} \boldsymbol{\phi}(s)ds\mathbf{\Pi} = \boldsymbol{\mu} + \hat{\boldsymbol{\phi}}_0\mathbf{\Pi} \quad (4.30)$$

So, we obtain the following.

$$\mathbf{\Pi} = (\mathbb{I} - \hat{\boldsymbol{\phi}}_0)^{-1}\boldsymbol{\mu} \quad (4.31)$$

where \mathbb{I} refers to a $K \times K$ identity matrix. \square

4.4.2 Martingale Representation of Hawkes Intensities

Bacry, Dayri and Muzy (2012) and Bacry and Muzy (2016) prove a martingale representation of $\boldsymbol{\lambda}(t)$ by using the Doob-Meyer decomposition to decompose the counting processes $\mathbf{N}(t)$ into finite increasing predictable compensators, $\boldsymbol{\Lambda}(t)$, and martingale processes, $\mathbf{M}(t)$. We follow a similar path as follows:

$$\mathbf{N}(t) = \boldsymbol{\Lambda}(t) + \mathbf{M}(t) \text{ with } \boldsymbol{\Lambda}(t) = \int_0^t \boldsymbol{\lambda}(s)ds \quad (4.32)$$

or:

$$d\mathbf{N}(t) = \boldsymbol{\lambda}(t)dt + d\mathbf{M}(t) \quad (4.33)$$

Then $\boldsymbol{\lambda}(t)$ can be formulated as a stochastic integration with respect to the martingale processes $(\mathbf{M}(t))_{t \geq 0}$:

Proposition 6. Let $(\mathbf{M}(t))_{t \geq 0}$ be the martingale compensated process of $(\mathbf{N}(t))_{t \geq 0}$, $(\boldsymbol{\lambda}(t))_{t \geq 0}$ can be represented as a stochastic integral with respect to the martingale $(\mathbf{M}(t))_{t \geq 0}$ as:

$$\boldsymbol{\lambda}(t) = \mathbf{\Pi} + (\boldsymbol{\Phi} \star d\mathbf{M})(t) = \mathbf{\Pi} + \int_{-\infty}^t \boldsymbol{\Phi}(t-s)d\mathbf{M}(s) \quad (4.34)$$

where $\boldsymbol{\Phi}(t)$ is defined as:

$$\boldsymbol{\Phi}(t) = \sum_{n=1}^{\infty} \boldsymbol{\phi}(t)^{(\star n)} \quad (4.35)$$

with $\boldsymbol{\phi}(t)^{(\star n)}$ refers to a n^{th} -times auto-convolution of $\boldsymbol{\phi}(t)$.

Proof. Substituting the decomposition of the counting function in Eqn. 4.33 into Eqn. 4.27, we have the following:

$$\boldsymbol{\lambda}(t) = \boldsymbol{\mu} + (\boldsymbol{\phi} \star d\mathbf{N})(t) = \boldsymbol{\mu} + (\boldsymbol{\phi} \star \boldsymbol{\lambda})(t) + (\boldsymbol{\phi} \star d\mathbf{M})(t) \quad (4.36)$$

Denote $\boldsymbol{\delta}(t)$ as a Diract delta function, $\boldsymbol{\lambda}(t) = (\mathbb{I}\boldsymbol{\delta} \star \boldsymbol{\lambda})(t)$. We can rewrite the above equation as:

$$((\mathbb{I}\boldsymbol{\delta} - \boldsymbol{\phi}) \star \boldsymbol{\lambda})(t) = \boldsymbol{\mu} + (\boldsymbol{\phi} \star d\mathbf{M})(t) \quad (4.37)$$

We will show that the inverse element of $(\mathbb{I}\delta - \phi)$ for the convolution is $(\mathbb{I}\delta + \Phi)$. Indeed, we have the following.

$$\begin{aligned} ((\mathbb{I}\delta - \phi) \star (\mathbb{I}\delta + \Phi))(t) &= (\mathbb{I}\delta \star \mathbb{I}\delta)(t) + (\mathbb{I}\delta \star \Phi)(t) - (\phi \star \mathbb{I}\delta)(t) - (\phi \star \Phi)(t) \\ &= \mathbb{I} + (\mathbb{I}\delta \star (\Phi - \phi))(t) - (\phi \star \Phi)(t) = \mathbb{I} \end{aligned} \quad (4.38)$$

Because $\Phi(t) = \sum_{n=1}^{\infty} \phi(t)^{(\star n)}$:

$$(\mathbb{I}\delta \star (\Phi - \phi))(t) = (\mathbb{I}\delta \star (\sum_{n=2}^{\infty} \phi(t)^{(\star n)}))(t) = \sum_{n=2}^{\infty} \phi(t)^{(\star n)} \quad (4.39)$$

$$(\phi \star \Phi)(t) = \sum_{n=2}^{\infty} \phi(t)^{(\star n)} \quad (4.40)$$

Thus, convoluting on both sides of [Eqn. 4.37](#) by $(\mathbb{I}\delta + \Phi)$, we get:

$$\lambda(t) = ((\mathbb{I}\delta + \Phi) \star \mu)(t) + (\Phi \star dM)(t) \quad (4.41)$$

Since μ is a constant, and by the definition of convolution:

$$\begin{aligned} ((\mathbb{I}\delta + \Phi) \star \mu)(t) &= \int_{-\infty}^t (\mathbb{I}\delta(t-s) + \Phi(t-s)) ds \mu = (\mathbb{I} + \int_0^{\infty} \Phi(s) ds) \mu \\ &= (\mathbb{I} + \hat{\Phi}_0) \mu \end{aligned} \quad (4.42)$$

By the convolution theorem, we get: $\mathbb{I} + \hat{\Phi}_0 = \sum_{n=1}^{\infty} \hat{\phi}_0^n = (\mathbb{I} - \hat{\phi}_0)^{-1}$. The above equation turns out to be the unconditional mean vector of the point processes Π , which completes the proof of the Proposition. \square

For the k -th point process, we note that $dM^k(t)$ only jumps at t if there is also a jump on $dN^k(t)$. Thus, [Eqn. 4.34](#) can be rewritten for each element $\lambda^k(t)$ as follows:

$$\lambda^k(t) = \Pi^k + \sum_{l=1}^K \int_0^t \Phi^{kl}(t-u) dM^l(u) \quad (4.43)$$

where $\Pi_{k \in [1, K]}^k$ and $\Phi^{kl}(t)_{k, l \in [1, K]}$ are elements of Π and $\Phi(t)$ respectively.

4.4.3 Conditional Covariance of Point Processes

Based on the previous martingale representation of conditional intensity, Bacry, Dayri and Muzy (2012) and Bacry and Muzy (2016) construct unconditional second-order characteristics of Hawkes processes, which are used for their non-parametric estimation method. We deviate from their unconditional approach to a conditional formulation of second-order moments. These conditional moments, then, are used to complete the missing parts of temporal co-variations amongst disjoint price change point processes, i.e. [Eqn. 4.24](#) in the conditional integrated covariance. We obtain the following Proposition:

Proposition 7. Let $N(t), t \geq 0$, be a K -dimensional Hawkes processes with a vector of conditional intensities $\lambda(t)$. Given $u \in [0, T], v \in [u, u + h]$ with $u + h \leq T$ and an information set up to T , \mathcal{H}_T , meaning that full paths of the point processes are observed. We have the following results:

$$\begin{aligned} \mathbb{E}_v[dN^k(u)dN^l(v)] &= N^k(u)\mathbb{1}_{k=l}\mathbb{1}_{v=u} + \mathbb{1}_{v>u} \left[\Phi^{lk}(v-u)dN^k(u)dv + \Pi^k\Pi^l \right. \\ &\quad \left. + \sum_{p=1}^K \int_0^u \Phi^{kp}(u-s)dN^p(s)\Phi^{lp}(v-s) \right] \end{aligned} \quad (4.44)$$

Proof. For $v \in [u, u + h]$ and $\forall k, l \in [1, K]$, $dN^k(u), dN^l(v)$ are both \mathcal{H}_v -measurable. Then, if $dN^k(u) = 0, dN^l(v) = 0$, we have $\mathbb{E}_v[dN^k(u)dN^l(v)] = 0$. Therefore, we consider only time points u, v with $dN^k(u), dN^l(v) \neq 0$.

For $v = u$ and $k \neq l$, then $\mathbb{E}_u[dN^k(u)dN^l(u)] = 0$ because N^k and N^l have no jump in common, i.e. the non-existence of simultaneous occurrence property of point processes by Assumption **(H4)**.

For $v = u$ but $k = l$, we have:

$$\mathbb{E}_u[dN^k(u)dN^k(u)] = \mathbb{E}_u[dN^k(u)] = dN^k(u) \quad (4.45)$$

For $v > u$, thanks to Eqn. 4.33, we can write:

$$\begin{aligned} \mathbb{E}_v[dN^k(u)dN^l(v)^\top] &= \mathbb{E}_v\left[[dM^k(u) + \lambda^k(u)dt][dM^l(v) + \lambda^l(v)ds]\right] = \mathbb{E}_v[dM^k(u)dM^l(v)] \\ &\quad + \mathbb{E}_v[\lambda^l(v)dM^k(u)]dv + \mathbb{E}_v[\lambda^k(u)dM^l(v)]du + \mathbb{E}_v[\lambda^k(u)\lambda^l(v)]dudv \end{aligned} \quad (4.46)$$

Due to the martingale difference sequence properties, $\mathbb{E}_v[dM^k(u)dM^l(v)^\top] = 0, \forall u \neq v$. Substituting the martingale representation of the conditional intensities, i.e. Eqn. 4.43 into the second term of Eqn. 4.46, we have:

$$\begin{aligned} \mathbb{E}_v[\lambda^l(v)dM^k(u)]dv &= \sum_{k=1}^K \int_0^v \mathbb{E}_s[\Phi^{lk}(v-s)dM^l(s)dM^k(u)]dsdv \\ &= \Phi^{lk}(v-u)\mathbb{E}_u[dM^k(u)dM^k(u)]dv = \Phi^{lk}(v-u)\mathbb{E}_u[dN^k(u)]dv \\ &= \Phi^{lk}(v-u)dN^k(u)dv \end{aligned} \quad (4.47)$$

Because $v > u$ and the point process evolve with ‘‘after-effects’’, i.e. Assumption **(H4)**, the conditional intensity $\lambda^k(u)$ does not contain the martingale $dM^l(v)$ in its formulation. Thus, we have the third term:

$$\mathbb{E}_v[\lambda^k(u)dM^l(v)]dv = 0 \quad (4.48)$$

And finally, we continue to utilize [Eqn. 4.43](#), and the last term can be rewritten as:

$$\begin{aligned} \mathbb{E}_v[\lambda^k(u)\lambda^l(v)]dudv &= \mathbb{E}_v\left[\left(\Pi^k + \sum_{p=1}^K \int_0^u \Phi^{kp}(u-s)dM^p(s)\right)\right. \\ &\quad \left.\left(\Pi^l + \sum_{p=1}^K \int_0^v \Phi^{lp}(v-s)dM^p(s)\right)\right]dudv \\ &= \Pi^k\Pi^l + \sum_{p=1}^K \int_0^u \Phi^{kp}(u-s)dN^p(s)\Phi^{lp}(v-s) \end{aligned} \quad (4.49)$$

Combining [Eqn. 4.45](#), [Eqn. 4.46](#), [Eqn. 4.47](#), [Eqn. 4.48](#), and [Eqn. 4.49](#) gives us the result in [Eqn. 4.44](#), which ends the proof of the [Proposition 7](#). \square

According to [Proposition 7](#), the conditional covariance of the disjoint point processes can be divided into two parts according to their contribution to the conditional integrated covariance. The first part, which is the first term of [Eqn. 4.44](#), refers to contemporaneous self-variations that partially govern the estimation of variance components. The second part, consisting of temporal self-variations, i.e. the case $k = l$, and temporal co-variations, i.e. the case $k \neq l$, of disjoint processes, accounts for the lead-lag effects between transaction events. These lead-lag correlations compensate for the loss in contemporaneous (co-)variations due to asynchronous trading, asymmetric information, and imperfect price formation. Moreover, the second part can be further broken down into smaller terms that accommodate different kinds of effects. The first term encodes the exciting feedback from a transaction on the occurrence of future events. The second term is driven by exogenous information (see [Eqn. 4.31](#)), while the last captures the endogenous effects incurred by common historical information.

4.4.4 Towards a fully parametric closed-form conditional covariance of point processes

The previous section provides a formulation of the conditional second moment structure in terms of parameters from the martingale representation of conditional intensity, i.e. Π^k, Φ^{kl} , which are constructed from the original Hawkes process parameters, i.e. μ^k, ϕ^{kl} . The formulation still misses a specification on the choice of the excitement function ϕ^{kl} to achieve a fully parametric closed-form. In most cases, ϕ^{kl} of Hawkes processes is a somewhat arbitrary parametric kernel, and the main decision is between exponential or power-law functions. Among the two kernels, the exponential excitement function yields a Markovian structure for the conditional intensity [Hawkes \(2017\)](#), and its likelihood function is much easier to handle by recursive representation [Ogata \(1988\)](#). Therefore, the exponential kernel is more mathematically attractive, and we chose the exponential decay function for the excitement kernel in our studies. The empirical analysis in the previous [Chapter 3](#) also confirms the validity of our choice. With the exponential decay kernel, the conditional intensity function [\(4.26\)](#) has the form:

$$\lambda^k(t) = \mu^k + \sum_{k=1}^k \int_{-\infty}^t \alpha^{kl} \beta^{kl} e^{-\beta^{kl}(t-s)} dN^r(s) \quad (4.50)$$

where $\alpha = \{\alpha^{kl}\}_{k,l \in [1,K]}$ are matrix-valued impact coefficients that specify the mean expected number of descendant of a given point event. Given that there is a transaction arrival in the point process l , the conditional intensity of the point process k increases proportionally to α^{kl} . The rate at which this effect decays over time is governed by $\beta = \{\beta^{kl}\}_{k,l \in [1,K]}$.

Using Hadamard symbols with \otimes , \oslash , \circ denoting element-wise multiplication, element-wise division, and element-wise power, respectively, we can rewrite the vector of exponential kernel intensity function with convolution operator (4.50) as:

$$\lambda(t) = \mu + \alpha \otimes \beta \otimes e^{\circ(-\beta t)} \star dN(t) \quad (4.51)$$

With the exponential kernel of fixed decay parameter, we can obtain a closed form of the conditional intensities under martingale representation as follows:

Proposition 8. *Let $(N(t))_{t \geq 0}$ be an K -dimensional vector of Hawkes processes with intensity vector $\lambda(t)$, satisfies Assumptions **H3** and **H4**. Let $(M_t)_{t \geq 0}$ be the martingale compensation processes of $N(t)$. Consider that $N(t)$ has an exponential decay kernel ϕ with the same constant parameter β for all D point processes. Then, the martingale representation of $\lambda(t)$ can have the form as follows:*

$$\lambda(t) = \Pi + \int_{-\infty}^t \alpha \beta e^{(\alpha - \mathbb{I})\beta(t-s)} dM(s) \quad (4.52)$$

Proof. By the convolution theorem, it is more convenient to rewrite $\Phi(t)$ defined by Eqn. 4.35 in the frequency domain of the Laplace transform:

$$\hat{\Phi}_z = \sum_{n=1}^{+\infty} \hat{\Phi}_z^n = \hat{\Phi}_z (\mathbb{I} - \hat{\Phi}_z)^{-1} \quad (4.53)$$

From Eqn. 4.51 and Eqn. 4.53, the Laplace transform of the matrix-valued kernel $\hat{\Phi}_z$ can be defined as

$$\hat{\Phi}_z = \alpha \otimes \beta \oslash (\beta + z) \quad (4.54)$$

Giving this result, the other term on the right-hand side of Eqn. 4.53 can also be formulated as:

$$(\mathbb{I} - \hat{\Phi}_z)^{-1} = \left[[\mathbb{I}z - (\alpha - \mathbb{I}) \otimes \beta] \oslash (\beta + z) \right]^{-1} \quad (4.55)$$

By fixing a decay parameter for all point processes, β is simplified to a constant, which leads $\hat{\Phi}_z$ to be as:

$$\hat{\Phi}_z = \alpha \beta [\mathbb{I}z - (\alpha - \mathbb{I})\beta]^{-1} \quad (4.56)$$

Applying the inverse Laplace transform, the convolution theorem, and the properties of the exponential matrix, we obtain the form of Φ in the time domain as:

$$\Phi(t) = \alpha \beta e^{(\alpha - \mathbb{I})\beta t} \quad (4.57)$$

which completes the proof of the Proposition 8 □

4.5 SIMULATION STUDY

This section presents a simulation study to uncover how the impacts of microstructure features such as trading activity, non-synchronicity trading, and microstructure noise to the IRC, and which bandwidth interval to choose when implementing the estimator. More importantly, it studies the relative finite sample performance of the IRC in comparison with other benchmark estimators in the literature. We opt to work with the simulation framework, rather than a real data-set, where we can have the information on the integrated variance-covariance matrix of efficient price that is not observable in empirical data, and investigate the performance of estimators by their deviations from the true value.

4.5.1 Simulation Design

The simulation framework is constructed to reproduce rich specifications of (i) efficient prices evolving with correlated stochastic volatility, (ii) independent and uncorrelated microstructure noises versus those with general properties, and (iii) asynchronous trading times. Throughout, we work with a bivariate stochastic volatility model over the interval $t \in [0, 1]$ that we think of as a day and contains 6.5 hours of trading. The simulation design follows that of Barndorff-Nielsen et al. (2011), Christensen, Kinnebrock and Podolskij (2010), Hansen and Lunde (2006a) and Li, Nolte and (Lechner) (2018).

4.5.1.1 Efficient Price

The efficient price diffusion is simulated using a bivariate stochastic volatility model. Each price process $d = 1, 2$ has the following specifications:

$$dY^d(t) = \sigma_d(t) \left[\sqrt{1 - (\gamma^k)^2} dW^d(t) + \gamma^d dZ^d(t) \right] \quad (4.58)$$

$$\sigma_d(t) = \exp [\theta^d + \eta^d v^d(t)] \quad (4.59)$$

$$dv^d(t) = \kappa^d v^d(t) dt + \zeta^d dZ^d(t) \quad (4.60)$$

where W^1 and Z^1 , W^1 and Z^2 , and Z^1 and Z^2 are pairwise independent Brownian motions. The correlation between $Y^1(t)$, $Y^2(t)$ is determined by $\rho = \iota \sqrt{1 - (\gamma^1)^2} \sqrt{1 - (\gamma^2)^2}$ with $\iota = d\langle W^1, W^2 \rangle_t$. The stochastic component of volatility is correlated with the efficient price change by $\gamma^d \zeta^d$. Thus, $\gamma^d \zeta^d$ controls the leveraged effect on the volatility of asset prices.

The efficient price processes are generated using a Euler scheme, where a trading day interval $[0, 1]$ is discretized into $M = 23,400$ intervals corresponding to the total seconds per trading day. We follow Li, Nolte and (Lechner) (2018) to set the parameters values for our simulation (see Table 4.1). With this configuration, the unconditional mean of daily volatility is roughly 0.0002. The first value of $v^d(t)$ is drawn from its stationary distribution $v^d(0) \sim \mathcal{N}\left(0, -\frac{(\zeta^d)^2}{2\kappa^d}\right)$.

Table 4.1: Parameters values for simulating the efficient price vectors.

θ^d	η^d	κ^d	γ^d	ζ^d	ι
$-5/\sqrt{2}$	$1/\sqrt{2}$	$-1/10\sqrt{2}$	-0.3	1	1

4.5.1.2 Asynchronous transaction times

To simulate the asynchronicity of observed transactions, we use two independent Poisson process sampling schemes to generate the time of transaction arrivals $\{t_i^d\}_{d=1,2}$. The arrival rates for the two Poisson processes are $\{\lambda_0^d\}_{d=1,2}$, so the expected number of transactions within a trading day is $\mathbb{E}[N^d(t)] = \int_0^1 \lambda_0^d ds = 23400\lambda_0^d$. This means that the simulated number of observed transactions will differ between repetitions but on average two simulated assets will have $23400\lambda_0^1$ and $23400\lambda_0^2$ observations, respectively.

We vary $(\lambda_0^1, \lambda_0^2)$ through the following configurations $(1/3, 1/6)$, $(1/4, 1/8)$, $(1/5, 1/10)$ to simulate different scenarios of liquidity.

4.5.1.3 Market microstructure noise

Market microstructure noise is an additive component to the efficient price. Empirically, we can not observe the efficient price because of the presence of market microstructure noise, and the following decomposition is frequently used in the literature:

$$\mathbf{X}(t_i) = \mathbf{Y}(t_i) + \mathbf{U}(t_i) \quad (4.61)$$

in which $\mathbf{U}(t_i)$ is modelled as identical independent stationary processes. We simulate the microstructure noise at observed transaction times generated above with the following settings:

$$\mathbf{U}(t_i) | \sigma_1, \sigma_2, \mathbf{Y} \stackrel{\text{i.i.d.}}{\sim} \mathcal{N}\left(0, \begin{pmatrix} \omega_1^2 & \rho\omega_1\omega_2 \\ \rho\omega_1\omega_2 & \omega_2^2 \end{pmatrix}\right) \quad \text{with } \omega_a^2 = \varphi \sqrt{[N^d(1)]^{-1} \sum_{i=1}^M \sigma_{d,i}^4} \quad (4.62)$$

The noise-to-signal ratio, φ , takes values 0, 0.001, and 0.01 which represent non-, moderate and high microstructure noise scenarios. This means that the variance of the noise can be set so that it increases with the volatility of the efficient price by a noise-to-signal ratio (Bandi and Russell, 2006). To examine our independent assumption between the microstructure noises, i.e. Assumptions **(H1)** and **(H2)**, the correlation between two noise terms, ρ , is set at 0 and 0.5 for the case of no and significant correlation between them.

4.5.1.4 Rounding error

The observed price process of asset d is decomposed as $\tilde{X}^d(t_i) = \tilde{Y}^d(t_i) \tilde{U}^d(t_i)$ where $\tilde{Y}^d(t_i) = \ln(Y^d(t_i))$ and $\tilde{U}^d(t_i) = \ln(U^d(t_i))$. The observed prices are forced to stay on the grid as follows:

$$\tilde{X}^d(t_i) = \xi \left\lfloor \frac{\exp[Y^d(t_i) + U^d(t_i)]}{\xi} \right\rfloor \quad (4.63)$$

where $\lfloor z \rfloor$ returns the nearest integer of a real number z . We set $\zeta = 0.01$ to emulate rounding errors on a grid. We note that the rounding will introduce additional flat trades, i.e. the transaction price does not move, to the observed price processes when the price is rounded to zero. The actual amount of flat trades depends on the initial observed price $\tilde{X}^d(0)$ since the rounding error is smaller when $\tilde{X}^d(0)$ is large and vice versa. We set $(\tilde{X}^1(0), \tilde{X}^2(0)) = (30, 30)$ and the resulting proportion of flat trades is mostly around 60 – 70%, which is in line with empirical finding in the literature (see, e.g. Jacod, Li and Zheng, 2017; Liesenfeld, Nolte and Pohlmeier, 2008).

4.5.2 Estimator and Tuning Parameters

We compare the performance of the intensity-based ex-post covariance estimator to both groups of quadratic covariation and point process estimators. The former includes realized covariance (RC) (Andersen et al., 2001; Andersen et al., 2003; Barndorff-Nielsen and Shephard, 2002a, 2004) of different sampling frequencies and multivariate realized kernel covariance (RK) (Barndorff-Nielsen et al., 2008, 2011) which is a state-of-the-art integrated covariance estimator, known to be highly efficient and robust to microstructure noise. The latter contains the non-parametric price duration volatility (PDV) estimator Engle and Russell, 1998; Hong et al., 2021; Li, Nolte and (Lechner), 2018; Tse and Yang, 2012 which is the closest one to the IRC.

The choice of tuning parameters for these estimators is non-trivial, as they have a very large impact on the performance of their performances. For the RC estimator, the choice of sampling frequency entails a bias-variance trade-off because the bias caused by the microstructure noise is most significant at high-frequency sampling, while the variance of the estimator increases as the sampling frequency is lowered. The recommendation in the literature has been to sample sparsely at some lower frequency (see, e.g. Bandi and Russell, 2008; Bandi and Russell, 2006; Hansen and Lunde, 2006b; Li et al., 2013; Liu and Tse, 2015). In our simulation, we chose the sampling frequencies of 1 min, 5 min, and 15 min for the RC estimator. For the RK estimator, the optimal choice of bandwidth is obtained following the implementation in Barndorff-Nielsen et al. (2011) and then the estimation is calculated using the Parzen kernel.

For the second group based on point process approach, the choice of sampling price change threshold is very important, since it plays the main role in eliminating the microstructure noise bias. Following Hong et al. (2021), Li, Nolte and (Lechner) (2018) and Tse and Yang (2012), we apply this estimator to the thresholds of 1 tick, 2 ticks, and 3 ticks.

Finally, for our intensity-based covariance estimator (IRC), we set a tolerance to determine the bandwidth interval h . We remind the reader that with the exponential decay kernel, the excitement effects from one event to others only converge to zero in infinity. But after an elapsed time interval, such effects decay to a trivial level, namely tolerance, and the magnitude smaller than the tolerance can be assumed to be negligible. The tolerance is chosen so that it is minor to the true value of the integrated covariance, i.e. less than

10^{-5} . Then the bandwidth interval h can be simply computed, with the estimated Hawkes parameters, as the time it takes for the excitement effects to decay to such a tolerance level.

4.5.3 *Simulation results*

The simulations are performed with 200 replications. In each replication, we calculate the bias as the difference of the estimated results with respect to the true value of the integrated variance-covariance matrix, and the squared error as the square of the difference for each of the estimators with respect to various tuning parameters. We then take the mean of biases and the root mean of squared errors over all replications. The final results are reported in Tables 4.2, 4.3, and 4.4, where the first two tables illustrate the results of the diagonal elements of the variance-covariance matrix estimation, variances, and the last are the non-diagonal elements, covariance/correlation. In each table, we report the results for different scenarios of microstructure noises, i.e. only pure rounding noise; moderate additive independent white noises and rounding error; strong additive independent white noises and rounding error; and strong additive correlated white noises and rounding error, and for different scenarios of high, moderate and low level of trading activities.

Table 4.2: Simulation results for integrated volatility estimators.

Integrated variance																
	Asset 1															
	RC ^{1m}		RC ^{5m}		RC ^{15m}		RK		PDV ^{1tick}		PDV ^{2ticks}		PDV ^{3ticks}		IRC	
	Bias	RMSE	Bias	RMSE	Bias	RMSE	Bias	RMSE	Bias	RMSE	Bias	RMSE	Bias	RMSE	Bias	RMSE
$\varphi^2 = 0, \rho = 0$																
$\lambda_0 = (1/3, 1/6)$	6,17E-06	2,06E-05	-3,00E-06	4,33E-05	-5,72E-06	7,32E-05	5,33E-07	2,11E-05	-5,54E-05	1,53E-04	-4,69E-05	1,04E-04	-4,00E-05	8,11E-05	8,37E-07	3,44E-05
$\lambda_0 = (1/4, 1/8)$	5,40E-06	1,89E-05	-4,31E-06	4,18E-05	-6,52E-06	7,13E-05	1,09E-06	2,49E-05	-7,45E-05	1,63E-04	-5,73E-05	1,15E-04	-4,66E-05	9,02E-05	-1,92E-06	3,58E-05
$\lambda_0 = (1/5, 1/10)$	7,54E-06	2,03E-05	-2,70E-06	4,36E-05	-4,60E-06	7,48E-05	-8,63E-07	2,60E-05	-8,89E-05	1,73E-04	-6,46E-05	1,23E-04	-5,10E-05	9,57E-05	-4,54E-06	3,85E-05
$\varphi^2 = 0.001, \rho = 0$																
$\lambda_0 = (1/3, 1/6)$	6,09E-06	2,07E-05	-2,94E-06	4,32E-05	-5,82E-06	7,32E-05	5,38E-07	2,11E-05	-5,53E-05	1,53E-04	-4,69E-05	1,04E-04	-4,03E-05	8,14E-05	1,77E-06	3,55E-05
$\lambda_0 = (1/4, 1/8)$	5,31E-06	1,89E-05	-4,20E-06	4,21E-05	-6,56E-06	7,13E-05	1,03E-06	2,50E-05	-7,44E-05	1,63E-04	-5,73E-05	1,15E-04	-4,65E-05	9,01E-05	-2,06E-06	3,68E-05
$\lambda_0 = (1/5, 1/10)$	7,56E-06	2,03E-05	-2,60E-06	4,37E-05	-4,67E-06	7,48E-05	-9,07E-07	2,60E-05	-8,88E-05	1,73E-04	-6,48E-05	1,23E-04	-5,09E-05	9,57E-05	-4,59E-06	3,91E-05
$\varphi^2 = 0.01, \rho = 0$																
$\lambda_0 = (1/3, 1/6)$	6,22E-06	2,06E-05	-3,01E-06	4,37E-05	-5,91E-06	7,34E-05	5,76E-07	2,12E-05	-5,48E-05	1,53E-04	-4,66E-05	1,04E-04	-3,97E-05	8,05E-05	1,54E-06	3,38E-05
$\lambda_0 = (1/4, 1/8)$	5,53E-06	1,92E-05	-4,09E-06	4,22E-05	-6,54E-06	7,13E-05	9,63E-07	2,50E-05	-7,41E-05	1,63E-04	-5,71E-05	1,14E-04	-4,63E-05	9,03E-05	-1,28E-06	3,47E-05
$\lambda_0 = (1/5, 1/10)$	7,56E-06	2,03E-05	-2,42E-06	4,34E-05	-4,58E-06	7,53E-05	-8,54E-07	2,62E-05	-8,85E-05	1,73E-04	-6,47E-05	1,23E-04	-5,07E-05	9,58E-05	-4,19E-06	3,86E-05
$\varphi^2 = 0.01, \rho = 0.5$																
$\lambda_0 = (1/3, 1/6)$	4,26E-06	1,98E-05	-3,71E-06	4,41E-05	-4,66E-06	7,26E-05	1,49E-07	2,04E-05	-5,47E-05	1,53E-04	-4,74E-05	1,04E-04	-3,91E-05	8,11E-05	1,20E-06	3,50E-05
$\lambda_0 = (1/4, 1/8)$	6,43E-06	1,96E-05	-2,65E-06	4,24E-05	-3,70E-06	7,60E-05	-2,61E-08	2,22E-05	-7,38E-05	1,63E-04	-5,69E-05	1,14E-04	-4,54E-05	8,93E-05	-1,37E-06	3,68E-05
$\lambda_0 = (1/5, 1/10)$	4,57E-06	1,93E-05	-2,56E-06	4,39E-05	-6,08E-06	7,35E-05	-1,73E-06	2,61E-05	-8,88E-05	1,73E-04	-6,59E-05	1,23E-04	-5,19E-05	9,70E-05	-2,40E-06	3,51E-05

Notes: Simulation results for estimating integrated variance of asset 1 using realized covariance (RC), multivariate realized kernel covariance (RK) with Parzen type, and price duration volatility (PDV) and intensity based realized covariance (IRC) estimators. The simulation framework is constructed with non-synchronous observations, microstructure noises and measurement error. The results are based on 200 repetitions.

Table 4.3: Simulation results for integrated volatility estimators.

Integrated variance																
Asset 2																
	RC ^{1m}		RC ^{5m}		RC ^{15m}		RK		PDV ^{1tick}		PDV ^{2ticks}		PDV ^{3ticks}		IRC	
	Bias	RMSE	Bias	RMSE	Bias	RMSE	Bias	RMSE	Bias	RMSE	Bias	RMSE	Bias	RMSE	Bias	RMSE
$\varphi^2 = 0, \varrho = 0$																
$\lambda_0 = (1/3, 1/6)$	4,72E-06	1,92E-05	-4,86E-06	3,98E-05	-6,07E-06	6,96E-05	-4,46E-07	1,73E-05	-9,57E-05	1,77E-04	-6,83E-05	1,28E-04	-5,41E-05	1,01E-04	-2,56E-06	3,22E-05
$\lambda_0 = (1/4, 1/8)$	5,53E-06	1,97E-05	-5,61E-06	3,88E-05	-5,48E-06	6,56E-05	2,45E-07	2,14E-05	-1,11E-04	1,89E-04	-7,97E-05	1,40E-04	-6,16E-05	1,11E-04	-8,46E-06	3,64E-05
$\lambda_0 = (1/5, 1/10)$	4,86E-06	2,04E-05	-5,19E-06	4,13E-05	-4,63E-06	7,02E-05	-2,36E-06	2,31E-05	-1,22E-04	1,98E-04	-8,78E-05	1,50E-04	-6,93E-05	1,21E-04	-9,85E-06	3,86E-05
$\varphi^2 = 0.001, \varrho = 0$																
$\lambda_0 = (1/3, 1/6)$	4,70E-06	1,94E-05	-4,77E-06	3,98E-05	-6,08E-06	6,92E-05	-3,90E-07	1,73E-05	-9,56E-05	1,77E-04	-6,81E-05	1,27E-04	-5,38E-05	1,00E-04	-2,40E-06	3,26E-05
$\lambda_0 = (1/4, 1/8)$	5,49E-06	2,00E-05	-5,68E-06	3,86E-05	-5,57E-06	6,55E-05	2,25E-07	2,15E-05	-1,11E-04	1,89E-04	-7,97E-05	1,40E-04	-6,16E-05	1,11E-04	-8,14E-06	3,63E-05
$\lambda_0 = (1/5, 1/10)$	4,92E-06	2,06E-05	-5,21E-06	4,11E-05	-4,76E-06	7,01E-05	-2,37E-06	2,32E-05	-1,22E-04	1,98E-04	-8,77E-05	1,49E-04	-6,94E-05	1,21E-04	-1,05E-05	3,94E-05
$\varphi^2 = 0.01, \varrho = 0$																
$\lambda_0 = (1/3, 1/6)$	4,70E-06	1,92E-05	-4,98E-06	3,98E-05	-6,16E-06	6,91E-05	-4,20E-07	1,74E-05	-9,53E-05	1,77E-04	-6,81E-05	1,27E-04	-5,37E-05	1,00E-04	-2,48E-06	3,21E-05
$\lambda_0 = (1/4, 1/8)$	5,74E-06	1,99E-05	-5,45E-06	3,84E-05	-5,48E-06	6,57E-05	2,27E-07	2,15E-05	-1,11E-04	1,89E-04	-7,95E-05	1,40E-04	-6,15E-05	1,10E-04	-8,06E-06	3,52E-05
$\lambda_0 = (1/5, 1/10)$	4,93E-06	2,04E-05	-5,13E-06	4,08E-05	-4,67E-06	7,04E-05	-2,27E-06	2,33E-05	-1,22E-04	1,98E-04	-8,77E-05	1,49E-04	-6,95E-05	1,21E-04	-1,04E-05	3,85E-05
$\varphi^2 = 0.01, \varrho = 0.5$																
$\lambda_0 = (1/3, 1/6)$	3,60E-06	2,00E-05	-5,47E-06	3,98E-05	-5,45E-06	6,95E-05	-5,80E-07	1,80E-05	-9,55E-05	1,77E-04	-6,85E-05	1,26E-04	-5,38E-05	1,01E-04	-2,00E-06	2,94E-05
$\lambda_0 = (1/4, 1/8)$	4,73E-06	2,03E-05	-5,89E-06	3,90E-05	-5,15E-06	6,99E-05	-1,00E-06	1,94E-05	-1,11E-04	1,89E-04	-7,94E-05	1,41E-04	-6,16E-05	1,12E-04	-6,73E-06	3,46E-05
$\lambda_0 = (1/5, 1/10)$	3,86E-06	2,06E-05	-4,06E-06	3,79E-05	-5,38E-06	6,88E-05	-2,47E-06	2,36E-05	-1,22E-04	1,98E-04	-8,73E-05	1,49E-04	-6,82E-05	1,19E-04	-8,04E-06	3,36E-05

Notes: Simulation results for estimating integrated variance of asset 2 using realized covariance (RC), multivariate realized kernel covariance (RK) with Parzen type, and price duration volatility (PDV) and intensity based realized covariance (IRC) estimators. The simulation framework is constructed with non-synchronous observations, microstructure noises and measurement error. The results are based on 200 repetitions.

Let us first analyze the estimated results of the integrated variance in Tables 4.2 and 4.3. For the first asset, the IRC estimator tends to outperform the RC and the PDV estimators in almost all scenarios of noise and trading activity. In the case with high transaction rates and only rounding noise, the performance of IRC estimator even is on par with the RK, which is a very well-known consistent quadratic covariation-type estimator. In the second asset, the IRC does not perform as well as the RK and suffers from large biases and RMSE. This might be due to the low level of the trading rate simulated on the second asset, which is always half that of the first asset. In addition, it is noticeable that the IRC's estimation performance in both assets is increasing with the simulated trading rates. The trading rate illustrates the degree to which the information set is available. We remind the reader that the IRC is a parametric designed estimator based on fitting a Hawkes exponential kernel to the realizations of disjoint price change states. Thus, the performance of the estimator is very sensitive to the size of the information set on which it is conditioning. In this study, it is the activity of the trading or the level of liquidity. The higher the liquidity of the asset, the better the volatility estimation can be obtained by the IRC. In sharp contrast, this pattern seems to be not valid for the remaining non-parametric estimators. The results obtained on the bias do not change much as the number of observed transactions increases.

We continue with Table 4.4 that illustrates the estimated results on the integrated covariance and correlation between two assets. Compared to other non-parametric estimators, we might expect an inferior performance for the IRC due to its intrinsic of parametric estimation. The parametric feature of the IRC, which relies on conditional expectation, might yield on-average or mean-reverting results, so it might exhibit a more modest performance compared to unconditional non-parametric estimators. However, we surprisingly observe that the IRC consistently over-performs the RC and is not significantly different from the RK. Moreover, similar to the integrated variance estimation, we also observe, amongst estimators, a tendency of increasing biases incurred by decreasing transaction rates. This tendency is most obvious in the RC with higher frequency subsampling, i.e. 1 minute and 5 minutes, of which the bias predominantly drives the RMSE. This tendency in the IRC is less severe but still significant.

On the right-hand side of Table 4.4, we report the estimated results on the correlation between assets. Interestingly, the IRC delivers very precise estimates of the correlation, and its estimations are much sharper than those of the RK in terms of bias. All quadratic covariation-type estimators deliver very precise estimates of the wrong quantity because their biases are the dominant components of the RMSE. But that is not the case for the IRC. Surprisingly, both the IRC and the RK estimators perform better when transaction rates decrease, indicating that there is less information available. It can be plausibly explained that the correlation is a nonlinear function of noise-contaminated integrated variance estimates and that the contamination is more severe in higher frequency transaction data, e.g. due to trading on the spread. Because the noise only exists when there is a transaction, it is clearly that a higher simulated transaction rate leads to a higher proportion of variance bias from the noise.

Table 4.4: Simulation results for integrated covariance/correlation estimators.

Integrated covariance/correlation																					
		Covariance										Correlation									
		RC ^{1m}		RC ^{5m}		RC ^{15m}		RK		IRC		RC ^{1m}		RC ^{5m}		RC ^{15m}		RK		IRC	
		Bias	RMSE	Bias	RMSE	Bias	RMSE	Bias	RMSE	Bias	RMSE	Bias	RMSE	Bias	RMSE	Bias	RMSE	Bias	RMSE	Bias	RMSE
$\varphi^2 = 0, \varrho = 0$																					
$\lambda_0 = (1/3, 1/6)$		-1,75E-05	2,97E-05	-8,26E-06	4,08E-05	-7,88E-06	6,90E-05	-3,01E-06	1,90E-05	-4,32E-06	3,29E-05	-1,27E-01	1,33E-01	-3,01E-02	4,11E-02	-1,96E-02	4,89E-02	-2,27E-02	2,88E-02	-1,15E-02	3,85E-02
$\lambda_0 = (1/4, 1/8)$		-2,28E-05	3,56E-05	-1,03E-05	3,98E-05	-8,10E-06	6,52E-05	-2,17E-06	2,25E-05	-6,92E-06	3,40E-05	-1,53E-01	1,59E-01	-3,52E-02	4,54E-02	-1,88E-02	4,78E-02	-2,05E-02	2,62E-02	-6,38E-03	3,48E-02
$\lambda_0 = (1/5, 1/10)$		-2,69E-05	4,12E-05	-1,04E-05	4,25E-05	-7,01E-06	7,03E-05	-4,33E-06	2,42E-05	-7,89E-06	3,67E-05	-1,75E-01	1,80E-01	-4,08E-02	5,07E-02	-2,19E-02	5,17E-02	-1,94E-02	2,43E-02	-1,63E-03	3,40E-02
$\varphi^2 = 0.001, \varrho = 0$																					
$\lambda_0 = (1/3, 1/6)$		-1,75E-05	2,98E-05	-8,14E-06	4,05E-05	-7,92E-06	6,89E-05	-2,97E-06	1,90E-05	-4,05E-06	3,38E-05	-1,27E-01	1,33E-01	-3,00E-02	4,11E-02	-1,96E-02	4,88E-02	-2,26E-02	2,87E-02	-1,28E-02	3,93E-02
$\lambda_0 = (1/4, 1/8)$		-2,28E-05	3,57E-05	-1,02E-05	3,99E-05	-8,11E-06	6,50E-05	-2,21E-06	2,26E-05	-6,85E-06	3,52E-05	-1,54E-01	1,59E-01	-3,53E-02	4,54E-02	-1,85E-02	4,78E-02	-2,06E-02	2,63E-02	-7,85E-03	3,31E-02
$\lambda_0 = (1/5, 1/10)$		-2,69E-05	4,12E-05	-1,03E-05	4,25E-05	-7,15E-06	7,01E-05	-4,37E-06	2,43E-05	-8,22E-06	3,72E-05	-1,75E-01	1,80E-01	-4,10E-02	5,10E-02	-2,21E-02	5,19E-02	-1,95E-02	2,44E-02	-3,16E-03	3,55E-02
$\varphi^2 = 0.01, \varrho = 0$																					
$\lambda_0 = (1/3, 1/6)$		-1,76E-05	2,98E-05	-8,38E-06	4,08E-05	-8,00E-06	6,88E-05	-2,99E-06	1,91E-05	-4,78E-06	3,30E-05	-1,28E-01	1,33E-01	-3,02E-02	4,12E-02	-1,95E-02	4,90E-02	-2,28E-02	2,88E-02	-1,48E-02	3,97E-02
$\lambda_0 = (1/4, 1/8)$		-2,27E-05	3,54E-05	-1,02E-05	4,00E-05	-8,00E-06	6,52E-05	-2,25E-06	2,26E-05	-6,84E-06	3,50E-05	-1,54E-01	1,59E-01	-3,58E-02	4,60E-02	-1,80E-02	4,73E-02	-2,06E-02	2,63E-02	-8,93E-03	3,50E-02
$\lambda_0 = (1/5, 1/10)$		-2,70E-05	4,12E-05	-1,02E-05	4,22E-05	-7,06E-06	7,03E-05	-4,31E-06	2,44E-05	-7,95E-06	3,66E-05	-1,76E-01	1,80E-01	-4,07E-02	5,04E-02	-2,18E-02	5,11E-02	-1,95E-02	2,43E-02	-3,00E-03	3,48E-02
$\varphi^2 = 0.01, \varrho = 0.5$																					
$\lambda_0 = (1/3, 1/6)$		-1,91E-05	3,23E-05	-8,85E-06	4,06E-05	-6,68E-06	6,83E-05	-3,32E-06	1,89E-05	-4,92E-06	3,24E-05	-1,29E-01	1,35E-01	-2,97E-02	4,03E-02	-1,62E-02	4,67E-02	-2,29E-02	2,85E-02	-1,88E-02	3,86E-02
$\lambda_0 = (1/5, 1/10)$		-2,25E-05	3,52E-05	-9,98E-06	3,95E-05	-6,81E-06	6,89E-05	-3,42E-06	2,04E-05	-5,05E-06	3,31E-05	-1,53E-01	1,58E-01	-3,61E-02	4,58E-02	-1,97E-02	4,95E-02	-2,12E-02	2,67E-02	-4,24E-03	3,37E-02
$\lambda_0 = (1/10, 1/20)$		-2,82E-05	4,30E-05	-8,04E-06	3,36E-05	-7,82E-06	6,61E-05	-4,82E-06	2,44E-05	-6,22E-06	3,35E-05	-1,74E-01	1,78E-01	-3,80E-02	4,79E-02	-1,95E-02	5,04E-02	-1,98E-02	2,46E-02	-7,04E-03	3,78E-02

Notes: Simulation results for estimating integrated variance of asset 2 using realized covariance (RC), multivariate realized kernel covariance (RK) with Parzen type, and price duration volatility (PDV) and intensity based realized covariance (IRC) estimators. The simulation framework is constructed with non-synchronous observations, microstructure noises and measurement error. The results are based on 200 repetitions.

Last but not least, we study the impact of noise components on the performance of the IRC in all the tables, which can verify the robustness of the estimator to the microstructure noise. Across different levels of noise, the results obtained by the IRC do not change much, except for the estimation of the integrated variance with the highest transaction rate of $\lambda_0 = 1/3$, where positive biases are observed. The positive biases might arise due to increasing the transaction frequency simultaneously adding more noise, leading to an upward bias in the estimation. Moreover, it is not, surprisingly, the design with pure rounding error producing the best performance in estimating integrated variance and covariance. It could be that IRC benefits from a significant additional layer of noise, which is the case of $\phi^2 = 0.01$, and delivers the best performance in terms of bias and RMSE. Meanwhile, the worst performance is found in the case of moderate noise $\phi^2 = 0.001$. We note that adding a significant additional layer of noise prior together with rounding error introduces an upward bias in the integrated variance estimation. This bias might compensate for attenuation biases incurred by the absence of observation in the observable price, and thereby turns out to improve the IRC's performance. However, in the case of a moderate or light layer of noise, this noise can be cancelled out by the rounding error if the deviation from the efficient price is not large enough to be a minimum price change unit, i.e. tick. Such a rounding error, due to discreteness, can also eliminate true small movements of the efficient price, thereby generating more significant downward biases. Finally, in the last simulation scenario, we add a correlation between additive microstructure noise with $\rho = 0.5$. However, correlated noise does not worsen the performance of the IRC. The other way around, it helps to improve the estimation in terms of both bias and RMSE. This finding confirms the validity of our previous statements pointing out the adequacy of independent uncorrelated white noise assumptions.

4.6 CONCLUSION

This chapter develops an intensity-based estimator (IRC) of integrated variance-covariance/correlation with noisy and asynchronous tick-by-tick data. The IRC is so far the first point process-based estimator that deals with covariation between multiple assets. It amalgamates both quadratic covariation and point process approaches by introducing the logic that the quadratic covariation of the price processes can be represented by the second-order moments of non-decreasing valued integer processes counting transactions associated with price change states. Via a martingale representation of conditional intensity, a closed-form of such second-order moments can be obtained, and thereby leads to a fully parametric specification of the IRC.

Compared to the realized covariance (RC) and the previous univariate point process (price duration) volatility estimator (PDV), the IRC has a number of outstanding features. First, thanks to its parametric form, the IRC allows for a feasible estimation for any arbitrary interval, even the short one, which lacks observations. Such a property overcomes the limitation of non-parametric realized volatility, which is often confined to only daily estimates. Second, the IRC does not need a pseudo-aligning scheme, which is necessary for

realized volatility to synchronize observations. Instead, it employs all transactions and utilizes all of transaction-related information, i.e. transaction price and time. Being designed to have a generic structure of temporal (cross-)autocovariation instead of ordered (cross-)autocovariation, the IRC accounts for the transaction time as an endogenous variable determining the strength of covariation. Moreover, to some extent, the temporal (cross-)autocovariation accounts for lead-lag effects and compensates for the loss of contemporaneous correlation incurred by asynchronous trading, asymmetric information, and imperfect price formation, which is still missing in the framework of PDV. Therefore, the IRC is not only the multivariate generalization of the PDV estimators but also accommodates a more general framework of price formation dynamics.

Our study has several limitations that provide ample room for future research. First, our simulation study is based on a relatively small number of repetitions due to the computationally intensive estimation of the model. It is therefore important to verify the robustness of our estimator in a more comprehensive simulation framework. Second, the current specification of the price dynamics in our theoretical framework can be further generalized for our estimator to account for any additional feature of the market micro-structure, e.g. asymmetry information, imperfect price formation and lead-lag effect and a more general version of microstructure noise. Finally, the estimator can be useful in various empirical applications, such as volatility forecasting and factor analysis, and is worth pursuing in empirical investigations.

DISJOINT HAWKES POINT PROCESSES ON MULTIVARIATE EXTENSION OF INTRADAY VALUE-AT-RISK

Abstract

We propose a multivariate intraday Value-at-Risk (IVaR) model which generalizes previous univariate intraday Value-at-Risk models. Our multivariate generalization, IIVaR, is based on modelling the occurrence of two-state directional price change events by stochastic conditional intensities and forecasting the paths of future returns by Monte Carlo simulation. The arrival times of future transactions are calculated by the cumulative conditional intensities between two consecutive events, which are predicted by an autoregressive conditional compensator. The performance of the IIVaR is illustrated in an empirical application with selected stocks listed on the Dow Jones Industrial Average index. Back-testing results show that the IIVaR forecasts can accurately capture multivariate market risk, and provide an empirical guide for optimal choice of forecasting interval lengths and sampling price change thresholds.

Keyword: Multivariate intraday value-at-risk, intensity-based risk measure, Hawkes process, back-testing.

5.1 INTRODUCTION

In the high-frequency financial world, trading is characterized by being extremely fast and information has a very short lifespan, living in the time frames of seconds-to-seconds or even only a few milliseconds (Goldstein, Kumar and Graves, 2014; Hasbrouck and Saar, 2013; Menkveld, 2018; O'Hara, 2015). Within these horizons, accurately capturing the entire distribution of asset return becomes impracticable and unfeasible. For example, to achieve a consistent estimate of the second-order moment through realized volatility, a large amount of data is needed, which is impossible in such small time windows (Tse and Yang, 2012). A more efficient and feasible solution is to consider only the tail of the distribution, which characterizes the probability of extreme events, rather than unnecessarily accounting for the whole distribution of all price events. The intuition is that in the time scales where much of the volatility is evoked by the market microstructure noise, the measures of extreme events seem to be more qualified market risk information than zero movements, or back-and-forth bounces of the prices due to the noise.

However, while the literature is full of efforts to develop sophisticated tail risk models, i.e. Value at Risk (VaR), for daily data and longer horizons, the issue of intraday market risk measurement has been less explored. The trading has been going at an extremely fast speed, so risk measures are now obliged to keep pace with the market. With increasingly available high-frequency financial databases and advanced computing power, it is now possible to address the question of how to define practical risk measures for traders or market makers operating on an intraday basis.

Consistent with this intuition, we are motivated to develop a new risk measure, effective on intraday time scales and for multiple assets, taking into account the cross-correlation structure of their extreme returns. Our multivariate intraday risk measure, namely intensity-based intraday value-at-risk (IIVaR), relies on the favorable results of multi-asset price dynamics modelling by the disjoint point process approach in Chapter 3. So far, the IIVaR can be considered as the first multivariate generalization of previous univariate intraday Value-at-Risk (IVaR) models based on the point process approach (see Liu and Tse, 2015 for a review on univariate IVaR). The univariate IVaR measures introduced in high-frequency financial econometrics literature was originally based on the modelling of serial dependence in duration for price change exceeding a threshold, i.e. price duration. We deviate from these discrete price duration measures and model continuous interdependence in the likelihood of occurring directional price change events by stochastic conditional intensities, which is a “multivariate-friendly” point process modelling approach. The cross- and auto-correlation in the tails of multivariate asset returns naturally arises as a result of the self- and cross-excitement mechanism in the conditional intensity formation process.

The econometric modelling of IVaR was first studied in Giot (2005), where the author recognizes the indispensability of the intradaily market risk measure. Reckoning on the importance of the information conveyed by irregularly spaced trading times, he employs a price duration volatility estimator with a log-ACD model (Bauwens and Giot, 2000), from

which the IVaR of the returns is estimated for a fixed time interval. Later, Dionne, Duchesne and Pacurar (2009) propose an IVaR for any arbitrary time interval using tick-by-tick data. The model is based on a log-ACD-ARMA-GARCH model (Engle, 2000) combining with Monte Carlo simulation. The log-ACD model yields the consecutive steps in time, while the ARMA-EGARCH model allows one to simulate the corresponding conditional tick-by-tick returns. The Monte Carlo simulation enables forecasting returns for any arbitrary interval length, and thus avoids complicated time manipulations, for the sake of obtaining results on a convenient regularly spaced framework. In another strand, Coroneo and Veredas (2012), by using a distribution-free approach of quantile regression, also propose an estimate of IVaR for equidistant sampled high-frequency return. Their approach of quantile regression allows one to construct conditional measures for return moments simply depending on explanatory variables and without necessary knowledge about the functional forms of these moments or of the distribution. More recently, Liu and Tse (2015) apply a two-state asymmetric auto-regressive conditional duration model (AACD) (Tay et al., 2011) to model bidirectional price duration events, which are duration events classified into upward and downward directional price movement. The estimated AACD then feeds into a Monte Carlo simulation to forecast ex-ante return distribution, from which IVaR is calculated. The results of the backtest show that the IVaR calculated using a sophisticated bidirectional price duration outperforms previous methods using simply the absolute threshold price duration in Dionne, Duchesne and Pacurar (2009) and Giot (2005).

The theoretical concept underlying the above-mentioned univariate IVaR methods is to look at slices of the conditional distribution of the transaction point process, that is, the transactions that move the price at least a certain level, to derive the risk, without any reliance on global distribution. Specifically, the strategy pursued in these methods is to concentrate on the waiting times for price change transaction events to occur, which is demonstrated to be significantly serial dependent. The IVaR forecasts are then given by the conditional expected duration between price change events, which can be consecutively estimated by the ACD-type models. However, the discreteness of ACD models hinders the extension of these univariate IVaR to a multivariate framework where the cross-effects between assets in an asynchronous transaction context need to be account for. The problem is that the ACD-type model cannot adjust the arrival rate of a new price event when novel information arrives within a duration. It has to wait till the arrival of point process terminates, which causes a loss of cross-correlation information between assets.

Moreover, it is usually not a true reflection of reality to assume that the price movements of two related assets are independent, especially when one considers the probability of their extreme moves, which are often the results of common information (Cousin and Bernardino, 2013; Grothe, Korniiichuk and Manner, 2014). For the univariate case, the marginal probability structure might be sufficient, but when it comes to a portfolio of multiple assets, one would need to take into account the interaction between assets in extreme events. Furthermore, while such contemporaneous correlation can be attributable to fundamental asset values, another type of correlation characterized by high-frequency data, that is, the temporal lead-lag correlation, arises as a consequence of the presence of asynchron-

ous trading, asymmetric information, strategic trading, and imperfect price adjustment in the market microstructure (see [Chapter 3](#)). Therefore, a multivariate IVaR model that reliably incorporates these features into its risk metrics would give a better/more informed measure of IVaR in one asset and in a combined way for an intraday portfolio.

Our proposed multivariate IIVaR deviates from the ACD-based IVaR models by directly modelling stochastic conditional intensity, and allows for an interdependence between assets in the likelihood of extreme price events' occurring. A predominant point process approach for this purpose, in temporal settings, is the Hawkes process (Bacry, Mastromatteo and Muzy, 2015; Bowsher, 2007; Hawkes, 1971; Hawkes and Oakes, 1974). The Hawkes process has also been used to model extreme price movements at a rather low frequency (Bieñ-Barkowska, 2020; Chavez-Demoulin, Davison and McNeil, 2005; Chavez-Demoulin, Embrechts and Sardy, 2014; Embrechts, Liniger and Lin, 2011; Grothe, Korniiichuk and Manner, 2014; Hautsch and Herrera, 2019). In an intra-daily trading context, the pioneer work of Chavez-Demoulin and McGill (2012) extends Chavez-Demoulin, Davison and McNeil (2005)'s Hawkes-Peak Over Threshold ([Hawkes-POT](#)), which models the clustering behaviour of extreme events over a threshold, to intraday risk measures. The Hawkes-POT has the same spirit as the IIVaR, which both focus on the temporal dependence of extreme price events in the tail and ignore the less important structure of moderate price events. However, the Hawkes-POT still exists only in a univariate framework due to the complexity of its structure and the selection of the exceedance threshold (Chavez-Demoulin, Embrechts and Sardy, 2014).

Working in the framework of the Hawkes process, we first partition multi-asset price dynamics into multivariate point processes of price change events. Using a price threshold δ as a filter, we develop a sample scheme to split the transaction-by-transaction data of each asset into bidirectional point processes associated with two states, that is, an over-upper bound ([OUB](#)) and over-lower bound ([OLB](#)). The OUB and OLB events are triggered if the cumulative price change on the upward (downward) equals or exceeds the threshold δ . The conditional intensities of all OUB and OLB transaction processes is then cast into multivariate Hawkes with an exponential decay kernel. The validity of this type of excitement kernel in modelling multi-asset disjoint price change dynamics has been proven in [Chapter 3](#). Contrasting with discrete duration-type models, the multivariate Hawkes conditional intensities update their information set continuously, thus accounting for both temporal self- and cross-asset effects induced by any new event arriving in the price dynamics. However, the conditional intensity provides rather a measure of event-occurrence probability than an indicator of certain transaction arrival. To facilitate future events forecasts, we propose an arrival detection mechanism based on an autoregressive conditional compensator, which estimates expected cumulative conditional intensities to arrive at a new price change event. Then, the Monte Carlo simulation is adopted to simulate the return distribution, from which the IVaR is calculated for any arbitrary intraday time interval.

To access the performance of the IIVaR, we use three well-known backtests: the LR test of Christoffersen (1998) based on a Markov chain model; the duration-based test of

Christoffersen (2004); and the generalized method of moments (GMM) duration-based test proposed by Candelon et al. (2010). We apply the IIVaR to two selected pairs of stocks with high and low trading activities listed on the Dow Jones Industrial Average index. Additionally, to investigate the impact of choosing the price change threshold and the forecast interval on the performance of the IIVaR, we examine different scenarios of sampling thresholds and forecast intervals. The IVaR forecast performance is sensitive to both the selection of the sampling threshold and the forecast intervals, which is different from the previous findings in Liu and Tse (2015). The back-testing results also show that filtered by the 4-ticks threshold, the IIVaR can capture accurately extreme price change dynamics of 30 or 60-minute forecast intervals.

The remainder of this chapter is organized as follows. In the next section 5.2 we summarize the existing univariate IVaR methods in the literature. Section 5.3 presents our proposed multivariate IVaR model consisting of the disjoint Hawkes point process of price dynamics, autoregressive conditional compensator modelling, and the forecast algorithm with the Monte Carlo simulation. Section 5.4 describes three backtesting methods for the evaluation of our IVaR model. In Sections 5.5, we describe the data and report the empirical results. The last section 5.6 concludes and suggests further research.

5.2 REVIEW EXISTING INTRADAY VALUE-AT-RISK MODELS

Value-at-Risk (VaR) model has emerged as a benchmark for the assessment of downside risk between practitioners (see, e.g. Basel Committee on Banking Supervision, 2011, 2021) and has been widely studied in the financial market literature (Basak and Shapiro, 2001; Jorion, 2006). It was implemented to quickly interpret, using a single value, the information about the risk of a portfolio. This value measures the minimal amount of accumulated loss and indicates how the value of the portfolio is likely to decrease over a certain period of time. Statistically, it is defined as the conditional quantile of the asset return distribution for a given shortfall probability ζ (typically chosen to be between 1% and 5%). Denoting $F_{t-1}(r_t)$ as the cumulative distribution function associated with portfolio return r_t during period $[t-1, t)$, the ex-ante VaR forecast with target probability ζ , denoted by $\text{VaR}_t(\zeta)$, is mathematically written as:

$$\text{VaR}_t(\zeta) := \inf\{r_t \in \mathbb{R} : F_{t-1}(r_t) \geq \zeta\} \quad (5.1)$$

and, equivalently:

$$\mathbb{P}r_{t-1}(r_t < -\text{VaR}_t(\zeta)) := \zeta \quad (5.2)$$

Consequently, VaR can be viewed as the boundary of the set $\{r_t \in \mathbb{R} : F_{t-1}(r_t) \geq \zeta\}$ where F_{t-1} denotes the conditional cumulative probability function given the information up to time $t-1$. Note that $\mathbb{P}r_{t-1}$ denotes the conditional probability and the negative sign in Eqn. 5.2 is due to the convention of reporting VaR as a positive number.

In this chapter, our objective is to propose multivariate market risk using the concept of intraday VaR (IVaR), which is an extension of VaR to intraday returns. As mentioned

in the Introduction, unlike the calculation of VaR for daily or longer horizons¹, the issue of intraday market risk measurement has been less explored (see, e.g. Banulescu et al., 2015; Dionne, Duchesne and Pacurar, 2009; Giot, 2005; Liu and Tse, 2015), and the current measures of IVaR are at one’s disposal with only univariate case of a single asset.

The limitation of use is due to some challenges posed by the features embedded in high-frequency returns. First, while it is naturally equidistant observations of return for daily VaR, the IVaR is characterized by using irregularly spaced transaction data. The market microstructure literature suggests that such irregular inter-trade durations are related to the existence of new information on the market and thereby interact with the price dynamics, leading to temporal clustering of the likelihood of extreme events occurring (see, e.g. Admati and Pfleiderer (1988), Diamond and Verrecchia (1987) and Easley and O’hara (1992) amongst others)². Consequently, a reliable measure of IVaR should take into account the mutual dependence between arrival times and extreme events.

In addition to clustering within a time series, the second challenge, which appears in multivariate IVaR, is the tendency of extreme event clusters to occur across assets. The reason for this tendency is not only contemporaneous correlations between assets but also temporal lead-lag correlations. While the former comes from fundamental analysis of true underlying values, the second arises as a consequence of the presence of asynchronous trading, asymmetric information, strategic trading, and imperfect price adjustment in the market microstructure (see Chapter 3), preventing the use of traditional multivariate techniques designed for aggregated low-frequency data.

Now, we will first briefly describe the univariate IVaR models in the literature and discuss the pros and cons of their approach to dealing with the first challenge. Then, our multivariate generalization, the IIVaR model, extending these univariate IVaR and capable of accommodating issues of the second challenge, will be developed in the next section.

5.2.1 The Giot model

Let r_i be the return over the given regular interval $[t_{i-1}, t_i)$ of the same duration. Giot (2005) assumes r_i follows an AR(1)-GARCH(1,1) model, which can be written as:

$$r_i = \mu + \eta r_{i-1} + \epsilon_i, \quad \epsilon_i = z_i \sqrt{h_i} \tag{5.3}$$

where ϵ_i are *iid* with unit variance and h_i is given by the GARCH(1,1) model:

$$h_i = \omega + \alpha z_{i-1}^2 + \beta h_{i-1} \tag{5.4}$$

1 This is motivated by the fact that financial institutions generally produce their market risk at the end of the business day to measure their total risk exposure over the next day. For minimum capital adequacy ratio requirements, banks usually calculate the VaR daily and then rescale it to a 10-day horizon (see, e.g. Basel Committee on Banking Supervision, 2019, 2021)

2 In Easley and O’hara (1992), informed traders only trade if they are endowed with superior price-relevant information. Therefore, in their model, long waiting times between trades are associated with no news and, as a consequence, with low volatility. The opposite relation between duration and volatility is suggested by Admati and Pfleiderer (1988). In their model, frequent trading is provoked by liquidity traders. Therefore, low trading corresponds to a high proportion of informed traders on the market, which can be interpreted as higher volatility

Upon estimating the parameters, the one-step-ahead IVaR at time t_i for period $[t_i, t_{i+1})$ is calculated as follows:

$$\text{IVaR}_{i+1}(\tilde{\zeta}) = -\left(\hat{\mu} + \hat{\eta}r_i + z_{\tilde{\zeta}}\sqrt{\hat{h}_{i+1}}\right) \quad (5.5)$$

where $z_{\tilde{\zeta}}$ is the $\tilde{\zeta}$ -quantile of ϵ_i . Based on the empirical results in Giot (2005)³, the t -GARCH model was found to be the one that has the best performance.

In the Giot method, the returns are first aggregated over a desired horizon to retrieve a regular spacing sample, to which traditional GARCH-type models can be applied. Thus, his approach does not only require finding an optimal aggregating scheme but also inevitably incurs a loss of information, lying in the observations removed and in the time intervals between transactions. Furthermore, speaking of practicality, since the interval is fixed, the GARCH model has to be re-estimated each time a different time interval is desired for the IVaR calculation. If market conditions change during the day, for example, the change in transaction observation frequency, a market practitioner might want to shorten the time horizon of his VaR. With the Giot method, she would need to resample the data on the new horizon and estimate a new model.

5.2.2 The Dionne-Duchesne-Pacurar model

Later, Dionne, Duchesne and Pacurar (2009) proposed a log-ACD-ARMA-GARCH model combining with a Monte Carlo simulation to forecast IVaR for any arbitrary interval length. Their method avoids complicated time manipulations and instead makes use of all tick-by-tick transaction data. In their method, a log-ACD part, originally proposed by Bauwens and Giot (2000), is used to forecast irregular waiting times between consecutive trades and an ARMA-GARCH part, which is also a UHF-GARCH-type model (Engle, 2000), is used to simulate the corresponding conditional distribution of tick-by-tick returns.

Let t_0, t_1, \dots, t_N denote the sequence of times at which the trades occur with the prices p_0, p_1, \dots, p_N , respectively, $x_i = t_i - t_{i-1}$ for $i = 1, 2, \dots, N$ are the duration between two consecutive trades, and $r_i = \log(p_i/p_{i-1})$ is the corresponding continuously compounded return. Denote by $\psi_i = \mathbb{E}(x_i|\mathcal{H}_{i-1})$ the conditional duration, where \mathcal{H}_{i-1} is the information set on the event at time t_{i-1} . The log-ACD model assumes that all temporal dependencies between inter-trade duration are captured by the conditional mean function in the way that the standardized duration $\epsilon_i = x_i/\psi_i$ is independently and identically distributed positive random variable with unit mean.

$$\psi_i = \exp\left\{\omega + \sum_{j=1}^m \alpha_j \epsilon_{i-j} + \sum_{j=1}^q \beta_j \ln \psi_{i-j}\right\} \quad (5.6)$$

The most common distribution choices for the standardized duration ϵ_i are generalized gamma distribution types.

³ Giot (2005) also proposes an IVaR measure based on a log-ACD model for irregularly spaced data. However, this IVaR is then cast onto a regularly time-spaced grid for back-testing purposes, and is not found to perform well.

The return r_i corresponding to the duration x_i is modelled using the ARMA (1,1) specification:

$$r_i = c + \phi_1 r_{i-1} + z_i \sqrt{h_i} + \theta(z_{i-1} \sqrt{h_{i-1}}) \tag{5.7}$$

where the standardized return z_i is an independent and identically distributed standard normal variable. The conditional volatility per transaction is given by h_i , which has the following specification:

$$\ln h_i = \gamma \ln(x_i) + \tilde{\omega} + \sum_{j=1}^P \tilde{\beta}_j (\ln h_{i-j} - \gamma \ln x_{i-j}) + \sum_{j=1}^Q [a_j (|z_{i-j}| + \mathbb{E}(|z_{i-j}|)) + \tilde{\alpha}_j z_{i-j}] \tag{5.8}$$

By assuming x_i to be weakly exogenous to r_i , the parameters of each component, i.e. log-ACD and ARMA-GARCH, are obtained separately by maximizing their log-likelihood functions. Using the estimated parameters, the inter-trade durations are generated using Eqn. 5.6, and the obtained durations are then used to generate the conditional volatility and thus the returns. The duration and the returns are generated iteratively until the accumulated duration reaches the intraday forecasting interval length. The simulation runs are repeated to obtain a distribution of the returns over the forecast period, from which the ζ -quantile of the returns is computed as $\text{IVaR}_{i+1}(\zeta)$.

5.2.3 The Liu-Tse model

Similar to the DDP method, the Liu and Tse (2015) model is also based on simulation to forecast IVaR for any arbitrary interval length. However, instead of considering the inter-trade duration as exogenous to return, the Liu and Tse method investigates the dynamics of price movements and duration jointly using a two-state asymmetric autoregressive conditional duration model (AACD) (Tay et al., 2011). With a predefined threshold δ , the two states are associated with possible price movements of δ ticks up and δ ticks down. Unlike the traditional ACD used in the DDP method that focuses on transaction duration, waiting times between consecutive transactions, the two states AACD focus on price change duration, waiting times such that the magnitude of price change since the previous event first equals or exceeds δ . These two states of price movements each follow a latent stochastic point process with independent exponential distributed inter-arrival times. Then, the observed price movement is the outcome of a competition between the two underlying point processes to be the first arrival.

Denote by $x_i = t_i - t_{i-1}$ the price duration where t_{i-1}, t_i are the occurrence times of the two consecutive price change events $i - 1$ and i -th. These price change events are said to occur if the cumulative price change since the last threshold price change event is at least equal to the threshold δ , regardless of whether it is downward or upward. Let $x_{ji}, j = -1, 1$ be the two latent duration variables associated with the two possible states of downward and upward, respectively, $\psi_{ji} = \mathbb{E}(x_{ji} | \mathcal{H}_{i-1})$ be the conditional price change duration of x_{ji} , and $\epsilon_{ji} = x_{ji} / \psi_{ji}$ be the standardized price change duration. Liu and Tse (2015) propose ψ_{ji} having the following specification:

$$\log\psi_{ji} = \sum_{k=-1,1} [\omega_{jk} + \alpha_{jk}\log x_{i-1}] dN^k(t_{i-1}) + \beta_j \log\psi_{j,i-1} \quad (5.9)$$

where $dN^k(t_{i-1})$ denotes the counting function that counts the last event of type -1 or 1 corresponding to the upward or downward price change, respectively. It takes the value 1 if the last event is of type k and 0 otherwise. The standardized price change duration, ϵ_{1i} and ϵ_{-1i} , are assumed to be independently Weibull distributed with unit mean.

Based on the estimated AACD model, price change events are generated with simulated independent Weibull-standardized duration. Note that while there are two possible states with waiting times x_{1i}, x_{-1i} , respectively, at each ex-ante price change event i th, there is only one state realized. Only the shortest of the two possible latent durations is observed and x_i is the outcome of the function $x_i = \min(x_{1i}, x_{-1i})$. The price change duration is generated iteratively to obtain the simulated return over the forecasting interval length. Repeated simulation runs produce the return distribution over the intraday period, from which the IVaR(ζ) is computed.

5.2.4 Limitations of existing univariate IVaR models for a multivariate extension

The theoretical concept underlying the VaR method is to look at slices of the conditional distribution of returns to derive the market risk, without any reliance on global distribution. Therefore, the strategy pursued in the above univariate IVaR methods is to focus on the waiting times to occur transactions associated with extreme price changes. And the widely adopted model is the ACD-type model. However, as we aforementioned in the introduction, although the ACD-type models are well suited to capture serially dependent properties of the price change duration for single asset in a discrete price duration setting, they are not compatible with a multivariate framework where the cross-effects between assets exist continuously. To be more specific, when new price-relevant information arrives within waiting times, the ACD-type model cannot update instantly but has to wait to adjust the conditional intensity of future event occurrence. Only when the arrival of a point process terminates, the latent conditional intensity of the ACD-type model starts updating the new information arriving in the cross-correlated point process, and this delay causes a potential loss of cross-correlation between assets.

Therefore, the ACD and its extensions cannot capture the cross-asset dependency and thus are inadequate for the multivariate IVaR measure. There is still a need for a model that can take into account the cross-dependence structure, in particular, in the context of intraday data for multiple assets in view of their clustering in extreme returns. In what follows, we will propose a new method to overcome these difficulties.

5.3 MULTIVARIATE INTENSITY-BASED INTRADAY VALUE-AT-RISK MODEL

Following Dionne, Duchesne and Pacurar (2009), and Liu and Tse (2015), we propose an IVaR method also based on a Monte Carlo simulation but for multiple assets. Instead of using duration models, our multivariate generalization, namely IIVaR, directly models

the stochastic conditional intensities of two-state price change transaction point processes. To do so, we continue applying the disjointing price change method that has been used to investigate multi-asset price formation processes and realized covariance in previous chapters. For our objective of forecasting IVaR, we concentrate on the tails of return distributions and, thus, on transaction events that lead to extreme price change. First, using a price threshold as filter, we split each asset’s tick-by-tick transaction data into two point processes associated with two states of price change as follows:

Definition 1. *Given an observed transaction-by-transaction price process of asset d , $X_i^d, 0 = t_0^d < t_1^d < \dots < t_i^d < \dots < T, i = 0, 1, \dots, N^d(T)$, and a price change threshold δ , an over-upper bound price transaction event (OUB), $\{t_i^{d+}\}_{i=0,1,\dots,N^d(T)}$, is triggered if the cumulative upward price change equals or greater than δ . And vice versa, an over-lower bound price transaction (OLB), $\{t_i^{d-}\}_{i=0,1,\dots,N^d(T)}$, is triggered if the cumulative downward price change exceeds δ . Thus, the two-state price change point processes for each asset d can be constructed as follows:*

1. Set a new event at $i = 0 : t_0^{d+} = 0, X_0^{d+} = X_0^d$ for the OUB point process and $t_0^{d-} = 0, X_0^{d-} = X_0^d$ for the OLB point process.
2. For $j = 1, 2, \dots, N^d(T)$, if $X_j^d - X_i^{d+} \geq \delta$, if $t_{i+1}^{d+} = t_j^d, X_{i+1}^{d+} = X_j^d$, we set a new event in the OUB point process. Else if $X_j^d - X_i^{d+} \leq 0$, we update a new dip to the price, i.e. $X_i^{d+} = X_j^d$ and remain the entry time t_i^{d+} unchanged. Otherwise, both the time and the price remain unchanged.

Vice versa, for the OLB point process, we also set a new event $t_{i+1}^{d-} = t_j^d, X_{i+1}^{d-} = X_j^d$ if $X_j^d - X_i^{d-} \leq -\delta$. Else if $X_j^d - X_i^{d-} \geq 0$ a new peak is updated to the price $X_i^{d-} = X_j^d$ but the entry time, t_i^{d-} , is still remaining. Otherwise, there is no update on the OLB point process.

Iterate until the sample is depleted.

We note that in the OUB and LOB point processes, $\Delta X_i^{d+} \geq X^d(t_i^{d+}) - X^d(t_{i-1}^{d+})$ and $\Delta X_i^{d-} \leq X^d(t_i^{d-}) - X^d(t_{i-1}^{d-})$. In our sampling scheme, we take into account directional price movements that are not only from the entry to the exit events, but also from a point in between and the exit event, i.e. the steps “Else if”. This is different from previous sampling schemes in the literature (see, e.g. Banulescu et al., 2015; Liu and Tse, 2015) that consider only price movements starting from the entry point. Our scheme is more extensive and entails the previous ones, avoiding dropping significant price movements in between. In what follows, we continue applying multivariate Hawkes point processes to models explicitly the vector of conditional intensities of two states, OUB and LOB, price change point processes for multiple assets.

5.3.1 Disjointing Hawkes point processes of price dynamics

We denote $(X^1, \dots, X^d, \dots)^T$ for $1 \leq d \leq D$ as a vector of transaction price realizations for D assets. For each asset, we obtain two-state disjoint point processes, OLB and OUB, associated with two states of price change $(X^{d+}, X^{d-})^T$, using the algorithm in Definition

1. We compose a new vector by concatenating all marginal bivariate vectors of the OLB and OUB processes and denote it as (X^1, \dots, X^k, \dots) for $1 \leq k \leq K$ with $K = 2 \times D$, that is, $X^1 \equiv X^{1+}, X^2 \equiv X^{1-}, \dots, X^{K-1} \equiv X^{D+}, X^K \equiv X^{D-}$. Then we denote by $t_1^k, \dots, t_{i-1}^k, t_i^k$ the sequence of clock times at which a transaction associated with the price change state k -th occurs and by $N^k(t)$ and $\lambda^k(t)$ the conditional counting and conditional intensity functions associated with the state k -th at time t . Note that if we let $t_j, \dots, t_{j-1}, t_j^4$ denote a pooled process of all K states, then its counting function is $N(t) = \sum_{k=1}^K N^k(t)$. Following multivariate Hawkes point processes, we model the conditional intensity $\lambda^k(t)$, measuring the instantaneous quantity of event arrival of the state k -th point process conditional on its information set \mathcal{H}_t , as a linear combination of past jumps of all K price change states of D assets:

$$\lambda^k(t) = \mu^k + \sum_{l=1}^K \int_{-\infty}^t \phi^{kl}(t-s) dN^l(s) \quad (5.10)$$

where $\{\mu^k\}_{k \in [1, K]}$ is a vector of exogenous intensities and $\{\phi^{kl}(t)\}_{k, l \in [1, K]}$ is a matrix-valued decay kernel.

Unlike duration models (e.g. ACD and its extension), this formulation, namely Hawkes point processes, parameterizes the conditional intensities as a measurable function conditional on a multivariate information set and thus allows for the interdependence between all point processes. The information set \mathcal{H}_t is common for all conditional intensities $\lambda^k(t), k \in [1, K]$ and accounts for any continuous change in the multi-asset price dynamics.

5.3.2 The compensator of counting function.

The disjointing point processes provide an efficient way to describe multi-asset price dynamics through the interdependence of their price change states. The most fundamental application of the model is to measure and forecast future transaction arrivals associated with those states. However, because the modelling involves solely conditional intensities, it provides rather the likelihood of a price change event's occurring than the indicator of a certain arrival. The model is short of a variable that exactly indicates the arrival time of new events in the disjoint processes. A natural candidate is the compensator of the counting function. By its definition, the conditional intensity measures the conditional expected instantaneous quantity of event arrival. Under the submartingale assumption of the counting process, the expected number of events can be well represented by the so-called compensator, which is the cumulative conditional intensity over an interval ⁵:

Definition 2. *Given a \mathcal{H}_t -submartingale point process $N^k(t)$ with $\mathbb{E}[N^k(t)] < \infty$, there is a unique \mathcal{H}_t predictable cumulative process $\Lambda^k(t) = \int_0^t \lambda^k(u) du$ called the compensator with the property:*

$$\mathbb{E}[N^k(t) | \mathcal{H}_s] = \mathbb{E}[\Lambda^k(t) | \mathcal{H}_s] = \mathbb{E}\left[\int_0^t \lambda^k(u) du | \mathcal{H}_s\right], \text{ almost surely.} \quad (5.11)$$

⁴ j denotes the index of the pooled point process while i denotes the index of the marginal price change state process

⁵ See, e.g. Daley and Vere-Jones (2006), Theorem A3.4.III; Hautsch (2012), Section 4.1.2

Thus, the expected number of events in the interval $(s, t]$, given \mathcal{H}_s , is computed as the conditional expectation of the so-called integrated intensity function defined as:

$$\mathbb{E}[N^k(t) - N^k(s) | \mathcal{H}_s] = \mathbb{E}\left[\int_s^t \lambda^k(u) du | \mathcal{H}_s\right] := \mathbb{E}[\Lambda^k(s, t) | \mathcal{H}_s], \text{ almost surely.} \quad (5.12)$$

The forecasting of a new event arrival based on the compensator is similar to simulating a new point process (see, e.g. Hautsch (2012) Section 4.1.7). Substituting estimated conditional intensities with the corresponding parameters obtained from the calibrated model yields a conditional compensator of the point process k over the interval $(s, t]$, $\hat{\Lambda}^k(s, t)$. The next price change event is predicted to occur in the point process k at time t if $\hat{\Lambda}^k(s, t)$ is greater than a given level. Once a new event is predicted to arrive, the conditional (integrated) intensities are updated immediately, taking into account the self- and cross-exciting impacts incurred by the arrival of that event.

To determine the level of $\Lambda^k(t)$ to have a new event, one way is to exploit the fact that $\Lambda^k(t_{i-1}^k, t_i^k) \sim \text{i.i.d. Exp}(1)$ due to random time change argument (see, in particular, Hautsch (2012) Theorem 4.5). However, this way ignores the temporal dependence in the occurrence of price change events induced by intraday periodicity. In the empirical application, we document that the two states of price duration processes exhibit a strong periodicity during the same day (see Figure 5.1). This pattern must be taken into account to avoid distortions in the results. One traditional way is to remove the periodicity from the transaction duration data prior to fitting the model. However, either increasing or decreasing the inter-trade duration will change the self- and cross-exciting between events (see Eqn. 5.10) and thus distort the interdependence between assets. Another solution is to adjust the periodicity on the estimated compensator without touching the original data. Thereby, in the next section we propose a statistical model for the estimated compensator time series given by the calibrated conditional intensities. The model is specified to take into account the temporal dependence of the occurrence over time and can explicitly forecast the future compensator.

5.3.3 The autoregressive conditional compensator - ACC model.

Because the compensator is closely linked to the duration between price change events by its definition, the most convenient way is to model the compensator with the same formulation to the duration. Denote by $\Lambda_i^k = \Lambda^k(t_i^k) - \Lambda^k(t_{i-1}^k)$ the compensator between two consecutive price change events associated with the marginal state k -th, and by ψ^k the conditional expectation of the compensator Λ_i^k such that $\psi_i^k = \mathbb{E}(\Lambda_i^k | \mathcal{H}_{i-1}^k)$. Let $\epsilon_i^k = \Lambda_i^k / \psi_i^k$ be the standardized compensator that is an independently standard exponential distributed variable. Our basic model for the compensator is as follows:

$$\Lambda_i^k = \psi_i^k \epsilon_i^k \quad (5.13)$$

$$\psi_i^k = \omega + \tilde{\alpha} \Lambda_{i-1}^k + \tilde{\beta} \psi_{i-1}^k \quad (5.14)$$

Because the filtration of Λ_i^k , \mathcal{H}_{i-1}^k only includes information on the marginal compensator process k -th to t_{i-1}^k , that is, the previous marginal compensator Λ_{i-1}^k and the lagged expected marginal compensator ψ_{i-1}^k , it is independent of the filtration of other marginal processes. Thus, the iterative forecast on the compensator for each future transaction i -th can be calculated independently and directly using Eqn. 5.13 and Eqn. 5.14. We recall that the interdependence between price change processes is captured by the dynamics of conditional intensities, from which the marginal compensator is composed.

5.3.4 Evaluation of IVaR by Monte Carlo simulation

We now describe the Monte Carlo simulation procedure for computing the IVaR based on calibrated Hawkes point processes and the estimated ACC model. Suppose that we want to estimate the IVaR of the ex-ante period $(T_1, T_2]$ given the ex-post sample period $[0, T_1]$, $T_1 < T_2$. We begin by estimating the matrix-valued parameters for K -price change point processes, $\hat{\mu}, \hat{\phi}$ based on the historical data up to T_1 and calculate the corresponding historical conditional intensities and compensator. Using the information of the calibrated historical compensator in the period $[0, T_1]$, we forecast the values of $\{\hat{\Lambda}_i^k\}_{1 \leq k \leq K}$. From the compensator forecasts, we can calculate future transaction arrival times t_i^k , $T_1 \leq t_i^k \leq T_2$. The simulation algorithm is as follows:

1. Simulate K (independent) sequences $\epsilon_1^k, \dots, \epsilon_n^k, \dots$, $1 \leq k \leq K$, of standard i.i.d. exponential random variables.
2. For $1 \leq k \leq K$, setting t_0^k as the last transaction time in the process k -th prior to T_1 , we calculate the initial values for ψ_0^k, Λ_0^k . Then using the simulated sequences of innovations ϵ_i^k , we iteratively calculate the compensator forecast of each future transaction $\hat{\Lambda}_i^k$.
3. Set $T_1 = 0$. If $W_1^k = \Lambda^k(0, t_1^k) = \int_0^{t_1^k} \lambda^k(u) du = \hat{\Lambda}_1^k - \Lambda^k(t_0^k, 0)$ with $W_{(\cdot)}^k$ denotes the integrated conditional intensity between two consecutive transactions of the pooled point process, we can express as $t_1^k = \Lambda^k(0, W_1^k)^{-1}$ with $\Lambda^k(\cdot)^{-1}$ denoting the inverse function of Λ^k depending only on $\hat{\Lambda}_1^k$ and T_1 .
4. Set a new point in the pooled process that occurs at $t_1 = \min\{t_1^1, \dots, t_1^k, \dots\}$ and its price change state index $\iota_1 = \operatorname{argmin}_k\{t_1^1, \dots, t_1^k, \dots\}$ for $1 \leq k \leq K$.
5. For all $1 \leq k \leq K, k \neq \iota_1$, we compute $\Lambda^k(0, t_1)$. Then, let $\Lambda^k(0, t_2^k) = \Lambda^k(0, t_1) + \Lambda^k(t_1, t_2^k)$. Because there is no transaction before t_1 in the marginal process k -th, we can write $\Lambda^k(0, t_2^k) = \hat{\Lambda}_1^k$ and $\Lambda^k(t_1, t_2^k) = \hat{\Lambda}_1^k - \Lambda^k(0, t_1) = W_2^k$. Therefore, we can compute $t_2^k = \Lambda^k(t_1, W_2^k)^{-1}$.
For $k = \iota_1$: Because there is a transaction at t_1 of the marginal process k -th, we can express $\Lambda^k(t_1, t_2^k) = \hat{\Lambda}_2^k$ and compute $t_2^k = \Lambda^k(t_1, \hat{\Lambda}_2^k)^{-1}$.
6. Set a new point in the pooled process that occurs at $t_2 = \min\{t_2^1, \dots, t_2^k, \dots\}$ and its price change state index $\iota_2 = \operatorname{argmin}_k\{t_2^1, \dots, t_2^k, \dots\}$ for $1 \leq k \leq K$.

7. Continue this procedure until the first event t_j such that $t_j \geq T_2$, at which a simulation of multivariate price change states point processes over the interval $(T_1, T_2]$ is obtained.

This simulation algorithm is repeated to obtain a distribution of returns over the interval $(T_1, T_2]$, from which the ξ -quantile of the return over the forecasting interval is computed as $\text{IVaR}(\xi)$.

5.4 BACK-TESTING IVAR

The standard assessment method of IVaR consists of back-testing or reality check procedures. As defined by Jorion (2006), backtesting is a formal statistical framework that verifies if the actual trading losses are in line with projected losses. This involves a systematic comparison of the history of IVaR forecasts generated by the model with the actual returns. The assessment is generally based on the concept of violation (also called Hit) (Candelon et al., 2010). An violation is said to occur if the ex-post realization of the portfolio returns is more negative than the IVaR forecast. Following the literature, we consider three well-known tests on violation realizations to assess the performance of our multivariate IVaR forecasts: unconditional coverage test by Kupiec (1995), correlated hit sequence test by Engle and Manganelli (2004), and random violation test by Candelon et al. (2010).

5.4.1 Unconditional coverage test

The test proposed by Kupiec (1995) considers exclusively the property of unconditional coverage. Under the unconditional coverage hypothesis, the expected frequency of observed IVaR violation is precisely equal to the coverage rate ξ . If the unconditional probability of violation is significantly higher than ξ , it means that the IVaR model understates the actual risk level of the portfolio. The opposite finding of too few IVaR violations would alternatively signal an overly conservative IVaR measure. Suppose that there are D -multivariate sequences of $\text{IVaR}_t^d, 1 \leq d \leq D, t \in [1, T]$ corresponding to D assets and T denoting the number of forecast intervals. The sequence of violations $I_t^d(\xi)$ for each asset with a target coverage probability ξ is defined as follows:

$$I_t^d(\xi) = \begin{cases} 1, & \text{if } r_t^d < -\text{IVaR}_t^d(\xi) \\ 0, & \text{otherwise.} \end{cases} \tag{5.15}$$

The probability of observing IVaR failures regardless of order in a sample of T forecasting intervals for asset d is:

$$\hat{\xi} = \frac{1}{T} I^d(\xi) = \frac{1}{T} \sum_{t=1}^T I_t^d(\xi) \tag{5.16}$$

Under the null hypothesis $H_0, \hat{\xi} = \xi$. To test that the underlying potential failure estimates are consistent with the null hypothesis, Kupiec (1995) proposes using the likelihood ratio

(LR) test procedure. Specifically, given a realization size T for $\hat{\zeta}$, the LR statistic at target probability ζ is as follows:

$$LR_T^d(\zeta) = 2[\log[(1 - \hat{\zeta})^{T-I^d(\hat{\zeta})} \hat{\zeta}^{I^d(\hat{\zeta})}] - \log[(1 - \zeta)^{T-I^d(\zeta)} \zeta^{I^d(\zeta)}]] \quad (5.17)$$

Under the null hypothesis, which means that the estimated IVaR achieves the target probability ζ , $LR_T^d(\zeta)$ has a chi-square distribution with 1 degree of freedom χ_1^2 .

5.4.2 Dynamic quantile test

The unconditional coverage is a very useful and straightforward test to evaluate whether the IVaR model reflects, overestimates, or underestimates the true level of risk. However, unconditional coverage cannot shed light on the possible dependence of IVaR violations. The serial correlation of violations in a marginal IVaR sequence and the cross-correlation of violations between assets can lead to the clustering of failures even if the IVaR model can reflect the true level of risk. IVaR violations at different dates or different assets must be distributed independently regardless of the coverage rate considered. Following Engle and Manganelli (2004), we use a linear regression model of current violations on a set of explanatory variables to test if the violations are serial or cross-correlated. Additionally, we consider tests for the cross-correlation of IVaR violations between assets by including the violation variables of other assets in the regression of Engle and Manganelli (2004). Let $\text{Hit}_t(\zeta) = I_t(\zeta) - \zeta$ be the de-meaned sequence of $I_t(\zeta)$. We consider a regression as follows:

$$\text{Hit}_t^d(\zeta) = a^d + \gamma^d \text{IVaR}_t(\zeta) + \sum_{r=1}^D b^{dr} \text{Hit}_t^r(\zeta) + \sum_{q=1}^Q b_q^d \text{Hit}_{t-q}^d(\zeta) + \epsilon_t \quad (5.18)$$

We test the following two null hypotheses for asset d : $a^d = \gamma^d = b^{d1} = \dots b^{dr} = \dots b_1^d = \dots = b_q^d = 0$. Under the null, the accompanying Wald statistic, denoted by $DQ_T^d(\zeta)$ is asymptotically chi-square distributed with $Q + D + 2$ degree of freedom, χ_{Q+D+2}^2 .

5.4.3 Duration-based GMM

Another method considered in the backtesting literature (see, e.g. Candelon et al., 2010; Christoffersen, 2004) uses the statistical properties of the duration between two consecutive hits in examining whether the IVaR violations occur randomly. The baseline idea is that if the IVaR correctly predicts the true level of coverage α , the duration between two consecutive hits associated with ζ must be geometrically distributed. Denote τ_i^d as the number of intervals between the violations $(i - 1)$ th and i th of the asset d with $i = 1, \dots, I^d(\zeta)$. The GMM test proposed by Candelon et al. (2010), denoted by G , is given by:

$$G = \left(\frac{1}{\sqrt{I^d(\zeta)}} \sum_{i=1}^{I^d(\zeta)} \Xi(\tau_i^d; \zeta) \right) \left(\frac{1}{\sqrt{I^d(\zeta)}} \sum_{i=1}^{I^d(\zeta)} \Xi(\tau_i^d; \zeta) \right)^\top \quad (5.19)$$

where $\Xi(d_i, \xi)$ denotes a $v \times 1$ vector whose components are orthonormal polynomials associated with the geometric distribution. Under the null hypothesis that the violations are randomly distributed, G must be asymptotically distributed as χ_v^2 .

5.5 EMPIRICAL APPLICATION

5.5.1 Data description

Table 5.1: Descriptive statistics for four selected stocks listed on the DJIA index.

Indicators	Group I		Group II	
	AAPL	MSFT	AXP	TRV
<i>Panel A: Trades</i>				
Average No. Trade	70886	58537	12231	6779
Max No. Trade	100837	80278	15865	8391
Min No. Trade	51490	47578	9437	5070
Nonzero Trade	31477	19653	5195	3842
Nonzero Percentage	44.20	33.56	42.69	56.89
Positive Extreme Trade	19	2	21	142
Positive Extreme Percentage	0.03	0.00	0.18	2.24
Negative Extreme Trade	19	2	20	149
Negative Extreme Percentage	0.02	0.00	0.19	2.16
Price Avg	174.01	109.61	107.45	129.88
<i>Panel B: Price Changes</i>				
Price Change Avg	7E-06	6E-06	3E-05	4E-05
Price Change SD	0.009	0.007	0.011	0.019
Price Change Skewness	18.486	11.613	9.647	4.485
Price Change Kurtosis	7108.059	4363.876	1892.687	715.584
<i>Panel C: Duration</i>				
Trade Duration Avg	0.317	0.376	1.802	3.236
Trade Duration SD	0.510	0.618	3.135	5.485
Trade Duration Skewness	3.106	3.124	3.280	3.110
Trade Duration Kurtosis	14.929	15.123	17.142	14.395

Notes: For each asset, we show the average statistics per day for some indicators such as number of trades; number of non-zero trades that move stock price; number of positive and negative extreme trades that move stock price more than 3 ticks; price average; and the average trade duration between consecutive observations.

Our dataset used in this empirical application, similar to the one in § 3.4 of the previous Chapter 3, is extracted and compiled from the Trade and Quote (TAQ) database and contains the high-frequency transaction data of four stocks listed on the Dow Jones Industrial Average (DJIA) index: Apple (ticker symbol AAPL) and Microsoft Corporation (ticker symbol MSFT); American Express (AXP) and The Traveler (TRV). The first pair of the selected stocks, namely Group I, including AAPL and MSFT belongs to the technology sector and also represents the stocks with the highest trading activities in the DJIA. Meanwhile, the second pair of the selected stocks, namely Group II, including AXP and TRC, is from the

financial services sector and represents the stocks with the lowest trading activity in the DJIA. The data used are in the period from 01 February 2019 to 15 March 2019, a total of 42 business days. The timestamp precision is in milliseconds. Prior to use, we perform data cleaning procedures of Barndorff-Nielsen et al. (2011) as in the previous chapter. The average of key statistics related to the trading activities of four selected stocks over all trading days is summarized in Table 5.1.

Amongst the four stocks, the AAPL are the most active trading stocks with the highest number of trades per day. Following AAPL, the other stock in the technology sector, MSFT, also has very high trading activities. These two stocks are considered high-liquidity stocks in our empirical study. In contrast, the two stocks of the financial services sector have the lowest number of trades per day and are considered low-liquidity stocks. On average, the trade duration is 0.317 seconds for AAPL, 0.376 seconds for MSFT, 1.802 seconds for AXP, and 3.235 for TRV. Nonzero trades that move stock prices occurred with a frequency of 30% to 50%, while extreme trades that move prices greater than 3 ticks occurred with very minor frequencies of less than 0.5%, except for TRV with a frequency of 4.4%. All the trade returns series display kurtosis and skewness much higher than normal distribution, especially the kurtosis. The leptokurticity arises as a consequence of the mass distribution mostly concentrated around zero ticks.

We then construct two-state price change point processes, OUB and OLB, from the transaction price data according to Definition 1. We let the price change thresholds take three values: 2 ticks, 3 ticks, and 4 ticks. We note that these values include the choice of threshold recommended by Hong et al. (2021), which is three times a measure of the average bid/ask spread. Detailed statistics on the OUB and OLB are reported in Table 5.2.

For all stocks, the average price duration is longer than the trade duration and increases with the price change threshold δ . The larger the price change, the more time it takes to move the price by this amount. The price changes associated with the OUB and OLB point processes display much lower kurtosis and skewness than the price changes from the transaction data. But these kurtosis and skewness do not decrease with increasing price change threshold δ . The mass distribution of the price change events seems to concentrate at 3 ticks, as this price change threshold displays the highest kurtosis and the lowest standard deviation.

We also present an example of the OUB and OLB price duration processes in Figure 5.1. The figure shows that there is a clear diurnal pattern in the two-state price duration processes, as documented in Engle and Russell (1998) for an absolute price duration process. Virtually, market activity (respectively, duration of price change) is higher (respectively, shorter) at the opening and lower (respectively, longer) at the closing of the trading day.

5.5.2 Empirical results

5.5.2.1 Out-of-sample IVaR forecasts

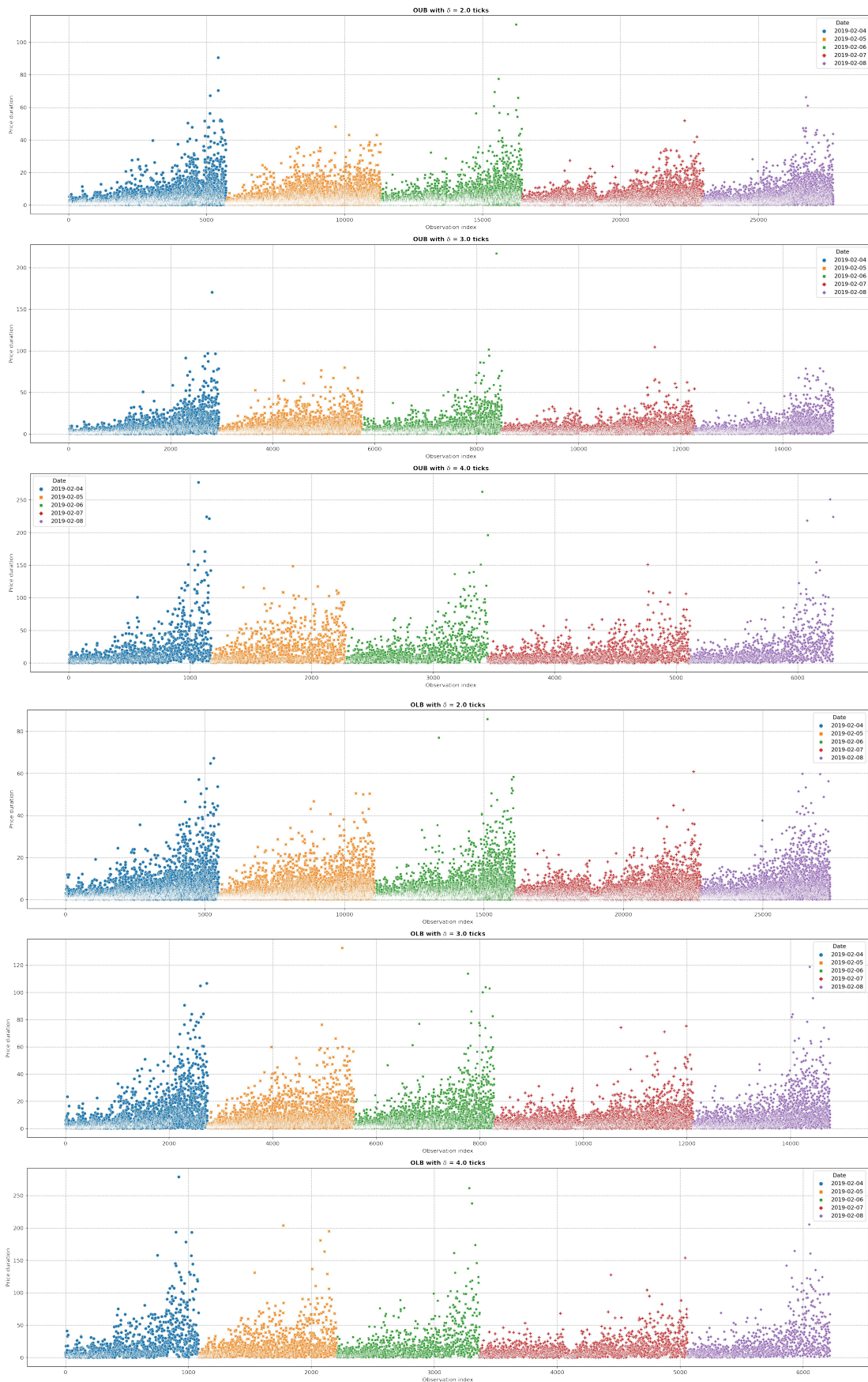
We calibrate the parameters of the conditional intensity functions and the ACC model using the OUB and OLB constructed from transaction data for one trading day (estima-

Table 5.2: Descriptive statistics for OUB and OLB point processes

Indicators	Group I				Group II			
	AAPL		MSFT		AXP		TRV	
	OUB	OLB	OUB	OLB	OUB	OLB	OUB	OLB
<i>δ = 2 ticks</i>								
Average No. of Events	3704	3675	1129	1135	597	598	848	842
Max No. of Events	5633	5617	1307	1372	667	702	773	756
Min No. of Events	3635	3495	1218	1152	740	716	836	838
Price Change Avg (ticks)	2.353	-2.354	2.599	-2.593	2.779	-2.784	3.056	-3.054
Price Change SD	0.522	0.526	0.497	0.497	0.644	0.652	1.134	1.134
Price Change Skewness	1.542	-1.678	0.015	-0.055	1.007	-1.062	2.040	-1.971
Price Change Kurtosis	6.432	9.502	-0.037	0.080	4.333	4.357	8.409	6.735
Price Duration Avg	6.387	6.426	20.224	20.174	37.626	37.614	26.302	26.561
Price Duration SD	7.927	8.303	25.128	24.904	42.512	43.893	28.921	29.336
Price Duration Skewness	3.046	3.197	3.268	2.971	2.637	2.693	2.400	2.501
Price Duration Kurtosis	15.590	16.272	17.738	14.222	10.613	11.081	8.861	10.281
<i>δ = 3 ticks</i>								
Average No. of Events	2093	2076	828	823	460	459	634	627
Max No. of Events	3177	3175	933	986	536	556	660	629
Min No. of Events	2027	1921	842	782	553	526	603	599
Price Change Avg (ticks)	3.127	-3.128	3.088	-3.088	3.221	-3.229	3.638	-3.647
Price Change SD	0.358	0.363	0.284	0.287	0.506	0.521	1.039	1.042
Price Change Skewness	3.701	-3.947	3.678	-3.766	2.897	-3.014	2.572	-2.469
Price Change Kurtosis	24.749	31.984	17.930	18.728	11.144	12.652	10.912	9.098
Price Duration Avg	11.261	11.330	27.763	27.947	49.154	49.195	35.305	35.745
Price Duration SD	13.180	14.074	33.485	33.362	54.455	57.455	39.646	39.496
Price Duration Skewness	2.866	3.036	3.105	2.816	2.500	2.719	2.729	2.640
Price Duration Kurtosis	14.272	14.323	15.590	12.170	9.044	11.200	12.471	11.933
<i>δ = 4 ticks</i>								
Average No. of Events	916	904	407	406	236	233	331	326
Max No. of Events	1318	1351	441	481	273	280	406	399
Min No. of Events	871	779	417	372	277	269	309	308
Price Change Avg (ticks)	4.690	-4.701	4.373	-4.367	4.524	-4.542	5.085	-5.103
Price Change SD	0.540	0.546	0.486	0.487	0.638	0.656	1.070	1.062
Price Change Skewness	0.549	-0.690	0.850	-0.916	1.256	-1.323	1.949	-1.778
Price Change Kurtosis	4.701	7.096	0.146	0.584	2.901	3.028	8.507	6.109
Price Duration Avg	25.594	25.961	56.639	57.002	96.134	97.287	68.677	69.735
Price Duration SD	29.506	32.104	67.718	66.828	104.893	111.954	79.951	79.629
Price Duration Skewness	2.782	3.071	2.987	2.784	2.460	2.525	2.744	2.588
Price Duration Kurtosis	12.072	15.009	14.214	12.848	8.613	8.988	11.486	9.911

Notes: For each price change threshold, we show the average statistics over all trading days for some indicators such as number of events; highest and lowest number of events per day; average price change and average price duration between consecutive events.

Figure 5.1: Price change duration processes over a trading week



Notes: The sample is extracted from the dataset of AAPL from 04/02/2019 to 08/02/2019, consisting of a trading week. The three upper panels are OUB price change processes and the three lower panels are OLB price changes processes, corresponding to 2, 3, and 4 ticks thresholds.

tion period) with price change thresholds of 2 ticks, 3 ticks, and 4 ticks. The calibrated parameters are used to simulate one-step-ahead price movements within next intervals of 5 minutes, 15 minutes, 30 minutes, and 1 hour. All the irregular simulated returns are summed up to give final returns over the fixed-time intervals. The simulation is run with 500 independent repetitions to simulate a full distribution of returns, from which the IVaR is extracted. After completing the IVaR forecast for an interval, we move the estimation period by including one interval forward and excluding the first interval, keeping the length of the estimation period to one day, and proceed with the next interval IVaR forecasting.

Table 5.3 displays the probability of observing failures of the IVaR out-of-sample forecast for two selected pairs of stocks. The results are reported for three levels of risk: 5%, 2.5% and 1% and for all selected intervals and sampling thresholds. The details of each case are illustrated in Figures 5.2 to 5.5. Entries in boldfaces denote the frequency of violation that is within 0.5% deviation from the nominal risk values.

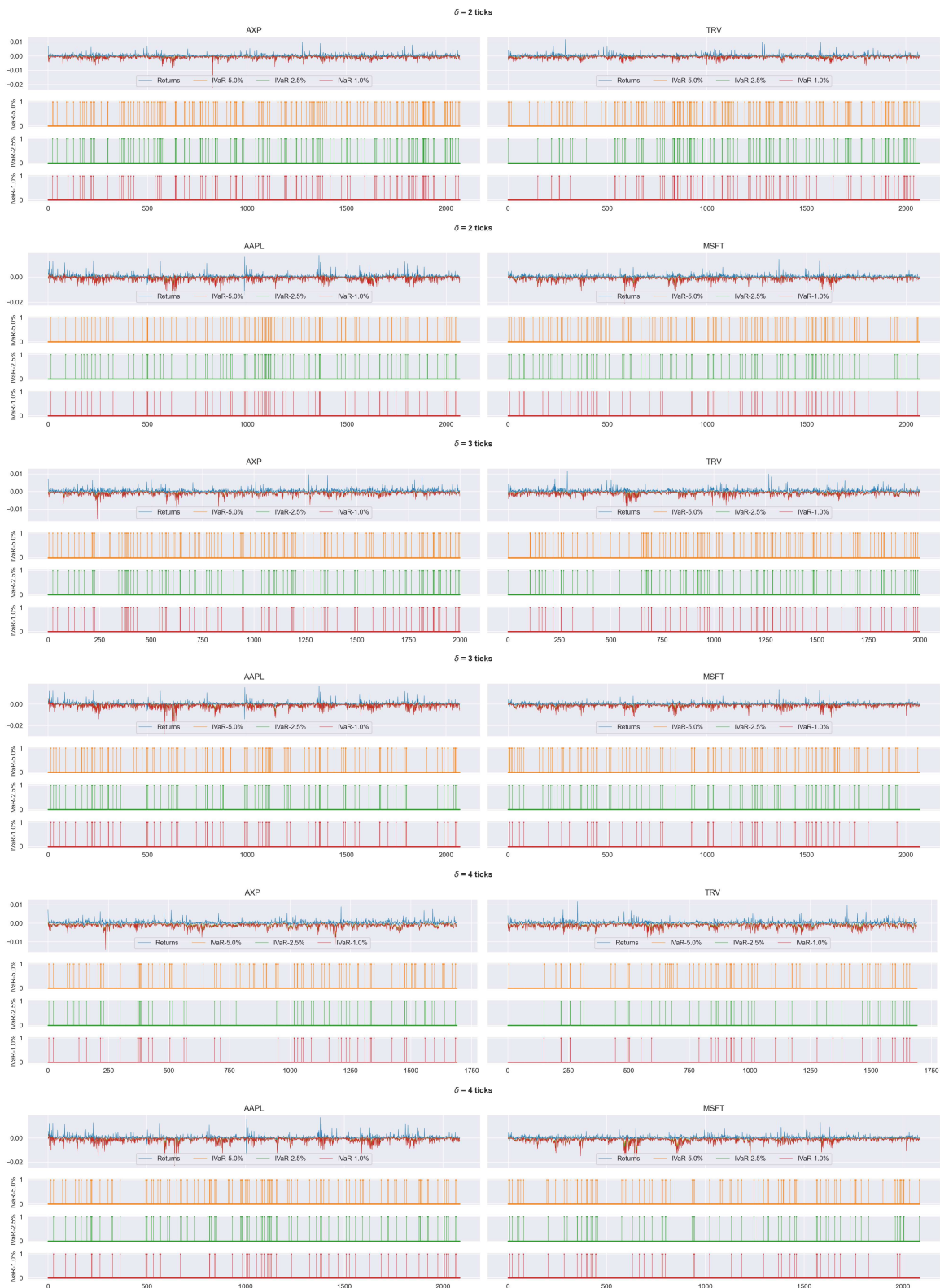
Table 5.3: Probability of observing IVaR failures for two selected pairs of stocks

IVaR level	5-min			15-min			30-min			60-min			
	5,0%	2,5%	1,0%	5,0%	2,5%	1,0%	5,0%	2,5%	1,0%	5,0%	2,5%	1,0%	
Low liquidity pair	Threshold: 2 ticks												
	AXP	0.079	0.061	0.046	0.067	0.046	0.026	0.073	0.052	0.038	0.076	0.047	0.035
	TRV	0.075	0.057	0.039	0.057	0.048	0.032	0.050	0.026	0.020	0.065	0.047	0.035
	Threshold: 3 ticks												
	AXP	0.066	0.051	0.038	0.064	0.046	0.024	0.060	0.039	0.027	0.073	0.061	0.042
	TRV	0.066	0.049	0.032	0.054	0.039	0.025	0.030	0.021	0.015	0.055	0.042	0.030
	Threshold: 4 ticks												
	AXP	0.052	0.034	0.025	0.044	0.032	0.025	0.032	0.025	0.011	0.057	0.050	0.043
	TRV	0.044	0.029	0.022	0.030	0.021	0.018	0.025	0.018	0.018	0.050	0.043	0.028
	High liquidity pair	Threshold: 2 ticks											
AAPL		0.051	0.042	0.029	0.045	0.032	0.027	0.052	0.034	0.023	0.040	0.023	0.023
MSFT		0.065	0.044	0.030	0.050	0.034	0.023	0.055	0.037	0.020	0.046	0.017	0.017
Threshold: 3 ticks													
AAPL		0.055	0.041	0.031	0.055	0.039	0.023	0.049	0.032	0.017	0.040	0.023	0.011
MSFT		0.055	0.041	0.027	0.050	0.039	0.026	0.052	0.037	0.023	0.040	0.029	0.017
Threshold: 4 ticks													
AAPL		0.051	0.041	0.028	0.049	0.040	0.027	0.052	0.043	0.029	0.029	0.023	0.011
MSFT		0.041	0.028	0.019	0.040	0.029	0.019	0.049	0.040	0.026	0.034	0.017	0.011

Notes: The figures are the unconditional probability of observing failures of IVaR out-of-sample forecast. Entries in bold-faces denote the frequency of violation within 0.5% deviation from the nominal risk values.

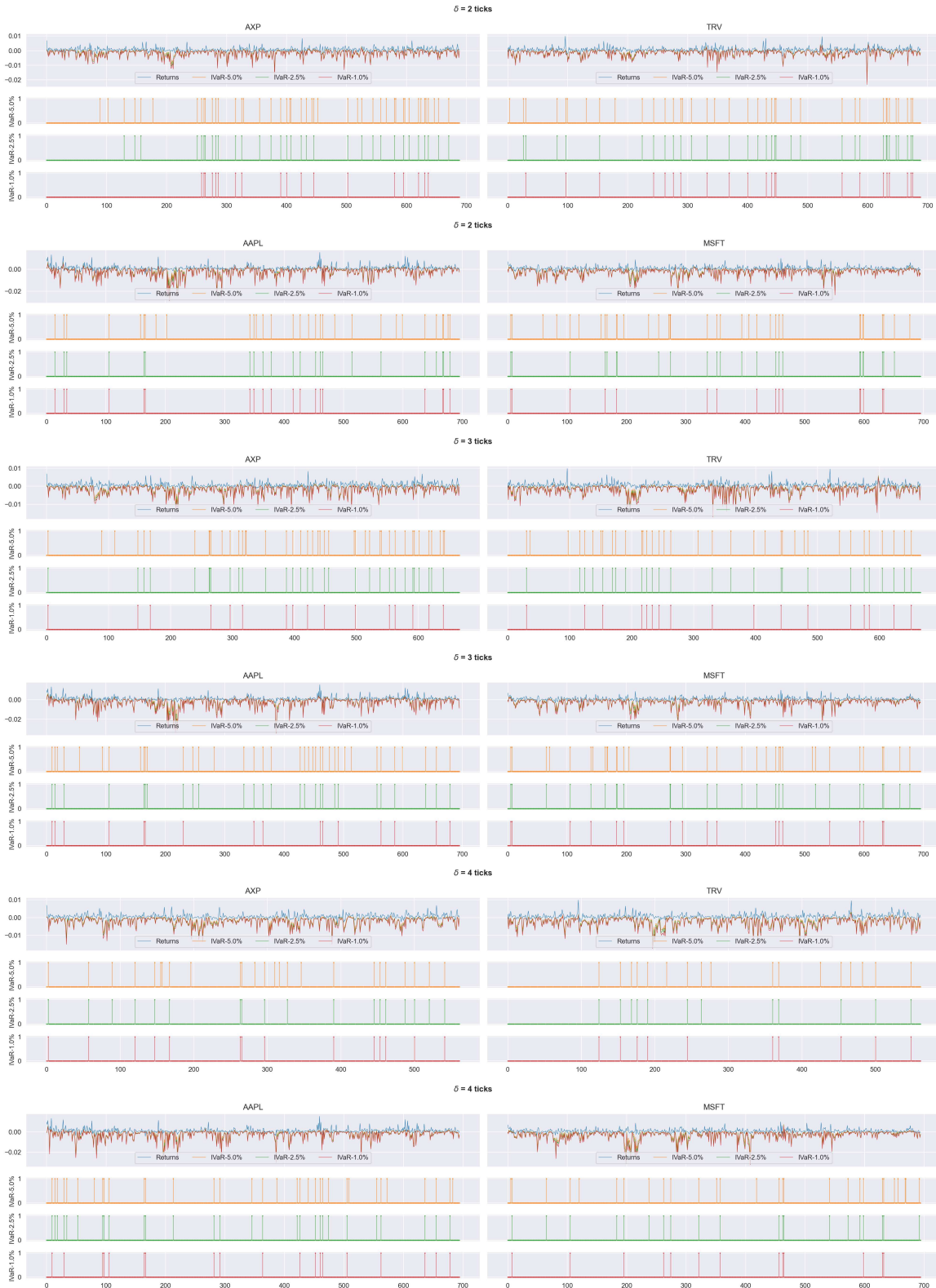
At first glance, we can observe that the violation frequency of IVaR tends to be closer to its nominal levels, e.g. 5%, 2.5% and 1%, when the forecasting interval length and the price change threshold are increased. For example, at the high risk level of 1%, the best IVaR performance of AAPL and MSFT, i.e. the frequency of IVaR violations is not significantly different from 1%, is achieved at 60-minute interval and 4-tick threshold, while for AXP and TRV it is at 30-minute and 4-tick.

Figure 5.2: 5-min IVaR out-of-sample forecasts with 2, 3, and 4 ticks thresholds



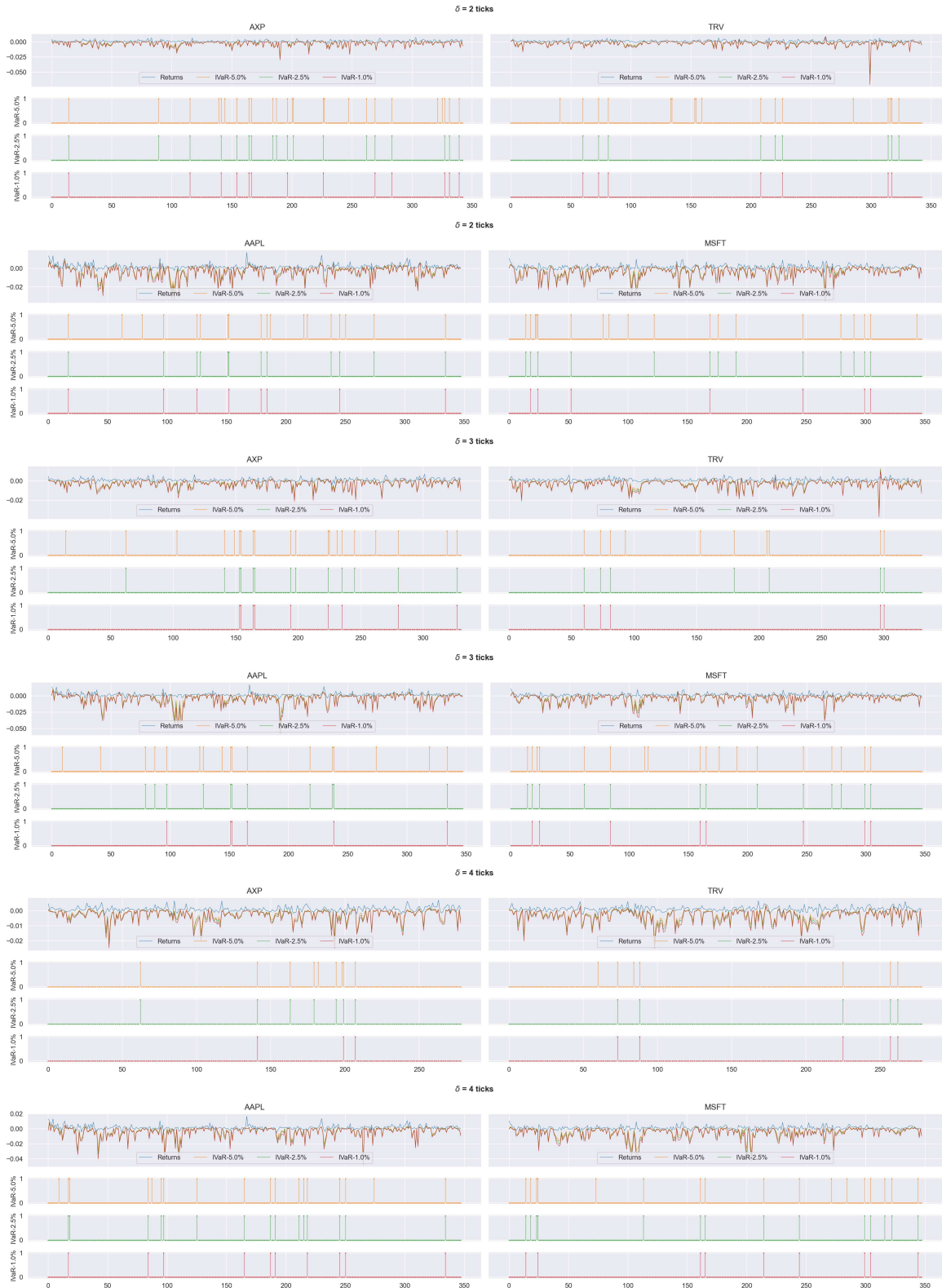
Notes: IVaR out-of-sample forecasts for AXP and TRV, AAPL and MSFT. The figure of each asset displays the forecasts of the intraday IVaR with 5% (in yellow), 2.5% (in green) and 1% (in red), the ex-post returns (in blue), as well as the violations series corresponding to each level of risks.

Figure 5.3: 15-min IVaR out-of-sample forecasts with 2, 3, and 4 ticks thresholds



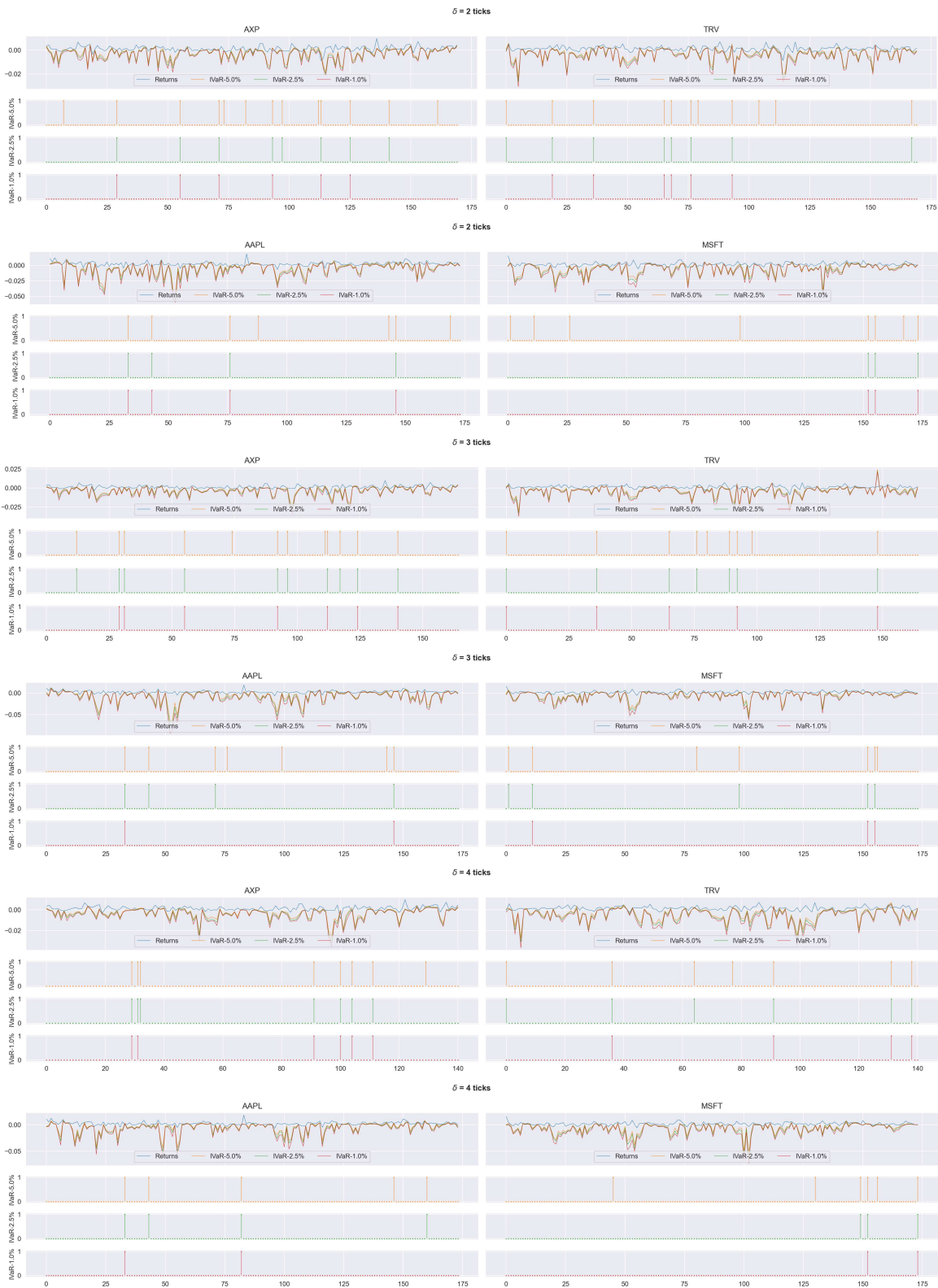
Notes: IVaR out-of-sample forecasts for AXP and TRV, AAPL and MSFT. The figure of each asset displays the forecasts of the intraday IVaR with 5% (in yellow), 2.5% (in green) and 1% (in red), the ex-post returns (in blue), as well as the violations series corresponding to each level of risks.

Figure 5.4: 30-min IVaR out-of-sample forecasts with 2, 3, and 4 ticks thresholds



Notes: IVaR out-of-sample forecasts for AXP and TRV, AAPL and MSFT. The figure of each asset displays the forecasts of the intraday IVaR with 5% (in yellow), 2.5% (in green) and 1% (in red), the ex-post returns (in blue), as well as the violations series corresponding to each level of risks.

Figure 5.5: 60-min IVaR out-of-sample forecasts with 2, 3, and 4 ticks thresholds



Notes: IVaR out-of-sample forecasts for AXP and TRV, AAPL and MSFT. The figure of each asset displays the forecasts of the intraday IVaR with 5% (in yellow), 2.5% (in green) and 1% (in red), the ex-post returns (in blue), as well as the violations series corresponding to each level of risks.

In addition, Figures 5.2 to 5.5 illustrate the realizations of the out-of-sample IVaR forecast results with different price change thresholds and different forecast intervals. The corresponding IVaR violations are also displayed in the panels below. From the figures, IVaR violations seem to cluster only in the cases of 5-minute and 15-minute one-step-ahead forecasting. For the longer forecasting intervals, i.e. 30 minutes and 60 minutes, they are not clustered and accurately capture the extreme return dynamics.

Finally, high liquid stocks, i.e. AAPL and MSFT, generally perform better in both aspects of IVaR violation probability and clustering than low liquid stocks, AXP and TRV. We remind the reader that our IIVaR estimator, basically, is a parametric-designed estimator based on fitting conditional intensities to the historical realizations of two-state price change processes. The performance of the estimator is very sensitive to the size of the information set on which it is conditioned, that is, in this study, the trading activity or the liquidity level. Therefore, the higher the liquid the asset, the better the IVaR estimation can be obtained by the IIVaR.

So far, we have presented the results obtained “upon the first glance” on the coverage and the serial independence of IVaR forecasts. In the next section, we will verify these findings using the back-testing methods mentioned in § 5.4.

5.5.2.2 Backtesting results

Tables 5.4 and 5.7 present the backtest results of the IVaR out-of-sample forecasts. For each forecast interval, sampling threshold, and level of risk, we perform Kupiec, dynamic quantile, and duration-based GMM tests on the realization of IVaR violations (hits) to test for unconditional coverage, independence, and random occurrence of IVaR forecast failures. To further examine the dependence of IVaR forecast failures, Tables 5.8 to 5.11 illustrate regressions of IVaR violation time series on relevant variables, i.e. lagged IVaR violations, IVaR violations of related stocks, IVaR magnitude, and trend. The t-test on the regression coefficient is performed to verify the correlation between the IVaR violation and its covariates. The entries reported in all tables are the corresponding p-values of the tests. The entries in boldfaces denote failures of the model at the 99% confidence level, as the p-values are less than 0.01, and the ones in italics denote failures at the 95% confidence level, as the p-values are less than 0.05.

From Table 5.4, the IIVaR model performs poorly in the 5-minute forecast interval. Especially, for low liquid stocks, AXP and TRV, p-values are rejected in almost all tests, except one case of the Kupiec test for IVaR forecasts at 5% risk level with 4-tick threshold. For high liquid stocks, significant p-values are obtained at the 5% risk level from the Kupiec test and the duration-based GMM test. Still, the null hypotheses of independence violations in the dynamic quantile test are all rejected.

Moving to IVaR forecasting over longer interval lengths, IIVaR tends to perform better. At 15 minutes, IVaR forecasts of the 2.5% risk level do not reject the null hypotheses of unconditional coverage in the Kupiec test and randomly distributed occurrences in the duration-based GMM test at all sampling thresholds for high liquid stocks, whereas for

Table 5.4: 5-min IVaR backtesting results for two selected pairs of stocks

IVaR level	Kupiec test			Dynamic quantile test			Duration GMM test			
	5,0%	2,5%	1,0%	5,0%	2,5%	1,0%	5,0%	2,5%	1,0%	
Low liquidity pair	Threshold: 2 ticks									
	AXP	0,000	0,000	0,000	0,000	0,000	0,000	0,000	0,000	0,000
	TRV	0,000	0,000	0,000	0,000	0,000	0,000	0,000	0,000	0,000
	Threshold: 3 ticks									
	AXP	0,002	0,000	0,000	0,000	0,000	0,000	0,000	0,000	0,000
	TRV	0,002	0,000	0,000	0,000	0,000	0,000	0,000	0,000	0,000
	Threshold: 4 ticks									
	AXP	0,353	<i>0,014</i>	0,000	0,000	0,000	0,000	0,000	0,000	0,000
TRV	0,278	0,307	0,000	0,000	0,001	0,000	0,000	0,000	0,000	
High liquidity pair	Threshold: 2 ticks									
	AAPL	0,798	0,000	0,000	0,000	0,000	0,000	0,846	0,005	0,000
	MSFT	0,003	0,000	0,000	0,000	0,000	0,000	0,066	0,000	0,000
	Threshold: 3 ticks									
	AAPL	0,345	0,000	0,000	0,000	0,000	0,000	0,323	0,000	0,000
	MSFT	0,345	0,000	0,000	0,000	0,000	0,000	0,905	0,009	0,000
	Threshold: 4 ticks									
	AAPL	0,787	0,000	0,000	0,000	0,000	0,000	0,951	0,006	0,000
MSFT	0,142	0,180	0,000	0,000	0,001	0,000	0,118	0,672	<i>0,010</i>	

Notes: The figures are the p-values of the backtests. Entries in boldfaces denote the p-values are less than 0.01 and italics ones denote the p-values are less than 0.05. The dynamic quantile test uses 3 lags of the IVaR as explanatory variables, and the duration-based GMM test tests for conditional coverage with 5 moment conditions.

Table 5.5: 15-min IVaR backtesting results for two selected pairs of stocks

IVaR level	Kupiec test			Dynamic quantile test			Duration GMM test			
	5,0%	2,5%	1,0%	5,0%	2,5%	1,0%	5,0%	2,5%	1,0%	
Low liquidity pair	Threshold: 2 ticks									
	AXP	0,054	0,001	0,000	0,000	0,000	0,000	0,222	<i>0,021</i>	0,001
	TRV	0,436	0,001	0,000	0,001	0,000	0,000	0,945	0,051	0,001
	Threshold: 3 ticks									
	AXP	0,100	0,001	0,002	0,000	0,000	0,004	0,377	<i>0,019</i>	0,085
	TRV	0,642	<i>0,032</i>	0,001	0,002	0,000	0,001	0,882	0,489	0,062
	Threshold: 4 ticks									
	AXP	0,541	0,306	0,003	0,001	0,000	0,000	0,000	0,000	0,007
TRV	<i>0,021</i>	0,570	0,094	0,000	0,000	0,002	0,000	0,000	0,000	
High liquidity pair	Threshold: 2 ticks									
	AAPL	0,501	0,283	0,000	0,001	<i>0,023</i>	0,001	0,132	0,619	0,000
	MSFT	0,972	0,129	0,003	0,002	0,001	0,000	0,590	0,185	<i>0,039</i>
	Threshold: 3 ticks									
	AAPL	0,583	<i>0,031</i>	0,003	0,000	0,008	<i>0,021</i>	0,977	0,436	0,126
	MSFT	0,972	<i>0,031</i>	0,000	0,003	0,005	0,003	0,789	0,473	<i>0,031</i>
	Threshold: 4 ticks									
	AAPL	0,896	<i>0,018</i>	0,000	0,005	0,003	0,000	0,989	0,327	<i>0,014</i>
MSFT	0,225	0,533	<i>0,040</i>	0,003	<i>0,027</i>	0,000	0,443	0,958	0,495	

Notes: The figures are the p-values of the backtests. Entries in bold-faces denote the p-values are less than 0.01 and italics ones denote the p-values are less than 0.05. The dynamic quantile test uses 3 lags of the IVaR as explanatory variables, and the duration-based GMM test tests for conditional coverage with 5 moment conditions.

Table 5.6: 30-min IVaR backtesting results for two selected pairs of stocks

IVaR level	Kupiec test			Dynamic quantile test			Duration GMM test			
	5,0%	2,5%	1,0%	5,0%	2,5%	1,0%	5,0%	2,5%	1,0%	
Low liquidity pair	Threshold: 2 ticks									
	AXP	0,068	0,004	0,000	<i>0,023</i>	<i>0,017</i>	<i>0,013</i>	0,231	0,100	0,002
	TRV	0,970	0,884	0,089	0,064	0,392	0,081	0,717	0,465	0,505
	Threshold: 3 ticks									
	AXP	0,399	0,124	<i>0,010</i>	0,002	0,004	0,000	<i>0,012</i>	0,212	<i>0,033</i>
	TRV	0,075	0,645	0,385	0,003	<i>0,025</i>	0,002	0,482	0,971	0,406
	Threshold: 4 ticks									
	AXP	0,147	0,992	0,901	0,057	0,706	0,932	0,785	0,931	0,992
	TRV	<i>0,035</i>	0,425	0,231	0,103	0,436	0,414	0,000	0,000	0,218
High liquidity pair	Threshold: 2 ticks									
	AAPL	0,883	0,284	<i>0,037</i>	<i>0,030</i>	0,073	0,227	0,991	0,906	0,439
	MSFT	0,698	0,168	0,095	<i>0,023</i>	0,067	0,340	0,971	0,818	0,629
	Threshold: 3 ticks									
	AAPL	0,921	0,448	0,218	0,166	<i>0,022</i>	0,007	0,980	0,865	0,832
	MSFT	0,883	0,168	<i>0,037</i>	0,126	0,122	<i>0,045</i>	0,967	0,811	0,433
	Threshold: 4 ticks									
	AAPL	0,883	<i>0,049</i>	0,004	0,282	0,084	0,111	0,911	0,355	0,107
	MSFT	0,921	0,094	<i>0,013</i>	0,074	<i>0,036</i>	0,098	0,949	0,387	0,133

Notes: The figures are the p-values of the backtests. Entries in bold-faces denote the p-values are less than 0.01 and italics ones denote the p-values are less than 0.05. The dynamic quantile test uses 3 lags of the IVaR as explanatory variables, and the duration-based GMM test tests for conditional coverage with 5 moment conditions.

Table 5.7: 60-min IVaR backtesting results for two selected pairs of stocks

IVaR level	Kupiec test			Dynamic quantile test			Duration GMM test			
	5,0%	2,5%	1,0%	5,0%	2,5%	1,0%	5,0%	2,5%	1,0%	
Low liquidity pair	Threshold: 2 ticks									
	AXP	0,140	0,100	<i>0,010</i>	0,194	0,296	0,166	0,686	0,548	0,173
	TRV	0,399	0,100	<i>0,010</i>	<i>0,037</i>	0,089	<i>0,027</i>	0,943	0,691	0,115
	Threshold: 3 ticks									
	AXP	0,208	<i>0,013</i>	0,002	0,163	0,089	<i>0,025</i>	0,716	0,272	<i>0,045</i>
	TRV	0,792	0,192	<i>0,035</i>	<i>0,030</i>	<i>0,015</i>	<i>0,022</i>	0,998	0,919	0,640
	Threshold: 4 ticks									
	AXP	0,719	0,098	0,004	0,202	0,080	<i>0,045</i>	0,296	0,438	<i>0,043</i>
	TRV	0,985	0,224	0,073	0,066	0,108	0,087	0,000	<i>0,022</i>	0,242
High liquidity pair	Threshold: 2 ticks									
	AAPL	0,541	0,863	0,141	0,231	0,888	0,744	0,987	0,895	0,678
	MSFT	0,805	0,488	0,384	0,226	0,000	0,000	0,701	0,360	0,874
	Threshold: 3 ticks									
	AAPL	0,541	0,863	0,847	0,356	0,888	0,965	0,903	0,939	0,980
	MSFT	0,541	0,758	0,384	0,084	0,106	0,002	0,580	0,823	0,592
	Threshold: 4 ticks									
	AAPL	0,163	0,863	0,847	0,440	0,891	0,976	0,833	0,989	0,928
	MSFT	0,321	0,488	0,847	0,165	0,000	0,959	0,710	0,448	0,999

Notes: The figures are the p-values of the backtests. Entries in bold-faces denote the p-values are less than 0.01 and italics ones denote the p-values are less than 0.05. The dynamic quantile test uses 3 lags of the IVaR as explanatory variables, and the duration-based GMM test tests for conditional coverage with 5 moment conditions.

low liquid stocks, these two tests start to be significant at the 4-tick threshold. However, rejections of dynamic quantile tests still persist at all thresholds and risk levels.

Table 5.8: 5-min IVaR backtesting results for two selected pairs of stocks

IVaR level	2 ticks			3 ticks			4 ticks		
	5,0%	2,5%	1,0%	5,0%	2,5%	1,0%	5,0%	2,5%	1,0%
Regression: $\text{Hit}_t^{AXP} = c + \delta\text{IVaR} + a\text{Hit}_t^{TRV} + b_1\text{Hit}_{t-1}^{AXP} + b_2\text{Hit}_{t-2}^{AXP} + b_3\text{Hit}_{t-3}^{AXP} + \epsilon_t$									
TRV	0,000	0,000	0,002	0,858	0,460	0,898	0,359	0,398	0,345
IVaR	0,000	0,000	0,000	0,000	0,000	0,000	0,000	0,000	0,000
AXP-3	0,345	0,960	0,310	0,782	0,902	0,751	0,698	0,423	0,290
AXP-2	0,586	0,599	0,427	0,790	0,496	0,104	0,032	0,100	0,981
AXP-1	0,560	0,742	0,685	0,971	0,589	0,521	0,509	0,568	0,324
const	0,000	0,000	0,000	0,000	0,000	0,000	0,000	0,000	0,000
Regression: $\text{Hit}_t^{TRV} = c + \delta\text{IVaR} + a\text{Hit}_t^{AXP} + b_1\text{Hit}_{t-1}^{TRV} + b_2\text{Hit}_{t-2}^{TRV} + b_3\text{Hit}_{t-3}^{TRV} + \epsilon_t$									
AXP	0,000	0,000	0,002	0,909	0,535	0,867	0,485	0,454	0,334
IVaR	0,000	0,000	0,000	0,000	0,000	0,000	0,000	0,000	0,000
TRV-3	0,226	0,440	0,681	0,715	0,557	0,125	0,930	0,742	0,810
TRV-2	0,626	0,435	0,817	0,601	0,579	0,411	0,839	0,911	0,679
TRV-1	0,762	0,307	0,032	0,449	0,408	0,401	0,225	0,514	0,135
const	0,000	0,000	0,000	0,000	0,000	0,000	0,000	0,000	0,000
Regression: $\text{Hit}_t^{AAPL} = c + \delta\text{IVaR} + a\text{Hit}_t^{MSFT} + b_1\text{Hit}_{t-1}^{AAPL} + b_2\text{Hit}_{t-2}^{AAPL} + b_3\text{Hit}_{t-3}^{AAPL} + \epsilon_t$									
MSFT	0,824	0,790	0,542	0,093	0,994	0,894	0,123	0,838	0,525
IVaR	0,000	0,000	0,000	0,000	0,000	0,000	0,000	0,000	0,000
AAPL-3	0,175	0,560	0,427	0,569	0,398	0,150	0,160	0,199	0,321
AAPL-2	0,573	0,538	0,990	0,080	0,250	0,591	0,887	0,456	0,887
AAPL-1	0,254	0,949	0,297	0,055	0,087	0,790	0,898	0,977	0,771
const	0,001	0,000	0,000	0,000	0,000	0,000	0,001	0,000	0,000
Regression: $\text{Hit}_t^{MSFT} = c + \delta\text{IVaR} + a\text{Hit}_t^{AAPL} + b_1\text{Hit}_{t-1}^{MSFT} + b_2\text{Hit}_{t-2}^{MSFT} + b_3\text{Hit}_{t-3}^{MSFT} + \epsilon_t$									
AAPL	0,935	0,768	0,521	0,079	0,905	0,991	0,151	0,927	0,584
IVaR	0,000	0,000	0,000	0,000	0,000	0,000	0,000	0,000	0,000
MSFT-3	0,147	0,418	0,934	0,084	0,326	0,559	0,528	0,413	0,271
MSFT-2	0,604	0,424	0,582	0,614	0,083	0,287	0,807	0,560	0,328
MSFT-1	0,703	0,339	0,549	0,829	0,215	0,770	0,749	0,992	0,293
const	0,000	0,000	0,000	0,000	0,000	0,000	0,068	0,000	0,000

Notes: The figures are the p-values of t-test on the regression's parameters. Entries in bold-faces denote the p-values are less than 0.01 and italics ones denote the p-values are less than 0.05.

Table 5.9: 15-min IVaR backtesting results for two selected pairs of stocks

IVaR level	2 ticks			3 ticks			4 ticks		
	5,0%	2,5%	1,0%	5,0%	2,5%	1,0%	5,0%	2,5%	1,0%
Regression: $\text{Hit}_t^{\text{AXP}} = c + \delta\text{IVaR} + a\text{Hit}_t^{\text{TRV}} + b_1\text{Hit}_{t-1}^{\text{AXP}} + b_2\text{Hit}_{t-2}^{\text{AXP}} + b_3\text{Hit}_{t-3}^{\text{AXP}} + \epsilon_t$									
TRV	<i>0,010</i>	0,000	0,000	0,081	<i>0,011</i>	<i>0,011</i>	0,007	0,000	0,000
IVaR	0,000	0,000	<i>0,017</i>	0,000	0,000	<i>0,013</i>	0,001	<i>0,013</i>	<i>0,019</i>
AXP-3	0,581	0,224	0,628	0,571	0,675	0,516	0,271	0,437	0,571
AXP-2	0,745	0,237	0,889	0,244	0,807	0,567	0,498	0,578	0,236
AXP-1	0,098	0,232	0,638	0,977	0,916	0,715	0,389	0,420	0,660
const	0,000	0,000	0,002	0,001	0,000	0,002	0,107	<i>0,022</i>	0,004
Regression: $\text{Hit}_t^{\text{TRV}} = c + \delta\text{IVaR} + a\text{Hit}_t^{\text{AXP}} + b_1\text{Hit}_{t-1}^{\text{TRV}} + b_2\text{Hit}_{t-2}^{\text{TRV}} + b_3\text{Hit}_{t-3}^{\text{TRV}} + \epsilon_t$									
AXP	0,008	0,000	0,000	0,114	<i>0,012</i>	<i>0,015</i>	0,008	0,000	0,000
IVaR	0,000	0,001	0,004	0,000	0,001	0,004	0,003	<i>0,026</i>	<i>0,032</i>
TRV-3	0,917	0,710	0,603	0,366	0,256	0,409	0,523	0,707	0,769
TRV-2	0,690	0,405	0,864	0,768	0,869	0,390	0,337	0,434	0,714
TRV-1	0,523	0,784	0,621	0,268	0,469	0,647	0,656	0,750	0,823
const	<i>0,020</i>	0,000	0,000	<i>0,012</i>	0,001	0,000	0,711	0,374	<i>0,022</i>
Regression: $\text{Hit}_t^{\text{AAPL}} = c + \delta\text{IVaR} + a\text{Hit}_t^{\text{MSFT}} + b_1\text{Hit}_{t-1}^{\text{AAPL}} + b_2\text{Hit}_{t-2}^{\text{AAPL}} + b_3\text{Hit}_{t-3}^{\text{AAPL}} + \epsilon_t$									
MSFT	0,058	0,201	<i>0,022</i>	0,097	0,326	0,342	0,163	0,246	<i>0,010</i>
IVaR	0,000	0,001	0,003	0,000	0,001	0,008	0,000	0,001	0,006
AAPL-3	0,638	0,309	0,381	0,282	0,860	0,535	0,749	0,375	0,662
AAPL-2	0,567	0,836	0,642	0,267	0,840	0,370	0,977	0,557	0,065
AAPL-1	0,745	0,721	0,464	0,115	0,357	0,628	0,289	0,435	0,609
const	0,272	<i>0,018</i>	0,000	<i>0,014</i>	0,001	0,001	0,097	0,001	0,000
Regression: $\text{Hit}_t^{\text{MSFT}} = c + \delta\text{IVaR} + a\text{Hit}_t^{\text{AAPL}} + b_1\text{Hit}_{t-1}^{\text{MSFT}} + b_2\text{Hit}_{t-2}^{\text{MSFT}} + b_3\text{Hit}_{t-3}^{\text{MSFT}} + \epsilon_t$									
AAPL	0,092	0,189	0,053	0,190	0,448	0,557	0,260	0,316	<i>0,023</i>
IVaR	0,000	0,000	0,003	0,000	0,001	<i>0,014</i>	0,001	0,006	<i>0,019</i>
MSFT-3	0,834	0,993	0,381	0,813	0,243	0,569	0,245	0,517	0,768
MSFT-2	0,415	0,379	0,018	0,493	0,521	<i>0,037</i>	0,088	0,080	0,001
MSFT-1	0,066	0,009	0,240	0,229	0,227	0,690	0,851	0,650	0,846
const	<i>0,037</i>	0,003	0,001	<i>0,042</i>	0,001	0,001	0,422	0,046	<i>0,016</i>

Notes: The figures are the p-values of t-test on the regression's parameters. Entries in bold-faces denote the p-values are less than 0.01 and italics ones denote the p-values are less than 0.05.

To investigate the failures of the independent violation hypothesis further in the dynamic quantile test at 15-minute forecasting, we examine t-tests for each estimated parameter of the IVaR Hits regression in Table 5.9. We note that p-values less than 0.05 indicate a significant dependence of IVaR Hits on the explanatory variables, which leads to the failures of the independence hypothesis. From Table 5.9, the failures are mainly caused by a trend illustrated by the constant coefficient and the correlation between IVaR values and IVaR violations. There still exists a correlation in IVaR violations between two less liquid stocks, TRV and AXP, while this correlation of the violations is not significant between high liquid stocks, AAPL and MSFT. Furthermore, IVaR violations are not serially correlated with its lagged variables. In other words, IVaR violations do not trace each other and are temporally independent.

The results of the backtest on 30- and 60-minute IVaR presented in Tables 5.6 and 5.7 continue to support the better performance of IIVaR in forecasting longer interval lengths. Overall, the 30-minute IVaR backtest results are satisfactory, and only a few cases are rejected even at the extreme risk level of 1 %. The 60-minute IVaR performs even better, especially with the pair AAPL and MSFT. In all the cases considered, the p-values associated with the Kupiec tests and the duration of the GMM tests exceed 15%. In other words, the null hypotheses of unconditional coverage and duration-based GMM tests can not be rejected, all the violations are randomly duration distributed and covered by nominal risk levels of the IVaR. However, in the dynamic quantile test, there are some rejections for MSFT. Further investigation on the t-test results in Table refc-3:tab11 indicates that these failures of the independent violation hypothesis are caused by the correlation with the third-order lagged violation variable. But there is no significance for the first- and second-order lagged coefficients. The significant third-order serial correlation in IVaR violations might plausibly arise as a consequence of the regression with a small sample at 60 minutes interval, i.e. 175 observations in this study. Moving back to the t-test results for shorter interval forecasts, that is, in Tables 5.8 to 5.10, it is evident that there is no serial correlation in IVaR violations of MSFT.

In other words, for high-liquidity assets, the IIVaR model accurately measures intraday market risks over the 60-minute forecast interval. This result provides evidence to support a reasonable choice of the IVaR forecast interval length. Indeed, when there is an abnormal deviation, that is, a shock to the true underlying values, it takes time for the market to correct and make the observable return converging to its mean (Brogaard, Hendershott and Riordan, 2014; O'Hara, 2015). Too frequently, IVaR forecasting cannot capture such an abnormal deviation and thereby fails more often. Meanwhile, with a reasonably long forecast interval, the IIVaR focuses on true price movements rather than noisy fluctuations around the underlying value, resulting in better IVaR performance. This is evidenced by the increasing performance of the IIVaR in all three backtests with increasing forecast interval length.

Finally, the performance of the IIVaR also depends on the choice of price change threshold from which the OUB and OLB point processes are constructed. Comparing the backtesting results on the IVaR forecasts associated with the different thresholds, the performance of IVaR is improved significantly when we increase the number of ticks on the threshold. Also, this tendency is stronger in the low-liquid stocks, AXP and TRV, than in the high-liquid stocks, AAPL and MSFT. This finding is slightly different from the one in the univariate AACD approach of Liu and Tse (2015) about the effects of the threshold choice. In their empirical analysis, the IVaR is not sensitive to the selection of a threshold. The difference in the finding can be due to the existence of a correlation structure in extreme returns of multiple assets, especially low liquidity. In fact, low liquid stocks are usually observed with heavy-tailed returns (see Section § 5.5.1). And the cross-correlation between stocks increases substantially with a large price move (see, e.g. Brogaard et al., 2018; Cizeau, Potters and Bouchaud, 2001; Longin and Solnik, 2001). In other words, the correlation structure of extreme returns is more pronounced in IVaR forecasts of low liquid

stocks. A high price change threshold better generates the realizations of interdependence in the tail, which, as a result, produces better IVaR forecasts.

Table 5.10: 30-min IVaR backtesting results for two selected pairs of stocks

IVaR level	2 ticks			3 ticks			4 ticks		
	5,0%	2,5%	1,0%	5,0%	2,5%	1,0%	5,0%	2,5%	1,0%
Regression: $\text{Hit}_t^{\text{AXP}} = c + \delta\text{IVaR} + a\text{Hit}_t^{\text{TRV}} + b_1\text{Hit}_{t-1}^{\text{AXP}} + b_2\text{Hit}_{t-2}^{\text{AXP}} + b_3\text{Hit}_{t-3}^{\text{AXP}} + \epsilon_t$									
TRV	0,610	0,541	0,171	0,779	0,503	0,657	0,559	0,599	0,743
IVaR	0,001	0,003	<i>0,020</i>	0,000	0,001	0,002	<i>0,025</i>	0,082	0,197
AXP-3	0,765	0,762	0,534	0,499	0,828	0,749	0,124	0,681	0,875
AXP-2	0,567	0,790	0,629	0,187	0,249	0,159	0,554	0,816	0,971
AXP-1	0,367	0,627	0,794	0,009	0,005	0,000	0,118	0,772	0,953
const	0,004	0,000	0,001	0,007	0,004	0,002	0,986	0,296	0,355
Regression: $\text{Hit}_t^{\text{TRV}} = c + \delta\text{IVaR} + a\text{Hit}_t^{\text{AXP}} + b_1\text{Hit}_{t-1}^{\text{TRV}} + b_2\text{Hit}_{t-2}^{\text{TRV}} + b_3\text{Hit}_{t-3}^{\text{TRV}} + \epsilon_t$									
AXP	0,723	0,529	0,158	0,654	0,526	0,651	0,719	0,846	0,944
IVaR	<i>0,020</i>	0,107	0,211	0,001	0,003	0,004	0,078	<i>0,030</i>	<i>0,031</i>
TRV-3	0,854	0,097	<i>0,017</i>	0,140	0,031	0,001	0,642	0,731	0,739
TRV-2	0,811	0,634	0,754	0,201	0,743	0,697	0,546	0,576	0,589
TRV-1	<i>0,015</i>	0,707	0,817	0,438	0,675	0,787	0,686	0,766	0,777
const	0,341	0,417	0,139	0,835	0,181	<i>0,025</i>	0,233	0,502	<i>0,026</i>
Regression: $\text{Hit}_t^{\text{AAPL}} = c + \delta\text{IVaR} + a\text{Hit}_t^{\text{MSFT}} + b_1\text{Hit}_{t-1}^{\text{AAPL}} + b_2\text{Hit}_{t-2}^{\text{AAPL}} + b_3\text{Hit}_{t-3}^{\text{AAPL}} + \epsilon_t$									
MSFT	0,823	0,369	0,712	0,972	0,351	<i>0,020</i>	0,256	0,088	0,173
IVaR	0,005	0,006	<i>0,028</i>	<i>0,014</i>	0,055	0,131	<i>0,034</i>	<i>0,038</i>	0,086
AAPL-3	<i>0,026</i>	0,327	0,613	0,650	0,706	0,905	0,251	0,709	0,514
AAPL-2	0,228	0,384	0,616	0,298	0,330	0,454	0,947	0,626	0,604
AAPL-1	0,765	0,261	0,712	0,104	0,003	0,003	0,774	0,557	0,665
const	0,166	<i>0,027</i>	0,009	0,312	0,152	0,164	0,293	<i>0,028</i>	0,008
Regression: $\text{Hit}_t^{\text{MSFT}} = c + \delta\text{IVaR} + a\text{Hit}_t^{\text{AAPL}} + b_1\text{Hit}_{t-1}^{\text{MSFT}} + b_2\text{Hit}_{t-2}^{\text{MSFT}} + b_3\text{Hit}_{t-3}^{\text{MSFT}} + \epsilon_t$									
AAPL	0,961	0,519	0,653	0,940	0,350	<i>0,020</i>	0,322	0,127	0,164
IVaR	0,000	0,004	<i>0,038</i>	0,003	<i>0,015</i>	<i>0,041</i>	0,005	<i>0,011</i>	<i>0,045</i>
MSFT-3	0,360	0,464	0,674	0,900	0,421	0,747	0,257	0,400	0,542
MSFT-2	0,967	0,338	0,620	0,981	0,495	0,619	0,369	0,448	0,555
MSFT-1	0,274	0,474	0,693	0,355	0,534	0,720	0,965	0,647	0,561
const	<i>0,030</i>	0,006	<i>0,017</i>	0,109	<i>0,016</i>	<i>0,014</i>	0,142	<i>0,010</i>	0,008

Notes: The figures are the p-values of t-test on the regression's parameters. Entries in bold-faces denote the p-values are less than 0.01 and italics ones denote the p-values are less than 0.05.

Table 5.11: 60-min IVaR backtesting results for two selected pairs of stocks

IVaR level	2 ticks			3 ticks			4 ticks		
	5,0%	2,5%	1,0%	5,0%	2,5%	1,0%	5,0%	2,5%	1,0%
Regression: $\text{Hit}_t^{AXP} = c + \delta\text{IVaR} + a\text{Hit}_t^{TRV} + b_1\text{Hit}_{t-1}^{AXP} + b_2\text{Hit}_{t-2}^{AXP} + b_3\text{Hit}_{t-3}^{AXP} + \epsilon_t$									
TRV	0,853	0,322	0,107	0,661	0,453	0,068	0,391	0,166	0,067
IVaR	0,018	0,095	0,123	0,011	0,030	0,054	0,024	0,068	0,131
AXP-3	0,258	0,444	0,597	0,496	0,535	0,623	0,589	0,394	0,640
AXP-2	0,745	0,669	0,763	0,636	0,421	0,139	0,644	0,350	0,132
AXP-1	0,806	0,716	0,812	0,640	0,683	0,734	0,366	0,245	0,855
const	0,021	0,035	0,025	0,022	0,006	0,012	0,132	0,074	0,037
Regression: $\text{Hit}_t^{TRV} = c + \delta\text{IVaR} + a\text{Hit}_t^{AXP} + b_1\text{Hit}_{t-1}^{TRV} + b_2\text{Hit}_{t-2}^{TRV} + b_3\text{Hit}_{t-3}^{TRV} + \epsilon_t$									
AXP	0,646	0,510	0,208	0,766	0,602	0,096	0,399	0,187	0,056
IVaR	0,004	0,012	0,020	0,001	0,001	0,003	0,002	0,008	0,027
TRV-3	0,037	0,194	0,148	0,275	0,109	0,942	0,727	0,783	0,791
TRV-2	0,272	0,431	0,521	0,433	0,585	0,511	0,310	0,438	0,569
TRV-1	0,525	0,649	0,725	0,869	0,993	0,982	0,408	0,553	0,711
const	0,051	0,028	0,011	0,107	0,020	0,013	0,156	0,033	0,026
Regression: $\text{Hit}_t^{AAPL} = c + \delta\text{IVaR} + a\text{Hit}_t^{MSFT} + b_1\text{Hit}_{t-1}^{AAPL} + b_2\text{Hit}_{t-2}^{AAPL} + b_3\text{Hit}_{t-3}^{AAPL} + \epsilon_t$									
MSFT	0,608	0,811	0,819	0,582	0,765	0,810	0,618	0,689	0,826
IVaR	0,026	0,169	0,182	0,059	0,172	0,266	0,100	0,173	0,304
AAPL-3	0,226	0,753	0,751	0,180	0,820	0,867	0,716	0,742	0,864
AAPL-2	0,545	0,706	0,710	0,602	0,734	0,814	0,711	0,706	0,841
AAPL-1	0,560	0,778	0,772	0,533	0,670	0,823	0,621	0,693	0,844
const	0,694	0,602	0,082	0,768	0,582	0,435	0,349	0,631	0,481
Regression: $\text{Hit}_t^{MSFT} = c + \delta\text{IVaR} + a\text{Hit}_t^{AAPL} + b_1\text{Hit}_{t-1}^{MSFT} + b_2\text{Hit}_{t-2}^{MSFT} + b_3\text{Hit}_{t-3}^{MSFT} + \epsilon_t$									
AAPL	0,570	0,919	0,905	0,366	0,682	0,789	0,644	0,845	0,856
IVaR	0,023	0,159	0,167	0,098	0,074	0,163	0,062	0,290	0,240
MSFT-3	0,187	0,000	0,000	0,078	0,006	0,000	0,049	0,000	0,867
MSFT-2	0,797	0,880	0,867	0,390	0,927	0,842	0,522	0,825	0,878
MSFT-1	0,499	0,805	0,805	0,049	0,668	0,768	0,608	0,821	0,851
const	0,513	0,508	0,157	0,967	0,468	0,222	0,894	0,646	0,393

Notes: The figures are the p-values of t-test on the regression's parameters. Entries in bold-faces denote the p-values are less than 0.01 and italics ones denote the p-values are less than 0.05.

5.6 CONCLUSION

In this chapter, we introduced IIVaR, a multi-asset intraday market risk model that extends the previous univariate intraday Value-at-Risk model. The model is based on modelling the occurrence of price change events by stochastic conditional intensities and forecasting arrivals of future transactions by Monte Carlo simulation. Tick-by-tick transaction data is first filtered by a threshold into two-state directional price change point processes, OUB and OLB. The conditional intensities of the OUB and OLB transaction processes are cast into multivariate Hawkes with exponential decay kernel. Contrasting to discrete duration-type models previously used in the literature, the multivariate Hawkes conditional intens-

ities update their information set continuously and thus account for both temporal self- and cross-asset effects induced by any new event arriving in the price change dynamics. Therefore, the IIVaR overcomes the limitations of the discrete model in updating cross-correlation information arriving within transaction waiting times. To facilitate forecasting future transactions, we propose an arrival detection mechanism by an autoregressive conditional compensator, estimating expected cumulative conditional intensities to have a new price change event arriving. Then a Monte Carlo simulation is adopted to simulate the return distribution, from which IVaR is calculated for any arbitrary intraday interval.

We applied our methodology to four stocks listed on the DJIA index. The results of the backtests indicate that IIVaR constitutes a real approach to measure intraday multivariate market risk. To investigate how the choice of price change threshold and forecasting intervals impact the performance of the IIVaR, we also compared the results of different scenarios for the thresholds and forecasting intervals. The model performs better in forecasting reasonably long intervals and with high price change thresholds. In our study, the 30-minute and 60-minute IVaR forecasts associated with the 4-tick threshold deliver the best performance.

Our study has several limitations that provide ample room for future research. First, our study can be further complemented by a comprehensive simulation framework and a comparison with other standard (univariate) IVaR models in the literature. It helps verifying the robustness of our estimator by additionally accounting for the cross-correlation in forecasting IVaR. Second, since the conditional intensity can be broken down into different factors, i.e. self-excitation, cross-excitation, and exogenous effects, it would be interesting to decompose the IVaR forecasts into the corresponding components. By doing so, the separated measures on the decomposed components would shed light on the structure of total IVaR by viewing it from different sources of risk. Finally, our current empirical application deals only with bivariate assets. Therefore, another natural development would be an extension to a larger number of assets and the development of an IIVaR for a portfolio.

CONCLUSIONS

6.1 SUMMARY AND MAIN FINDINGS

This thesis introduces a new mathematical formulation of intraday price changes that relaxes the EMH assumption that new information is incorporated instantaneously into prices. In a high-frequency trading setup, with inter-transaction times well under the human-attention span, it is unrealistic to assume that there is enough time for new information to be assimilated instantaneously. Instead, we introduce the concept of “information lifespan”, which enables a more structural formulation of price in term of information diffusion over time. Using this concept, we extend existing microstructure models and introduce generalizations of the following aspects: (1) a comprehensive multi-asset price formation dynamics at the transaction-by-transaction frequency accommodating microstructure complications of asymmetric information, strategic trading, and imperfect learning (2) an intensity-based estimator of locally integrated variance-covariance matrix accounting for lead-lag correlation and robust to microstructure noise, and asynchronous trading; and (3) a multivariate intraday Value-at-Risk (IVaR) generalizing previous univariate IVaR and taking into account cross-correlations of extreme asset returns.

In [Chapter 3](#), motivated by the intuition that information and time are inherently linked, we propose that information has a life span, decaying over time. Then we extend the classic “martingale plus noise” model and introduce a multi-asset price formation dynamic, generalizing previous microstructure models of lagged price adjustment to accommodate various complications of asymmetric information, information lifespan, and temporal lagged price adjustment. Our multivariate generalization, the MALA model, strengthens the theoretical results of previous lagged price adjustment models by decomposing the driving sources of the adjustment as two distinct and subsequent imperfections of the market: pricing errors due to asymmetric information inherent in transaction-by-transaction frequency and partial adjustment due to imperfect learning of residual (trade) information over time. The MALA relaxes constancy and analogy assumptions on the impacts of order flows and historical trade; and thus accounts for the distinct roles of informed trading in causing the delayed assimilation of information. Also, as long-lived residual information has a lifespan, the MALA allows trades across assets to become temporally lead-lag correlated. This lead-lag correlation gives an alternative explanation to Epps effects, which documents the bias towards zero of cross-correlation between related assets when the sampling frequency shrinks to the transaction-by-transaction level.

We also built a bridge between the microstructure price dynamics model and Hawkes point process. In a disjoint manner, the instantaneous increment of the observable price can be represented by the Hawkes stochastic conditional intensity. Then, the multivariate Hawkes process allows the estimation of price adjustments to be computed at every point in time. This property alleviates the complications that arise from the embedded features of high-frequency trading data. The obtained parameters of the MALA are robust to asynchronous trading, irregular spacing time, and microstructure noise.

Using transaction data on a cross section of DJIA stocks, we provide empirical evidence for the indispensability of a price formation mechanism for multiple assets at a transaction-by-transaction frequency. We found the significance of the cross-asset effects at all levels, the level of price change, the level of transaction, and the level of asset. In particular, at the price change level, there exists strong excitement amongst states belonging to within-asset as well as cross-asset. The within-asset excitements mainly exhibit a mean-reverting behaviour, whereas the cross-asset excitements implies co-movement in the extreme returns. At the transaction level, the life-span of the residual information gives rise to the temporal lead-lag correlation, which is, by Epps effects, considered to vanish in contemporaneous time in asynchronous trading settings. This temporal lead-lag correlation is then normalized by the factor of liquidity, resulting in a measure of the lead-lag relationship at the asset level which takes into account the combined effects from the information content of trade and liquidity.

Furthermore, the MALA shows its advantage in recovering the lead-lag structure of the true underlying values over previous models of aggregating prices. The empirical analysis provides evidence of the existence of lead-lag correlations over a time interval less than the duration of a trade. While the models of aggregating prices destroy all correlations that are exhausted at a rate higher than the sampling frequency, the MALA model can account for true short-term lead-lag correlations at the finest frequency of transaction level. Thus, the lead-lag correlation between assets can be simply recovered by integrating for any arbitrary interval.

In [Chapter 4](#), on the ground that the price formation dynamics captures well the lead-lag correlations, we continue to estimate the integrated covariation for multiple assets, taking into account this temporal cross-correlation. Our estimator, the IRC, combines features of both quadratic covariation, e.g. RK, and point process-based approaches, e.g. PDV. It not only preserves superior features of the PDV by providing local estimations on the intraday variation of asset returns, but also accommodates a generic temporal (cross-) autocovariation structure of RK estimators, facilitating the estimation of local cross-correlation between assets. To some extent, the temporal (cross-) autocovariation structure accounts for lead-lag effects and compensates for the loss of contemporaneous correlation incurred by asynchronous trading, asymmetric information, and imperfect price formation.

To overcome the limitation of discrete price duration modelling in the PDV, the IRC utilizes multivariate Hawkes processes to model stochastic conditional intensities of all possible observable disjoint states of a price change, taking advantage of the discreteness of the transaction-by-transaction price and a finite number of price change states. We con-

struct a link between the quadratic covariation of the return process and the second-order moment structure of the disjoint price change counting process. Under a martingale representation, a parametric structure of the quadratic covariation can be obtained and expressed in terms of the estimated parameters of the conditional intensities corresponding to these counting processes.

We placed the mapping between the quadratic covariation and the disjoint price change process under a noise-contaminated semi-martingale hypothesis for the observable price. And by a reasonable assumption that the microstructure noises are only updated at transaction times and independent of the efficient prices, we propose an efficient way, also based on the intensities of the disjoint point processes, to directly estimate the bias incurred by the noises, which complements the robustness of our IRC estimator.

We examine the properties of the IRC estimator in detail, and analyze its bias with the presence of microstructure noise, time discretization, and price discretization. The simulation results illustrate that the IRC estimator is robust to these elements. Compared to the PDV and RC estimators, the IRC outperforms them in estimating all elements of the variance-covariance matrix. More importantly, the results also show that the IRC delivers a much sharper estimation of the correlation than the consistency, noise-robust RK estimator.

In [Chapter 5](#), we develop an intensity-based intraday Value-at-Risk, motivated by the favourable results on the extreme returns co-movements of multi-asset prices dynamics modelling in [Chapter 3](#). Our IIVaR model nests previous univariate IVaR models based on modelling of the price duration. The IIVaR uses stochastic conditional intensities to model the occurrence of price change events and adopts a Monte Carlo simulation to forecast arrivals of future price-change transactions. Contrasting with discrete duration-type models previously used in the literature, the multivariate stochastic conditional intensities are adjusted to newly arrived information continuously and thus account for both temporal self- and cross-asset effects induced by any new event arriving at the price change dynamics. Therefore, the IIVaR overcomes the limitations of the discrete models in continuously updating cross-correlation information. In order to facilitate forecasting future transactions, we also propose an arrival detection mechanism by an autoregressive conditional compensator, estimating expected cumulative conditional intensities to have a new price-change event arriving. Then a Monte Carlo simulation is utilized to simulate the return distribution, from which IVaR is calculated for any arbitrary intraday interval.

We applied our methodology to four stocks listed on the DJIA index. The results of the backtest indicate that IIVaR constitutes a reliable approach to measure intraday multivariate market risk. To investigate how the choice of the price change threshold and the forecast intervals impact the performance of the IIVaR, we compare the results of different scenarios for the thresholds and forecast intervals. The model performs better in forecasting reasonably long intervals and with a high price change threshold. In our study, 30-minute and 60-minute IVaR forecasts associated with the 4-tick threshold deliver the best performance.

6.2 IMPLICATIONS

This thesis has several important implications for both academic researchers and practitioners.

First, the model in [Chapter 3](#) has demonstrated a strong deviation from the traditional null assumption of semi-martingale prices in market micro-structure. A coherent alternative assumption is one in which a role is given to the asymmetries in information, as well as to the life span of information in determining asset prices. This natural alternative hypothesis assumes that the price process is driven by imperfect semi-martingales price adjustment plus noise processes, an assumption of which the lead-lag effects arise as a consequence.

The empirical results on measuring lead-lag effects provide theoretical and empirical evidence for the existence of a multi-asset price formation mechanism at the finest transaction-by-transaction frequency. The presence of a lead-lag correlation is due not only to the information content of trade that contributes to the cross-asset price formations, but also to the level of liquidity, which can be expressed in terms of trading activity. One asset can be highly informative per trade but low trading activity, and consequently incurs a small aggregated impact on prices of other assets. In the other way around, a high-liquidity asset with a high number of trades but low information content can stimulate a large price impact in total. Thus, to uncover the lead-lag correlation at asset level, it is necessary to account for the liquidity together with the cross-transaction information content. Moreover, the empirical results document that the cross-adjustments between assets live on effective time scales less than the average waiting time of a trade. This result confirms the inevitability of modelling lead-lag effects from the transaction-by-transaction level. While the previous model of aggregating prices destroys all correlations that are exhausted at a rate higher than the sampling frequency, our model on transaction-by-transaction data can account for true short-term lead-lag correlations.

Furthermore, the model also provides a formal treatment of second-moment structure of price process, which enables separable estimation of contemporaneous, lead, and lag correlations at different time scales and the possibility of developing an efficient estimator of locally integrated covariance over any time interval.

Second, [Chapter 4](#) shows that the second-order moment structure of the true underlying values on the coarse scale can be recovered from the temporal (cross-)autocovariance of intraday observable price movements. This chapter presents a new methodology, the IRC, that aims to obtain better estimates of such second-order moments by using high-frequency data. While the stylized facts of high-frequency transaction data, i.e. the random time arrival of price moves, discreteness of prices, non-synchronous price changes, are partially or wholly discarded in previous RV and PDV estimators, the IRC illustrates the important contributions of all these elements to the dynamics of quadratic covariation. We also propose that not only the contemporaneous covariation should be captured but also the temporal (cross-)covariation. To do so, we advocate the combination of both quadratic covariation and point process approaches in a parametric structure of the IRC. The new

methodology overcomes difficulties of its predecessors and can be used for a wider set of applications, from locally realized estimates to future forecasts of the intraday portfolio covariance-variance matrix.

Finally, [Chapter 5](#) presents other possibilities for the application of point process-based price change dynamics to market risk measurement. Although a complete description of the return distribution is desirable but impracticable and unfeasible with the time frames of intraday trading, the more efficient solution is to analyze only the tail of the distribution, which characterizes the probability of extreme events. The stochastic conditional intensities modelling provides a convenient way to capture the occurrence of price change events and, at the same time, accounts for a multi-asset interdependence relationship in the price dynamics. Our methodology, IIVaR, extends the previous univariate IVaR and enables multivariate intraday market risk measures. It also helps researchers understand the structure of IVaR from different sources of risk. Last but not least, the IIVaR are efficient at the relatively short time interval of the intraday level and can render empirical applications in defining practical risk measures for traders or practitioners operating their activities on an intraday basis.

6.3 LIMITATIONS AND FUTURE RESEARCHES

As with all studies, this thesis has various limitations that provide grounds for future research.

One of the limitations that applies to all chapters is a similar kernel shape for all decay functions of disjoint price change processes, which is determined by decay coefficients β . In [Chapter 3](#) and [Chapter 5](#), we choose the same decay coefficients for each asset for simplicity and reducing the computation burden, which increases exponentially with the number of different decay coefficients. In [Chapter 4](#), we impose only a single decay coefficient for all disjoint price change point processes to derive conveniently a fully parametric closed form of conditional intensity function under martingale representation. One would then need to introduce, for each asset, different decay kernels that account for cross-adjustments of other assets on that asset and the kernels that account for self-adjustments of that asset on itself (see [Eqn. 3.41](#)). The estimation of the kernels contains additional components and requires much more computational capacity but still follows the same procedure. By imposing different decaying kernel shapes, one could quantify the difference in the cross-asset effects of an asset in the lead-lag relationship with other assets. In addition, the effective time scale of the effects, directly determined by the decay coefficients, measures the life span of information, a criterion for market efficiency. More importantly, this extended framework would open the door to precise estimation and obvious interpretations in order to get better insights into the multi-asset price formation dynamics.

Another limitation is the simple structure of the microstructure noise u in all the chapters. We assumed that microstructure noises follow an independent normal distribution and are also uncorrelated with efficient price processes. In general, the transaction costs are significantly smaller than the change in the true underlying values, the noise

variation can be negligible compared to the variation in the efficient price processes, and thus the simplistic nature of microstructure noise is acceptable. However, the assumption may be empirically questionable in some circumstances of significant asymmetric information where market makers can set nontrivial transaction costs. The large microstructure noise (transaction cost) can be induced by a large amount of informed trading, represented by the coefficients γ . The idea is that the market maker would respond to significant asymmetric information by increasing the transaction cost to compensate for their adverse selection risks.

Finally, our current application in all chapters deals only with bivariate assets. Therefore, another natural development would be an extension to a larger number of assets.

We have drawn the potential limitations that can be applied to all chapters. In the following, we will give details on the specific limitation in each chapter and attempt to detail potential further researches:

In [Chapter 3](#), we do not provide a comparison with other traditional price formation dynamics. This result is actually derived in the work of Bucchini, Corsi and Peluso (2020) and our model is the generalized version of their work. In the following paper, we will cover this comparison with a simulation study. [Chapter 3](#) also leaves some interesting questions that call for future research. First, the model can be more generalized by allowing the adjustment speed of the price quotes to the efficient price to depend on the pricing errors due to asymmetric information. The larger the pricing errors, the higher the proportion of informed trading in the market. And the higher the informed trading, the faster the market maker learns. Second, it would be interesting to address the measure of market efficiency by parameter γ , together with the information lifespan.

[Chapter 4](#) also leaves some open questions to be addressed. First, we need to extend the theoretical framework and provide the asymptotic properties of the estimator in terms of the number of price-change states. The impact of the truncated state spaces of price changes can be further examined. In addition, the method we used to correct for the bias of the microstructure noise is still unclear. The precision of the denoise term we derived in [Eqn. 4.14](#) needs to be investigated in detail. Second, it would be interesting to apply the estimator to real data in an empirical analysis. Although one of the difficulties in accessing the performance of the volatility estimator with empirical analysis is that we do not observe the true value of the variance-covariance matrix, we can still compare the estimation to the outer products of the open-to-close returns, which when averaged over many days provide an estimator of the average covariance between asset returns (see, in particular, Barndorff-Nielsen et al., 2011). Finally, the estimator can be useful in various empirical applications, such as volatility forecasting and factor analysis, and is worth further investigation.

[Chapter 5](#) also has several limitations that provide ample space for further research. First, the evaluation of the IIVaR performance can be further complemented by a comprehensive simulation framework and a comparison with other standard (univariate) IVaR models existing in the literature. It helps verify the robustness of the estimator by additionally accounting for the cross-correlation in forecasting IVaR. Second, since the conditional in-

tensity can be broken down into different factors, i.e. self-excitation, cross-excitation, and exogenous effects, it would be interesting to decompose the IVaR forecasts into the corresponding components. By doing so, the separated measures on the decomposed components would shed light on the structure of total IVaR by viewing it from different sources of risk.

6.4 FINAL REMARKS

In summary, this thesis presents tailor-made mathematical models that contribute to the literature on price dynamics and risk measurement in the high-frequency trading market. The findings show that our proposed model on multi-asset price formation dynamics and multivariate intraday risk measures can overcome limitations of classical models and provide a more structured framework to capture special properties of the high-frequency market embedded at transaction-by-transaction frequency. This thesis establishes the theoretical foundation on these models and advocates the use of them in future researches on the themes of asset pricing and empirical market microstructure.

A

APPENDIX

A.1 HAWKES PROCESS MODELS

In this section of the Appendix, we recall some essential definitions and estimations on the point process theory, and particularly interesting class of the Hawkes point process introduced in Hawkes (1971) and Hawkes and Oakes (1974).

A.1.1 Point Process

Point process is a useful mathematical tool for describing phenomena occurring at random locations and/or times. A point process is a random element whose values are point patterns in a set S . Here we present useful results on the temporal point process where the set S is the interval $[0, T)$ and the points are timestamps of events. The book of Daley and Vere-Jones (2006) is regarded as the main reference on point process theory.

Every realization ω of a point process d , i.e. the transaction arrival time series of asset d , can be represented by a counting process $N_t^d = \int_0^t w(s)ds = \sum_{i=1}^n \mathbb{1}_{t_i^d \leq t}$, where n is an integer-valued random variable, and t_i^d are random elements of $[0, T)$. The usual characterization of the point process is done using the conditional intensity function, which is defined as the infinitesimal rate at which events are expected to occur after t , given the history of $N^d(s)$ prior to t :

$$\lambda^d(t|\mathcal{F}_t) = \lim_{dt \rightarrow 0} \frac{\mathbb{Pr}\{N^d(t) - N^d(t - dt) > 0 | \mathcal{F}_t\}}{dt} \quad (\text{A.1})$$

where \mathcal{F}_t is the filtration of the process that encodes information available up to (but not including) the time t . The most simple temporal point process is the Poisson process, which assumes that events arrive at a constant rate, which corresponds to a constant intensity function $\lambda^d(t) = \lambda > 0$. Note that temporal point processes can also be characterized by the distribution of inter-event times (the duration between two consecutive events).

The temporal point process we consider in this thesis is the Hawkes point process, which models how past events increase the probability of future events.

A.1.2 Hawkes Point Processes

In order to model joint dynamics of several point processes (for example, transaction arrivals of different assets), we will consider the multidimensional Hawkes point process model, introduced in Hawkes (1971) and Hawkes and Oakes (1974). The model implemented the idea that the point processes are tractable with self- and cross-exciting behaviour between different processes. By definition, the conditional intensity, $\lambda^d(t)$, measuring the instantaneous quantity of the event arrival of the point process d conditional on its information set \mathcal{F}_t , can be formulated as a linear combination of past jumps of all D processes:

$$\lambda^d(t) = \mu^d + \sum_{r=1}^D \int_{-\infty}^t \phi^{dr}(t-s) dN^r(s) \quad (\text{A.2})$$

where:

- $\{\mu^d\}_{d \in [1,D]}$ is a vector of exogenous intensities, or also called immigration intensities. The immigrant of type $d, 1 \leq d \leq D$ arrives at a Poisson process with intensity of immigration μ^d .
- $\{\phi^{dr}(t)\}_{d,r \in [1,D]}$ is a matrix-valued decay kernel assumed to be positive and causal. Whenever a point event occurs, be it an immigrant or descendant, the intensity is temporarily increased. This intensity increase causes the arrival of point events, which in turn can spawn descendants of their own. The occurrence in time t of the d -type descendant of a point event type r , who was born or migrated in time s , is governed by $\phi^{dr}(t-s)$.

This formulation of the conditional intensity yields a natural way to measure the causality between events. Let us define a projection $t \rightarrow G^{dr}(t)$ with each element $G^{dr}(t)$ computed as the truncated L^1 norm of the kernels $\phi^{dr}(t)$:

$$G^{dr}(t) := \|\phi^{dr}\|_t := \int_0^t \phi^{dr}(s) ds \geq 0 \text{ for } 1 \leq i, j \leq D \quad (\text{A.3})$$

As in the clustering representation of Hawkes processes Hawkes and Oakes (1974), $G^{dr}(t)$ weights the direct influence of an event type r on the point process d within t seconds after its arrival. Thus, $G^{dr}(\infty)$ can be interpreted as the mean total number of events of type d directly triggered by an event of type r . To ensure that the intensity processes $\lambda^d(t)$ are not explosive and that the point process N_t^d has asymptotically stationary increments, the following stability conditions needs to be hold:

The point processes N_t^d admits a version of stationary intensities if the following conditions are satisfied:

(A.H.1) $\phi^{dr}(t) \forall d, r \in [1, D]$ are bounded functions;

(A.H.2) $\sum_{d,r} \int_0^\infty \phi^{dr}(s) ds < 1 \forall d, r \in [1, D]$.

Through this thesis, we will always consider that the Assumption **(A.H.1)** and **(A.H.2)** holds. In addition, following Bacry, Jaisson and Muzy (2016), Engle and Russell (1998),

Hawkes (1971), Hawkes and Oakes (1974) and Russell and Engle (2005), among others, we also impose the following assumptions on the point process:

(A.H.3) *It is assumed that each point process $\{N^d(t)\}_{d=1}^D$ evolves with “after effects” and “conditionally orderly”, having the following properties:*

$$\mathbb{P}\{N^d(t) - N^d(t - dt) = 1 | \mathcal{H}_t\} = \lambda^d(t)dt + o(dt) \quad (\text{A.4})$$

$$\mathbb{P}\{N^d(t) - N^d(t - dt) > 1 | \mathcal{H}_t\} = o(dt) \quad (\text{A.5})$$

On the one hand, a point process is considered to evolve with after-effect if for any $t > 0$, the likelihood of occurring an event at t depends on the sequence of historical events that occurred only before but not after t , i.e. the interval $[0, t)$. This means that each past event arrival only has impacts on the future event arrivals after its presence. On the other hand, a point process satisfying conditionally orderly is that, for a sufficiently short time interval, there exists at most one event arrival. In other words, conditioned on the information set up to t , \mathcal{H}_t , the probability of occurring two or more events is infinitesimal relative to the probability of occurring one event.

Let us define that N_t and $\lambda(t)$ are D -dimensional vectors of stationary processes. By matrix representation and using convolution notation, we can express the conditional intensity vector, $\lambda(t) = \{\lambda^d(t)\}_{d \in [1, D]}$ as:

$$\lambda(t) = \mu + (\phi \star dN)(t) \quad (\text{A.6})$$

where $\mu = \{\mu^d\}_{d \in [1, D]}$, $\phi(t) = \{\phi^{dr}(t)\}_{d, r \in [1, D]}$ are vector and matrix sizes D and $D \times D$, respectively. The operator \star stands for convolution.

A.2 THE DISJOINT REPRESENTATION AND MARKED HAWKES POINT PROCESSES

The intensity process given above is a time-intensity process. It only describes the dynamic of the ground process of the component index d , i.e. the transaction arrival process with the form *(time, index)* without (price) marks. We consider here marked-point processes with each point event being triples of the form *(time, index, mark)*.

For a full specification of a marked-point process, we need to specify the distribution of the mark. However, the mark distribution is often complicated since it depends on the past of the processes, i.e. the history of the ground process and also the historical marks. To model a point process and its marks jointly, Engle and Manganelli (2004) assume the independence between the conditional distribution of marks and the marginal distribution of arrival times. But this assumption is quite strict, and empirical high-frequency data show that there exists an interdependence between inter-event duration and price changes. Here, we will propose an alternative representation to a marked-point process with finite mark spaces as a multidimensional vector of new disjoint point processes.

Definition 3. *A marked point process with time on the real line \mathbb{R}^+ and marks in the complete separable metric space \mathcal{M}^d is a point process $\{t_i^d, m_i^d\}$ on $\mathbb{R} \times \mathcal{M}^d$ with $i \in I$, I countable, $d \in$*

$[0, D]$ is the component index, $t_i^d \in \mathbb{R}$ is the time, and m_i^d is the mark value of the i th point type- d . The unmarked process $\{t_i^d\}$ on \mathbb{R} is a point process in its own right, called the ground process denoted by $N^d(\cdot)$.

When \mathcal{M}^d is a finite set, we say that the point process is marked with a finite mark space. Intuitively, one may think of a marked point process as follows: (a) consists of events occurring at random points in continuous time; (b) every time an event occurs, one assigns a mark to these events by drawing a sample from a distribution which may very well depend on time, as well as the history of the ground process and/or past marks.

Given that a point event i -th is part of component d , the associated mark m_i^d may depend on the history of the ground process N^d or the past marks. We denote by $\lambda^d(t, m|\mathcal{F}_t)$, $1 \leq d \leq D$, as a family of multivariate marked intensity functions. We will show that a marked point process with finite mark space can be represented by new disjoint multivariate point processes and $\lambda^d(t, m|\mathcal{F}_t)$ can be rewritten as a vector $\{\lambda^{d,m}(t|\mathcal{F}_t)\}_{m \in \mathcal{M}^d}$.

Let M^d be the number of possible outcomes of \mathcal{M}^d at time t . We define new point processes, $\{N^{d,m}(t)\}_{m \in \mathcal{M}^d}$ as disjoint outcomes of $N^d(t)$. That is, each component $N^{d,m}(t)$ is a counting process for one and only one of the M^d outcomes of $N^d(t)$. Due to the singularity of the Hawkes point process, for any t , the vector $\{dN^{d,m}(t)\}_{m \in \mathcal{M}^d}$ has at most one nonzero element, and this nonzero element (if any) is an indicator that at time t an outcome of $dN^d(t)$ occurs. Denoting $0 < t_1^d < \dots < t_i^d < \dots \leq T$ as the event arrival times of ground process d , where $dN^d(t_i^d) = 1$, in the observation period $[0, T]$. Then we can express a ground process $dN^d(t)$ with its M^d dimensional mark space as multivariate disjoint marked processes $\{t_i, dN^{d,m}(t_i)\}_{i \in I}$. The mark, which is denoted by m , indicates exactly which outcome in the mark space \mathcal{M}^d occurs at t_i . We define the conditional intensity function of $N^{d,m}(t)$ as:

$$\lambda^{d,m}(t|\mathcal{F}_t) = \lim_{dt \rightarrow 0} \frac{\mathbb{P}\{N^{d,m}(t) - N^{d,m}(t - dt) > 0|\mathcal{F}_t\}}{dt} \quad (\text{A.7})$$

The \mathcal{F}_t is the information set that includes all the information about the history of the ground process and the past marks. In other words, the conditional intensity at time t is not independent of these factors. We call $dN^{d,m}(t)$ and $\lambda^{d,m}(t|\mathcal{F}_t)$ a disjoint process and its conditional intensity.

Proposition 9. *The disjoint processes and the ground process are mapped via the following properties:*

$$N^d(t) = \sum_{m \in \mathcal{M}^d} N^{d,m}(t) \quad (\text{A.8})$$

$$\lambda^d(t|\mathcal{F}_t) = \sum_{m \in \mathcal{M}^d} \lambda^{d,m}(t|\mathcal{F}_t) \quad (\text{A.9})$$

Proof. The Eqn. A.8 simply follows the decomposition of the ground process based on a finite mark state space.

By definition of the conditional intensity:

$$\lambda^d(t|\mathcal{F}_t) = \lim_{dt \rightarrow 0} \frac{\mathbb{P}r[dN^d(t) = 1|\mathcal{F}_t]}{dt} \quad (\text{A.10})$$

We have the following:

$$\mathbb{P}r[dN^d(t) = 1|\mathcal{F}_t] = \mathbb{P}r\left[\bigcup_{m \in \mathcal{M}^d} dN_t^{d,m} = 1|\mathcal{F}_t\right] = \bigcup_{m \in \mathcal{M}^d} \mathbb{P}r[dN^{d,m}(t) = 1|\mathcal{F}_t] + o(dt) \quad (\text{A.11})$$

where the second equality is from the property [Eqn. A.5](#) and that $\{dN^{d,m_1} = 1 \cap dN^{d,m_2} = 1\} = \emptyset, \forall (m_1, m_2) \in \mathcal{M}^d$ given a complete history. Substituting this into [A.10](#), we obtain [Eqn. A.9](#). \square

Proposition 10. *The probability of the marks is given by the multinomial probability mass function:*

$$\mathbb{P}r[dN^{d,m}(t) = 1 | dN^d(t) = 1, \mathcal{F}_t] = \frac{\lambda^{d,m}(t|\mathcal{F}_t)}{\lambda^d(t|\mathcal{F}_t)} \quad (\text{A.12})$$

Proof. By Bayes' Theorem, we have the following:

$$\mathbb{P}r[dN^{d,m}(t) = 1 | dN^d(t) = 1, \mathcal{F}_t] = \lim_{dt \rightarrow 0} \mathbb{P}r\left[\frac{dN^{d,m}(t) = 1 \cap dN^d(t) = 1|\mathcal{F}_t}{[dN^d(t) = 1|\mathcal{F}_t]}\right] \quad (\text{A.13})$$

$$= \lim_{dt \rightarrow 0} \mathbb{P}r\left[\frac{dN^{d,m}(t) = 1|\mathcal{F}_t}{[dN^d(t) = 1|\mathcal{F}_t]}\right] \quad (\text{A.14})$$

$$= \frac{\lambda^{d,m}(t|\mathcal{F}_t)}{\lambda^d(t|\mathcal{F}_t)} \quad (\text{A.15})$$

where the equality between [Eqn. A.13](#) and [Eqn. A.14](#) follows the singularity assumption of [Eqn. A.5](#). So, the marks follow a multinomial distribution with probabilities given as above. \square

The disjoint representation provides an efficient way to describe a marked point process without specifying the distribution of the marks. The probability of arriving an event is governed by the conditional intensity function $\lambda^d(t|\mathcal{F}_t)$ of the ground process, while the marks are drawn from a M^d -dimensional multinomial distribution to produce the corresponding event in $N^{d,m}$. Note that if we have D -dimensional marked point processes and for each component $d \in [1, D]$, we can disjoint into new M^d point processes. So, in total, we have the $K = \sum_{d=1}^D M^d$ dimensional vector of disjoint processes from the D -dimensional marked point processes. Instead of estimating the joint distribution of the marks and the ground point processes, we will concentrate on the estimation of these disjoint processes. To simplify the notation, we will use $N^k(\cdot)$ and $\lambda^k(\cdot)$ with $k \in [1, K]$ denoting the index of the disjoint process component, substituting for $N^{d,m}(\cdot)$ and $\lambda^{d,m}(\cdot)$.

A.3 PARAMETER ESTIMATION AND GOODNESS-OF-FIT TEST

The standard way to estimate the parameters of the Hawkes process is the maximum likelihood method. In order to define the likelihood function, we fix an observation period of $[0, T]$ as the time interval during which empirical data have been collected.

Definition 4. For all $t \in [0, T]$, the compensator is defined as:

$$\Lambda^k(t) = \int_0^t \lambda^k(s) ds, \text{ where } 1 \leq k \leq K \quad (\text{A.16})$$

The log-likelihood of given intensities $(\lambda^k(t))_{k \in [1, K]}$ with a sample of a pooled point process, i.e. the single process is formed by pooling all the point events of disjoint processes, $\{t_i\}_{i \in [1, N(T)]} = \bigcup_{k \in [1, K]} \{t_i^k\}_{i \in [1, N^k(T)]}$ where $N(t)$ denoting its right-continuous counting function of the pooled point process, is defined as:

$$\mathcal{L}(\theta) = \sum_{k=1}^K \mathcal{L}^d(\theta^k) = \sum_{k=1}^K \left[\int_0^T \log \lambda^k(t) dN^k(t) - \int_0^T \lambda^k(t) dt \right] \quad (\text{A.17})$$

$$= \sum_{k=1}^K \left[\sum_{t_i^k < T} \log \left(\mu^k + \sum_{l=1}^k \sum_{t_j^l < t_i^k} \alpha^{kl} \beta^{kl} e^{-\beta^{kl}(t_i^k - t_j^l)} \right) - \mu^k T - \int_0^T \sum_{l=1}^k \sum_{t_j^l < t} \alpha^{kl} \beta^{kl} e^{-\beta^{kl}(t - t_j^l)} dt \right] \quad (\text{A.18})$$

The log-likelihood can be separated into K independent sub-problems with goodness of fit $\mathcal{L}^k(\theta^k)$ that correspond to the intensity of each asset k . A straightforward computation gives the following:

$$\mathcal{L}^k(\theta^k) = \sum_{t_i^k < T} \log \left[\mu^k + \sum_{l=1}^k \sum_{t_j^l < t_i^k} \alpha^{kl} \beta^{kl} e^{-\beta^{kl}(t_i^k - t_j^l)} \right] - \mu^k T - \sum_{l=1}^k \sum_{t_j^l < T} \alpha^{kl} [1 - e^{-\beta^{kl}(T - t_j^l)}] \quad (\text{A.19})$$

Standard numerical maximization algorithms can now be used to estimate the parameters of a corresponding exponential Hawkes model. It then remains to assess goodness-of-fit of an estimated Hawkes model, which is what we will discuss now. The basic idea is to construct the residual process and compare the observed residual process with its theoretically expected counterpart.

Definition 5. Let $\{t_i\}_{i \in [1, N(T)]} = \bigcup_{k \in [1, K]} \{t_i^k\}_{i \in [1, N^k(T)]}$ be the pooled point process. The residual process is a transformed time sequence $\{\tau_i^k\}_{i \in [1, N(T)]}$ that is computed as:

$$\tau_i^k := \Lambda^k(t_i) \quad (\text{A.20})$$

According to Daley and Vere-Jones (2006), we have the following property:

Proposition 11. Let $\{N^k(t)\}_{k \in [1, K]}$ be a multivariate disjoint point processes defined on $[0, \infty)$ with a finite set of components, filtration \mathcal{F}_t , and the corresponding K dimensional vector of left-continuous \mathcal{F}_t -intensity $\lambda^k(t|\mathcal{F}_t)$. $\forall k \in [1, K]$, suppose that the conditional intensities are strictly

positive and that $\lim_{t \rightarrow \infty} \Lambda^k(t) = \infty$. Then, under simultaneous random-time transformations, the residual processes $\{\tau_i^k\}_{i \in [1, N(T)]}$, $k \in [1, K]$ are independent Poisson processes with unit intensity.

This property is used to test the goodness-of-fit of the model to the data by drawing Q-Q plots of empirical quantiles with respect to the theoretical exponential distribution quantiles.

A.4 ADDITIONAL TABLES AND FIGURES

Table A.1: Empirical results of pair-wise interdependence for selected DJIA stocks (*continued*)

		AAPL					XOM				
		-3	-2	-1	1	2	3	-2	-1	1	2
AAPL	-3	0.58 (0.95)	0.27 (0.40)	0.23 (0.33)	0.70 (0.99)	2.54 (4.54)	14.87 (36.24)	1.25 (1.52)	0.62 (0.87)	0.47 (0.66)	1.10 (1.51)
	-2	2.58 (0.54)	2.05 (0.40)	2.16 (0.41)	6.63 (1.32)	20.37 (4.43)	17.63 (3.96)	4.53 (0.89)	4.40 (0.85)	3.58 (0.70)	4.27 (0.84)
	-1	16.81 (0.49)	17.91 (0.53)	24.73 (0.73)	48.15 (1.41)	40.53 (1.19)	32.12 (0.94)	26.27 (0.77)	31.28 (0.92)	27.88 (0.82)	23.75 (0.70)
	1	30.34 (0.89)	39.51 (1.17)	48.00 (1.42)	24.17 (0.72)	17.91 (0.53)	17.22 (0.51)	25.11 (0.74)	27.30 (0.81)	32.37 (0.96)	28.56 (0.84)
	2	19.43 (4.27)	21.21 (4.54)	6.76 (1.33)	1.95 (0.37)	1.98 (0.39)	2.31 (0.48)	4.08 (0.80)	3.77 (0.72)	4.87 (0.93)	4.94 (0.99)
	3	15.80 (36.82)	3.00 (5.01)	0.70 (0.93)	0.20 (0.27)	0.25 (0.36)	0.48 (0.65)	0.83 (0.90)	0.55 (0.76)	0.79 (1.06)	1.04 (1.32)
	XOM	-2	0.30 (1.24)	0.22 (1.01)	0.18 (0.89)	0.14 (0.70)	0.17 (0.81)	0.26 (1.02)	0.23 (1.12)	0.07 (0.31)	0.50 (2.55)
-1		8.59 (0.85)	9.07 (0.91)	9.58 (0.96)	8.10 (0.81)	6.83 (0.69)	6.38 (0.63)	5.35 (0.57)	5.65 (0.58)	23.90 (2.45)	22.82 (2.38)
1		5.40 (0.54)	6.65 (0.66)	7.55 (0.75)	9.81 (0.98)	9.24 (0.92)	8.46 (0.84)	24.77 (2.55)	25.99 (2.64)	5.59 (0.57)	6.16 (0.62)
2		0.16 (0.79)	0.11 (0.61)	0.11 (0.65)	0.15 (0.91)	0.18 (1.02)	0.28 (1.43)	7.56 (59.18)	0.38 (2.36)	0.05 (0.30)	0.14 (0.74)
Total		0.72	5.08	34.04	33.81	5.16	0.76	0.21	9.97	10.07	0.17

Notes: Conditional probabilities of occurrences of event type k (in rows) given the last occurrence of event type l (in columns): $\Pr(dN^k(t_i) = 1 | dN^l(t_{i-1}) = 1)$. The result is reported in percentage. The last row **Total** presents the unconditional probabilities of each type of events.

Table A.2: Empirical results of pair-wise interdependence for selected DJIA stocks (*continued*)

		AAPL					CVX						
		-3	-2	-1	1	2	3	-3	-2	-1	1	2	3
AAPL	-3	0.58 (1.02)	0.27 (0.45)	0.21 (0.33)	0.67 (1.02)	2.45 (4.70)	14.56 (38.06)	1.35 (2.35)	0.67 (1.06)	0.48 (0.78)	0.38 (0.56)	0.53 (0.94)	1.00 (2.32)
	-2	2.48 (0.56)	1.94 (0.41)	2.09 (0.43)	6.37 (1.37)	19.53 (4.57)	16.62 (3.98)	5.56 (1.21)	4.62 (0.98)	3.76 (0.78)	3.13 (0.66)	3.56 (0.76)	4.22 (0.90)
	-1	16.44 (0.52)	17.28 (0.55)	23.74 (0.75)	46.03 (1.46)	38.88 (1.23)	30.39 (0.96)	27.56 (0.85)	28.40 (0.88)	28.72 (0.90)	25.61 (0.80)	24.71 (0.77)	24.17 (0.75)
	1	29.28 (0.92)	38.06 (1.21)	46.00 (1.46)	22.81 (0.73)	16.97 (0.54)	16.54 (0.52)	24.14 (0.76)	24.77 (0.78)	25.68 (0.81)	29.59 (0.93)	28.95 (0.91)	27.28 (0.85)
	2	19.09 (4.53)	20.44 (4.71)	6.46 (1.37)	1.84 (0.37)	1.88 (0.39)	2.15 (0.47)	5.34 (1.14)	4.06 (0.85)	3.32 (0.68)	4.16 (0.85)	4.92 (1.04)	5.33 (1.12)
	3	15.28 (37.99)	2.90 (5.21)	0.67 (0.96)	0.19 (0.28)	0.25 (0.42)	0.45 (0.65)	0.82 (1.12)	0.63 (0.93)	0.46 (0.65)	0.59 (0.85)	0.86 (1.40)	1.55 (2.82)
	Total	0.67	4.74	31.90	31.68	4.81	0.71	0.52	2.16	10.06	10.10	2.14	0.52

		AAPL					V						
		-3	-2	-1	1	2	3	-3	-2	-1	1	2	3
CVX	-3	1.10 (2.37)	0.67 (1.43)	0.48 (1.01)	0.36 (0.74)	0.50 (1.03)	0.70 (1.48)	0.28 (0.61)	0.15 (0.33)	0.12 (0.23)	0.51 (0.99)	1.85 (3.97)	8.30 (17.45)
	-2	2.51 (1.22)	2.38 (1.15)	2.06 (0.98)	1.61 (0.76)	1.60 (0.75)	1.82 (0.85)	1.25 (0.58)	1.26 (0.61)	1.15 (0.56)	3.45 (1.62)	9.35 (4.26)	7.04 (3.33)
	-1	6.70 (0.68)	7.93 (0.80)	9.07 (0.92)	7.78 (0.78)	6.33 (0.63)	5.46 (0.54)	7.70 (0.82)	8.86 (0.94)	11.58 (1.23)	20.41 (2.07)	14.72 (1.51)	11.61 (1.20)
	1	4.49 (0.45)	6.05 (0.60)	7.32 (0.72)	9.67 (0.97)	8.51 (0.86)	7.61 (0.76)	10.99 (1.13)	15.53 (1.58)	20.80 (2.12)	11.09 (1.17)	9.28 (0.98)	7.76 (0.82)
	2	1.46 (0.65)	1.59 (0.75)	1.54 (0.73)	2.15 (1.04)	2.41 (1.18)	2.50 (1.25)	7.18 (3.39)	9.06 (4.25)	3.43 (1.61)	0.96 (0.47)	1.14 (0.56)	1.50 (0.76)
	3	0.58 (1.19)	0.50 (1.01)	0.36 (0.73)	0.51 (1.05)	0.68 (1.43)	1.19 (2.81)	7.84 (17.64)	2.00 (4.17)	0.49 (0.90)	0.12 (0.22)	0.13 (0.25)	0.24 (0.45)
	Total	0.67	4.74	31.90	31.68	4.81	0.71	0.52	2.16	10.06	10.10	2.14	0.52

		AAPL					V						
		-3	-2	-1	1	2	3	-3	-2	-1	1	2	3
AAPL	-3	0.50 (0.92)	0.24 (0.41)	0.20 (0.30)	0.65 (0.98)	2.39 (4.57)	13.95 (36.11)	1.85 (4.74)	0.93 (1.51)	0.55 (0.90)	0.39 (0.62)	0.58 (0.96)	1.18 (2.02)
	-2	2.29 (0.53)	1.84 (0.39)	1.96 (0.40)	6.25 (1.35)	19.40 (4.58)	16.33 (3.95)	5.93 (1.32)	5.18 (1.15)	4.03 (0.85)	3.12 (0.66)	3.60 (0.79)	4.46 (0.97)
	-1	14.77 (0.47)	16.05 (0.51)	22.58 (0.72)	45.33 (1.45)	37.96 (1.21)	29.94 (0.96)	26.92 (0.86)	28.83 (0.92)	29.98 (0.96)	25.32 (0.81)	23.17 (0.74)	20.02 (0.64)
	1	27.91 (0.89)	37.16 (1.19)	45.24 (1.45)	21.72 (0.70)	15.73 (0.51)	15.33 (0.49)	22.37 (0.72)	23.48 (0.75)	25.08 (0.81)	30.97 (0.99)	30.06 (0.97)	28.55 (0.92)
	2	18.21 (4.31)	20.17 (4.69)	6.34 (1.35)	1.69 (0.34)	1.71 (0.37)	1.84 (0.40)	4.67 (0.98)	3.99 (0.84)	3.38 (0.70)	4.47 (0.94)	5.70 (1.23)	6.81 (1.57)
	3	15.00 (38.13)	2.81 (5.10)	0.64 (0.91)	0.17 (0.24)	0.21 (0.34)	0.41 (0.59)	1.30 (1.97)	0.71 (1.02)	0.47 (0.68)	0.69 (1.04)	1.11 (1.86)	1.88 (3.48)
	Total	0.67	4.69	31.35	31.14	4.76	0.71	0.36	1.70	11.25	11.35	1.69	0.35

Notes: Conditional probabilities of occurrences of event type k (in rows) given the last occurrence of event type l (in columns): $\Pr(dN^k(t_i) = 1 | dN^l(t_{i-1}) = 1)$. The result is reported in percentage. The last row **Total** presents the unconditional probabilities of each type of events.

Table A.3: Empirical results of pair-wise interdependence for selected DJIA stocks (*continued*)

		AXP						CVX					
		-3	-2	-1	1	2	3	-3	-2	-1	1	2	3
AXP	-3	0.43 (1.00)	0.34 (0.44)	0.22 (0.26)	0.68 (0.91)	2.40 (4.13)	10.43 (22.56)	1.71 (2.50)	1.13 (1.56)	0.72 (0.97)	0.50 (0.68)	0.72 (1.04)	1.10 (1.51)
	-2	1.86 (0.79)	1.49 (0.63)	1.28 (0.53)	3.61 (1.53)	9.83 (4.44)	7.58 (3.41)	3.59 (1.50)	3.07 (1.27)	2.41 (0.97)	1.77 (0.72)	2.09 (0.87)	2.52 (1.07)
	-1	10.38 (0.80)	11.68 (0.92)	14.70 (1.17)	23.95 (1.86)	16.46 (1.26)	11.95 (0.93)	11.26 (0.80)	12.34 (0.89)	13.17 (0.95)	10.18 (0.74)	8.99 (0.65)	8.37 (0.60)
	1	12.70 (0.96)	17.80 (1.35)	24.16 (1.85)	14.32 (1.12)	12.15 (0.95)	10.01 (0.79)	8.35 (0.60)	8.98 (0.64)	10.06 (0.73)	13.60 (0.98)	12.82 (0.91)	11.52 (0.82)
	2	8.27 (3.78)	9.74 (4.49)	3.33 (1.41)	1.14 (0.46)	1.49 (0.60)	1.99 (0.87)	2.33 (1.02)	2.12 (0.88)	1.84 (0.75)	2.46 (1.01)	3.14 (1.28)	3.66 (1.53)
	3	9.86 (19.69)	2.49 (4.11)	0.61 (0.85)	0.19 (0.24)	0.27 (0.38)	0.39 (0.59)	1.24 (1.72)	0.82 (1.20)	0.54 (0.75)	0.69 (0.93)	1.11 (1.61)	1.76 (2.72)
	Total	0.74	2.46	13.72	13.81	2.44	0.73	1.34	5.66	26.03	26.15	5.59	1.35
CVX	-3	3.65 (2.95)	2.27 (1.83)	1.25 (0.95)	0.83 (0.65)	1.31 (1.05)	2.29 (1.66)	0.75 (0.67)	0.43 (0.36)	0.32 (0.25)	1.22 (0.93)	4.04 (3.29)	16.13 (13.81)
	-2	8.59 (1.59)	7.09 (1.27)	5.22 (0.93)	3.86 (0.68)	5.04 (0.90)	6.21 (1.12)	3.07 (0.55)	2.91 (0.53)	2.56 (0.45)	7.36 (1.30)	18.06 (3.23)	14.29 (2.63)
	-1	20.03 (0.77)	22.89 (0.88)	24.52 (0.95)	19.82 (0.76)	18.31 (0.70)	16.23 (0.62)	14.20 (0.55)	16.61 (0.65)	22.19 (0.86)	37.60 (1.44)	28.15 (1.08)	22.23 (0.86)
	1	16.45 (0.62)	18.20 (0.69)	19.86 (0.76)	24.96 (0.96)	23.75 (0.91)	21.16 (0.81)	21.75 (0.84)	29.20 (1.12)	37.78 (1.44)	21.99 (0.85)	17.77 (0.69)	14.55 (0.56)
	2	5.69 (1.04)	4.63 (0.83)	4.00 (0.72)	5.37 (0.97)	6.97 (1.27)	8.01 (1.45)	15.21 (2.80)	17.83 (3.25)	7.26 (1.30)	2.31 (0.42)	2.72 (0.50)	3.29 (0.62)
	3	2.07 (1.72)	1.37 (1.02)	0.86 (0.64)	1.27 (0.98)	2.02 (1.68)	3.73 (3.11)	16.54 (14.75)	4.55 (3.72)	1.16 (0.86)	0.31 (0.23)	0.36 (0.29)	0.59 (0.46)
	Total	0.74	2.46	13.72	13.81	2.44	0.73	1.34	5.66	26.03	26.15	5.59	1.35
AXP	-3	0.46 (0.46)	0.40 (0.42)	0.26 (0.25)	0.83 (0.86)	2.93 (3.66)	12.15 (20.37)	2.37 (2.84)	1.39 (1.46)	0.85 (0.90)	0.68 (0.71)	0.96 (1.08)	1.70 (2.02)
	-2	1.84 (0.61)	1.82 (0.60)	1.53 (0.46)	4.18 (1.35)	11.50 (4.04)	9.31 (3.46)	4.77 (1.60)	3.78 (1.23)	3.07 (0.98)	2.24 (0.72)	2.77 (0.90)	3.28 (1.15)
	-1	11.11 (0.67)	12.56 (0.75)	16.48 (0.99)	27.05 (1.61)	18.85 (1.12)	13.90 (0.84)	13.87 (0.82)	15.41 (0.91)	16.80 (0.99)	12.52 (0.74)	10.91 (0.65)	10.14 (0.60)
	1	13.98 (0.83)	20.10 (1.18)	27.25 (1.61)	15.98 (0.95)	13.51 (0.80)	10.79 (0.64)	10.28 (0.60)	11.10 (0.65)	12.47 (0.73)	17.21 (1.01)	16.05 (0.94)	14.75 (0.87)
	2	9.92 (3.53)	11.18 (3.99)	3.97 (1.29)	1.34 (0.41)	1.73 (0.57)	2.06 (0.72)	3.14 (1.06)	2.64 (0.85)	2.26 (0.72)	3.20 (1.04)	4.08 (1.38)	4.72 (1.59)
	3	11.00 (17.03)	3.09 (4.01)	0.73 (0.73)	0.24 (0.25)	0.32 (0.38)	0.39 (0.38)	1.83 (2.26)	1.06 (1.17)	0.64 (0.69)	0.92 (0.97)	1.42 (1.66)	2.59 (2.96)
	Total	0.96	3.13	16.89	17.03	3.10	0.95	1.77	5.34	21.87	21.92	5.21	1.83
IBM	-3	5.04 (3.09)	2.94 (1.66)	1.62 (0.88)	1.20 (0.67)	1.85 (1.03)	3.13 (2.11)	0.96 (0.60)	0.70 (0.44)	0.51 (0.28)	1.61 (0.93)	4.87 (3.14)	15.98 (11.77)
	-2	7.80 (1.47)	6.88 (1.30)	5.32 (0.98)	3.66 (0.68)	4.29 (0.81)	5.34 (1.00)	2.91 (0.55)	2.78 (0.53)	2.75 (0.51)	7.07 (1.33)	15.73 (3.08)	12.48 (2.46)
	-1	17.08 (0.77)	20.32 (0.93)	21.62 (0.99)	16.29 (0.74)	14.72 (0.67)	12.98 (0.59)	13.07 (0.60)	16.01 (0.74)	20.90 (0.96)	31.16 (1.43)	23.83 (1.09)	18.05 (0.83)
	1	13.63 (0.62)	14.39 (0.66)	16.41 (0.75)	22.11 (1.01)	20.52 (0.93)	17.66 (0.81)	16.09 (0.73)	24.02 (1.10)	31.50 (1.44)	20.44 (0.94)	16.18 (0.74)	12.39 (0.57)
	2	5.11 (0.98)	4.38 (0.84)	3.67 (0.70)	5.31 (1.01)	6.63 (1.27)	7.21 (1.41)	13.94 (2.83)	15.77 (3.17)	6.66 (1.29)	2.46 (0.46)	2.61 (0.50)	2.94 (0.57)
	3	3.04 (1.82)	1.95 (1.11)	1.14 (0.63)	1.80 (0.95)	3.15 (1.78)	5.07 (2.89)	16.76 (11.53)	5.36 (3.34)	1.58 (0.87)	0.49 (0.26)	0.60 (0.33)	0.97 (0.57)
	Total	0.96	3.13	16.89	17.03	3.10	0.95	1.77	5.34	21.87	21.92	5.21	1.83

Notes: Conditional probabilities of occurrences of event type k (in rows) given the last occurrence of event type l (in columns): $\Pr(dN^k(t_i) = 1 | dN^l(t_{i-1}) = 1)$. The result is reported in percentage. The last row **Total** presents the unconditional probabilities of each type of events.

Table A.4: Empirical results of pair-wise interdependence for selected DJIA stocks (*continued*)

		CVX						IBM					
		-3	-2	-1	1	2	3	-3	-2	-1	1	2	3
CVX	-3	0.69 (0.70)	0.37 (0.34)	0.27 (0.24)	1.06 (0.90)	3.63 (3.31)	14.76 (14.07)	2.72 (2.37)	1.56 (1.40)	1.10 (0.96)	0.78 (0.68)	1.20 (1.03)	2.04 (1.83)
	-2	2.81 (0.57)	2.55 (0.52)	2.29 (0.46)	6.53 (1.30)	16.29 (3.28)	12.65 (2.62)	7.37 (1.50)	5.87 (1.18)	4.62 (0.92)	3.63 (0.72)	4.32 (0.88)	5.51 (1.12)
	-1	12.53 (0.55)	14.88 (0.65)	19.99 (0.88)	34.18 (1.47)	25.32 (1.10)	20.05 (0.87)	18.36 (0.80)	20.78 (0.90)	21.85 (0.95)	18.25 (0.79)	16.90 (0.73)	15.96 (0.69)
	1	19.39 (0.84)	26.20 (1.13)	34.59 (1.49)	19.45 (0.85)	15.78 (0.69)	13.08 (0.57)	15.55 (0.67)	16.81 (0.72)	18.10 (0.78)	22.56 (0.98)	21.04 (0.91)	19.21 (0.83)
	2	13.56 (2.80)	16.19 (3.32)	6.47 (1.30)	2.01 (0.41)	2.27 (0.46)	2.88 (0.62)	4.96 (1.03)	4.20 (0.85)	3.70 (0.75)	4.84 (0.98)	5.98 (1.23)	6.48 (1.34)
	3	14.53 (14.37)	3.94 (3.59)	1.03 (0.84)	0.26 (0.22)	0.33 (0.31)	0.44 (0.36)	2.04 (1.87)	1.21 (1.03)	0.83 (0.72)	1.12 (1.00)	1.60 (1.43)	2.48 (2.11)
	IBM	-3	2.81 (2.09)	1.94 (1.52)	1.22 (0.95)	0.87 (0.69)	1.21 (0.98)	1.89 (1.45)	0.74 (0.63)	0.46 (0.39)	0.38 (0.30)	1.17 (0.95)	3.57 (3.35)
-2		5.65 (1.49)	4.63 (1.20)	3.82 (0.99)	2.78 (0.73)	3.02 (0.80)	3.28 (0.88)	2.25 (0.61)	2.06 (0.56)	2.08 (0.55)	5.31 (1.46)	12.04 (3.45)	9.35 (2.66)
-1		13.20 (0.83)	14.24 (0.90)	15.00 (0.96)	11.96 (0.77)	10.59 (0.67)	9.22 (0.58)	10.84 (0.74)	12.81 (0.86)	16.64 (1.12)	24.32 (1.64)	18.12 (1.21)	13.82 (0.92)
1		9.37 (0.59)	10.67 (0.68)	11.70 (0.75)	15.79 (1.00)	14.95 (0.94)	13.06 (0.81)	12.79 (0.84)	18.25 (1.22)	24.58 (1.65)	15.85 (1.06)	12.86 (0.86)	9.96 (0.67)
2		3.45 (0.96)	3.13 (0.85)	2.71 (0.73)	3.83 (1.02)	4.61 (1.22)	5.26 (1.41)	10.01 (2.99)	12.07 (3.51)	5.02 (1.41)	1.84 (0.49)	1.89 (0.51)	2.25 (0.63)
3		2.03 (1.77)	1.25 (0.97)	0.91 (0.71)	1.29 (0.99)	2.00 (1.53)	3.44 (2.72)	12.37 (12.15)	3.92 (3.55)	1.11 (0.89)	0.34 (0.26)	0.46 (0.35)	0.62 (0.42)
Total		1.20	5.03	23.11	23.23	4.97	1.20	1.25	3.80	15.57	15.62	3.71	1.29

		IBM						V					
		-3	-2	-1	1	2	3	-3	-2	-1	1	2	3
IBM	-3	0.67 (0.65)	0.43 (0.40)	0.32 (0.26)	1.05 (0.89)	3.32 (3.18)	11.38 (13.14)	2.85 (2.69)	1.88 (1.63)	1.21 (1.01)	0.87 (0.74)	1.15 (1.03)	1.81 (1.77)
	-2	1.95 (0.56)	1.86 (0.53)	1.89 (0.52)	4.98 (1.41)	11.28 (3.32)	8.85 (2.61)	4.90 (1.39)	4.49 (1.26)	3.70 (1.04)	2.61 (0.73)	2.86 (0.80)	3.01 (0.85)
	-1	9.68 (0.68)	11.64 (0.81)	15.23 (1.06)	23.22 (1.60)	17.19 (1.18)	13.13 (0.90)	10.95 (0.76)	12.99 (0.89)	14.45 (0.99)	11.15 (0.76)	9.41 (0.64)	8.11 (0.55)
	1	11.55 (0.79)	17.48 (1.19)	23.52 (1.61)	14.44 (1.00)	11.49 (0.79)	8.96 (0.62)	7.84 (0.53)	9.09 (0.62)	10.75 (0.73)	15.30 (1.05)	13.78 (0.94)	12.17 (0.83)
	2	9.41 (2.85)	11.33 (3.40)	4.68 (1.35)	1.61 (0.45)	1.64 (0.47)	1.79 (0.51)	3.43 (1.01)	2.85 (0.83)	2.54 (0.73)	3.71 (1.07)	4.56 (1.34)	4.82 (1.44)
	3	11.28 (11.68)	3.61 (3.38)	1.04 (0.85)	0.31 (0.25)	0.38 (0.30)	0.55 (0.45)	1.78 (1.82)	1.28 (1.07)	0.87 (0.72)	1.27 (1.05)	1.90 (1.62)	3.01 (2.91)
	V	-3	2.02 (2.83)	1.19 (1.48)	0.76 (0.92)	0.50 (0.60)	0.76 (1.01)	1.22 (1.68)	0.45 (0.49)	0.38 (0.55)	0.23 (0.28)	0.79 (0.99)	3.04 (4.67)
-2		6.20 (1.60)	5.06 (1.29)	3.81 (0.95)	2.60 (0.65)	3.09 (0.81)	4.13 (1.07)	2.58 (0.71)	2.08 (0.53)	1.87 (0.46)	5.22 (1.35)	14.27 (3.99)	13.02 (3.70)
-1		23.44 (0.91)	24.63 (0.95)	25.83 (1.00)	20.30 (0.79)	19.10 (0.74)	17.97 (0.70)	12.05 (0.47)	15.29 (0.60)	20.16 (0.79)	37.39 (1.45)	30.40 (1.18)	24.32 (0.94)
1		18.28 (0.70)	19.01 (0.73)	19.83 (0.76)	26.31 (1.01)	25.59 (0.98)	24.18 (0.93)	24.24 (0.94)	31.38 (1.21)	38.52 (1.48)	19.74 (0.77)	16.29 (0.63)	13.53 (0.52)
2		4.23 (1.14)	3.05 (0.80)	2.60 (0.66)	3.91 (0.99)	5.00 (1.29)	5.66 (1.47)	15.04 (4.19)	15.10 (4.24)	5.01 (1.31)	1.72 (0.44)	2.00 (0.51)	2.62 (0.71)
3		1.30 (1.75)	0.70 (0.90)	0.50 (0.59)	0.76 (0.93)	1.17 (1.59)	2.20 (2.85)	13.89 (28.67)	3.20 (5.22)	0.68 (0.83)	0.22 (0.28)	0.34 (0.48)	0.45 (0.57)
Total		1.18	3.57	14.61	14.67	3.48	1.22	0.83	3.93	25.79	26.03	3.89	0.81

Notes: Conditional probabilities of occurrences of event type k (in rows) given the last occurrence of event type l (in columns): $\Pr(dN^k(t_i) = 1 | dN^l(t_{i-1}) = 1)$. The result is reported in percentage. The last row **Total** presents the unconditional probabilities of each type of events.

Table A.5: Empirical results of pair-wise interdependence for selected DJIA stocks (*continued*)

		AXP					XOM				
		-3	-2	-1	1	2	3	-2	-1	1	2
AXP	-3	0.57 (1.36)	0.32 (0.34)	0.24 (0.24)	0.80 (0.88)	2.87 (3.91)	11.24 (20.55)	1.46 (1.94)	0.98 (1.11)	0.72 (0.80)	0.76 (0.85)
	-2	2.03 (0.75)	1.70 (0.57)	1.49 (0.48)	4.06 (1.39)	11.06 (4.09)	8.42 (3.21)	2.73 (0.96)	3.10 (1.05)	2.23 (0.76)	1.98 (0.68)
	-1	10.87 (0.69)	12.84 (0.82)	16.42 (1.05)	26.44 (1.66)	18.63 (1.16)	13.13 (0.83)	11.98 (0.76)	14.75 (0.92)	11.84 (0.74)	9.39 (0.59)
	1	13.32 (0.83)	19.41 (1.21)	26.55 (1.65)	16.39 (1.04)	13.87 (0.88)	10.76 (0.68)	8.47 (0.52)	11.11 (0.69)	15.71 (0.97)	12.97 (0.79)
	2	9.44 (3.58)	10.65 (4.00)	3.89 (1.34)	1.34 (0.45)	1.68 (0.58)	1.82 (0.64)	2.14 (0.79)	2.14 (0.73)	3.25 (1.12)	3.51 (1.23)
	3	10.89 (18.75)	2.86 (3.78)	0.70 (0.79)	0.22 (0.22)	0.29 (0.40)	0.45 (0.49)	0.83 (1.10)	0.70 (0.81)	1.04 (1.20)	1.49 (2.14)
	Total		0.89	2.95	16.02	16.13	2.92	0.88	0.60	29.43	29.69

		XOM				V					
		-2	-1	1	2	-3	-2	-1	1	2	3
XOM	-2	0.30 (0.68)	0.10 (0.24)	0.80 (2.02)	9.95 (27.70)	0.84 (2.05)	0.46 (1.10)	0.33 (0.84)	0.26 (0.66)	0.29 (0.67)	0.46 (1.16)
	-1	8.62 (0.44)	9.95 (0.50)	36.98 (1.85)	35.08 (1.76)	18.63 (0.93)	18.83 (0.94)	19.23 (0.96)	16.33 (0.81)	14.63 (0.73)	14.36 (0.71)
	1	36.95 (1.84)	39.44 (1.96)	9.63 (0.48)	9.40 (0.47)	14.08 (0.70)	13.92 (0.69)	15.31 (0.76)	19.24 (0.96)	19.53 (0.97)	18.34 (0.91)
	2	10.53 (39.78)	0.59 (1.81)	0.08 (0.25)	0.17 (0.44)	0.33 (0.74)	0.26 (0.83)	0.20 (0.61)	0.26 (0.83)	0.34 (1.02)	0.55 (1.59)
V	-3	1.60 (1.85)	0.86 (1.07)	0.60 (0.76)	0.66 (0.77)	0.36 (0.40)	0.37 (0.61)	0.23 (0.30)	0.75 (0.97)	2.86 (4.59)	12.27 (24.12)
	-2	3.74 (0.99)	3.85 (0.99)	2.81 (0.74)	2.53 (0.66)	2.34 (0.67)	2.07 (0.56)	1.84 (0.48)	5.06 (1.36)	13.84 (4.01)	12.95 (3.82)
	-1	19.68 (0.79)	23.41 (0.94)	20.05 (0.81)	16.37 (0.65)	12.37 (0.50)	15.52 (0.63)	20.01 (0.81)	36.14 (1.46)	29.69 (1.19)	23.97 (0.96)
	1	15.41 (0.61)	18.65 (0.74)	24.25 (0.97)	20.31 (0.81)	23.05 (0.92)	30.74 (1.22)	37.30 (1.49)	19.99 (0.80)	16.48 (0.66)	14.07 (0.56)
	2	2.46 (0.64)	2.62 (0.70)	3.94 (1.03)	3.82 (1.03)	14.63 (4.32)	14.74 (4.30)	4.88 (1.32)	1.74 (0.46)	2.02 (0.54)	2.58 (0.73)
	3	0.71 (0.93)	0.54 (0.68)	0.87 (1.11)	1.70 (2.32)	13.37 (29.41)	3.09 (5.21)	0.66 (0.85)	0.23 (0.31)	0.32 (0.45)	0.45 (0.68)
Total		0.41	20.04	20.21	0.33	0.79	3.78	24.86	25.08	3.74	0.77

Notes: Conditional probabilities of occurrences of event type k (in rows) given the last occurrence of event type l (in columns): $\mathbb{P}\text{r}(dN^k(t_i) = 1 | dN^l(t_{i-1}) = 1)$. The result is reported in percentage. The last row **Total** presents the unconditional probabilities of each type of events.

BIBLIOGRAPHY

- Admati, Anat R. and Paul Pfleiderer (Jan. 1988). 'A Theory of Intraday Patterns: Volume and Price Variability'. In: *Review of Financial Studies* 1.1, pp. 3–40. doi: [10.1093/rfs/1.1.3](https://doi.org/10.1093/rfs/1.1.3).
- Aitken, Michael, Douglas Cumming and Feng Zhan (Oct. 2015). 'High frequency trading and end-of-day price dislocation'. In: *Journal of Banking & Finance* 59, pp. 330–349. doi: [10.1016/j.jbankfin.2015.06.011](https://doi.org/10.1016/j.jbankfin.2015.06.011).
- Amihud, Yakov and Haim Mendelson (July 1987). 'Trading Mechanisms and Stock Returns: An Empirical Investigation'. In: *The Journal of Finance* 42.3, pp. 533–553. doi: [10.1111/j.1540-6261.1987.tb04567.x](https://doi.org/10.1111/j.1540-6261.1987.tb04567.x).
- Andersen, Torben G. and Tim Bollerslev (June 1997). 'Intraday periodicity and volatility persistence in financial markets'. In: *Journal of Empirical Finance* 4.2-3, pp. 115–158. doi: [10.1016/s0927-5398\(97\)00004-2](https://doi.org/10.1016/s0927-5398(97)00004-2).
- Andersen, Torben G., Tim Bollerslev and Francis X. Diebold (2010). 'Parametric and Nonparametric Volatility Measurement'. In: *Handbook of Financial Econometrics: Tools and Techniques*. Elsevier, pp. 67–137. doi: [10.1016/b978-0-444-50897-3.50005-5](https://doi.org/10.1016/b978-0-444-50897-3.50005-5).
- Andersen, Torben G., Tim Bollerslev, Francis X. Diebold and Paul Labys (Mar. 2001). 'The Distribution of Realized Exchange Rate Volatility'. In: *Journal of the American Statistical Association* 96.453, pp. 42–55. doi: [10.1198/016214501750332965](https://doi.org/10.1198/016214501750332965).
- Andersen, Torben G., Tim Bollerslev, Francis X. Diebold and Paul Labys (Mar. 2003). 'Modeling and Forecasting Realized Volatility'. In: *Econometrica* 71.2, pp. 579–625. doi: [10.1111/1468-0262.00418](https://doi.org/10.1111/1468-0262.00418).
- Andersen, Torben G., Tim Bollerslev and Nour Meddahi (Jan. 2005). 'Correcting the Errors: Volatility Forecast Evaluation Using High-Frequency Data and Realized Volatilities'. In: *Econometrica* 73.1, pp. 279–296. doi: [10.1111/j.1468-0262.2005.00572.x](https://doi.org/10.1111/j.1468-0262.2005.00572.x).
- Andersen, Torben G., Dobrislav Dobrev and Ernst Schaumburg (Mar. 2009). *Duration-Based Volatility Estimation*. Global COE Hi-Stat Discussion Paper Series gd08-034. Institute of Economic Research, Hitotsubashi University. URL: <https://ideas.repec.org/p/hst/ghsdps/gd08-034.html>.
- Aquilina, Matteo, Eric Budish and Peter O'Neill (Sept. 2021). 'Quantifying the High-Frequency Trading "Arms Race"'. In: *The Quarterly Journal of Economics* 137.1, pp. 493–564. doi: [10.1093/qje/qjab032](https://doi.org/10.1093/qje/qjab032).
- Asai, Manabu, Michael McAleer and Jun Yu (Sept. 2006). 'Multivariate Stochastic Volatility: A Review'. In: *Econometric Reviews* 25.2-3, pp. 145–175. doi: [10.1080/07474930600713564](https://doi.org/10.1080/07474930600713564).
- Aït-Sahalia, Yacine, Jianqing Fan and Dacheng Xiu (Dec. 2010). 'High-Frequency Covariance Estimates With Noisy and Asynchronous Financial Data'. In: *Journal of the American Statistical Association* 105.492, pp. 1504–1517. doi: [10.1198/jasa.2010.tm10163](https://doi.org/10.1198/jasa.2010.tm10163).
- Aït-Sahalia, Yacine and Jean Jacod (Dec. 2012). 'Analyzing the Spectrum of Asset Returns: Jump and Volatility Components in High Frequency Data'. In: *Journal of Economic Literature* 50.4, pp. 1007–1050. doi: [10.1257/jel.50.4.1007](https://doi.org/10.1257/jel.50.4.1007).
- Aït-Sahalia, Yacine, Per A. Mykland and Lan Zhang (2005). 'How Often to Sample a Continuous-Time Process in the Presence of Market Microstructure Noise'. In: *Review of Financial Studies* 18.2, pp. 351–416. doi: [10.1093/rfs/hhi016](https://doi.org/10.1093/rfs/hhi016).
- Aït-Sahalia, Yacine and Dacheng Xiu (Oct. 2016). 'Increased correlation among asset classes: Are volatility or jumps to blame, or both?' In: *Journal of Econometrics* 194.2, pp. 205–219. doi: [10.1016/j.jeconom.2016.05.002](https://doi.org/10.1016/j.jeconom.2016.05.002).
- Aït-Sahalia, Yacine and Jialin Yu (Mar. 2009). 'High frequency market microstructure noise estimates and liquidity measures'. In: *The Annals of Applied Statistics* 3.1. doi: [10.1214/08-aoas200](https://doi.org/10.1214/08-aoas200).
- Bacry, E., K. Dayri and J. F. Muzy (May 2012). 'Non-parametric kernel estimation for symmetric Hawkes processes. Application to high frequency financial data'. In: *The European Physical Journal B* 85.5. doi: [10.1140/epjb/e2012-21005-8](https://doi.org/10.1140/epjb/e2012-21005-8).
- Bacry, E., S. Delattre, M. Hoffmann and J. F. Muzy (Jan. 2013). 'Modelling microstructure noise with mutually exciting point processes'. In: *Quantitative Finance* 13.1, pp. 65–77. doi: [10.1080/14697688.2011.647054](https://doi.org/10.1080/14697688.2011.647054).
- Bacry, Emmanuel, Martin Bompain, Philip Deegan, Stéphane Gaïffas and Søren V. Poulsen (2018). 'tick: a Python Library for Statistical Learning, with an emphasis on Hawkes Processes and Time-Dependent Models'. In: *Journal of Machine Learning Research* 18.214, pp. 1–5. URL: <http://jmlr.org/papers/v18/17-381.html>.
- Bacry, Emmanuel, Thibault Jaisson and Jean-François Muzy (Apr. 2016). 'Estimation of slowly decreasing Hawkes kernels: application to high-frequency order book dynamics'. In: *Quantitative Finance* 16.8, pp. 1179–1201. doi: [10.1080/14697688.2015.1123287](https://doi.org/10.1080/14697688.2015.1123287).
- Bacry, Emmanuel, Iacopo Mastromatteo and Jean-François Muzy (June 2015). 'Hawkes Processes in Finance'. In: *Market Microstructure and Liquidity* 01.01, p. 1550005. doi: [10.1142/s2382626615500057](https://doi.org/10.1142/s2382626615500057).

- Bacry, Emmanuel and Jean-Francois Muzy (Apr. 2016). 'First- and Second-Order Statistics Characterization of Hawkes Processes and Non-Parametric Estimation'. In: *IEEE Transactions on Information Theory* 62.4, pp. 2184–2202. doi: [10.1109/tit.2016.2533397](https://doi.org/10.1109/tit.2016.2533397).
- Ball, Clifford A. (Sept. 1988). 'Estimation Bias Induced by Discrete Security Prices'. In: *The Journal of Finance* 43.4, pp. 841–865. doi: [10.1111/j.1540-6261.1988.tb02608.x](https://doi.org/10.1111/j.1540-6261.1988.tb02608.x).
- Bandi, F. M. and J. R. Russell (Apr. 2008). 'Microstructure Noise, Realized Variance, and Optimal Sampling'. In: *Review of Economic Studies* 75.2, pp. 339–369. doi: [10.1111/j.1467-937x.2008.00474.x](https://doi.org/10.1111/j.1467-937x.2008.00474.x).
- Bandi, Federico M. and Jeffrey R. Russell (Mar. 2006). 'Separating microstructure noise from volatility'. In: *Journal of Financial Economics* 79.3, pp. 655–692. doi: [10.1016/j.jfineco.2005.01.005](https://doi.org/10.1016/j.jfineco.2005.01.005).
- Banulescu, Denisa, Gilbert Colletaz, Christophe Hurlin and Sessi Tokpavi (Nov. 2015). 'Forecasting High-Frequency Risk Measures'. In: *Journal of Forecasting* 35.3, pp. 224–249. doi: [10.1002/for.2374](https://doi.org/10.1002/for.2374).
- Barndorff-Nielsen, Ole E., Peter Reinhard Hansen, Asger Lunde and Neil Shephard (2008). 'Designing Realized Kernels to Measure the ex post Variation of Equity Prices in the Presence of Noise'. In: *Econometrica* 76.6, pp. 1481–1536. doi: [10.3982/ecta6495](https://doi.org/10.3982/ecta6495).
- (June 2011). 'Multivariate realised kernels: Consistent positive semi-definite estimators of the covariation of equity prices with noise and non-synchronous trading'. In: *Journal of Econometrics* 162.2, pp. 149–169. doi: [10.1016/j.jeconom.2010.07.009](https://doi.org/10.1016/j.jeconom.2010.07.009).
- Barndorff-Nielsen, Ole E. and Neil Shephard (May 2002a). 'Econometric analysis of realized volatility and its use in estimating stochastic volatility models'. In: *Journal of the Royal Statistical Society: Series B (Statistical Methodology)* 64.2, pp. 253–280. doi: [10.1111/1467-9868.00336](https://doi.org/10.1111/1467-9868.00336).
- (2002b). 'Estimating quadratic variation using realized variance'. In: *Journal of Applied Econometrics* 17.5, pp. 457–477. doi: [10.1002/jae.691](https://doi.org/10.1002/jae.691).
- (May 2004). 'Econometric Analysis of Realized Covariation: High Frequency Based Covariance, Regression, and Correlation in Financial Economics'. In: *Econometrica* 72.3, pp. 885–925. doi: [10.1111/j.1468-0262.2004.00515.x](https://doi.org/10.1111/j.1468-0262.2004.00515.x).
- (2007). 'Variation, Jumps, and High-Frequency Data in Financial Econometrics'. In: *Advances in Economics and Econometrics: Theory and Applications, Ninth World Congress*. Ed. by Richard Blundell, Whitney Newey and Torsten Editors Persson. Vol. 3. Econometric Society Monographs. Cambridge University Press, 328–372. doi: [10.1017/CB09780511607547.011](https://doi.org/10.1017/CB09780511607547.011).
- Barndorff-Nielsen, Ole E., Neil Shephard and Matthias Winkel (May 2006). 'Limit theorems for multipower variation in the presence of jumps'. In: *Stochastic Processes and their Applications* 116.5, pp. 796–806. doi: [10.1016/j.spa.2006.01.007](https://doi.org/10.1016/j.spa.2006.01.007).
- Basak, Suleyman and Alexander Shapiro (Apr. 2001). 'Value-at-Risk-Based Risk Management: Optimal Policies and Asset Prices'. In: *Review of Financial Studies* 14.2, pp. 371–405. doi: [10.1093/rfs/14.2.371](https://doi.org/10.1093/rfs/14.2.371).
- Basel Committee on Banking Supervision (Feb. 2011). *Revisions to the Basel II market risk framework*. <https://www.bis.org/publ/bcbs193.pdf>. Accessed: 30 July 2022.
- (Jan. 2019). *Minimum capital requirements for market risk*. <https://www.bis.org/bcbs/publ/d457.pdf/>. Accessed: 30 July 2022.
- (Nov. 2021). *The Basel Framework*. https://www.bis.org/basel_framework/. Accessed: 30 July 2022.
- Bauwens and Giot (2000). 'The Logarithmic ACD Model: An Application to the Bid-Ask Quote Process of Three NYSE Stocks'. In: *Annales d'Économie et de Statistique* 60, p. 117. doi: [10.2307/20076257](https://doi.org/10.2307/20076257).
- Bauwens, L. (May 2006). 'Stochastic Conditional Intensity Processes'. In: *Journal of Financial Econometrics* 4.3, pp. 450–493. doi: [10.1093/jjfinec/nbj013](https://doi.org/10.1093/jjfinec/nbj013).
- Bauwens, Luc, Sébastien Laurent and Jeroen V. K. Rombouts (Jan. 2006). 'Multivariate GARCH models: a survey'. In: *Journal of Applied Econometrics* 21.1, pp. 79–109. doi: [10.1002/jae.842](https://doi.org/10.1002/jae.842).
- Bernhardt, Dan and Reza S. Mahani (July 2007). 'Asymmetric information and stock return cross-autocorrelations'. In: *Economics Letters* 96.1, pp. 14–22. doi: [10.1016/j.econlet.2006.12.004](https://doi.org/10.1016/j.econlet.2006.12.004).
- Bibinger, Markus (June 2012). 'An estimator for the quadratic covariation of asynchronously observed Itô processes with noise: Asymptotic distribution theory'. In: *Stochastic Processes and their Applications* 122.6, pp. 2411–2453. doi: [10.1016/j.spa.2012.04.002](https://doi.org/10.1016/j.spa.2012.04.002).
- Bieñ-Barkowska, Katarzyna (July 2020). 'Looking at Extremes without Going to Extremes: A New Self-Exciting Probability Model for Extreme Losses in Financial Markets'. In: *Entropy* 22.7, p. 789. doi: [10.3390/e22070789](https://doi.org/10.3390/e22070789).
- Bien, Katarzyna, Ingmar Nolte and Winfried Pohlmeier (2006). *A Multivariate Integer Count Hurdle model: Theory and application to exchange rate dynamics*. eng. urn:nbn:de:bsz:352-opus-32361. Konstanz. URL: <http://hdl.handle.net/10419/32153>.
- Bloomfield, Robert, Maureen O'Hara and Gideon Saar (Jan. 2005). 'The "make or take" decision in an electronic market: Evidence on the evolution of liquidity'. In: *Journal of Financial Economics* 75.1, pp. 165–199. doi: [10.1016/j.jfineco.2004.07.001](https://doi.org/10.1016/j.jfineco.2004.07.001).
- Bollerslev, Tim (Apr. 1986). 'Generalized autoregressive conditional heteroskedasticity'. In: *Journal of Econometrics* 31.3, pp. 307–327. doi: [10.1016/0304-4076\(86\)90063-1](https://doi.org/10.1016/0304-4076(86)90063-1).

- (1987). 'A Conditionally Heteroskedastic Time Series Model for Speculative Prices and Rates of Return'. In: *The Review of Economics and Statistics* 69.3, pp. 542–547. ISSN: 00346535, 15309142. URL: <http://www.jstor.org/stable/1925546>.
- Bollerslev, Tim and Michael Melvin (May 1994). 'Bid - ask spreads and volatility in the foreign exchange market'. In: *Journal of International Economics* 36.3-4, pp. 355–372. doi: [10.1016/0022-1996\(94\)90008-6](https://doi.org/10.1016/0022-1996(94)90008-6).
- Boulatov, A., T. Hendershott and D. Livdan (Apr. 2012). 'Informed Trading and Portfolio Returns'. In: *The Review of Economic Studies* 80.1, pp. 35–72. doi: [10.1093/restud/rds020](https://doi.org/10.1093/restud/rds020).
- Bowsher, Clive G. (Dec. 2007). 'Modelling security market events in continuous time: Intensity based, multivariate point process models'. In: *Journal of Econometrics* 141.2, pp. 876–912. doi: [10.1016/j.jeconom.2006.11.007](https://doi.org/10.1016/j.jeconom.2006.11.007).
- Brennan, Michael J., Narasimhan Jegadeesh and Bhaskaran Swaminathan (Oct. 1993). 'Investment Analysis and the Adjustment of Stock Prices to Common Information'. In: *Review of Financial Studies* 6.4, pp. 799–824. doi: [10.1093/rfs/6.4.799](https://doi.org/10.1093/rfs/6.4.799).
- Brogaard, Jonathan, Allen Carrion, Thibaut Moyaert, Ryan Riordan, Andriy Shkilko and Konstantin Sokolov (May 2018). 'High frequency trading and extreme price movements'. In: *Journal of Financial Economics* 128.2, pp. 253–265. doi: [10.1016/j.jfineco.2018.02.002](https://doi.org/10.1016/j.jfineco.2018.02.002).
- Brogaard, Jonathan, Terrence Hendershott and Ryan Riordan (May 2014). 'High-Frequency Trading and Price Discovery'. In: *Review of Financial Studies* 27.8, pp. 2267–2306. doi: [10.1093/rfs/hhu032](https://doi.org/10.1093/rfs/hhu032).
- Brownlees, Christian, Eulalia Nualart and Yucheng Sun (Mar. 2020). 'On the estimation of integrated volatility in the presence of jumps and microstructure noise'. In: *Econometric Reviews* 39.10, pp. 991–1013. doi: [10.1080/07474938.2020.1735751](https://doi.org/10.1080/07474938.2020.1735751).
- Buccheri, Giuseppe, Giacomo Bormetti, Fulvio Corsi and Fabrizio Lillo (Mar. 2019). 'Comment on: Price Discovery in High Resolution'. In: *Journal of Financial Econometrics* 19.3, pp. 439–451. doi: [10.1093/jjfinec/nbz008](https://doi.org/10.1093/jjfinec/nbz008).
- Buccheri, Giuseppe, Fulvio Corsi and Stefano Peluso (Jan. 2020). 'High-Frequency Lead-Lag Effects and Cross-Asset Linkages: A Multi-Asset Lagged Adjustment Model'. In: *Journal of Business & Economic Statistics* 39.3, pp. 605–621. doi: [10.1080/07350015.2019.1697699](https://doi.org/10.1080/07350015.2019.1697699).
- Candelon, B., G. Colletaz, C. Hurlin and S. Tokpavi (Aug. 2010). 'Backtesting Value-at-Risk: A GMM Duration-Based Test'. In: *Journal of Financial Econometrics* 9.2, pp. 314–343. doi: [10.1093/jjfinec/nbq025](https://doi.org/10.1093/jjfinec/nbq025).
- Carnero, M. A. (Mar. 2004). 'Persistence and Kurtosis in GARCH and Stochastic Volatility Models'. In: *Journal of Financial Econometrics* 2.2, pp. 319–342. doi: [10.1093/jjfinec/nbh012](https://doi.org/10.1093/jjfinec/nbh012).
- Chan, Kalok (Jan. 1992). 'A Further Analysis of the Lead-Lag Relationship Between the Cash Market and Stock Index Futures Market'. In: *Review of Financial Studies* 5.1, pp. 123–152. doi: [10.1093/rfs/5.1.123](https://doi.org/10.1093/rfs/5.1.123).
- (Sept. 1993). 'Imperfect Information and Cross-Autocorrelation among Stock Prices'. In: *The Journal of Finance* 48.4, pp. 1211–1230. doi: [10.1111/j.1540-6261.1993.tb04752.x](https://doi.org/10.1111/j.1540-6261.1993.tb04752.x).
- Chao, Yong, Chen Yao and Mao Ye (May 2017). 'Discrete Pricing and Market Fragmentation: A Tale of Two-Sided Markets'. In: *American Economic Review* 107.5, pp. 196–199. doi: [10.1257/aer.p20171046](https://doi.org/10.1257/aer.p20171046).
- (July 2018). 'Why Discrete Price Fragments U.S. Stock Exchanges and Disperses Their Fee Structures'. In: *The Review of Financial Studies* 32.3, pp. 1068–1101. doi: [10.1093/rfs/hhy073](https://doi.org/10.1093/rfs/hhy073).
- Chavez-Demoulin, V., A. C. Davison and A. J. McNeil (Apr. 2005). 'Estimating value-at-risk: a point process approach'. In: *Quantitative Finance* 5.2, pp. 227–234. doi: [10.1080/14697680500039613](https://doi.org/10.1080/14697680500039613).
- Chavez-Demoulin, V., P. Embrechts and S. Sardy (July 2014). 'Extreme-quantile tracking for financial time series'. In: *Journal of Econometrics* 181.1, pp. 44–52. doi: [10.1016/j.jeconom.2014.02.007](https://doi.org/10.1016/j.jeconom.2014.02.007).
- Chavez-Demoulin, V. and J.A. McGill (Dec. 2012). 'High-frequency financial data modeling using Hawkes processes'. In: *Journal of Banking & Finance* 36.12, pp. 3415–3426. doi: [10.1016/j.jbankfin.2012.08.011](https://doi.org/10.1016/j.jbankfin.2012.08.011).
- Chiao, Chaoshin, Ken Hung and Cheng F. Lee (Dec. 2004). 'The price adjustment and lead-lag relations between stock returns: microstructure evidence from the Taiwan stock market'. In: *Journal of Empirical Finance* 11.5, pp. 709–731. doi: [10.1016/j.jempfin.2003.09.002](https://doi.org/10.1016/j.jempfin.2003.09.002).
- Chordia, Tarun, Richard Roll and Avanidhar Subrahmanyam (Apr. 2000). 'Commonality in liquidity'. In: *Journal of Financial Economics* 56.1, pp. 3–28. doi: [10.1016/s0304-405x\(99\)00057-4](https://doi.org/10.1016/s0304-405x(99)00057-4).
- Chordia, Tarun, Asani Sarkar and Avanidhar Subrahmanyam (Feb. 2011). 'Liquidity Dynamics and Cross-Autocorrelations'. In: *Journal of Financial and Quantitative Analysis* 46.3, pp. 709–736. doi: [10.1017/s0022109011000081](https://doi.org/10.1017/s0022109011000081).
- Christensen, Kim, Silja Kinnebrock and Mark Podolskij (Nov. 2010). 'Pre-averaging estimators of the ex-post covariance matrix in noisy diffusion models with non-synchronous data'. In: *Journal of Econometrics* 159.1, pp. 116–133. doi: [10.1016/j.jeconom.2010.05.001](https://doi.org/10.1016/j.jeconom.2010.05.001).
- Christensen, Kim, Mark Podolskij and Mathias Vetter (Sept. 2013). 'On covariation estimation for multivariate continuous Itô semimartingales with noise in non-synchronous observation schemes'. In: *Journal of Multivariate Analysis* 120, pp. 59–84. doi: [10.1016/j.jmva.2013.05.002](https://doi.org/10.1016/j.jmva.2013.05.002).
- Christoffersen, P. (Dec. 2004). 'Backtesting Value-at-Risk: A Duration-Based Approach'. In: *Journal of Financial Econometrics* 2.1, pp. 84–108. doi: [10.1093/jjfinec/nbh004](https://doi.org/10.1093/jjfinec/nbh004).
- Christoffersen, Peter F. (Nov. 1998). 'Evaluating Interval Forecasts'. In: *International Economic Review* 39.4, p. 841. doi: [10.2307/2527341](https://doi.org/10.2307/2527341).

- Cizeau, P., M. Potters and J-P. Bouchaud (2001). 'Correlation structure of extreme stock returns'. In: *Quantitative Finance* 1.2, pp. 217–222. doi: [10.1080/713665669](https://doi.org/10.1080/713665669). eprint: <https://doi.org/10.1080/713665669>. URL: <https://doi.org/10.1080/713665669>.
- Coroneo, Laura and David Veredas (Oct. 2012). 'A simple two-component model for the distribution of intraday returns'. In: *The European Journal of Finance* 18.9, pp. 775–797. doi: [10.1080/1351847x.2011.601649](https://doi.org/10.1080/1351847x.2011.601649).
- Corsi, Fulvio, Stefano Peluso and Francesco Audrino (Jan. 2014). 'Missing in Asynchronicity: A Kalman-em Approach for Multivariate Realized Covariance Estimation'. In: *Journal of Applied Econometrics* 30.3, pp. 377–397. doi: [10.1002/jae.2378](https://doi.org/10.1002/jae.2378).
- Cousin, Areski and Elena Di Bernardino (Aug. 2013). 'On multivariate extensions of Value-at-Risk'. In: *Journal of Multivariate Analysis* 119, pp. 32–46. doi: [10.1016/j.jmva.2013.03.016](https://doi.org/10.1016/j.jmva.2013.03.016).
- Curci, Giuseppe and Fulvio Corsi (Feb. 2012). 'Discrete sine transform for multi-scale realized volatility measures'. In: *Quantitative Finance* 12.2, pp. 263–279. doi: [10.1080/14697688.2010.490561](https://doi.org/10.1080/14697688.2010.490561).
- Curme, Chester, Michele Tumminello, Rosario N. Mantegna, H. Eugene Stanley and Dror Y. Kenett (2015). 'How Lead-Lag Correlations Affect the Intraday Pattern of Collective Stock Dynamics'. In: *SSRN Electronic Journal*. doi: [10.2139/ssrn.2648490](https://doi.org/10.2139/ssrn.2648490).
- Daley, D. J. and D. Vere-Jones (Apr. 2006). *An Introduction to the Theory of Point Processes*. Springer New York. 471 pp. ISBN: 9780387215648.
- Damodaran, Aswath (Mar. 1993). 'A Simple Measure of Price Adjustment Coefficients'. In: *The Journal of Finance* 48.1, pp. 387–400. doi: [10.1111/j.1540-6261.1993.tb04716.x](https://doi.org/10.1111/j.1540-6261.1993.tb04716.x).
- Dao, Thong Minh, Frank McGroarty and Andrew Urquhart (Jan. 2018). 'Ultra-high-frequency lead-lag relationship and information arrival'. In: *Quantitative Finance* 18.5, pp. 725–735. doi: [10.1080/14697688.2017.1414484](https://doi.org/10.1080/14697688.2017.1414484).
- Darolles, Gouriéroux and Le Fol (2000). 'Intraday Transaction Price Dynamics'. In: *Annales d'Économie et de Statistique* 60, p. 207. doi: [10.2307/20076261](https://doi.org/10.2307/20076261). URL: <https://www.jstor.org/stable/20076261>.
- Diamond, Douglas W. and Robert E. Verrecchia (June 1987). 'Constraints on short-selling and asset price adjustment to private information'. In: *Journal of Financial Economics* 18.2, pp. 277–311. doi: [10.1016/0304-405x\(87\)90042-0](https://doi.org/10.1016/0304-405x(87)90042-0).
- Diebold, F. X. and G. Strasser (Feb. 2013). 'On the Correlation Structure of Microstructure Noise: A Financial Economic Approach'. In: *The Review of Economic Studies* 80.4, pp. 1304–1337. doi: [10.1093/restud/rdt008](https://doi.org/10.1093/restud/rdt008).
- Dionne, Georges, Pierre Duchesne and Maria Pacurar (Dec. 2009). 'Intraday Value at Risk (IVaR) using tick-by-tick data with application to the Toronto Stock Exchange'. In: *Journal of Empirical Finance* 16.5, pp. 777–792. doi: [10.1016/j.jempfin.2009.05.005](https://doi.org/10.1016/j.jempfin.2009.05.005).
- Duffie, Darrell (2010). *Dynamic asset pricing theory*. Princeton University Press.
- Dufour, Alfonso and Robert F. Engle (Dec. 2000). 'Time and the Price Impact of a Trade'. In: *The Journal of Finance* 55.6, pp. 2467–2498. doi: [10.1111/0022-1082.00297](https://doi.org/10.1111/0022-1082.00297). URL: <https://doi.org/10.1111/0022-1082.00297>.
- Easley, David and Maureen O'hara (June 1992). 'Time and the Process of Security Price Adjustment'. In: *The Journal of Finance* 47.2, pp. 577–605. doi: [10.1111/j.1540-6261.1992.tb04402.x](https://doi.org/10.1111/j.1540-6261.1992.tb04402.x).
- Embrechts, Paul, Thomas Liniger and Lu Lin (Aug. 2011). 'Multivariate Hawkes processes: an application to financial data'. In: *Journal of Applied Probability* 48.A, pp. 367–378. doi: [10.1239/jap/1318940477](https://doi.org/10.1239/jap/1318940477).
- Engle, Robert F. (1982). 'Autoregressive Conditional Heteroscedasticity with Estimates of the Variance of United Kingdom Inflation'. In: *Econometrica* 50.4, pp. 987–1007. ISSN: 00129682, 14680262. URL: <http://www.jstor.org/stable/1912773>.
- (2000). 'The Econometrics of Ultra-High-Frequency Data'. In: *Econometrica* 68.1, pp. 1–22. ISSN: 00129682, 14680262. URL: <http://www.jstor.org/stable/2999473>.
- Engle, Robert F and Simone Manganelli (Oct. 2004). 'CAViaR: Conditional Autoregressive Value at Risk by Regression Quantiles'. In: *Journal of Business & Economic Statistics* 22.4, pp. 367–381. doi: [10.1198/073500104000000370](https://doi.org/10.1198/073500104000000370).
- Engle, Robert F. and Jeffrey R. Russell (1998). 'Autoregressive Conditional Duration: A New Model for Irregularly Spaced Transaction Data'. In: *Econometrica* 66.5, pp. 1127–1162. ISSN: 00129682, 14680262. URL: <http://www.jstor.org/stable/2999632>.
- Engle, Robert and Jeffrey Russell (Dec. 1994). *Forecasting Transaction Rates: The Autoregressive Conditional Duration Model*. Tech. rep. doi: [10.3386/w4966](https://doi.org/10.3386/w4966).
- Epps, Thomas W. (June 1979). 'Comovements in Stock Prices in the Very Short Run'. In: *Journal of the American Statistical Association* 74.366a, pp. 291–298. doi: [10.1080/01621459.1979.10482508](https://doi.org/10.1080/01621459.1979.10482508).
- Fama, Eugene F. (Sept. 1998). 'Market efficiency, long-term returns, and behavioral finance'. In: *Journal of Financial Economics* 49.3, pp. 283–306. doi: [10.1016/s0304-405x\(98\)00026-9](https://doi.org/10.1016/s0304-405x(98)00026-9).
- Fernandes, Marcelo and Joachim Grammig (Jan. 2006). 'A family of autoregressive conditional duration models'. In: *Journal of Econometrics* 130.1, pp. 1–23. doi: [10.1016/j.jeconom.2004.08.016](https://doi.org/10.1016/j.jeconom.2004.08.016).
- Filimonov, Vladimir and Didier Sornette (May 2012). 'Quantifying reflexivity in financial markets: Toward a prediction of flash crashes'. In: *Physical Review E* 85.5, p. 056108. doi: [10.1103/physreve.85.056108](https://doi.org/10.1103/physreve.85.056108).
- Filimonov, Vladimir, Spencer Wheatley and Didier Sornette (May 2015). 'Effective measure of endogeneity for the Autoregressive Conditional Duration point processes via mapping to the self-excited Hawkes

- process'. In: *Communications in Nonlinear Science and Numerical Simulation* 22.1-3, pp. 23–37. doi: [10.1016/j.cnsns.2014.08.042](https://doi.org/10.1016/j.cnsns.2014.08.042).
- Garman, Mark B. (June 1976). 'Market microstructure'. In: *Journal of Financial Economics* 3.3, pp. 257–275. doi: [10.1016/0304-405x\(76\)90006-4](https://doi.org/10.1016/0304-405x(76)90006-4).
- Gerhard, Frank and Nikolaus Hautsch (Jan. 2002). 'Volatility estimation on the basis of price intensities'. In: *Journal of Empirical Finance* 9.1, pp. 57–89. doi: [10.1016/s0927-5398\(01\)00045-7](https://doi.org/10.1016/s0927-5398(01)00045-7).
- Giot, Pierre (Aug. 2005). 'Market risk models for intraday data'. In: *The European Journal of Finance* 11.4, pp. 309–324. doi: [10.1080/1351847032000143396](https://doi.org/10.1080/1351847032000143396).
- Glosten, Lawrence R. and Paul R. Milgrom (1985). 'Bid, ask and transaction prices in a specialist market with heterogeneously informed traders'. In: *Journal of Financial Economics* 14.1, pp. 71–100. issn: 0304-405X. doi: [https://doi.org/10.1016/0304-405X\(85\)90044-3](https://doi.org/10.1016/0304-405X(85)90044-3). URL: <https://www.sciencedirect.com/science/article/pii/0304405X85900443>.
- Gloter, Arnaud and Jean Jacod (2001). 'Diffusions with measurement errors. I. Local Asymptotic Normality'. In: *ESAIM: Probability and Statistics* 5, pp. 225–242. doi: [10.1051/ps:2001110](https://doi.org/10.1051/ps:2001110).
- Goldstein, Michael A., Pavitra Kumar and Frank C. Graves (Apr. 2014). 'Computerized and High-Frequency Trading'. In: *Financial Review* 49.2, pp. 177–202. doi: [10.1111/fire.12031](https://doi.org/10.1111/fire.12031).
- Gomes, C. and H. Waelbroeck (Oct. 2014). 'Is market impact a measure of the information value of trades? Market response to liquidity vs. informed metaorders'. In: *Quantitative Finance* 15.5, pp. 773–793. doi: [10.1080/14697688.2014.963140](https://doi.org/10.1080/14697688.2014.963140).
- Gottlieb, Gary and Avner Kalay (Mar. 1985). 'Implications of the Discreteness of Observed Stock Prices'. In: *The Journal of Finance* 40.1, pp. 135–153. doi: [10.1111/j.1540-6261.1985.tb04941.x](https://doi.org/10.1111/j.1540-6261.1985.tb04941.x).
- Gouriéroux, Christian, Joanna Jasiak and Gaëlle Le Fol (1999). 'Intra-day market activity'. In: *Journal of Financial Markets* 2.3, pp. 193–226. issn: 1386-4181. doi: [https://doi.org/10.1016/S1386-4181\(99\)00004-X](https://doi.org/10.1016/S1386-4181(99)00004-X). URL: <https://www.sciencedirect.com/science/article/pii/S138641819900004X>.
- Grammig, Joachim and Kai-Oliver Maurer (June 2000). 'Non-monotonic hazard functions and the autoregressive conditional duration model'. In: *The Econometrics Journal* 3.1, pp. 16–38. doi: [10.1111/1368-423x.00037](https://doi.org/10.1111/1368-423x.00037).
- Grothe, Oliver, Volodymyr Korniihuk and Hans Manner (Oct. 2014). 'Modeling multivariate extreme events using self-exciting point processes'. In: *Journal of Econometrics* 182.2, pp. 269–289. doi: [10.1016/j.jeconom.2014.03.011](https://doi.org/10.1016/j.jeconom.2014.03.011).
- Hall, Anthony D. and Nikolaus Hautsch (Aug. 2007). 'Modelling the buy and sell intensity in a limit order book market'. In: *Journal of Financial Markets* 10.3, pp. 249–286. doi: [10.1016/j.finmar.2006.12.002](https://doi.org/10.1016/j.finmar.2006.12.002).
- Hansen, Peter R. and Asger Lunde (Apr. 2006a). 'Realized Variance and Market Microstructure Noise'. In: *Journal of Business & Economic Statistics* 24.2, pp. 127–161. doi: [10.1198/073500106000000071](https://doi.org/10.1198/073500106000000071).
- (Apr. 2006b). 'Realized Variance and Market Microstructure Noise'. In: *Journal of Business & Economic Statistics* 24.2, pp. 127–161. doi: [10.1198/073500106000000071](https://doi.org/10.1198/073500106000000071).
- Harford, Jarrad and Aditya Kaul (Mar. 2005). 'Correlated Order Flow: Pervasiveness, Sources, and Pricing Effects'. In: *Journal of Financial and Quantitative Analysis* 40.1, pp. 29–55. doi: [10.1017/s0022109000001733](https://doi.org/10.1017/s0022109000001733).
- Harris, Lawrence (Sept. 1990). 'Estimation of Stock Price Variances and Serial Covariances from Discrete Observations'. In: *The Journal of Financial and Quantitative Analysis* 25.3, p. 291. doi: [10.2307/2330697](https://doi.org/10.2307/2330697).
- Hasbrouck, J (Mar. 2001). 'Common factors in prices, order flows, and liquidity'. In: *Journal of Financial Economics* 59.3, pp. 383–411. doi: [10.1016/s0304-405x\(00\)00091-x](https://doi.org/10.1016/s0304-405x(00)00091-x).
- Hasbrouck, Joel (Mar. 1991). 'Measuring the Information Content of Stock Trades'. In: *The Journal of Finance* 46.1, pp. 179–207. doi: [10.1111/j.1540-6261.1991.tb03749.x](https://doi.org/10.1111/j.1540-6261.1991.tb03749.x).
- (1996). 'Modeling market microstructure time series'. In: *Handbook of Statistics*. Elsevier, pp. 647–692. doi: [10.1016/s0169-7161\(96\)14024-4](https://doi.org/10.1016/s0169-7161(96)14024-4).
- (Feb. 1999a). 'Security bid/ask dynamics with discreteness and clustering: Simple strategies for modeling and estimation'. In: *Journal of Financial Markets* 2.1, pp. 1–28. URL: <https://ideas.repec.org/a/eee/finmar/v2y1999i1p1-28.html>.
- (1999b). 'The Dynamics of Discrete Bid and Ask Quotes'. In: *The Journal of Finance* 54.6, pp. 2109–2142. issn: 00221082, 15406261. URL: <http://www.jstor.org/stable/797989>.
- (Sept. 2019). 'Price Discovery in High Resolution'. In: *Journal of Financial Econometrics* 19.3, pp. 395–430. doi: [10.1093/jjfinc/nbz027](https://doi.org/10.1093/jjfinc/nbz027).
- Hasbrouck, Joel and Thomas S. Y. Ho (Sept. 1987). 'Order Arrival, Quote Behavior, and the Return-Generating Process'. In: *The Journal of Finance* 42.4, pp. 1035–1048. doi: [10.1111/j.1540-6261.1987.tb03926.x](https://doi.org/10.1111/j.1540-6261.1987.tb03926.x).
- Hasbrouck, Joel and Gideon Saar (Nov. 2013). 'Low-latency trading'. In: *Journal of Financial Markets* 16.4, pp. 646–679. doi: [10.1016/j.finmar.2013.05.003](https://doi.org/10.1016/j.finmar.2013.05.003).
- Hausman, Jerry A., Andrew W. Lo and A.Craig MacKinlay (June 1992). 'An ordered probit analysis of transaction stock prices'. In: *Journal of Financial Economics* 31.3, pp. 319–379. doi: [10.1016/0304-405x\(92\)90038-y](https://doi.org/10.1016/0304-405x(92)90038-y).
- Hautsch, Nikolaus (2001). 'Modelling Intraday Trading Activity Using Box-Cox ACD Models'. In: *SSRN Electronic Journal*. doi: [10.2139/ssrn.289643](https://doi.org/10.2139/ssrn.289643).

- Hautsch, Nikolaus (2012). *Econometrics of Financial High-Frequency Data*. Springer Berlin Heidelberg. DOI: [10.1007/978-3-642-21925-2](https://doi.org/10.1007/978-3-642-21925-2).
- Hautsch, Nikolaus and Rodrigo Herrera (Dec. 2019). 'Multivariate dynamic intensity peaks-over-threshold models'. In: *Journal of Applied Econometrics* 35.2, pp. 248–272. DOI: [10.1002/jae.2741](https://doi.org/10.1002/jae.2741).
- Hautsch, Nikolaus, Lada M. Kyj and Roel C. A. Oomen (Oct. 2010). 'A blocking and regularization approach to high-dimensional realized covariance estimation'. In: *Journal of Applied Econometrics* 27.4, pp. 625–645. DOI: [10.1002/jae.1218](https://doi.org/10.1002/jae.1218).
- Hawkes, Alan G. (Oct. 1971). 'Point Spectra of Some Mutually Exciting Point Processes'. In: *Journal of the Royal Statistical Society: Series B (Methodological)* 33.3, pp. 438–443. DOI: [10.1111/j.2517-6161.1971.tb01530.x](https://doi.org/10.1111/j.2517-6161.1971.tb01530.x).
- (Dec. 2017). 'Hawkes processes and their applications to finance: a review'. In: *Quantitative Finance* 18.2, pp. 193–198. DOI: [10.1080/14697688.2017.1403131](https://doi.org/10.1080/14697688.2017.1403131).
- Hawkes, Alan G. and David Oakes (Sept. 1974). 'A cluster process representation of a self-exciting process'. In: *Journal of Applied Probability* 11.3, pp. 493–503. DOI: [10.2307/3212693](https://doi.org/10.2307/3212693).
- Hayashi, Takaki and Yuta Koike (Aug. 2017). 'Multi-scale analysis of lead-lag relationships in high-frequency financial markets'. In: arXiv: [1708.03992 \[stat.ME\]](https://arxiv.org/abs/1708.03992).
- (Jan. 2018). 'Wavelet-Based Methods for High-Frequency Lead-Lag Analysis'. In: *SIAM Journal on Financial Mathematics* 9.4, pp. 1208–1248. DOI: [10.1137/18m1166079](https://doi.org/10.1137/18m1166079).
- (Nov. 2019). 'No arbitrage and lead – lag relationships'. In: *Statistics & Probability Letters* 154, p. 108530. DOI: [10.1016/j.spl.2019.06.006](https://doi.org/10.1016/j.spl.2019.06.006).
- Hayashi, Takaki and Nakahiro Yoshida (Apr. 2005). 'On covariance estimation of non-synchronously observed diffusion processes'. In: *Bernoulli* 11.2. DOI: [10.3150/bj/1116340299](https://doi.org/10.3150/bj/1116340299).
- Hoffmann, M., M. Rosenbaum and N. Yoshida (May 2013). 'Estimation of the lead-lag parameter from non-synchronous data'. In: *Bernoulli* 19.2. DOI: [10.3150/11-bej407](https://doi.org/10.3150/11-bej407).
- Holden, Craig W. and Avanidhar Subrahmanyam (Mar. 1992). 'Long-Lived Private Information and Imperfect Competition'. In: *The Journal of Finance* 47.1, pp. 247–270. DOI: [10.1111/j.1540-6261.1992.tb03985.x](https://doi.org/10.1111/j.1540-6261.1992.tb03985.x).
- Hong, Seok Young, Ingmar Nolte, Stephen J Taylor and Xiaolu Zhao (Mar. 2021). 'Volatility Estimation and Forecasts Based on Price Durations'. In: *Journal of Financial Econometrics*. DOI: [10.1093/jjfinec/nbab006](https://doi.org/10.1093/jjfinec/nbab006).
- Huang, Roger D. and Hans R. Stoll (Jan. 1994). 'Market Microstructure and Stock Return Predictions'. In: *Review of Financial Studies* 7.1, pp. 179–213. DOI: [10.1093/rfs/7.1.179](https://doi.org/10.1093/rfs/7.1.179).
- Huth, Nicolas and Frédéric Abergel (Mar. 2014). 'High frequency lead/lag relationships — Empirical facts'. In: *Journal of Empirical Finance* 26, pp. 41–58. DOI: [10.1016/j.jempfin.2014.01.003](https://doi.org/10.1016/j.jempfin.2014.01.003).
- Jacod, Jean, Yingying Li, Per A. Mykland, Mark Podolskij and Mathias Vetter (July 2009). 'Microstructure noise in the continuous case: The pre-averaging approach'. In: *Stochastic Processes and their Applications* 119.7, pp. 2249–2276. DOI: [10.1016/j.spa.2008.11.004](https://doi.org/10.1016/j.spa.2008.11.004).
- Jacod, Jean, Yingying Li and Xinghua Zheng (2017). 'Statistical Properties of Microstructure Noise'. In: *Econometrica* 85.4, pp. 1133–1174. DOI: [10.3982/ecta13085](https://doi.org/10.3982/ecta13085).
- (Jan. 2019). 'Estimating the integrated volatility with tick observations'. In: *Journal of Econometrics* 208.1, pp. 80–100. DOI: [10.1016/j.jeconom.2018.09.006](https://doi.org/10.1016/j.jeconom.2018.09.006).
- Jasiak, Joanna (1999). 'Persistence in Intertrade Durations'. In: *SSRN Electronic Journal*. DOI: [10.2139/ssrn.162008](https://doi.org/10.2139/ssrn.162008).
- Jong, Frank de and Theo Nijman (June 1997). 'High frequency analysis of lead-lag relationships between financial markets'. In: *Journal of Empirical Finance* 4.2-3, pp. 259–277. DOI: [10.1016/s0927-5398\(97\)00009-1](https://doi.org/10.1016/s0927-5398(97)00009-1).
- Jorion, Philippe (Nov. 2006). *Value at Risk, 3rd Ed.: The New Benchmark for Managing Financial Risk*. MCGRAW HILL BOOK CO. 624 pp. ISBN: 0071464956.
- Karr, Alan (2017). *Point Processes and Their Statistical Inference*. New York: Routledge. ISBN: 9781351423830.
- Kirchner, Matthias (Sept. 2016a). 'An estimation procedure for the Hawkes process'. In: *Quantitative Finance* 17.4, pp. 571–595. DOI: [10.1080/14697688.2016.1211312](https://doi.org/10.1080/14697688.2016.1211312).
- (Aug. 2016b). 'Hawkes and INAR(∞) processes'. In: *Stochastic Processes and their Applications* 126.8, pp. 2494–2525. DOI: [10.1016/j.spa.2016.02.008](https://doi.org/10.1016/j.spa.2016.02.008).
- Koike, Yuta (Apr. 2015). 'Estimation of integrated covariances in the simultaneous presence of nonsynchronicity, microstructure noise $\text{noi}_{10.1016/j.jeconom.2008.09.016}$ and jumps'. In: *Econometric Theory* 32.3, pp. 533–611. DOI: [10.1017/s0266466614000954](https://doi.org/10.1017/s0266466614000954).
- Kupiec, Paul H. (Nov. 1995). 'Techniques for Verifying the Accuracy of Risk Measurement Models'. In: *The Journal of Derivatives* 3.2, pp. 73–84. DOI: [10.3905/jod.1995.407942](https://doi.org/10.3905/jod.1995.407942).
- Kyle, Albert S. (Nov. 1985). 'Continuous Auctions and Insider Trading'. In: *Econometrica* 53.6, p. 1315. DOI: [10.2307/1913210](https://doi.org/10.2307/1913210).
- Large, Jeremy (2007a). 'Accounting for the Epps effect: Realized covariation, cointegration and common factors'. In: *Unpublished paper: Oxford-Man Institute, University of Oxford*.
- (Feb. 2007b). 'Measuring the resiliency of an electronic limit order book'. In: *Journal of Financial Markets* 10.1, pp. 1–25. DOI: [10.1016/j.finmar.2006.09.001](https://doi.org/10.1016/j.finmar.2006.09.001).
- Lee, Suzanne S. and Per A. Mykland (Dec. 2007). 'Jumps in Financial Markets: A New Nonparametric Test and Jump Dynamics'. In: *Review of Financial Studies* 21.6, pp. 2535–2563. DOI: [10.1093/rfs/hhm056](https://doi.org/10.1093/rfs/hhm056).

- Li, Sida, Xin Wang and Mao Ye (Apr. 2021). 'Who provides liquidity, and when?' In: *Journal of Financial Economics*. DOI: [10.1016/j.jfineco.2021.04.020](https://doi.org/10.1016/j.jfineco.2021.04.020).
- Li, Yifan, Ingmar Nolte and Sandra Nolte (Lechner) (2018). 'Asymptotic Theory for Renewal Based High-Frequency Volatility Estimation'. In: *SSRN Electronic Journal*. DOI: [10.2139/ssrn.3123062](https://doi.org/10.2139/ssrn.3123062).
- Li, Yifan, Ingmar Nolte and Sandra Nolte-Lechner (2015). 'High-Frequency Volatility Estimation and the Relative Importance of Market Microstructure Variables: An Autoregressive Conditional Intensity Approach'. In: *SSRN Electronic Journal*. DOI: [10.2139/ssrn.2665639](https://doi.org/10.2139/ssrn.2665639).
- Li, Yifan, Ingmar Nolte and Sandra Nolte (Mar. 2021). 'High-frequency volatility modeling: A Markov-Switching Autoregressive Conditional Intensity model'. In: *Journal of Economic Dynamics and Control* 124, p. 104077. DOI: [10.1016/j.jedc.2021.104077](https://doi.org/10.1016/j.jedc.2021.104077).
- Li, Yifan, Ingmar Nolte, Michalis Vasios, Valeri Voev and Qi Xu (Apr. 2022). 'Weighted Least Squares Realized Covariation Estimation'. In: *Journal of Banking & Finance* 137, p. 106420. DOI: [10.1016/j.jbankfin.2022.106420](https://doi.org/10.1016/j.jbankfin.2022.106420).
- Li, Yingying, Per A. Mykland, Eric Renault, Lan Zhang and Xinghua Zheng (Nov. 2013). 'Realized Volatility When Sampling Times Are Possibly Endogenous'. In: *Econometric Theory* 30.3, pp. 580–605. DOI: [10.1017/s0266466613000418](https://doi.org/10.1017/s0266466613000418).
- Li, Yingying, Shangyu Xie and Xinghua Zheng (Nov. 2016). 'Efficient estimation of integrated volatility incorporating trading information'. In: *Journal of Econometrics* 195.1, pp. 33–50. DOI: [10.1016/j.jeconom.2016.05.017](https://doi.org/10.1016/j.jeconom.2016.05.017).
- Li, Yingying, Zhiyuan Zhang and Xinghua Zheng (July 2013). 'Volatility inference in the presence of both endogenous time and microstructure noise'. In: *Stochastic Processes and their Applications* 123.7, pp. 2696–2727. DOI: [10.1016/j.spa.2013.04.002](https://doi.org/10.1016/j.spa.2013.04.002).
- Liesenfeld, Roman, Ingmar Nolte and Winfried Pohlmeier (2008). 'Modelling financial transaction price movements: a dynamic integer count data model'. In: *High Frequency Financial Econometrics*. Physica-Verlag HD, pp. 167–197. DOI: [10.1007/978-3-7908-1992-2_8](https://doi.org/10.1007/978-3-7908-1992-2_8).
- Liu, Lily Y., Andrew J. Patton and Kevin Sheppard (July 2015). 'Does anything beat 5-minute RV? A comparison of realized measures across multiple asset classes'. In: *Journal of Econometrics* 187.1, pp. 293–311. DOI: [10.1016/j.jeconom.2015.02.008](https://doi.org/10.1016/j.jeconom.2015.02.008).
- Liu, Shouwei and Yiu Kuen Tse (Dec. 2015). 'Intraday Value-at-Risk: An asymmetric autoregressive conditional duration approach'. In: *Journal of Econometrics* 189.2, pp. 437–446. DOI: [10.1016/j.jeconom.2015.03.035](https://doi.org/10.1016/j.jeconom.2015.03.035).
- Lo, Andrew W. and A. Craig MacKinlay (July 1990). 'An econometric analysis of nonsynchronous trading'. In: *Journal of Econometrics* 45.1-2, pp. 181–211. DOI: [10.1016/0304-4076\(90\)90098-e](https://doi.org/10.1016/0304-4076(90)90098-e).
- Longin, François and Bruno Solnik (Apr. 2001). 'Extreme Correlation of International Equity Markets'. In: *The Journal of Finance* 56.2, pp. 649–676. DOI: [10.1111/0022-1082.00340](https://doi.org/10.1111/0022-1082.00340).
- Luca, Giovanni De and Giampiero M. Gallo (Jan. 2004). 'Mixture Processes for Financial Intradaily Durations'. In: *Studies in Nonlinear Dynamics & Econometrics* 8.2. DOI: [10.2202/1558-3708.1223](https://doi.org/10.2202/1558-3708.1223).
- Lunde, Asger (1999). 'A generalized gamma autoregressive conditional duration model'. In: *Stylized Facts of Financial Time Series and Three Popular Models of Volatility*. SSE/EFI Working Paper Series in Economics and Finance 563. Stockholm School of Economics. URL: <https://EconPapers.repec.org/RePEc:hhs:hastef:0563>.
- Malmsten, Hans and Timo Teräsvirta (2004). 'Extreme Correlation of International Equity Markets'. In: *The Journal of Finance* 56.2, pp. 649–676. DOI: [10.1111/0022-1082.00340](https://doi.org/10.1111/0022-1082.00340).
- Mancino, M. E. and S. Sanfelici (Feb. 2008). 'Robustness of Fourier estimator of integrated volatility in the presence of microstructure noise'. In: *Computational Statistics & Data Analysis* 52.6, pp. 2966–2989. DOI: [10.1016/j.csda.2007.07.014](https://doi.org/10.1016/j.csda.2007.07.014).
- (Jan. 2011). 'Estimating Covariance via Fourier Method in the Presence of Asynchronous Trading and Microstructure Noise'. In: *Journal of Financial Econometrics* 9.2, pp. 367–408. DOI: [10.1093/jjfinec/nbq031](https://doi.org/10.1093/jjfinec/nbq031).
- Martens, Martin P.E. (2004). 'Estimating Unbiased and Precise Realized Covariances'. In: *SSRN Electronic Journal*. DOI: [10.2139/ssrn.556118](https://doi.org/10.2139/ssrn.556118).
- Mcneil, Alexander J., Rudiger Frey and Paul Embrechts (May 2015). *Quantitative Risk Management*. Princeton University Press. 720 pp. ISBN: 0691166277.
- Mech, Timothy S. (Dec. 1993). 'Portfolio return autocorrelation'. In: *Journal of Financial Economics* 34.3, pp. 307–344. DOI: [10.1016/0304-405x\(93\)90030-f](https://doi.org/10.1016/0304-405x(93)90030-f).
- Meddahi, Nour (2002). 'A theoretical comparison between integrated and realized volatility'. In: *Journal of Applied Econometrics* 17.5, pp. 479–508. DOI: [10.1002/jae.689](https://doi.org/10.1002/jae.689).
- Menkveld, Albert J. (Oct. 2016). 'The Economics of High-Frequency Trading: Taking Stock'. In: *Annual Review of Financial Economics* 8.1, pp. 1–24. DOI: [10.1146/annurev-financial-121415-033010](https://doi.org/10.1146/annurev-financial-121415-033010).
- (Apr. 2018). 'High-Frequency Trading as Viewed through an Electron Microscope'. In: *Financial Analysts Journal* 74.2, pp. 24–31. DOI: [10.2469/faj.v74.n2.1](https://doi.org/10.2469/faj.v74.n2.1).
- Merton, Robert C. (Dec. 1980). 'On estimating the expected return on the market'. In: *Journal of Financial Economics* 8.4, pp. 323–361. DOI: [10.1016/0304-405x\(80\)90007-0](https://doi.org/10.1016/0304-405x(80)90007-0).
- Muller, U. A., Michel Dacorogna, R. D. Dave, O. V. Pictet, Richard Olsen and J.R. Ward (1993). *Fractals and Intrinsic Time - a Challenge to Econometricians*. Working Papers 1993-08-16. Olsen and Associates.

- Mykland, Per A. and Lan Zhang (2009). 'Inference for Continuous Semimartingales Observed at High Frequency'. In: *Econometrica* 77.5, pp. 1403–1445. ISSN: 00129682, 14680262. URL: <http://www.jstor.org/stable/25621366>.
- Nelson, Daniel B. (1991). 'Conditional Heteroskedasticity in Asset Returns: A New Approach'. In: *Econometrica* 59.2, pp. 347–370. ISSN: 00129682, 14680262. URL: <http://www.jstor.org/stable/2938260>.
- Nolte, Ingmar and Valeri Voev (Jan. 2012). 'Least Squares Inference on Integrated Volatility and the Relationship Between Efficient Prices and Noise'. In: *Journal of Business & Economic Statistics* 30.1, pp. 94–108. DOI: [10.1080/10473289.2011.637876](https://doi.org/10.1080/10473289.2011.637876).
- O'Hara, Maureen (Jan. 1998). *Market Microstructure Theory*. John Wiley & Sons. 304 pp. ISBN: 0631207619.
- (July 2003). 'Presidential Address: Liquidity and Price Discovery'. In: *The Journal of Finance* 58.4, pp. 1335–1354. DOI: [10.1111/1540-6261.00569](https://doi.org/10.1111/1540-6261.00569).
- (May 2015). 'High frequency market microstructure'. In: *Journal of Financial Economics* 116.2, pp. 257–270. DOI: [10.1016/j.jfineco.2015.01.003](https://doi.org/10.1016/j.jfineco.2015.01.003).
- O'Hara, Maureen, Chen Yao and Mao Ye (Sept. 2014). 'What's Not There: Odd Lots and Market Data'. In: *The Journal of Finance* 69.5, pp. 2199–2236. DOI: [10.1111/jofi.12185](https://doi.org/10.1111/jofi.12185).
- Ogata, Yoshihiko (Mar. 1988). 'Statistical Models for Earthquake Occurrences and Residual Analysis for Point Processes'. In: *Journal of the American Statistical Association* 83.401, pp. 9–27. DOI: [10.1080/01621459.1988.10478560](https://doi.org/10.1080/01621459.1988.10478560).
- Pacurar, Maria (Sept. 2008). 'Autoregressive Conditional Duration, ACD, Models in Finance: A Survey of the Theoretical and Empirical Literature'. In: *Journal of Economic Surveys* 22.4, pp. 711–751. DOI: [10.1111/j.1467-6419.2007.00547.x](https://doi.org/10.1111/j.1467-6419.2007.00547.x).
- Park, Sujin, Seok Young Hong and Oliver Linton (Apr. 2016). 'Estimating the quadratic covariation matrix for asynchronously observed high frequency stock returns corrupted by additive measurement error'. In: *Journal of Econometrics* 191.2, pp. 325–347. DOI: [10.1016/j.jeconom.2015.12.005](https://doi.org/10.1016/j.jeconom.2015.12.005).
- Pasquariello, Paolo and Clara Vega (Dec. 2013). 'Strategic Cross-Trading in the U.S. Stock Market'. In: *Review of Finance* 19.1, pp. 229–282. DOI: [10.1093/rof/rft055](https://doi.org/10.1093/rof/rft055).
- Podolskij, Mark and Mathias Vetter (Aug. 2009). 'Estimation of volatility functionals in the simultaneous presence of microstructure noise and jumps'. In: *Bernoulli* 15.3. DOI: [10.3150/08-bej167](https://doi.org/10.3150/08-bej167).
- Protter, Philip (2013). *Stochastic Integration and Differential Equations*. Vol. 21. Springer.
- Rambaldi, Marcello, Vladimir Filimonov and Fabrizio Lillo (Mar. 2018). 'Detection of intensity bursts using Hawkes processes: An application to high-frequency financial data'. In: *Physical Review E* 97.3, p. 032318. DOI: [10.1103/physreve.97.032318](https://doi.org/10.1103/physreve.97.032318).
- Roll, Richard (Sept. 1984). 'A Simple Implicit Measure of the Effective Bid-Ask Spread in an Efficient Market'. In: *The Journal of Finance* 39.4, pp. 1127–1139. DOI: [10.1111/j.1540-6261.1984.tb03897.x](https://doi.org/10.1111/j.1540-6261.1984.tb03897.x).
- Russell, Jeffrey R (1999). 'Econometric modeling of multivariate irregularly-spaced high-frequency data'. In: *Manuscript, GSB, University of Chicago*.
- Russell, Jeffrey R and Robert F Engle (Apr. 2005). 'A Discrete-State Continuous-Time Model of Financial Transactions Prices and Times'. In: *Journal of Business & Economic Statistics* 23.2, pp. 166–180. DOI: [10.1198/073500104000000541](https://doi.org/10.1198/073500104000000541).
- Russell, Jeffrey R. and Robert F. Engle (2010). 'Analysis of High-Frequency Data'. In: *Handbook of Financial Econometrics: Tools and Techniques*. Elsevier, pp. 383–426. DOI: [10.1016/b978-0-444-50897-3.50010-9](https://doi.org/10.1016/b978-0-444-50897-3.50010-9).
- Rydberg, Tina Hviid and Neil Shephard (1999a). 'A Modelling Framework for the Prices and Times of Trades Made on the New York Stock Exchange'. In: *SSRN Electronic Journal*. DOI: [10.2139/ssrn.164170](https://doi.org/10.2139/ssrn.164170).
- (1999b). 'Modelling Trade-By-Trade Price Movements of Multiple Assets Using Multivariate Compound Poisson Processes'. In: *SSRN Electronic Journal*. DOI: [10.2139/ssrn.182248](https://doi.org/10.2139/ssrn.182248).
- (Aug. 2000). *BIN Models for Trade-by-Trade Data. Modelling the Number of Trades in a Fixed Interval of Time*. Econometric Society World Congress 2000 Contributed Papers 0740. Econometric Society. URL: <https://ideas.repec.org/p/econ/wc2000/0740.html>.
- (Mar. 2003). 'Dynamics of Trade-by-Trade Price Movements: Decomposition and Models'. In: *Journal of Financial Econometrics* 1.1, pp. 2–25. DOI: [10.1093/jfinec/nbg002](https://doi.org/10.1093/jfinec/nbg002).
- Schatz, Michael, Spencer Wheatley and Didier Sornette (Dec. 2021). 'The ARMA Point Process and its Estimation'. In: *Econometrics and Statistics*. DOI: [10.1016/j.ecosta.2021.11.002](https://doi.org/10.1016/j.ecosta.2021.11.002).
- Tay, Anthony S., Christopher Ting, Yiu Kuen Tse and Mitch Warachka (Mar. 2011). 'The impact of transaction duration, volume and direction on price dynamics and volatility'. In: *Quantitative Finance* 11.3, pp. 447–457. DOI: [10.1080/14697680903405742](https://doi.org/10.1080/14697680903405742).
- Taylor, Stephen (2008). *Modelling financial time series*. New Jersey: World Scientific. ISBN: 9789812770851.
- Tookes, Heather E. (Jan. 2008). 'Information, Trading, and Product Market Interactions: Cross-sectional Implications of Informed Trading'. In: *The Journal of Finance* 63.1, pp. 379–413. DOI: [10.1111/j.1540-6261.2008.01319.x](https://doi.org/10.1111/j.1540-6261.2008.01319.x).
- Tse, Yiu kuen and Thomas Tao Yang (Oct. 2012). 'Estimation of High-Frequency Volatility: An Autoregressive Conditional Duration Approach'. In: *Journal of Business & Economic Statistics* 30.4, pp. 533–545. DOI: [10.1080/07350015.2012.707582](https://doi.org/10.1080/07350015.2012.707582).

- Varneskov, Rasmus Tangsgaard (Dec. 2016a). 'Estimating the quadratic variation spectrum of noisy asset prices using generalized flat-top realized kernels'. In: *Econometric Theory* 33.6, pp. 1457–1501. doi: [10.1017/s0266466616000475](https://doi.org/10.1017/s0266466616000475).
- (Jan. 2016b). 'Flat-Top Realized Kernel Estimation of Quadratic Covariation With Nonsynchronous and Noisy Asset Prices'. In: *Journal of Business & Economic Statistics* 34.1, pp. 1–22. doi: [10.1080/07350015.2015.1005622](https://doi.org/10.1080/07350015.2015.1005622).
- Vives, Xavier (Oct. 1995). 'The Speed of Information Revelation in a Financial Market Mechanism'. In: *Journal of Economic Theory* 67.1, pp. 178–204. doi: [10.1006/jeth.1995.1070](https://doi.org/10.1006/jeth.1995.1070).
- Voev, V. and A. Lunde (Nov. 2006). 'Integrated Covariance Estimation using High-frequency Data in the Presence of Noise'. In: *Journal of Financial Econometrics* 5.1, pp. 68–104. doi: [10.1093/jjfinec/nbl011](https://doi.org/10.1093/jjfinec/nbl011).
- Wheatley, Spencer, Vladimir Filimonov and Didier Sornette (Feb. 2016). 'The Hawkes process with renewal immigration & its estimation with an EM algorithm'. In: *Computational Statistics & Data Analysis* 94, pp. 120–135. doi: [10.1016/j.csda.2015.08.007](https://doi.org/10.1016/j.csda.2015.08.007).
- Wheatley, Spencer, Alexander Wehrli and Didier Sornette (Jan. 2019). 'The endo–exo problem in high frequency financial price fluctuations and rejecting criticality'. In: *Quantitative Finance* 19.7, pp. 1165–1178. doi: [10.1080/14697688.2018.1550266](https://doi.org/10.1080/14697688.2018.1550266).
- Wuensche, Oliver, Erik Theissen and Joachim Grammig (2011). 'Time and the Price Impact of a Trade: A Structural Approach'. In: *SSRN Electronic Journal*. doi: [10.2139/ssrn.968241](https://doi.org/10.2139/ssrn.968241).
- Xiu, Dacheng (Nov. 2010). 'Quasi-maximum likelihood estimation of volatility with high frequency data'. In: *Journal of Econometrics* 159.1, pp. 235–250. doi: [10.1016/j.jeconom.2010.07.002](https://doi.org/10.1016/j.jeconom.2010.07.002).
- Yao, Chen and Mao Ye (Apr. 2018). 'Why Trading Speed Matters: A Tale of Queue Rationing under Price Controls'. In: *The Review of Financial Studies* 31.6, pp. 2157–2183. doi: [10.1093/rfs/hhy002](https://doi.org/10.1093/rfs/hhy002).
- Zhang, Lan (2006). 'Efficient Estimation of Stochastic Volatility Using Noisy Observations: A Multi-Scale Approach'. In: *Bernoulli* 12.6, pp. 1019–1043. issn: 13507265. url: <http://www.jstor.org/stable/25464852>.
- (Jan. 2011). 'Estimating covariation: Epps effect, microstructure noise'. In: *Journal of Econometrics* 160.1, pp. 33–47. doi: [10.1016/j.jeconom.2010.03.012](https://doi.org/10.1016/j.jeconom.2010.03.012).
- Zhang, Lan, Per A. Mykland and Yacine Aït-Sahalia (2005). 'A Tale of Two Time Scales: Determining Integrated Volatility with Noisy High-Frequency Data'. In: *Journal of the American Statistical Association* 100.472, pp. 1394–1411. issn: 01621459. url: <http://www.jstor.org/stable/27590680>.
- Zhang, Michael Yuanjie, Jeffrey R. Russell and Ruey S. Tsay (2001). 'A nonlinear autoregressive conditional duration model with applications to financial transaction data'. In: *Journal of Econometrics* 104.1, pp. 179–207. issn: 0304-4076. doi: [https://doi.org/10.1016/S0304-4076\(01\)00063-X](https://doi.org/10.1016/S0304-4076(01)00063-X). url: <https://www.sciencedirect.com/science/article/pii/S030440760100063X>.
- (Sept. 2008). 'Determinants of bid and ask quotes and implications for the cost of trading'. In: *Journal of Empirical Finance* 15.4, pp. 656–678. doi: [10.1016/j.jempfin.2007.12.003](https://doi.org/10.1016/j.jempfin.2007.12.003).

Titre : Dynamique de formation des prix à haute fréquence et mesures multivariées du risque de marché intra-journalier.

Mots clés : Dynamique de formation des prix, matrice de variance-covariance, IVaR multivariée.

Résumé : Cette thèse porte sur les marchés électroniques modernes et développe des modèles mathématiques sur mesure pour le trading à haute fréquence. Observées à la résolution la plus fine, la formation des prix et les transactions intra-journalières présentent des propriétés fondamentalement différentes de celles du trading à plus basse fréquence. En effet, plusieurs "frictions de marché" semblent désormais être la norme plutôt que l'exception, ce qui remet en question l'hypothèse de l'efficacité des marchés. Par conséquent, les modèles mathématiques établis de longue date et appliqués à une dynamique de prix à basse fréquence, inadaptés au contexte actuel de trading à haute fréquence, ne parviennent plus à expliquer l'environnement complexe généré par les frictions de microstructure des marchés.

Pour remédier à ces lacunes, nous développons dans la première partie de cette thèse une dynamique généralisée de formation des prix, basée sur l'idée que l'information et le

temps intrinsèquement liés, considérant que l'information a une durée de vie et qu'elle se dégrade avec le temps. Plus précisément, nous proposons une extension du modèle classique "martingale plus bruit" et permettons un traitement plus structurel de la dynamique à haute fréquence qui reflète les sources d'information asymétrique, la durée de vie de l'information et l'ajustement des prix retardé dans le temps.

Les deuxième et troisième parties de la thèse contribuent à la mesure du risque multivarié à haute fréquence, mesure développée à partir de la dynamique des prix exposée en première partie. En particulier, la deuxième partie de la thèse introduit un nouvel estimateur de la structure des moments de second ordre pour le rendement d'actifs. La troisième partie de la thèse contribue à la modélisation directe de la queue de la distribution des rendements en développant une nouvelle Value-at Risk intra-journalière multivariée.

Title : High-Frequency Price Formation Dynamics and Multivariate Intraday Risk Measurement.

Keywords : Price formation dynamics, variance-covariance matrix, multivariate IVaR.

Abstract : This thesis focuses on modern electronic markets and develops tailor-made mathematical models of high-frequency trading. When focusing on the finest frequency of trading, such as transaction-by-transaction, intraday price formation and trading exhibit fundamentally different properties compared to lower trading frequencies. Several "market frictions" appear to be the norm, rather than the exception and this poses a great challenge to the efficient market hypothesis. Consequently, long-established mathematical models that are applied on lower-frequency price dynamics, are no longer adequate in the context of high-frequency trading and fail to explain the complex environment generated by the frictions of market microstructure.

To address these shortcomings, in the first part of this thesis, we develop a generalized price

formation dynamics based on the view that time and information are inherently linked, considering that information has a life span and decays over time. More precisely, we extend the classic "martingale-plus-noise" model and allow for a more structural treatment of high-frequency dynamics that capture the sources of asymmetric information, information life span, and temporal lagged price adjustment.

The second and third parts of the thesis contribute to high-frequency multivariate risk measurement, developed on the ground of the price dynamics in the first part. In particular, the second part of the thesis introduces a novel estimator of second-order moment structure of asset returns and the third part of the thesis contributes on direct modelling of the tail distribution of asset returns by developing a new multivariate intraday Value-at-Risk.

